Anaerobic Oxidation of Methane in Paddy Soil

Dissertation

to obtain the Dr. rer. nat. degree

of the Faculty of Forest Sciences and Forest Ecology

Georg-August-University Göttingen

Submitted by

Lichao Fan

Born in Shandong, China

Göttingen, October 2020

Members of the disputation committee:

Prof. Dr. Michaela Dippold, Biogeochemistry of Agroecosystems, Georg-August-University Göttingen, Germany

Prof. Dr. Volker Thiel, Geobiology, Geoscience Center, Georg-August-University Göttingen, Germany

Dr. Maxim Dorodnikov, Soil Science of Temperate Ecosystems, Georg-August-University Göttingen, Germany

Prof. Dr. Mats B Nilsson, Swedish University of Agricultural Sciences, Sweden

Prof. Dr. Tida Ge, Ningbo University, China

Referee

1st Referee: Prof. Dr. Michaela Dippold

2nd Referee: Prof. Dr. Volker Thiel

Date of the oral examination: 30-09-2020

To my best friend

Maxim Dorodnikov

Table of content

Acknowledgements

Time flies! It seems that I just arrived here yesterday – Göttingen, in fact, almost four years have passed. I still clearly remember each thing of the first day. In the early morning just after the rain on November 25th 2016, I first set foot on this exotic land, Germany. I was so excited but at the same time a little timid. I boarded the ICE train to Göttingen from Frankfurt International Airport. I stood at the junction of the train cabins and looked out through the window. I saw the bright sun shining on the grass, and three gorgeous horses were eating leisurely. Beyond, beautiful houses and big trees were crossed together in the distance, that I have only seen such kind scenery from movies. It was so beautiful and unforgettable. That was the moment I started to like this exotic land, even it is ten thousand kilometers away from my hometown. I arrived in Göttingen at noon. When I came to my apartment, I found it was a small but nice room, outside of the window was lawn and cheers. In the evening, I went to the laboratory under the guidance of friends, and I met with Prof. Dr. Yakov Kuzyakov, I did not clearly remember what we have talked about, but I did remember that exciting and aspirational feelings: The four-year journey as an international PhD student at the University of Göttingen began.

This is a wonderful and fruitful studying journey, undoubtedly. I spent a qualified time in the excellent soil science research group and I would like to acknowledge everyone I met here. First of all, I would like to express my sincere thanks to my supervisors Prof. Dr. Michaela Dippold, Prof. Dr. Volker Thiel, Dr. Maxim Dorodnikov, and Prof. Dr. Yakov Kuzyakov. I appreciate they given me a large extent of the flexibility and independence to conduct my PhD work, I cannot reach this version of myself if without their continuous support and their wealth of knowledge. Special thanks to Dr. Maxim Dorodnikov, he is not only as my supervisor but also my best friend, for his generous guidance, support, and understand whenever I need it.

I would like to appreciate all my co-authors Dr. Maxim Dorodnikov, Prof. Yakov Kuzyakov, Prof. Michaela A. Dippold, Prof. Volker Thiel, Prof. Tida Ge, Prof. Jinshui Wu, Dr. Muhammad Shahbaz, Dr. Dominik Schneider, Dr. Weichao Wu, and Dr. Heng Gui for their insightful suggestions and brilliant ideas to improve the quality of the manuscripts in this thesis.

Sincere thanks to my colleagues of the Department of Soil Science of Temperate Ecosystems, Agricultural Soil Science, Biogeochemistry of Agroecosystems, Chinese Academy of Sciences Institute of Subtropical Agriculture, Chinese Academy of Agricultural Sciences Tea Research Institute, and a special group of friends in the Büsgenweg 2 departments for the together-shared-memorable moments. I also would like to thank the technical staff for their assistance and guidance in the laboratory. Specific thanks to the lunch group of my Chinese friends.

I am very grateful to the China Scholarship Council (CSC) to sponsor my PhD study in Germany, and thanks to the German Research Foundation (DFG, Do 1533/2-1) and Graduate School Forest and Agricultural Sciences (GFA) to fund my research and conference travels.

Finally, I am greatly indebted to my family for their unconditional love, continued spiritual support, and encouragement during my study and life in general. I sincerely appreciate my beautiful wife Suyan Xie and my dear son Yichen Fan. They are my strength and motivation to success in this journey.

Vielen Dank!

Summary

The anaerobic oxidation of methane (AOM) is a globally important CH_4 sink that offsets potential CH_4 emission into the atmosphere. AOM is estimated to consume up to 90% of CH_4 produced in marine sediments before it reaches atmosphere, but it is an underappreciated CH_4 sink in terrestrial ecosystems. This calls for the study of the specific mechanisms of terrestrial AOM and the estimation of the ecological relevance for CH_4 sink, especially in ecosystems exposed to long-term anaerobic conditions such as rice paddies. Flooded paddy soils are the hotspot area of methanogenesis along with a high availability of alternative electron acceptors (AEAs) needed by methanotrophic microorganisms to oxidize CH_4 anaerobically. However, the role of AEAs and the intensity of the AOM process in reducing the CH_4 fluxes from rice paddies remain unclear. Moreover, it remains unclear how AEAs from different fertilization modes affect anaerobic microbial interactions, and whether a preferred AOM pathway exists in these interactions.

Current studies on AOM are largely based on microcosm incubations with headspace CH_4 injection and shaking. However, shaking introduces mechanical disturbances but the lack of shaking may lead to a systematical underestimation of CH_4 oxidation due to the relatively low solubility of CH_4. To address these and the above challenges, four research aspects were investigated in this: (i) utility of the silicone tube approach for CH_4 oxidation studies, (ii) the occurrence of AOM under shaking and steady conditions with silicone tubes, (iii) role of AEAs and fertilization for AOM, (iv) active AOM pathways and functioning of the microbial community network in paddy soils. These aspects were investigated by tracing the ^{13}C-label from CH_4 into CO_2, soil organic matter, total microbial biomass and phospholipid fatty acids (PLFA) in fertilized (manure, biochar, NPK) paddy soils amended with alternative electron acceptors (NO_3^-, Fe^{3+}, SO_4^{2-}, humic-acids) to quantify CH_4 oxidation, and identify microbial groups by 16S rRNA sequencing analyses.

Our results implied the injection of CH_4 belowground via porous silicone tubes to compensate for the poor solubility of CH_4 and replace the common shaking method. During a 29-day incubation of soil slurry, the highest net CH_4 oxidation rate was 1.6 μg $C\text{-}CO_2$ g^{-1} dry soil h^{-1} after injecting $^{13}CH_4$ into the slurry through a silicone tube without shaking. This was 1.5-2.5 times faster than the respective CH_4 oxidation after headspace injection without shaking. Furthermore, it was found that CH_4 oxidation rates were similar between silicone tube injection without shaking and headspace injection with shaking. Consequently, the silicone tube approach can substitute the common shaking method. As the silicone tube approach maintains the gas concentration gradients, it can more realistically reflect natural soil conditions.

Secondly, by ^{13}C enrichment of CO_2 after $^{13}CH_4$ injection we clearly confirmed the hypothesized occurrence of AOM in paddy soil during a 59-day anaerobic incubation. The cumulative AOM reached 0.16-0.24 μg $C\text{-}CO_2$ g^{-1} dry soil without shaking, but it was 33-80% lower with shaking. Unexpectedly, the effect of silicone tubes on AOM was insignificant either with or without shaking, suggesting that the main limiting factor for AOM was not the CH_4 concentration in water (slurry) but the availability of AEAs. Without shaking, the methanogenesis control (no CH_4 addition) revealed a steady increase of CH_4 in the headspace/tube, whereas the CH_4 concentration in jars with shaking was constantly low during 59 days. This suggests that shaking inhibited methanogenesis, possibly by disturbing the AOM-related microorganisms which were co-localized to the substrates (*i.e.* CH_4 and AEAs).

Added NO_3^- was the most effective electron acceptor during 84 days of anaerobic incubation. The highest AOM rate was 0.80 ng C g^{-1} dry soil h^{-1} under pig manure fertilization followed by the control and NPK, while AOM was the lowest under biochar application. The role of Fe^{3+} in AOM remained unclear. SO_4^{2-} inhibited AOM but strongly stimulated the production of unlabeled CO_2, indicating intensive sulfate-induced decomposition of native organic matter. Added humic acids were the second most effective electron acceptor for AOM, but increased methanogenesis by 5-6 times in all

fertilization treatments. We demonstrated for the first time that organic electron acceptors are among the key AOM drivers and are crucial in paddy soils.

Finally, we determined AOM pathways by tracing ^{13}C incorporation from $^{13}CH_4$ into total microbial biomass and PLFA, and related these pathways to the microbial community's network. The co-occurrence network revealed a set of major and minor AOM pathways with synergistic relations between complementary anaerobic microbial groups. A set of comparative analyses confirmed that NO_3^--driven AOM was the major AOM pathway. It co-existed with minor pathways involving NO_2^- reduction by NC10 bacteria, putative reduction of humic acids and Fe^{3+} by *Geobacter* species, and SO_4^{2-} reduction by sulfate-reducing bacteria linked with anaerobic methanotrophs.

In a broader ecological view, AOM is ubiquitous in paddy soils but still is an underappreciated CH_4 sink. NO_3^--induced AOM together with manure fertilization has the potential to recycle ~3.9 Tg C-CH_4 annually before the produced CH_4 released to the atomsphere, which was equivalent to roughly ~10–20% of the global net CH_4 emissions from rice paddies. Consequently, the application of suitable organic and mineral fertilization strategies can provide an effective control on the CH_4 sink under anaerobic conditions in submerged agricultural ecosystems.

Zusammenfassung

Die anaerobe Oxidation von Methan (AOM) ist eine wichtige globale CH_4-Senke, die potenzielle CH_4-Emission in die Atmosphäre ausgleicht. Es wird geschätzt, dass die AOM bis zu 90% des in marinen Sedimenten produzierten CH_4 verbraucht, bevor es in die Atmosphäre gelangt. In terrestrischen Ökosystemen ist die AOM hingegen eine unzureichend erforschte CH_4-Senke. Die spezifischen Mechanismen der terrestrischen AOM sind weitgehend unbekannt; ebenso fehlt eine Abschätzung der ökologischen Relevanz der AOM als CH_4-Senke, insbesondere in Ökosystemen, die lang anhaltenden anaeroben Bedingungen ausgesetzt sind, wie z.B. Reisfelder. Überflutete Reisfeldböden sind Hotspots der Methanogenese, gleichzeitig aber verfügen sie potenziell große Mengen alternativer Elektronenakzeptoren (AEAs), die von methanotrophen Mikroorganismen benötigt werden um CH_4 anaerob zu oxidieren. Die Rolle individueller AEAs und die Intensität des AOM-Prozesses bei der Kompensation der CH_4-Flüsse aus Reisfeldern sind bislang jedoch unklar. Darüber hinaus bleibt unklar, wie verschiedene AEAs aus unterschiedlichen Düngemitteln die anaeroben mikrobiellen Interaktionen beeinflussen, und ob ein bevorzugter AOM-Pfad aus diesen Interaktionen resultiert.

Aktuelle Studien zur AOM basieren weitgehend auf Mikrokosmos-Inkubationen mit Headspace-CH_4-Injektion und Schütteln. Während das Schütteln einerseits zu mechanischen Störungen führt, kann der Verzicht auf das Schütteln aufgrund der relativ geringen CH_4-Löslichkeit zu einer systematischen Unterschätzung der CH_4-Oxidation führen. Zur Lösung dieser analytischen Probleme und zur Beantwortung der oben genannten Forschungsfragen wurden vier Aspekte in dieser Studie untersucht: (i) Nutzen der Silikonschlauch-Methode für die Bestimmung der CH_4-Oxidation, (ii) Bestimmung der AOM unter Schütteln gegenüber stationären Bedingungen mit Silikonschläuchen, (iii) Rolle der AEAs und der applizierten Düngemittel für die AOM, (iv) aktive AOM-Pfade in Abhängigkeit von der mikrobiellen Gemeinschaft in Reisböden. Diese Aspekte wurden durch die Verfolgung von ^{13}C-Markierungen aus CH_4 in CO_2, organische Bodensubstanz, mikrobielle Biomasse und Phospholipid-Fettsäuren (PLFA) in gedüngten (Schweinemist, Biokohle, NPK) Reisböden untersucht, die mit alternativen Elektronenakzeptoren (NO_3^-, Fe^{3+}, SO_4^{2-}, Huminsäuren) ergänzt wurden. Die CH_4-Oxidation wurde quantifizieret und beteiligte mikrobiellen Gruppen wurden durch 16S rRNA-Sequenzanalysen identifiziert.

Unsere Ergebnisse zeigten, dass die Injektion von CH_4 über poröse Silikonschläuche direkt in den Reisboden die schlechte Löslichkeit von CH_4 ausgleichen kann und somit die übliche Schüttelmethode durch diese ersetzt werden kann. Mit dieser Methode betrug die höchste Netto-Oxidationsrate von CH_4 während einer 29-tägigen Inkubation 1,6 µg C-CO_2 g^{-1} trockener Boden pro Stunde. Dies war 1,5-2,5-mal schneller als die entsprechende CH_4-Oxidation nach Headspace-Injektion ohne Schütteln. Die CH_4-Oxidationsraten von Injektionen mit Silikonschlauch ohne Schütteln und Headspace-Injektionen mit Schütteln waren ähnlich. Folglich kann der Silikonschlauchansatz die übliche Schüttelmethode ersetzen. Da die Gaskonzentrationsgradienten erhalten bleiben, werden die natürlichen Bodenbedingungen mit dieser Methode deutlich realistischer wiedergeben.

Das Auftreten der AOM in Reisböden konnte anhand der ^{13}C-Anreicherung von CO_2 nach $^{13}CH_4$-Injektion während einer 59-tägigen anaeroben Inkubation eindeutig bestätigt werden. Die kumulative AOM erreichte ohne Schütteln 0,16-0,24 µg C-CO_2 g^{-1} trockenen Boden, mit Schütteln war sie 33-80% niedriger. Unerwarteterweise war bei Verwendung von Silikonschläuchen der Effekt des Schüttelns unbedeutend, was darauf hindeutet, dass der wichtigste limitierende Faktor für die AOM nicht die CH_4-Konzentration in der Wasser-Boden-Suspension sondern die Verfügbarkeit von AEAs war. Ohne Schütteln zeigte die Kontrolle (keine CH_4-Zugabe) einen stetigen Anstieg der CH_4-Konzentration im Headspace/Schlauch durch Methanogenese, während sie mit Schütteln während 59 Tagen konstant niedrig blieb. Dies deutet darauf hin, dass Schütteln die Methanogenese hemmte, möglicherweise

durch die Störung der Co-Lokalisierung zwischen AOM-verwandten Mikroorganismen untereinander, und ihren Substraten (d.h. CH_4 und AEAs).

NO_3^- erwies sich während der 84-tägigen anaeroben Inkubation als der wirksamste Elektronenakzeptor. Die höchste AOM-Rate betrug 0,80 ng C g-1 TB h-1 unter Schweinemistdüngung, gefolgt von der Kontrolle, NPK, und Biokohle. Die Rolle von Fe^{3+} bei AOM blieb unklar. SO_4^{2-} hemmte AOM, stimulierte aber stark die Produktion von unmarkiertem CO_2, was auf eine intensive sulfatinduzierte Zersetzung von organischem Material hinweist. Nach NO_3^- waren Huminsäuren der zweitwirksamste Elektronenakzeptor für die AOM, erhöhten jedoch gleichzeitig die Methanogenese bei allen Düngungsbehandlungen um das 5-6-fache. Wir konnten zum ersten Mal zeigen, dass organische Elektronenakzeptoren zu den wichtigsten AOM-Treibern gehören und in Reisböden von entscheidender Bedeutung sind.

Schließlich wurden mittels nachverfolgung der ^{13}C-Inkorporation von $^{13}CH_4$ in die mikrobielle Biomasse und PLFA die wichtigsten AOM-Pfade untersucht, und Verbindungen zwischen diesen Pfaden und dem Netzwerk der mikrobiellen Gemeinschaft hergestellt. Das Co-occurrence Network zeigte eine Reihe von Haupt- und Neben-AOM-Pfaden mit synergistischen Beziehungen zu komplementären anaeroben mikrobiellen Gruppen. Eine Reihe vergleichender Analysen bestätigte, dass die NO_3^--getriebene AOM der Hauptpfad der AOM war. Sie interagierte mit mehreren Nebenpfaden, insbesondere der NO_2^- Reduktion durch NC10-Bakterien, die Reduktion Fe^{3+} und (mutmaßlich) Huminsäuren durch *Geobacter*-Arten, sowie die SO_4^{2-} Reduktion durch sulfatreduzierende Bakterien in Verbindung mit anaeroben Methanotrophen.

Schätzungsweise hat die NO_3^--induzierte AOM unter Schweinemistdüngung das Potential, jährlich ~3,9 Tg C-CH_4 zu recyceln, was etwa ~10-20% der globalen Netto-CH_4-Emissionen von Reisfeldern ausgleicht. Geeignete organische und mineralische Düngestrategien bieten daher einen wirksamen Hebel zur Reduktion von CH_4-Emissionen aus unter Nassanbau bewirtschafteten Agrarökosystemen.

Abbreviations

C	Carbon
N	Nitrogen
SOM	Soil organic matter
SOC	Soil organic carbon
CO_2	Carbon dioxide
CH_4	Methane
DOC	Dissolved organic carbon
MBC	Microbial biomass carbon
AOM	Anaerobic oxidation of methane
AEA	Alternative electron acceptor
HA	Humic acids
ASV	Amplicon sequence variant
SRB	Sulfate-reducing bacteria
SBM	Syntrophy bacteria with menthaogens
PLFA	Phospholipid fatty acid (biomarker)
NO_3^-	Nitrate
NO_2^-	Nitrite
Fe^{3+}	Ferric iron
SO_4^{2-}	Sulfate
ANOVA	Analysis of variance
ACE	Abundance-based coverage estimator
PD	Faith's phylogenetic diversity
PCoA	Principal coordinate analysis
PCA	Principal component analysis
LEfSe	Linear discriminant analysis effect size
PERMANOVA	Permutational multivariate analysis of variance

List of figures

Extended summary

Study 1:

Study 2:

with sampling from headspace (tube-headspace), (d) headspace injection and sampling without silicone tube (headspace-headspace-no-tube), (e) control without CH_4 injection with headspace sampling (control-headspace) and (f) silicone tube sampling (control-tube).

Fig. 2 Dynamics of $\delta^{13}C$ of CO_2 over 59 days of incubation with and without shaking in the microcosms subjected to 6 treatments (see (a)-(f) in Fig. 1). Error bars: standard error of means (n = 3).

Fig. 3 Anaerobic CH_4 oxidation (AOM) rates over 59 days of incubation with and without shaking in the microcosms subjected to 6 treatments (see (a)-(f) in Fig. 1).

Fig. 4 Cumulative anaerobic CH_4 oxidation (AOM, CH_4-derived CO_2) over 59 days of incubation with and without shaking. Estimations based on isotope mixing model (Eq. 1) for the microcosms subjected to 6 treatments (see (a)-(f) in Fig. 1).

Fig. 5 Relationships between gross CH_4 production and anaerobic CH_4 oxidation (AOM) with and without shaking.

Fig. 6 Conceptual scheme demonstrating the effects of shaking vs. static conditions on anaerobic oxidation of methane (AOM) estimated based on the ^{13}C-labelled CH_4 (blue arrows).

Fig. 7 Box plots of aerobic and anaerobic CH_4 oxidation rates in paddy soils.

Fig. S1 The design of the soil silicone tube and its parameters (a, b), a set-up with a needle (c), an assembled incubation jar (d), the set-up for sampling with simultaneous N_2 replacement from silicone tube (e) and headspace (f). A plastic holder on a needle (c) is a site for an anaerobic indicator to control availability of O_2 in the headspace during incubation. S, outside surface area of silicone tube.

Fig. S2 Conceptual diagram of incubation experimental design and sample codes

Fig. S3 Soil microbial biomass carbon, MBC (a) and CH_4-derived C in MBC (b), dissolved organic carbon, DOC (c), and CH_4-derived C in DOC (d) in microcosms with CH_4 injection into the headspace (Headspace), into the silicone tube (Tube), into the headspace without silicone tube (Headspace-no-tube) and the control without CH_4 injection (Control, for DOC and MBC only) with and without shaking.

Fig. S4 N_2O production over 59 days of incubation with and without shaking in the microcosms.

Study 3:

Fig. 1 Dynamics of CH_4 concentration ($[CH_4]$) in the headspace of microcosms from three field fertilization treatments over 84 days of incubation.

Fig. 2 Dynamics of $\delta^{13}CO_2$ signatures over 84 days of incubation without and with $^{13}CH_4$ injection nested with electron acceptor amendments and the non-amended reference under field fertilization treatments.

Fig. 3 Box plots of the average rates of anaerobic oxidation of methane (AOM) over 84 days of incubation under field fertilization treatments.

Fig. 4 Cumulative anaerobic oxidation of methane (AOM) over 84 days' incubation under field fertilization treatments (Control (a), Pig manure (b), Biochar (c), NPK (d)) and electron acceptor amendments (NO_3^-, Fe^{3+}, SO_4^{2-}, and humic acids (HA)).

Fig. 5 Relationships between the amounts of gross CH_4 production (net + AOM) and anaerobic oxidation of methane (AOM) in reference soils without electron acceptor amendments: Control (a), Pig manure (b), Biochar (c) and NPK (d).

Fig. 6 Conceptual scheme demonstrating the effects of alternative electron acceptors (*i.e.* NO_3^-, Fe^{3+}, SO_4^{2-}, and humic acids (HA)) on anaerobic oxidation of methane (AOM) and anaerobic soil organic matter (SOM) decomposition.

Fig. S1 Dynamics of CO_2 concentration ($[CO_2]$) in headspace of microcosms from three field fertilization treatments (Pig manure, Biochar, NPK) and the low-fertilized Control over 84 days of incubation.

Fig. S2 Relationship between rate of anaerobic oxidation of methane (AOM) and microbial biomass carbon (MBC) in reference soil without electron acceptor amendments.

Fig. S3 Box plots of the average gross rates of CH_4 production (net + AOM) over 84 days of incubation under field fertilization treatments: Control (a), Pig manure (b), Biochar (c) and NPK (d).

Study 4:

Fig. 1 Changes in bacterial communities between pre- and post-incubated paddy soils.

Fig. 2 Phospholipid fatty acids (PLFA) of individual microbial groups affected by fertilization and electron acceptors.

Fig. 3 Relative abundance of the AOM-related microorganisms

Fig. 4 The co-occurrence networks reflecting anaerobic methane oxidation (AOM) metabolism.

Fig. 5 Microbial drivers of anaerobic oxidation of methane (AOM).

Fig. 6 Conceptual model of microbial anaerobic methane oxidation (AOM) pathways in paddy soils.

Fig. S1 Schematic diagram of the experimental design and the selected samples for downstream 16S rRNA gene sequencing.

Fig. S2 Relative abundance of archaea co-amplified with bacteria.

Fig. S3 Number of depleted and enriched ASV (Amplicon Sequence Variants) in post-incubation soil compared to pre-incubation.

Fig. S4 Predicted functions of the bacterial communities based on FAPROTAX database.

Fig. S5 The amounts of CH_4-derived ^{13}C in CO_2 (AOM) (A and B), cumulative CO_2 (C, D) and CH_4 production (E and F) in different fertilization treatments and electron acceptor amendments.

Fig. S6 Relative abundance of NC10, *Geobacter*, Sulfate reducing bacteria, and strophic bacteria with methanogens.

Fig. S7 The bacterial co-occurrence networks based on ASVs (Amplicon Sequence Variants) correlation analysis under different fertilization treatments (A). (B) The relative abundances and amounts of nodes contributed into co-occurrence networks grouped by phyla. (C) The relative abundances and amounts of nodes of co-occurrence networks grouped by phyla. *Geobacter*, NC10, SRB (sulfate reducing bacteria), and SBM (syntrophic bacteria with methanogens) in the co-occurrence networks considered as AOM-related microorganisms in each fertilization treatment.

Fig. S8 The bacterial co-occurrence networks based on ASV (Amplicon Sequence Variants) correlation analysis under different electron acceptor amendments (A). (B) The relative abundances and amounts of nodes contributed into co-occurrence networks grouped by phyla. (C) Relative abundances of *Geobacter*, NC10, SRB (sulfate reducing bacteria), and SBM (syntrophic bacteria with methanogens) shown in the co-occurrence networks in each electron acceptor amendment.

Fig. S9 Bacterial communities in paddy soils under different fertilization treatments.

Fig. S10 Enrichment and depletion of ASV (Amplicon Sequence Variants) under different fertilization in paddy soils.

Fig. S11 Functional community profiles based on BugBase prediction.

Fig. S12 LEfSe results revealed bacterial biomarkers (from phylum to genus level) sensitive to fertilization treatments (Control, Pig manure, Biochar, NPK).

Fig. S13 Bacterial communities in paddy soils with different electron acceptor amendments.

Fig. S14 Principal Coordinates Analysis (PCoA) of electron acceptor amendments under each fertilization treatment by using the unweighted Unifrac distance metric.

Fig. S15 Different electron acceptor amendments have enriched and depleted ASV (Amplicon Sequence Variants).

Fig. S16 Different fertilized paddy soils nested with different electron acceptor amendments are enriched and depleted for certain ASV (Amplicon Sequence Variants).

Fig. S17 LEfSe results revealed bacterial biomarkers (from phylum to genus level) sensitive to electron acceptors amendments under each fertilization treatment.

List of tables

1. Extended summary

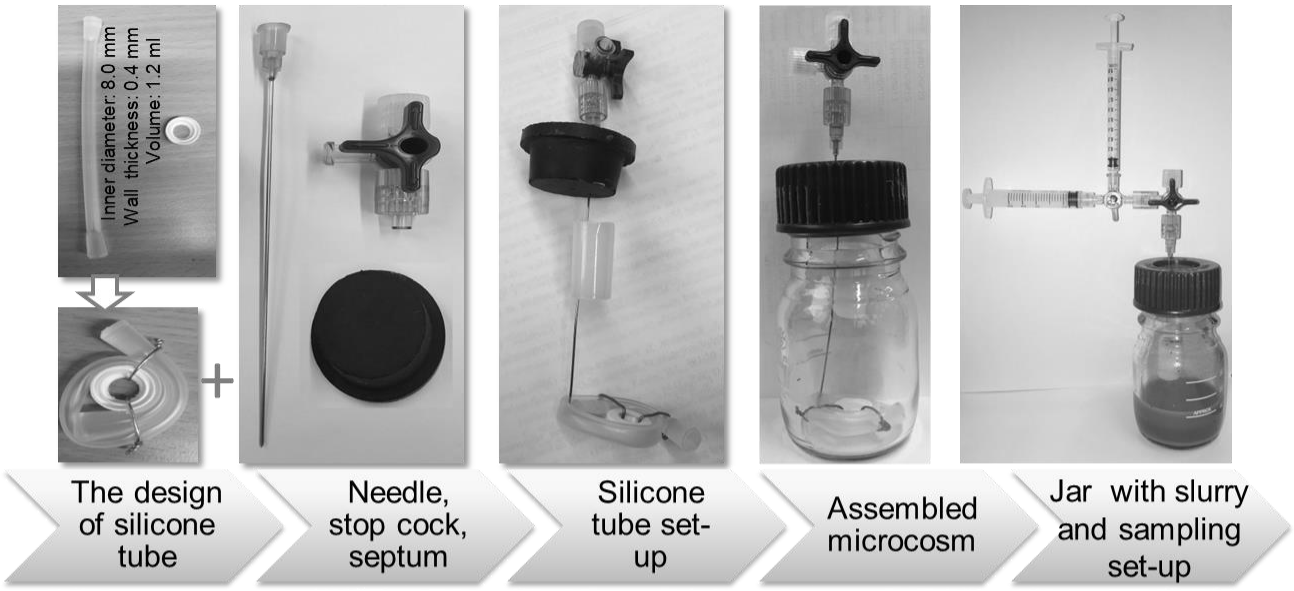

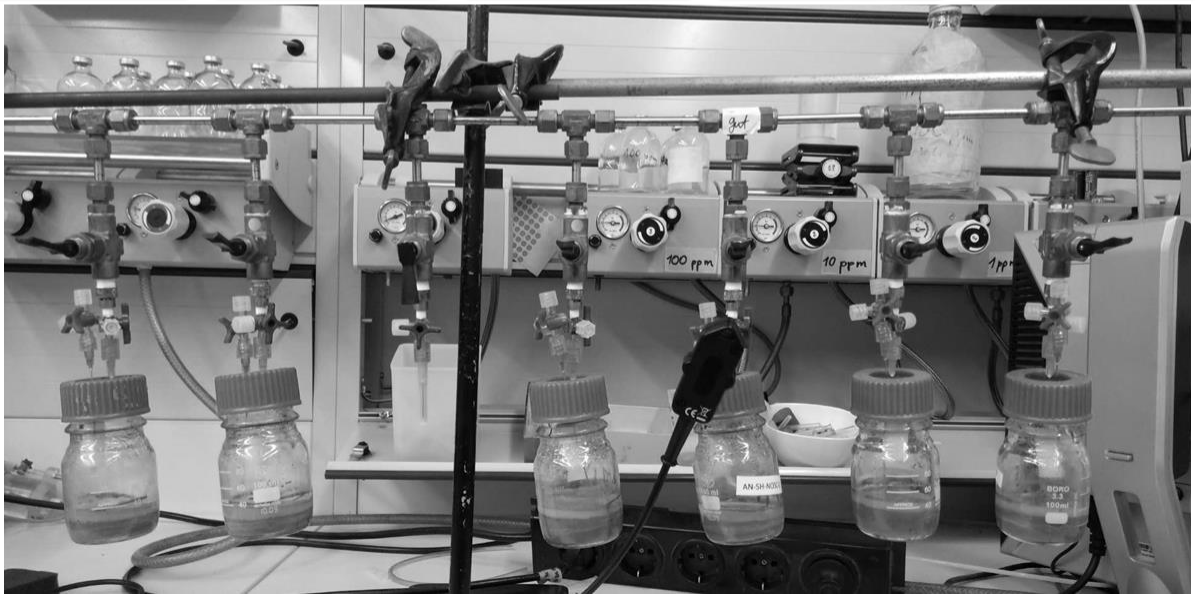

1.1 Introduction

Methane (CH_4) is an important greenhouse gas with a 28-fold greater global warming potential compared to carbon dioxide (CO_2) (Forster et al., 2007). Importantly, the global CH_4 concentrations in the atmosphere have increased ~ 2.5-3.0 times since the industrial revolution (Keppler et al., 2006). Investigations of the biogeochemical cycle of CH_4 in terrestrial ecosystems have focused mainly on methanogenesis and aerobic CH_4 oxidation (Lai, 2009; Tate, 2015), whereas another global process, the anaerobic oxidation of methane (AOM), has been largely underappreciated. AOM in marine ecosystems is a globally important biogeochemical process. In marine sediments, AOM is mainly linked to microbial sulfate reduction and consumes 20-300 Tg CH_4 yr^{-1} – equivalent to as much as 90% of the CH_4 produced by methanogenesis (Smemo and Yavitt, 2011; Valentine, 2002). This makes AOM crucial for the global CH_4 balance and represents a potential constraint on climate change (Hu et al., 2014; Segarra et al., 2015). Due to the global significance in marine ecosystems, the exact mechanisms (potential electron acceptors, optimal biochemical conditions, etc.) and relevance of AOM in terrestrial ecosystems have received increasing attention (Bai et al., 2019; Shen et al., 2019). However, the evidence on AOM in terrestrial ecosystems is sporadic and cannot be directly compared to available information from the marine environment (Reeburgh, 2007). The process has therefore not been considered in most process-based biogeochemical models (Gauthier et al., 2015). This calls for studying the specific mechanisms of terrestrial AOM and for estimating the relevance for CH_4 consumption in oxygen-free environments, especially in ecosystems exposed to prolonged anaerobic conditions such as peatlands and rice paddies.

Wetlands and submerged agricultural areas such as paddy fields are the primary sources of the increasing biogenic CH_4 concentrations in the atmosphere (Nisbet et al., 2016; Saunois et al., 2016). Submerged rice paddies are the hotspot area of methanogenesis (Keppler et al., 2006) which generate 31 million tons of CH_4 per year, and rice paddies account for >9% of total anthropogenic sources to atmospheric CH_4 (Bousquet et al., 2006). Paddy soils have specific physical and chemical properties compared to natural wetlands due to rice field management practices including fertilizer application (Kögel-Knabner et al., 2010). Ample organic (e.g., livestock manure, biochar) and mineral (NPK) fertilizers routinely supply sufficient nutrient elements, which alongside serve as electron donors and acceptors in redox reactions. Therefore, sustainable methanogenic conditions along with high availability of alternative electron acceptors (AEAs) due to mineral and organic fertilization argue further for the ecologically relevant AOM process.

1.1.1 Incubation approach for CH_4 oxidation studies

CH_4 is anaerobically produced by methanogens, and oxidized to CO_2 by methanotrophs under aerobic and anaerobic conditions. Nonetheless, substantial uncertainties about CH_4 oxidation rates remain because of the large temporal and spatial variability of *in situ* CH_4 oxidation (Guo et al., 2017). The uncertainties associated with the current methods of CH_4 oxidation measurements under controlled conditions compound the problem. A common approach to standardize measurements of CH_4 oxidation potential is based on controlled incubation experiments. Almost all laboratory CH_4 oxidation experiments on submerged soils use incubation microcosms with CH_4 injection into the microcosms' headspace and subsequent shaking of soil as slurry (Khalil and Baggs, 2005; Nayak et al., 2007; Whalen et al., 1990). Because the transition of CH_4 from air to water is a limiting factor for the CH_4 oxidation process (Templeton et al., 2006), this this entails a strong risk of underestimating CH_4 oxidation in the incubation microcosms compared to natural submerged soils. To compensate for the low CH_4 solubility, the common microcosm approach requires continuous shaking of the slurry during incubation. Shaking, however, completely removes the *in situ* CH_4 and O_2 gradients. Shaking also induces forced mixing of the gases (CH_4 and O_2) with the slurry, and the high headspace CH_4 concentration maintains a high rate of CH_4 oxidation (Cai and Mosier, 2000). Finally, shaking also affects various other processes in soil (e.g. CO_2 efflux, pH gradients, substrate localization).

Thus, in contrast to pulse headspace injection with shaking, the relatively slow CH_4 delivery belowground and O_2 diffusion from the headspace into soil should better mimic the common *in situ* gas gradients. This would mitigate the above-mentioned shortcomings in measuring the soil CH_4 oxidation potential. CH_4 can be continuously delivered into the soil slurry by using a silicone tube approach. This approach is commonly used for belowground gas sampling under field conditions (Kammann et al., 2001; Pausch and Kuzyakov, 2012). The porous silicone material allows exclusively gas to diffuse through the tube walls from the zone of high to low concentration, thereby promoting continuous release of CH_4. Therefore, in the studies 1 and 2, we developed and tested a silicone tube approach to measure CH_4 oxidation potential under aerobic and anaerobic conditions.

1.1.2 The occurrence of AOM

The studies on AOM occurrence in terrestrial ecosystem are still sporadic. This is because *in situ* AOM measurements are rather challenging to conduct (Roland et al., 2017) due to the dynamics of the physicochemical conditions in deeper soil layers and problems in separating gross and net processes of CH_4 cycling (Smemo and Yavitt, 2011). Current studies on AOM in terrestrial ecosystems are largely based on microcosm incubations with headspace CH_4 injection with or without shaking (Gupta et al., 2013; He et al., 2015; Hu et al., 2015). We hypothesized that the shortcomings of headspace CH_4 injection into microcosm can be overcome with an approach that partly mimics *in situ* conditions: the belowground injection of CH_4 via silicone tubes directly to the slurry simulates the natural release via methanogenesis and diffusion throughout the soil profile.

The use of stable carbon isotope signatures for determining the fraction of CO_2 derived from CH_4 oxidation is a straightforward and relatively simple approach, which gives a more comprehensive and better constrained picture of the qualitative and quantitative carbon cycle. The ^{13}C excess in the headspace CO_2 under strictly controlled anaerobic conditions enabled us to confirm the earlier reported occurrence of AOM in submerged paddy soils (Shen et al., 2014; Zhou et al., 2014; Shi et al., 2017). The AOM rates were reported between 0.11-1.05 ng C g^{-1} dry soil h^{-1} (Shen et al., 2014; Shi et al., 2017). These AOM rates were also comparable to those documented in wetlands (Shen et al., 2015) and tropical mineral soils (Blazewicz et al., 2012). Interestingly, the observed rates are 1 to ~2 orders of magnitude lower than in peatlands (Gupta et al., 2013), freshwater sediments (Roland et al., 2016), and marine systems (Orcutt et al., 2005). Therefore, the mechanisms controlling AOM may strongly differ in various ecosystems. In the studies 2, 3 and 4, we confirmed the occurrence of AOM and estimated its rate based on the incorporation of ^{13}C from ^{13}C-labeled CH_4 into CO_2 relative to the natural abundance control. We also traced CH_4-derived C into phospholipid fatty acids (PLFA) biomarkers to identify AOM-related microbial groups.

1.1.3 Alternative electron acceptors for AOM

AOM depends strongly on the availability of alternative-to-oxygen electron acceptors (AEAs) (Luna-Guido, 2014; Smemo and Yavitt, 2011). Previous studies have reported the occurrence of AOM in freshwater sediments (Beal et al., 2009; Deutzmann et al., 2014; Deutzmann and Schink, 2011; Roland et al., 2017; Segarra et al., 2015; Weber et al., 2016), peatlands (Gupta et al., 2013; Putkinen et al., 2018; Shi et al., 2017; Smemo and Yavitt, 2007), rice paddies (Shen et al., 2014; Shi et al., 2017; Zhou et al., 2014), as well as in boreal and tropical soils (Blazewicz et al., 2012; Mohanty et al., 2017; Pozdnyakov et al., 2011). Despite the increasing recognition of AOM in these environments, no systematic studies are available on the role of potential AEAs, whose identification will be a key to elucidating the driving factors behind terrestrial AOM.

In marine environments, SO_4^{2-} is the most common and dominant alternative electron acceptor (AEA), and microbial sulfate reduction is intimately linked to AOM (Knittel and Boetius, 2009). In contrast, available information on AEAs for AOM in terrestrial ecosystems is elusive. Several potential predominately inorganic AEAs have been suggested, including sulfate (SO_4^{2-}), nitrate (NO_3^-), nitrite (NO_2^-), and ferric iron (Fe^{3+}) but with conflicting results. Gauthier et al., (2015) demonstrated that adding SO_4^{2-} suppressed methanogenesis rather than enhancing AOM in soils. This is because of SO_4^{2-}

concentrations in terrestrial ecosystems are typically too low (~0.01-0.2 mM in freshwater vs. 28 mM in sea water). On the other hand, Gupta et al., (2013) suggested that SO_4^{2-} served as the AEA accelerating AOM rates in a fen peat, where SO_4^{2-} concentrations were higher. Likewise, NO_3^- application in peatland soils revealed both positive (Pozdnyakov et al., 2011) and negative effects (Gupta et al., 2013) on AOM.

In tropical soils, AOM is linked to Fe^{3+} reduction-oxidation (Mohanty et al., 2017), the possible mechanism of providing energy for AOM being similar to microbial sulfate reduction (Smemo and Yavitt, 2011). In addition to inorganic AEAs, there is also evidence that organic AEAs such as humic acids and humic substances actively participate in redox processes driving AOM (Blodau and Deppe, 2012). Humic substances can act as direct AEAs for AOM driven by ANME-2d (Bai et al., 2019), or as indirect AEAs via the re-oxidation of other AEAs (e.g. Fe^{2+}) (Valenzuela et al., 2019) or intermediate sulfur species (Blodau et al., 2007; Kappler et al., 2004; Yu et al., 2015). As yet, however, the specific role of organic substances as AEAs for AOM remains largely unclear. In the study 3, we tested the potential of alternative electron acceptors (NO_3^-, Fe^{3+}, SO_4^{2-}, humic acids) on AOM in fertilized paddy soils.

1.1.4 Microbial active AOM pathways

AOM was firstly identified in 1970s as a microbial process coupled to SO_4^{2-} reduction in marine sediments (Barnes and Goldberg, 1976) whichwas performed by methanotrophic archaea of the ANME-1, ANME-2 subgroups -2a, -2b, and 2c, and ANME-3 clades and consortia with sulfate-reducing bacteria (Knittel and Boetius, 2009). Later, AOM was found to be linked to other terminal electron acceptors, such as metal oxides (Fe^{3+} and Mn^{4+}) (Beal et al., 2009), NO_2^- (Ettwig et al., 2010), NO_3^- (Haroon et al., 2013), and humic acids (Bai et al., 2019; Scheller et al., 2016). Regarding microorganisms, archaea *Candidatus "*Methanoperedens ferrireducens*"* (*M. ferrireducens*) can perform Fe^{3+}-dependent AOM via "reverse methanogenesis" and putative extracellular electron transfer pathways (Cai et al., 2018). It was also demonstrated that *M. nitroreducens*-like archaea can anaerobically oxidize methane using Fe^{3+} (Ettwig et al., 2016). NO_2^--dependent AOM is driven by *Candidatus* "Methylomirabilis oxyfera" (*M. oxyfera*) of the NC10 phylum bacteria via the "intra-aerobic denitrification" pathway — producing oxygen from NO_2^- and using it to consume CH_4 (Ettwig et al., 2010). NO_3^--dependent AOM is performed by *Candidatus* "Methanoperedens nitroreducens" (*M. nitroreducens*) archaea of the ANME-2d clade via "reverse methanogenesis" pathway with NO_3^- reduced to NO_2^-. *M. nitroreducens* is either in a co-culture with *M. oxyfera* or in a syntrophic relationship with an anaerobic ammonium-oxidizing (Anammox) bacterium (Haroon et al., 2013).

Recently it was identified that humic substances serve as electron acceptors for AOM driven by ANME-2d (Bai et al., 2019). Humic acids-dependent AOM is linked with *Geobacter* species (i.e., a representative iron reducing bacteria), it plays a role in transporting electrons directly or via electron shuttles to the available electron acceptors. Humic substances may act as direct electron acceptors for humic acids-reducing bacteria (Heitmann et al., 2007; Roden et al., 2010), or as indirect organic electron acceptors via the re-oxidation of mineral electron acceptors (Kappler et al., 2004; Valenzuela et al., 2019). However, the specific role of organic substances as electron acceptors and soil microorganisms involved in AOM remains largely unclear.

Contribution of NO_3^-/NO_2^--dependent pathway to total AOM is expected to strongly increase globally following the extensive anthropogenic nitrogen inputs in marine ecosystems (e.g., river runoff and N deposition) and terrestrial habitats (e.g., agricultural N fertilization and municipal waste). Also, NO_3^- and NO_2^- are prevailing electron acceptors and NO_3^-/NO_2^--dependent AOM has been observed in paddy soils (Hu et al., 2014; Vaksmaa et al., 2016). The role of other AEAs, especially organic electron acceptors, related to AOM in rice paddies needs verification. It is of critical importance to understand how these mineral and organic electron acceptors shape microbial interactions and ecological functions in anaerobic environments. In study 4, we identify a set of major and minor AOM pathways with synergistic relations to complementary anaerobic microbial groups.

1.2 Aims and main hypotheses

This thesis was aimed to evaluate the new methodology of silicone tube approach for CH_4 oxidation studies (study 1 and 2), the role of AEAs and fertilization practices in AOM (study 3), and microbial mechanism of AOM pathways (study 4).

We put forward and tested the following hypotheses:

i. Poor CH_4 diffusion in soil slurry would be compensated by directly delivering CH_4 into the soil through a silicone tube, yielding a faster CH_4 oxidation rate (aerobic: study 1; anaerobic: study 2) without shaking and, consequently, shaking of microcosms can be efficiently substituted with the soil CH_4 silicone tube injection approach because the latter better reflects the common *in situ* gas gradients.

ii. NO_3^- is the most preferential AEA for AOM in paddy soils because it is present in high amounts and has a higher energy release by reduction compared to other AEAs. In comparison, humic acids, Fe^{3+} and SO_4^{2-} could be relevant but less effective than NO_3^-. Further, pig manure and NPK fertilization are hypothesized to induce the highest AOM rate due to larger availability of organic and inorganic AEAs as compared with the low-fertilized control and biochar addition (study 3).

iii. Several active AOM pathways co-exist in paddy soils depending on the AEAs avialibilty. We hypothesize that NO_3^--driven AOM is the major AOM pathway and it co-exists with minor pathways involving reduction of NO_2^-, humic acids, Fe^{3+}, and SO_4^{2-} (study 4).

1.3 Materials and methods

1.3.1 Site description

The soil sampling site was located near Jinjing town, Changsha county of Hunan province in China (28°33′04″N, 113°19′52″E). The area is characterized by a subtropical humid monsoon climate. The mean annual air temperature of the region is 17.5 °C and the mean annual precipitation is 1330 mm. The typical paddy field has a tillage history of more than 1000 years of rice production (double cropping, with early rice growth season in late April to mid-July and late rice growth season in mid-July to late October).

Soil samples were collected from an ongoing long-term field experiment under different fertilization treatments conducted by the Institute of Subtropical Agriculture, Chinese Academy of Sciences. Four fertilization treatments were chosen: (i) Control with conventional fertilization (60 kg N ha^{-1} yr^{-1} as urea, 18 kg P ha^{-1} as $Ca(H_2PO_4)_2$, and 83 kg K ha^{-1} were applied before the seedling transplanting in each of the rice seasons), (ii) Pig manure (60 Mg ha^{-1} yr^{-1}, half of which was applied before transplanting in the early and another half in the late rice season; containing 250 g C kg^{-1}, 16.8 g N kg^{-1}, 5.3 g P kg^{-1}, 2.5 g K kg^{-1}; pH 8.0) with conventional fertilization, (iii) Biochar (24,000 kg ha^{-1} applied in spring 2016; biochar was pyrolyzed from wheat straw at 500 °C by Sanli New Energy Ltd. (Shangqiu, Henan Province, China); containing 418 g C kg^{-1}, 2.8 g N kg^{-1}; pH 9.8) with conventional fertilization, and (iv) NPK (240 kg N ha^{-1} yr^{-1} as urea, 120 kg N ha^{-1} in the early rice season and the rest in the late rice season; 18 kg P ha^{-1} as $Ca(H_2PO_4)_2$ and 83 kg K ha^{-1} were applied before the seedling transplanting in each of the rice seasons as basal fertilizer). Each plot was flooded for one week before the early rice transplanting, and through the whole growing season till rice harvesting when water was drained from the rice field. Each of these fertilization treatments was applied independently on three field plot replicates (35 m^2 per plot), and the rice cultivars and managements were similar (Fig. ES1).

Fig. ES1 An overview photo of the field plots

1.3.2 Soil sampling

Soil samples were collected from abovementioned fields after the late season rice harvesting in December 2016, when the plots were field-moist but not over-flooded. From each of the plots, we collected four soil cores from 10-30 cm depth (bottom layer of a plow horizon 0-30 cm) with a soil auger (d = 5 cm). The core samples were mixed and homogenized to form one composite sample per plot. There were no large stones in the paddy soil and un-decomposed plant remnants were carefully removed before incubation. All soil samples (ca. 30% soil weight-based water content) were immediately sealed in plastic bags. The air in the bags was evicted to minimize exposure to atmospheric oxygen (O_2). Soil samples for laboratory incubation were not sieved because the paddy field has been thoroughly and regularly plowed for more than 1000 years, and also to avoid un-natural overexposure to air and minimize unfavorable effects on the anaerobic processes studied. Soil samples were transported from China to the University of Göttingen, Germany, at room temperature during one day; thereafter they were stored in a cooling room (4 ℃) until the incubation experiment.

1.3.3 Experimental setup

1.3.3.1 Studies (1) and (2)

To test a new approach for a lab incubation with soil CH_4 injection by silicone tubes, we developed and constructed a special microcosm (see the cover photo of this chapter). A silicone tube (Carl Roth GmbH + Co. KG, Germany, inner diameter: 4 mm, wall thickness: 1 mm, surface area: 18.8 cm^2, volume: 1.2 ml) was fixed around a plastic cap and tied in place with stainless steel wires. Both ends of the tube were sealed with silicone rubber septa, and one end was connected with a needle as a sampling port, sealed with a 3-way stopcock. Labeled CH_4 (4.8 ml 5 atom% $^{13}CH_4$) was added to the headspace or to the soil silicone tube to quantify the net oxidation of $^{13}CH_4$ to $^{13}CO_2$ over time. Importantly, for the silicone tube, only CH_4 (no O_2) was injected. All the treatments are shown in Fig. ES2. For the incubation, field-moist soil (20 g, 30% soil weight-based water content) was placed into 120 ml glass jars with wide necks, and 15 ml of deionized water was added to make soil slurry. Visible plant debris and small stones were hand-removed prior to loading. Jars were sealed with gas-impermeable butyl rubber septa and fixed with plastic screw caps. All jars and septa were autoclaved twice at 121 ^{o}C for 20 min before loading soil into jars. The slurry was pre-incubated in the dark at 18 ℃ for 10 days to establish equilibrium after disturbance caused by soil slurry preparation. At the end of the pre-incubation, the headspace was flushed with synthetic air (20/80% O_2/N_2) in study 1 or with N_2 in study 2 for 10 min through needles inserted in the septa. The soil silicone tubes were also

flushed with synthetic air/N_2 using two 25 ml syringes as input and exhaust ports switched by a three-way stopcock. Headspace and soil tube pressures were equilibrated to 101.3 *kPa*. Thereafter, gas was sampled for background values, after which 4.8 ml of 5 atom% $^{13}CH_4$ was immediately injected into the jars designated to receive CH_4. To monitor oxygen availability after CH_4 injection, anaerobic indicators (Thermo scientific, Oxoid Ltd. Wade Road, Basingstoke, Hants, RG24 8PW, UK) were placed inside the jars and the color was regularly recorded.

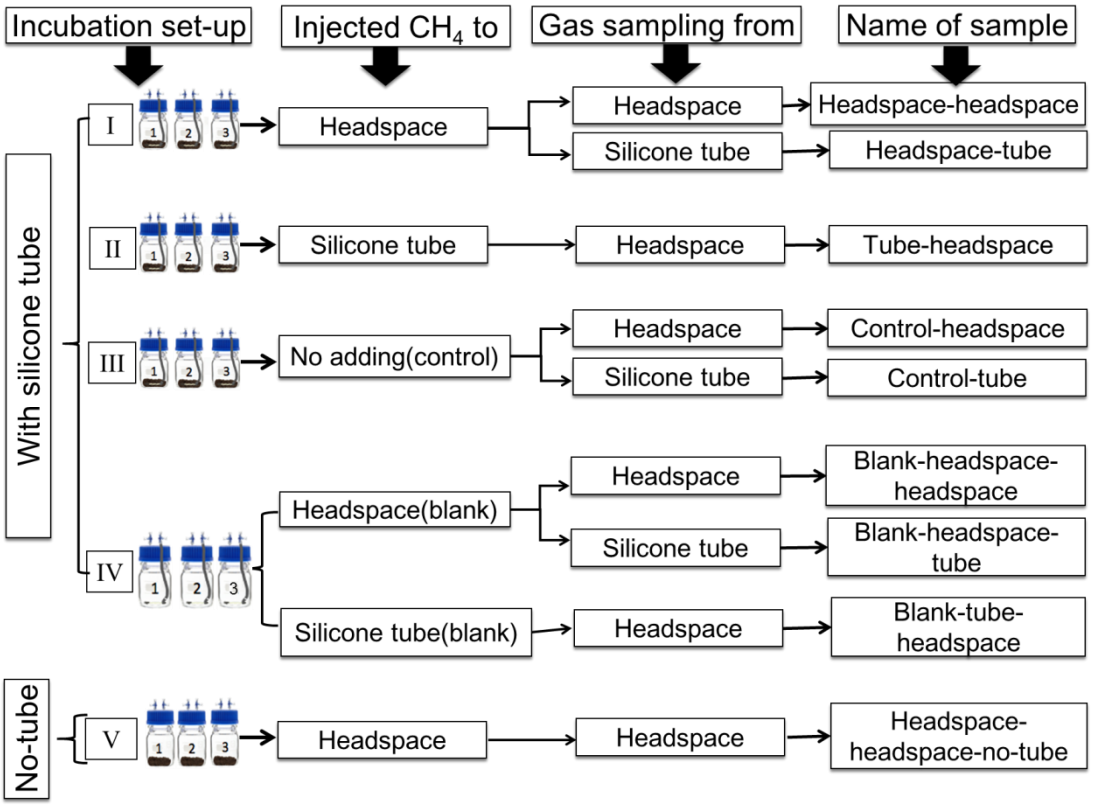

Fig. ES2 Conceptual diagram of incubation experimental design and sample codes

1.3.3.2 Studies (3) and (4)

The anaerobic incubation experiment was designed to test paddy soils under different fertilization treatments for AOM induced by addition of several AEAs, *i.e.* Fe^{3+}, NO_3^-, SO_4^{2-}, and humic acids (Sigma-Aldrich Chemie GmbH, Kappelweg 1, D-91625 Schnelldorf, Germany) (Fig. ES3).

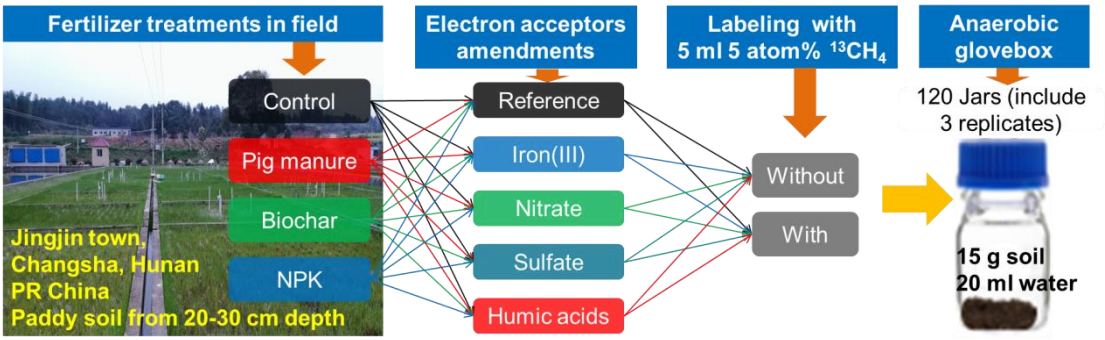

Fig. ES3 Conceptual diagram of experimental design

To prepare the microcosms, 15 g field-moist soil was loaded into the jars. The headspace of jar was back-flushed with high-purity N_2, then the N_2-flushed microcosms were left overnight to allow for consumption of any remaining O_2. Therafter, to exclude further contamination with atmospheric O_2, all manipulations with soils were conducted in a glovebox (N_2/H_2, 97/3%) under fully controlled anaerobic conditions. Inside the glovebox, the jars were opened and 20 ml deionized sterile water or

chemical solutions (see below) were added to make the soil slurries. To quantify the anaerobic oxidation of $^{13}CH_4$ to $^{13}CO_2$ over time, labeled CH_4 (5 ml 5 atom% $^{13}CH_4$) was injected into the headspace of the microcosms, resulting in an initial average headspace CH_4 concentration of 3.1%. The anaerobic indicators were also used.

The added AEA amounts corresponded to the upper limits of the respective concentration ranges measured in the soil. NO_3^- (22.3 μg g^{-1}) was added as $NaNO_3$, SO_4^{2-} (12.7 mg g^{-1}) was added as Na_2SO_4, and HA (1.25 mg g^{-1}) were added as solution dissolved in deionized sterile water with help of sonication (RK 100H, Bandelin Sonorex, Heinrichstr. 3-4, 12207 Berlin, Germany). Fe^{3+} was added as Fe_2O_3 (23.3 mg Fe g^{-1}) powder. Finally, 84 soil samples were chosen for further sequencing and PLFA analysis. These were: 12 original and not incubated soil samples (Control, Pig manure, Biochar and NPK × 3 field replicates each), and 12 reference soil samples incubated without electron amendments and without $^{13}CH_4$ addition, and 60 samples after incubation with four electron acceptors amendments (NO_3^-, SO_4^{2-}, Fe^{3+}, humic acids) and reference, all with $^{13}CH_4$ addition.

1.3.4 Gas sampling and measurements

For study (1) gas samples were collected at 1, 3, 7, 12, 17, and 29 days after $^{13}CH_4$ injection. For study (2) gas samples were collected at 1, 3, 7, 12, 17, 29, and 59 days after $^{13}CH_4$ injection. For study (3) gas samples were collected at 2, 7, 14, 21, 28, 42, 56 and 84 days after $^{13}CH_4$ injection. One-ml gas-tight syringes fitted with stopcocks were used to collect gas from the headspace (through septa with needles) and from soil tubes (through outlet ports). After each sampling, the equivalent volume of N_2 was injected to compensate any pressure loss and to maintain a slight overpressure. All gas samples were transferred to evacuated, N_2-flushed glass vials and diluted with N_2 (1 ml sample into 12 ml N_2). The CO_2 and CH_4 concentrations were then measured on a gas chromatograph (GC-14B, Shimadzu, Ld. Nds., Japan) equipped with a flame ionization detector (for CH_4) and an electron capture detector (for CO_2). A separate set of vials was used to determine the ^{13}C isotope composition, with a dilution of 1 ml sample into 15 ml N_2.

1.3.5 Soil samples analysis

SOC and total N were determined with a Vario Max CN Analyzer (Elementar Analysensysteme GmbH, Langenselbold, Germany). Other elements (*i.e.* S, Fe) in the soils were determined using inductively coupled plasma optical emission spectroscopy (ICP-OES; iCAP 6000 series, ASX-520 Auto-Sampler, Thermo Scientific, Germany). Soil microbial biomass carbon (MBC), NH_4^+, and NO_3^- contents were measured from incubated soil. MBC was determined by a chloroform fumigation K_2SO_4 extraction method, and calculated based on the difference between extracted organic C content of fumigated and non-fumigated soils by using a k_{EC} factor = 0.45 (after Joergensen, 1996). Extractable dissolved organic carbon (eDOC) was determined from the extracts of the non-fumigated samples. The extracts obtained were analyzed for total C content using a TOC/TIC analyzer (Multi N/ C 2100, Analytik Jena, Germany). NH_4^+ and NO_3^- were extracted with 0.05 M K_2SO_4 and measured using continuous flow injection colorimetry (SEAL Analytical AA3, SEAL Analytical GmbH, Norderstedt, Germany).

Microbial biomass was characterized by PLFA analysis with the modified Bly and Dyer extraction method (Gunina et al., 2014). Total PLFA was calculated by summing up the abundance of all biomarkers, and bacterial PLFA was calculated as a sum of the abundances of Gram-positive, Gram-negative and Actinobacteria, and expressed as ng PLFA g^{-1} dry soil. Total DNA was extracted from about 0.3 g of soil from each sample using the DNeasy PowerSoil DNA isolation kit (100) (QIAGEN GmbH, 40724 Hilden, Germany) according to the vendor instruction. The polymerase chain reaction (PCR) amplification mixture was prepared with Phusion High-Fidelity DNA Polymerase kit (Thermo scientific, Germany). Sequencing was performed on an Illumina MiSeq platform (at the Institute for Microbiology and Genetics, University of Göttingen, Göttingen, Germany). For the calculation of the pairwise distance and generation of the distance matrix, a 100% identity threshold was used to cluster sequences into Amplicon Sequence Variant (ASV) (Callahan et al., 2017).

1.3.6 Isotope analysis and calculations

Stable C isotope analysis was conducted using an isotope ratio mass spectrometer (Delta plus IRMS, Thermo Fisher Scientific, Bremen, Germany). Data are reported as $\delta^{13}C$-values. The quantity of $^{13}CH_4$ oxidized was expressed by the amount of $^{13}CO_2$, ^{13}C-PFLA, and CH_4-derived C into MBC and DOC using the following equation:

$$C_{OX} = \frac{(\delta^{13}C_{Total} - \delta^{13}C_{Control})}{(\delta^{13}C_{OX} - \delta^{13}C_{Control})} \times C_{Total} \quad (1)$$

where C_{OX} (ng) represents the amount of $^{13}CH_4$ transformed into $^{13}CO_2$, ^{13}C-PFLA, and CH_4-derived C into MBC and DOC. C_{Total} represents the total amount of C in the corresponding pool (i.e. CO_2, PLFA, MBC and DOC), $\delta^{13}C_{Total}$ is the delta value of $^{13}CO_2$, ^{13}C-PFLA, and CH_4-derived C into MBC and DOC in the samples treated with $^{13}CH_4$, $\delta^{13}C_{Control}$ is the delta value of CO_2 or PLFA or MBC or DOC in the control without $^{13}CH_4$ addition, and $\delta^{13}C_{OX}$ is the delta value of $^{13}CH_4$ with 5 atom% enrichment. Due to the standard deviation of 0.7‰ for PLFA, the difference between $\delta^{13}C_{Total}$ and $\delta^{13}C_{Control}$ above 1.4‰ was considered as valid ^{13}C tracer incorporation into PLFA. When the difference was below 1.4‰, it was considered as no ^{13}C incorporation and C_{OX} was taken as zero.

1.3.7 Statistical analysis

Analyses of variance (ANOVA) including ANOVA with repeated measures, two-way ANOVA, One-way ANOVA and *t*-tests were used to verify the significance of the obsereved differences. The Shapiro–Wilk test was used to test the normality, when equal variances were assumed using the least significant difference (LSD) otherwise using Games-Howell post hoc test. Multiple topological properties were calculated and visualized using igraph package. All statistical analyses were performed using SPSS software (ver. 19.0, SPSS Inc., Chicago, IL, USA), SigmaPlot software (ver. 12.5, Systat Software, Inc, San Jose, California, USA), and R (v3.5.3).

1.4 Main results and discussion

1.4.1 Silicone tube approach for incubation studies on CH_4 oxidation

The highest net CH_4 oxidation rate was 1.6 μg C g^{-1} dry soil h^{-1}, which was measured between the 3rd and 7th day after injecting $^{13}CH_4$ into the slurry via a silicone tube without shaking. This rate was 1.5-2.5 times faster than the respective CH_4 oxidation after headspace injection without shaking (Fig. ES4). Indeed, the continuous delivery of CH_4 into the slurry increased its availability for methanotrophs (Khalil and Baggs, 2005; Nayak et al., 2007) in contrast to CH_4 diffusion from the headspace. This supported our first hypothesis claiming that direct CH_4 delivery into the slurry via a silicone tube should compensate for poor CH_4 diffusion without shaking.

Our measured CH_4 oxidation rates agree with the respective rates for microcosms with shaking reported elsewhere. Conrad & Rothfuss, (1991) and Krüger & Frenzel, (2003) observed maximum rates between 1.9 and 4.7 μg C g^{-1} dry soil h^{-1} (our rates were 1.7-2.7 μg C g^{-1} dry soil h^{-1}) under continuous shaking (75-120 rpm) in slurry from paddy soils. The rates without shaking also coincided moderately well to several reported values, e.g. 0.3-0.6 μg C g^{-1} dry soil h^{-1} (Blazewicz et al., 2012) vs. 0.1-0.7 μg C g^{-1} dry soil h^{-1} in the current study (Fig. ES4). We therefore conclude that the tube-based CH_4 injection facilitates gas diffusion between gas-solution-soil phases, which has a similar effect as shaking on CH_4 oxidation, as hypothesized. Moreover, the CH_4 oxidation rate via silicone tube injection (1.6 μg C g^{-1} dry soil h^{-1}) was 2-4 times faster than headspace CH_4 injection without shaking and ca. 1.1 times slower (1.7 μg C g^{-1} dry soil h^{-1}) than conventional headspace CH_4 injection with shaking. Therefore, we conclude that direct soil CH_4 injection via silicone tubes is advantageous in incubation experiments because gas concentration gradients are maintained and thereby more realistically reflect natural soil conditions.

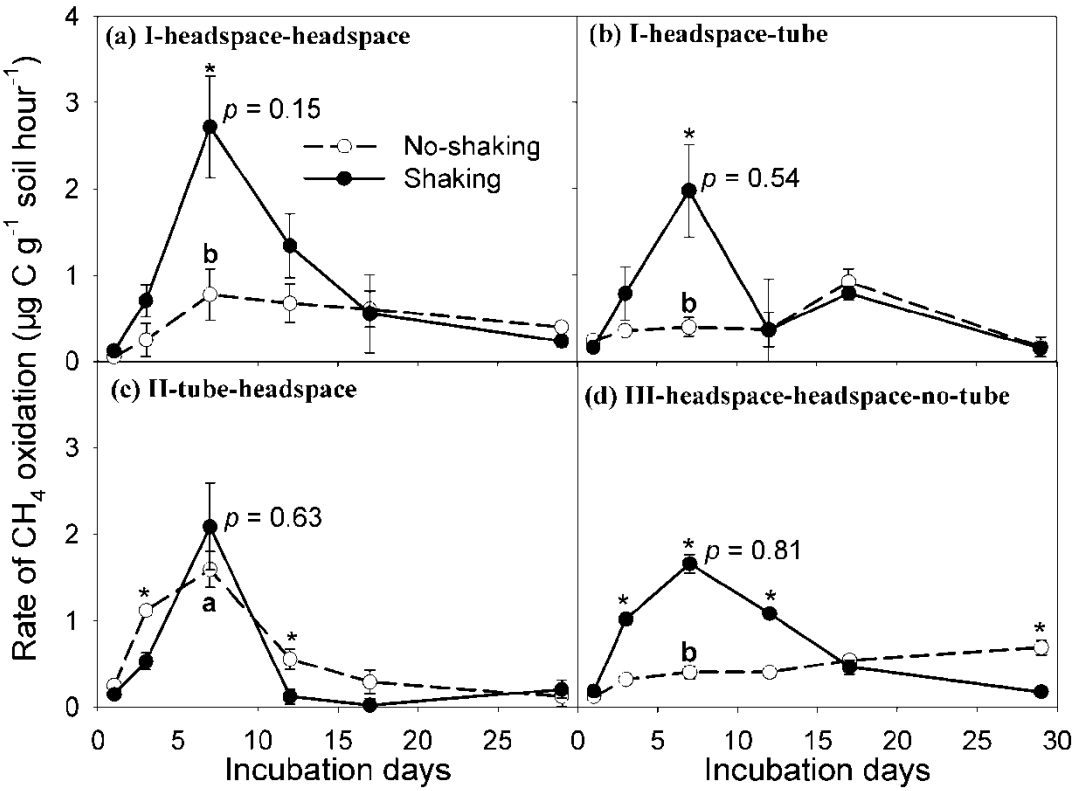

Fig. ES4 CH_4 oxidation rates over 29 days of incubation with and without shaking. Lowercase letters: significant differences ($p < 0.05$) of the maximum CH_4 oxidation rates (day 7) between microcosms under no-shaking. Asterisks: significant difference ($p < 0.05$) between shaking and no-shaking at each instance of measurement. *p* values refer to t-test of the maximum CH_4 oxidation rates (day 7) between the soil injection without shaking (II-tube-headspace, white circles) and both injection approaches with shaking. Error bars: standard error of means ($n = 3$).

1.4.2 ^{13}C-based evidence on AOM with/without shaking in paddy soil

^{13}C enrichment in CO_2 occurred under anaerobic conditions in soil after $^{13}CH_4$ addition irrespective of shaking and injection/sampling approaches (Fig. ES5), that demonstrated AOM takes place in submerged paddy soil. During the 59-day incubation, however, the effect of the silicone tube on AOM was not significant either with ($p = 0.21$) or without shaking ($p = 0.20$).

This rejected our hypothesis claiming that direct CH_4 delivery into the slurry via a silicone tube should have a faster CH_4 rate under anaerobic condition. This is because the amount of CH_4 dissolved in water (slurry) was 2 orders of magnitude higher than the cumulative AOM (500 µg vs. 1.0-3.9 µg CH_4 per jar). We conclude that the CH_4 concentration in water (slurry) was not the main limiting factor for the AOM.

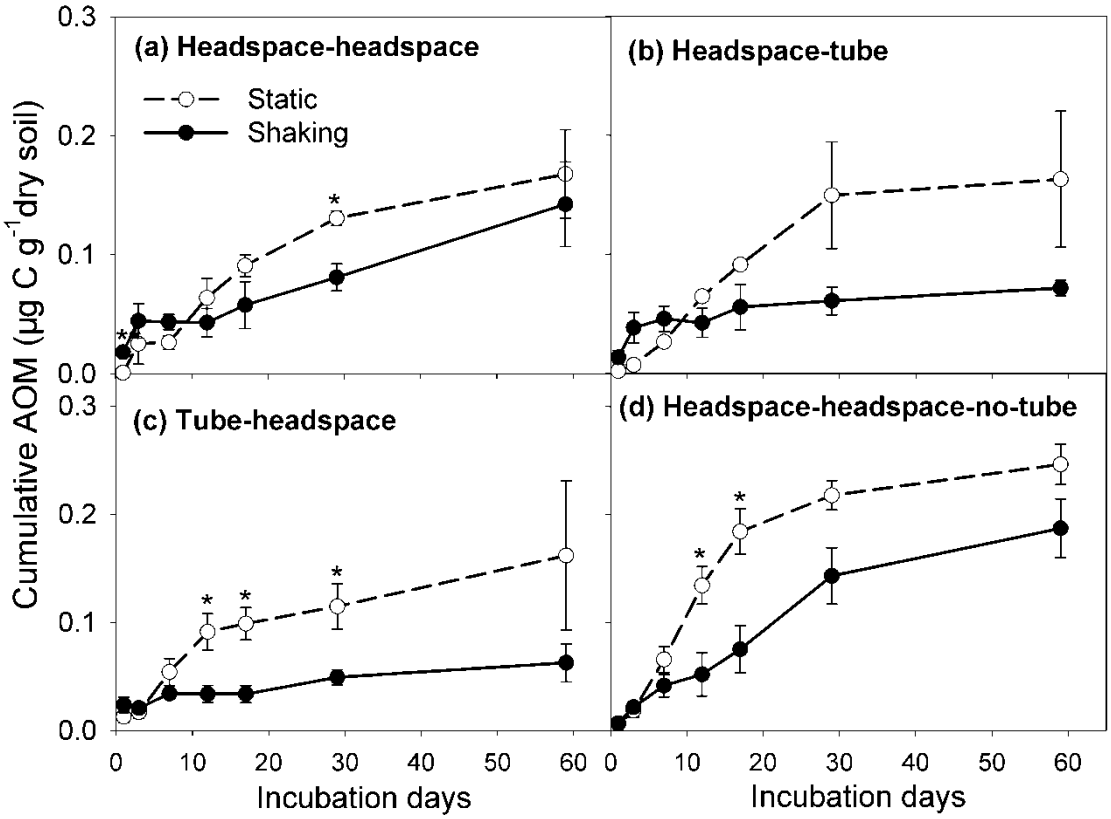

Fig. ES5 Cumulative anaerobic CH_4 oxidation (AOM, CH_4-derived CO_2) over 59 days of incubation with and without shaking. Asterisks: significant difference ($p < 0.05$) between shaking and static treatments at each day of measurements. Error bars: standard error of means ($n = 3$).

The cumulative AOM was lower ($p = 0.01$) under shaking vs. static conditions (Fig. ES5), demonstrating the overall negative effect of shaking on AOM. The following mechanisms may be responsible for the negative effects of shaking:

1. AOM is controlled by CH_4 production, and one of the pathways is carried out by methanogens via "reverse methanogenesis" (Blazewicz et al., 2012; Gauthier et al., 2015; Smemo and Yavitt, 2007 & 2011). In the experiment, CH_4 oxidation was dependent on gross CH_4 production with shaking, and also without shaking when the CH_4 production was low (Fig. ES6, dashed fitting line, and b, solid line), indicating that AOM is related to methanogenic activity. One possible reason for the negative effect of shaking could be a mechanical disturbance of microbial communities (e.g. syntrophic bacteria, (Liu and Conrad, 2017)), thus preventing them from organizing in a way that stimulates CH_4 production and/or oxidation. So, although AOM was detected in submerged paddy soil in microcosms with shaking, the shaking strongly inhibited methanogenic activity. In contrast to the linear relationship of AOM at lower rates of methanogenesis, as CH_4 production increased, AOM slowed down (Fig. ES6, power growth regression). This suggests that "reverse methanogenesis" was not the only (dominating) process, and that unidentified electron acceptors drive AOM in submerged paddy soil.

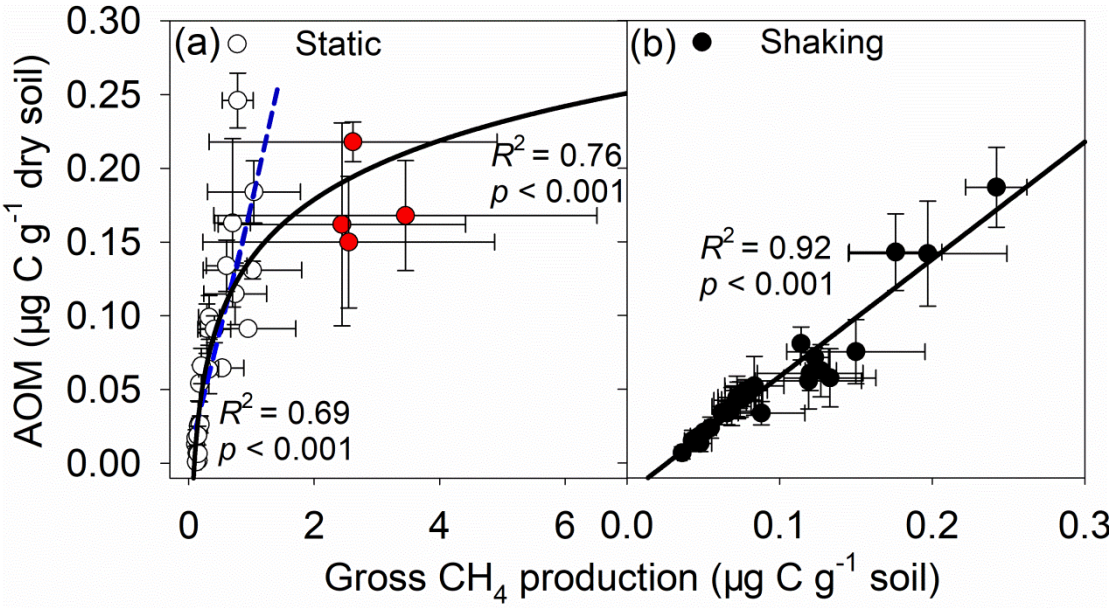

Fig. ES6 Relationships between gross CH_4 production and anaerobic CH_4 oxidation (AOM) with and without shaking. Solid lines are regressions of all data measured (a) under static conditions ($y = 246x^{(2.34\times10^{-4})} - 246$) and (b) with shaking ($y = 0.79x - 0.021$). Dashed blue line is a regression of data ($y = 0.17x + 0.004$) excluding the highest CH_4 production rates (the red circles). Gross CH_4 production was calculated as the sum of net CH_4 oxidation (from different injection/sampling approaches) plus net CH_4 production (from control without added CH_4). Vertical error bars: standard error of AOM means (n = 3); horizontal error bars: standard error of gross CH_4 production means (n = 3).

2. Electron acceptors ultimately control redox processes under anaerobic conditions, including AOM. Shaking can maximize mass transfer and equilibration; it thereby increases the probability of interactions between methanotrophs and electron acceptors, so the maximal AOM rate occurred in the early incubation phase. In static systems, the interactions would be much less probable, especially initially when the relevant microbial populations are likely to be less active. Accordingly, it took two weeks to reach the peak AOM rate that optimally co-localized the electron acceptors and the methane oxidizers. As the AOM proceeds, the concentration of electron acceptors decreases, triggering a reduction in the AOM rate. Shaking, which destroys gradients and moments of co-localization, leads to lower AOM rates (Fig. ES12 B). This suggests that AOM was limited by the amount of available electron acceptors. Therefore, for the first time we obtained the important information that static condition but not shaking is favorable for AOM process (Fig. ES12 B).

1.4.3 Role of electron acceptors and fertilization in AOM

NO_3^- was the most effective AEA in the paddy soil and probably fueled the nitrate/nitrite-dependent AOM, particularly under pig manure fertilization (Fig. ES7). This finding verified our second hypothesis on NO_3^- as the most preferential AEA for the AOM process. Indeed, NO_3^- is most favorable thermodynamically to fuel ATP generation because the Gibb's Free Energy of nitrate-dependent AOM process is one order of magnitude higher than that of other AEAs (*e.g.* SO_4^{2-}) (reviewed in Smemo and Yavitt, 2011).

SO_4^{2-} amendment yielded close-to-zero AOM (and even inhibited AOM), independent of fertilization (Fig. ES7). This fully rejects our hypothesis of SO_4^{2-} being a relevant AEA for AOM in paddy soils. On average, unlabeled CO_2 increased by 140% and methanogenesis was suppressed by 50% after SO_4^{2-} amendment under all fertilization treatments. This stimulation of CO_2 release suggests that

sulfate-induced anaerobic organic matter degradation was thermodynamically more favorable than AOM in the examined paddy soils (Fig. ES8).

Amendment with Fe^{3+} did not significantly support AOM and even partially suppressed the AOM rates in the control and manure fertilization (Fig. ES7). This contradicts the hypothesized relevance of Fe^{3+} for AOM in paddy soil. Fe^{3+}-dependent AOM has been reported in tropical soils, freshwater and brackish wetland sediments, and marine sediments (Mohanty et al., 2017; Ettwig et al., 2016; Segarra et al., 2013; Beal et al., 2009). Recently, Cai et al., (2018) reported Fe^{3+}-dependent AOM can be performed by *M. ferrireducens*.

We demonstrated a distinct temporal delay of AOM under humic acids amendment as compared with *e.g.* NO_3^- (Fig. ES7). Two mechanisms may explain this: (i) unlike NO_3^- which is readily available for AOM, humic acids must undergo decomposition and be partly re-utilized for methanogenesis (as acetate) before the intermediate decomposition products could serve as AEAs for AOM. (ii) AOM may be driven by different microbial groups – with lower and higher affinity to CH_4. Raghoebarsing et al., (2006) reported that the affinity of SO_4^{2-}-dependent AOM for methane is four orders of magnitude lower than NO_2^--dependent AOM. The role of humic acids in AOM appears to be particularly important in DOC-depleted paddy soils or when CH_4 concentration is high enough for low-affinity methanotrophs (Fig. ES8).

Among the fertilization types, manure fertilization demonstrated the highest AOM potential (Fig. ES7) as compared to other organic/inorganic fertilizers and the control. This only partly confirms our second hypothesis because NPK (which was expected to demonstrate a high AOM rate due to larger availability of inorganic AEAs) resulted in lower AOM compared to the control. The NO_3^- content was almost 2 times higher under pig manure than NPK and about 4 times higher than the control. Thus, long-term fertilization with pig manure increased the amount of NO_3^- in paddy soil, thereby providing a suitable environment for AOM-performing microorganisms such as *M. oxyfera*, *M. oxyfera*-like bacteria and/or anaerobic methanotrophic archaea.

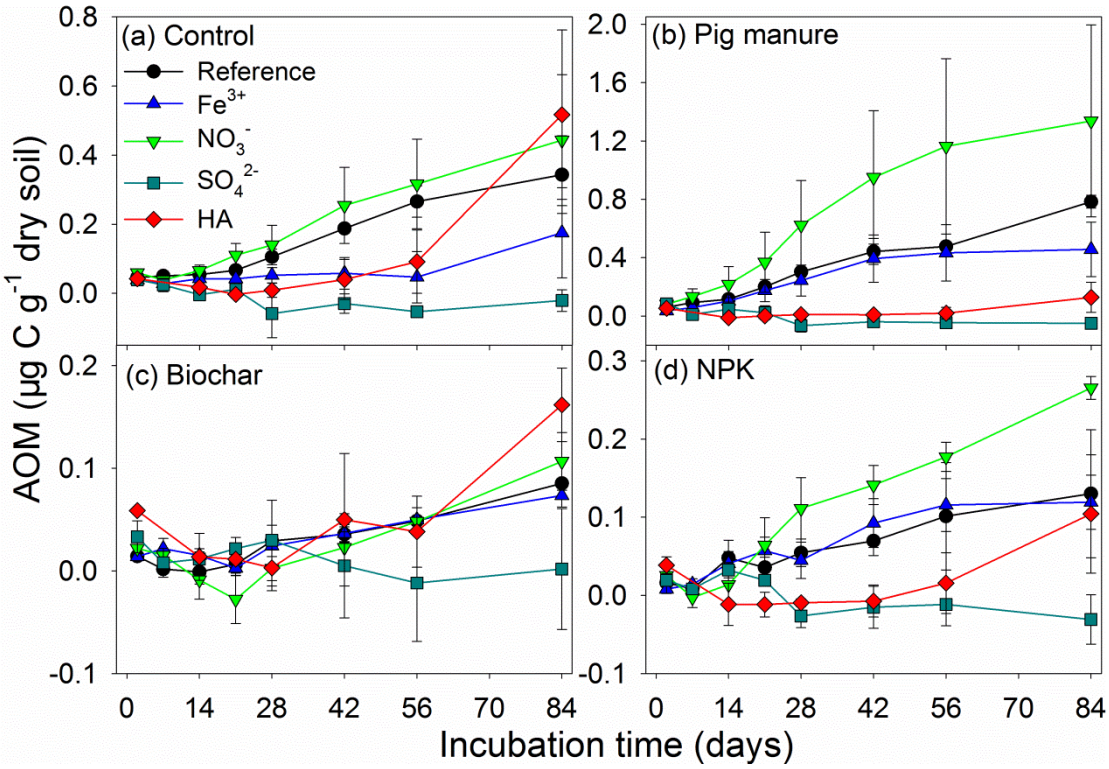

Fig. ES7 Cumulative anaerobic oxidation of methane (AOM) over 84 days' incubation under field fertilization treatments (Control (a), Pig manure (b), Biochar (c), NPK (d)) and electron acceptor amendments (NO_3^-, Fe^{3+}, SO_4^{2-}, and humic acids (HA)). Error bars: standard error of mean (*n*=3).

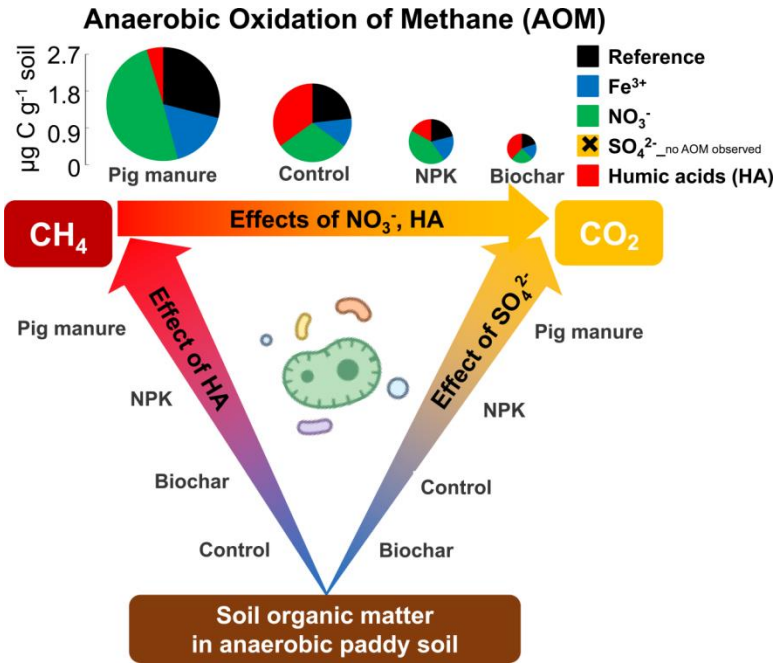

Fig. ES8 Conceptual scheme demonstrating the effects of alternative electron acceptors (*i.e.* NO_3^-, Fe^{3+}, SO_4^{2-}, and humic acids (HA)) on anaerobic oxidation of methane (AOM) and anaerobic soil organic matter (SOM) decomposition. The field fertilization treatments included Control, Pig manure, Biochar, and NPK. Pie size reflects the amount of cumulative AOM during the 84-day incubation, and pie sectors correspond to the contribution of tested electron acceptors to cumulative AOM. Colour gradients: an increasing effect of (i) HA on CH_4 production (blue to red), (ii) SO_4^{2-} on CO_2 production (blue to yellow) and (iii) NO_3^- and HA on AOM (red to yellow).

Assuming that the physical parameters of our paddy soil are representative of those globally (namely a bulk density of 1.3 g cm^{-3} and plow layer of 25.5 cm (Pan et al., 2004)), and considering the AOM rate observed for manure-fertilized NO_3^--amended paddy soil (0.80 ng C g^{-1} soil h^{-1}), then the AOM has the potential to recycle ~3.9 Tg C-CH_4 yr^{-1}. This is roughly 10-20% of the global CH_4 emissions from paddy fields (comprising 19.5-37.5 Tg C yr^{-1} (Keppler et al., 2006; Sass et al., 1999)). Our results clearly point at the impact of fertilization management on AOM in submerged agroecosystems, and its key role to decrease the net CH_4 flux to the atmosphere and hence the potential global warming.

1.4.4 Active AOM pathways and functioning of the microbial community network

Incorporation of ^{13}C from added $^{13}CH_4$ PLFA under strict anoxic conditions confirmed the ^{13}C use for anabolism for 16 ^{13}C-enriched PLFA (Fig. ES10), which demonstrated the cellular uptake of CH_4-derived ^{13}C into microbial biomass (Raghoebarsing et al., 2006; Segarra et al., 2015) and. The partitioning of CH_4-derived ^{13}C between Gram-negative, Gram-positive and Actinobacterial PLFA, and the incorporation of ^{13}C into these 16 PLFA, strongly depended on fertilization and AEA availability (Fig. ES10). This suggests that microorganisms involved in AOM used different metabolic pathways (Segarra et al., 2015). Fertilization can introduce various AEAs in paddy soils for AOM. The highest AOM potential was reached under manure fertilization because of its high NO_3^- load. Consequently, AOM occurred (as a strongly interlinked process) solely in the co-occurrence microbial network of manure-fertilized soil (Fig. ES10). The relative abundance of ANME-2d was highest under pig manure fertilization, but abundances of *Geobacter*, NC10, and SRB were similar to the control (p>0.05, Fig. ES11). This indicates that ANME-2d conducted NO_3^--AOM independently as the dominant pathway (Fig. ES13). This support our third hypothesis that NO_3^--driven AOM is the major AOM pathway.

Biochar application resulted in a higher abundance of NC10 but lowest AOM, suggesting that NC10-derived AOM (i.e., NO_2^--dependent AOM) is one of the active pathways but with minor intensity (Fig. ES13). Higher *Geobacter* abundance was recorded under biochar and NPK fertilization, but ANME-2d abundance and cumulative AOM were lower relative to manure fertilization (Figs. ES8, 11). Thus, biochar application hindered the proposed pathway of extracellular electron transfer between *Geobacter* and ANME-2d, where CH_4 oxidation is coupled to the reduction of anthraquinone-2,6-disulfonate (AQDS) or humic substances (Bai et al., 2019; Scheller et al., 2016). Accordingly, the various AOM pathways are ongoing in parallel at microsites under specific redox conditions, whereby AEA depend on fertilization.

The co-occurrence patterns clearly revealed robust coupling between methanogens, ANME-2d, *Geobacter*, NC10, SRB, and SBM from one side, and AOM, ^{13}C-PLFA, CH_4, and CO_2 from another (Fig. ES10). This suggests mutually beneficial relationships for energy acquisition under anaerobic conditions (Barberán et al., 2012; Berry et al., 2014). Accordingly, the observed clustering in the co-occurrence networks underlines (i) a tight association between methanogenesis and AOM, (ii) that ANME-2d, *Geobacter*, NC10, and SRB jointly contributed to AOM by several co-existing AOM pathways, (iii) that co-occurrence networks after individual AEA amendments demonstrated multiple AOM pathway co-exist in paddy soil.

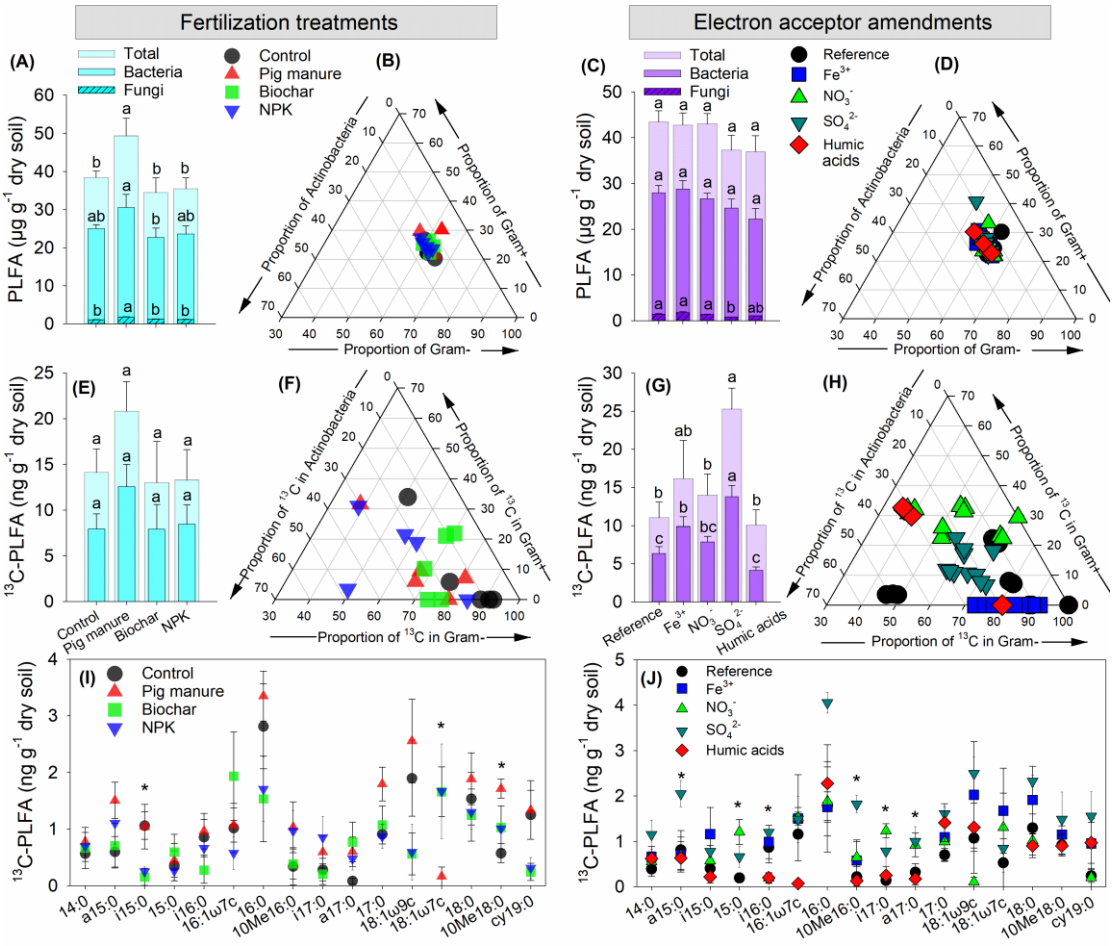

Fig. ES9 Phospholipid fatty acids (PLFA) of individual microbial groups affected by fertilization and electron acceptors. (**A**) The amount of PLFA and (**B**) the proportion of Gram-negative, Gram-positive and Actinobacteria in each fertilization. (**C**) The amount of PLFA and (**D**) the proportion of individual microbial groups in each electron acceptor amendment. (**E**) CH_4-derived ^{13}C incorporation in PLFA and (**F**) proportional ^{13}C partitioning of individual microbial groups in each fertilization. (**G**) CH_4-derived ^{13}C incorporation in PLFA and (**H**) proportional ^{13}C partitioning of individual microbial groups in each electron acceptor amendment. (**I**) 16 ^{13}C-enriched PLFA in each fertilization. (**J**) 16

^{13}C-enriched PLFA in each electron acceptor amendment. Lowercase letters: significant differences of total PLFA and ^{13}C-enriched PLFA at p<0.05. Asterisks (*): significant differences between individual ^{13}C-enriched PLFA at p<0.05.

The AOM pathways were subsequently determined based on the thermodynamic energy yield in reactions with the main electron acceptors (NO_3^-, humic acids, Fe^{3+}, SO_4^{2-}) (Cui et al., 2015; Shen et al., 2019; Smemo and Yavitt, 2011). AOM was highest under NO_3^- amendment, with a high relative abundance of ANME-2d but NC10 abundance was similar to the reference (Fig. ES11). In contrast, ^{13}C incorporation from CH_4 into 10Me16:0 was lowest under NO_3^-, and 10Me16:0 was identified as one of the key PLFA of "*M. oxyfera*" (Kool et al., 2012). This suggests that NO_3^-, rather than NO_2^- (which is used by NC10 *M. oxyfera*), was the dominant electron acceptor for AOM, supported by excess of NO_3^- applied with manure and N fertilization. This again support our third hypothesis that NO_3^--driven AOM is the major AOM pathway. Moreover, AOM was associated in the co-occurrence network of NO_3^--amended microbial communities (Fig. ES10). A plausible candidate for an AOM-performing microorganism using NO_3^- is *M. nitroreducens*, which is dominant in the ANME-2d cluster and broadly distributed in paddy soils (Vaksmaa et al., 2016; Vaksmaa et al., 2017). Another AEA, namely Fe^{3+}, had a minor effect on CH_4-derived C in PLFA and demonstrated a low potential to fuel AOM in the tested paddy soils.

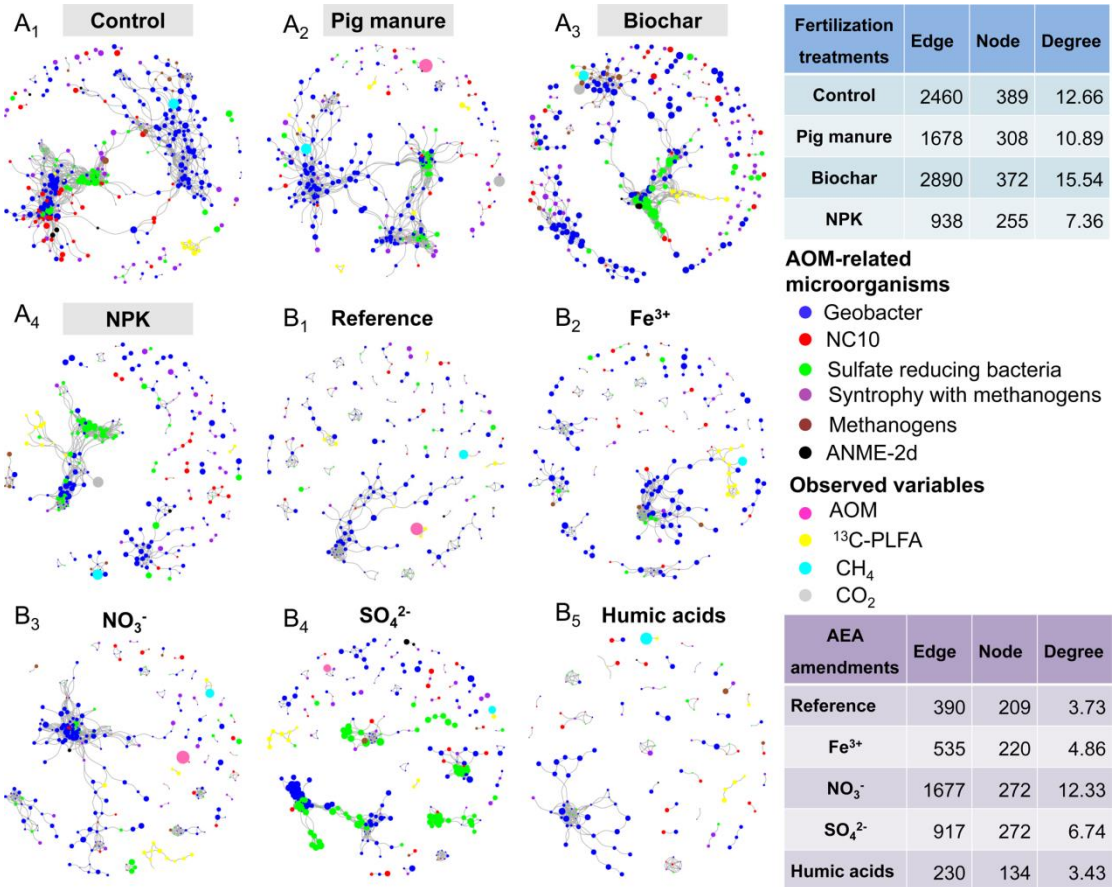

Fertilization treatments	Edge	Node	Degree
Control	2460	389	12.66
Pig manure	1678	308	10.89
Biochar	2890	372	15.54
NPK	938	255	7.36

AEA amendments	Edge	Node	Degree
Reference	390	209	3.73
Fe^{3+}	535	220	4.86
NO_3^-	1677	272	12.33
SO_4^{2-}	917	272	6.74
Humic acids	230	134	3.43

Fig. ES10 The co-occurrence networks reflecting anaerobic methane oxidation (AOM) metabolism. (**A$_{1\text{-}5}$**) The co-occurrence networks under fertilization treatments. (**B$_{1\text{-}5}$**) The co-occurrence networks for each fertilization with electron acceptor amendments. The co-occurrence networks associated with AOM-related microorganisms (methanogens, ANME-2d, *Geobacter*, NC10, SRB (sulfate-reducing bacteria), and SBM (syntrophic bacteria with methanogens)) and the observed variables which reflecting $^{13}CH_4$ metabolism (AOM, ^{13}C-PLFA, CH_4, CO_2) based on Amplicon Sequence Variants correlation analysis, and a connection stands for a strong (Pearson's r>0.6) and significant (p<0.01) correlation. The size of each node is proportional to the microbial relative abundance and recorded values.

Surprisingly, SO_4^{2-} addition increased the relative abundance of ANME-2d and NC10, and induced higher ^{13}C incorporation into the PLFA 10Me16:0 (Figs. ES9, 11). The measured AOM, however, was the lowest. There are several possible reasons for this: (i) Highest CO_2 production under SO_4^{2-} amendment (Fig. ES8) suggests that organic matter oxidation with SO_4^{2-} was thermodynamically more favorable than AOM. (ii) AOM was clustered in the co-occurrence network of SO_4^{2-}-amended microbial communities (Fig. ES10), suggesting that SO_4^{2-}-dependent AOM performed by consortia of ANME-2d with SRB was one of the active AOM pathways. Nonetheless, similar to NC10-derived AOM, SO_4^{2-}-dependent AOM was of minor intensity. (iii) SO_4^{2-}-driven organic matter decomposition by *Geobacter* and SRB may have diluted the ^{13}C-label of the CH_4 by non-labeled SOM-derived CH_4, thereby masking the ongoing AOM. (iv) 10Me16:0 might be ^{13}C-enriched as derived from cross-feeding of other microbial groups (e.g., Actinobacteria), which are also functional and can grow under these conditions. Especially for the 10Me-branched fatty acids of Actinobacteria, a growth based on necromass of other microbial groups incorporating $^{13}CH_4$ is very likely (Apostel et al., 2018).

Humic substances were previously acknowledged as important AEAs for organic matter decomposition (Keller et al., 2009) and AOM (Bai et al., 2019). Humic acids increased the abundance of methanogens, *Geobacter* and SBM, and led to the highest CH_4 production (Figs. ES8, 11). Reportedly, *Geobacter* also plays a role in oxidizing acetate, and its activity is coupled to the reduction of humic acids (Voordeckers et al., 2010). A mutual linkage of *Geobacter* with methanogens is possible, whereas humic substances served as methanogenesis substrates (Voordeckers et al., 2010). We therefore conclude that active AOM pathways co-exist, which NO_3^--driven AOM is the major AOM pathway and it co-exists with minor pathways involving reduction of NO_2^-, humic acids, Fe^{3+}, and SO_4^{2-}, as hypothesized.

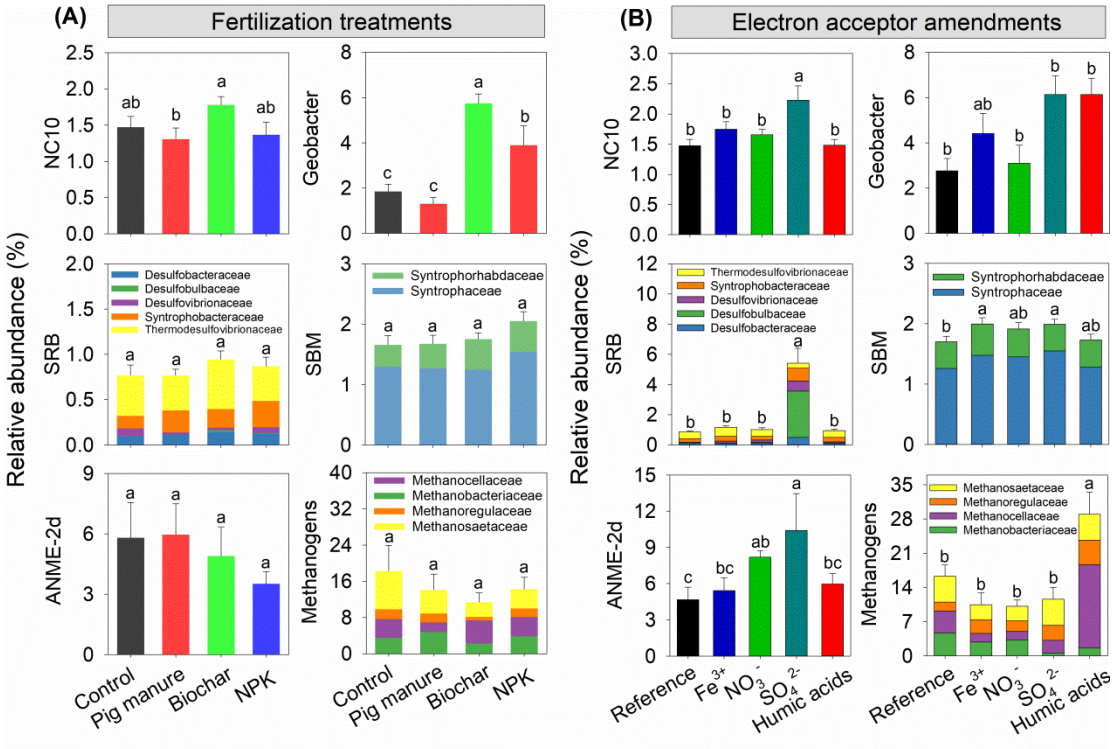

Fig. ES11 Relative abundance of AOM-related microorganisms. AOM-related microorganisms including NC10, *Geobacter*, SRB (sulfate-reducing bacteria), SBM (strophy bacteria with methangens), ANME-2d, and methangens. **(A)** AOM-related microorganisms under fertilization. **(B)** AOM-related microorganisms under electron acceptor amendments. Lowercase letters represent significant differences at $p<0.05$.

1.5 Integration and conclusions

Based on ^{13}C labeling, this thesis demonstrated for the first time that CH_4 injection through a silicone tube directly into the soil is an efficient approach for incubation studies on CH_4 oxidation (Fig. ES12B). The AOM experimental data highlighted the occurrence of AOM in submerged paddy soil. A static setup is superior to shaking when estimating AOM due to lesser disturbance (Fig. ES12C). NO_3^- is the most effective AEA. Fe^{3+} had no effect and SO_4^{2-} negatively affected AOM. Humic acids obviously played a dual role, *i.e.* as a substrate for methanogenesis and as an AEA for AOM in DOC-depleted paddy soils. The most pronounced AOM in paddy soils occurred under pig manure fertilization, followed by the control and NPK, while AOM was the lowest under biochar application (Fig. ES12D). Furthermore, we open new perspectives for studies on highly complex interactions of anaerobic communities in paddy soils including AOM. The latter was disentangled by jointly applying microbial co-occurrence network analysis and ^{13}C tracing from $^{13}CH_4$ in CO_2 and PLFA. The pronounced co-occurrence network revealed a set of major and minor AOM pathways with synergistic relations to other anaerobic microbial groups. We identified AOM independently conducted by ANME-2d as being the major AOM pathway in paddy soils, whereby manure fertilization had greatest effect, followed by NPK, with the lowest effect after biochar application. This pathway co-existed with the minor AOM pathways independently conducted by NC10 and with the AOM conducted by consortia of ANME-2d with *Geobacter* or sulfate-reducing bacteria (Fig. ES12E). On a larger scale, NO_3^--induced AOM together with manure fertilization has the potential to recycle ~3.9 Tg C-CH_4 annually, which represents a roughly ~10–20% offset of global net CH_4 emissions from rice paddies. Consequently, from a broader ecological perspective, organic and mineral fertilization are important controls of the CH_4 sink under anaerobic conditions in submerged agricultural ecosystems.

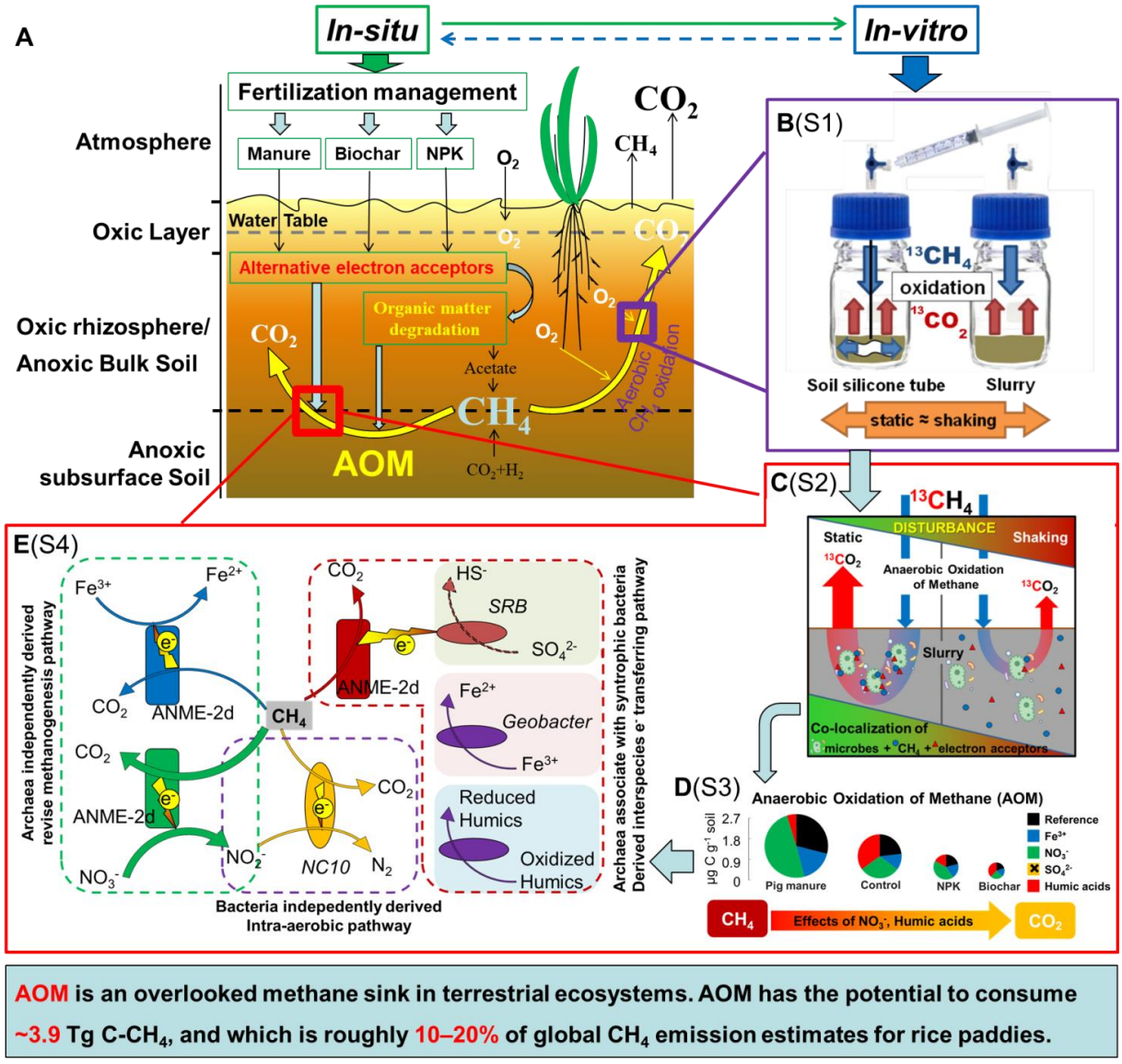

Fig. ES12 Conceptual scheme of the whole study. **(A)** Schematic diagram of the in-situ CH4 cycling under fertilization rice paddy. **(B)** Schematic diagram of the incubation experiment set-up with and without soil silicone tube (white color on the left), and with and without shaking. **(C)** The effects of shaking vs. static conditions on anaerobic oxidation of methane (AOM) estimated based on the ^{13}C-labelled CH_4 (blue arrows). The colour gradient from green to red and shape of triangles mean the increasing disturbance on AOM due to shaking, and the decreasing co-localization of substrate (CH_4, blue circles), electron acceptors (red circles) and microorganisms from shaking vs. static conditions. **(D)** Conceptual scheme demonstrating the effects of alternative electron acceptors (*i.e.* NO_3^-, Fe^{3+}, SO_4^{2-}, and humic acids) on AOM. **(E)** Conceptual model of microbial anaerobic methane oxidation (AOM) pathways in paddy soils. Green box, archaea independently conduct "reverse methanogenesis" pathway associated with reduction of (i) NO_3^- to NO_2^- by *M. nitroreducens* of ANME-2d (Haroon et al., 2013), (ii) Fe^{3+} to Fe^{2+} by *M. ferrireducens* of ANME-2d (Cai et al., 2018). Purple box, bacteria independently conducted "intra-aerobic denitrification" pathway by NC10 *M. oxyfera*, where O_2 is derived from intracellular NO_2^- dismutation (Ettwig et al., 2010). Red box, interspecies-extracellular electron transferring "reverse methanogenesis" pathway by archaea and associated syntrophic bacteria (McAnulty et al., 2017), the putative reduction of (i) Fe^{3+} and (ii) humic substances by consortia of ANME with *Geobacter*, and (iii) reduction of SO_4^{2-} by consortia of ANME with sulfate reducing bacteria. Thick green arrow: the most potent AOM pathway, i.e., NO_3^--dependent AOM.

1.6 Outlook

Here we present the synthesis of broader literature findings and also some results from unpublished and ongoing work, together with an outline of promising future research directions.

1.6.1 The challenge of field AOM potential measurements

AOM measurements in *situ* are still challenging to conduct, if ever, reported due to the dynamics of the physicochemical conditions in deeper soil layers and problems in separating gross and net processes of CH_4 cycling, but of great scientific interest. The most common approach to estimate AOM potential is incubation studies via microcosms under the controlled laboratory conditions. However, the microcosm's incubation may cause systematical under- or overestimation because the controlled incubation systems lack the structural and biological complexity of field reality. For example, soil slurry in microcosms totally destroyed the physical structure of soil profile, and ignored the effects of roots rhizosphere on soil nutrition and the sensitive response of microorganisms. Segarra et al., (2015), Hu et al., (2014) and our estimations (study 2 and 3) used AOM rates from microcosm studies to upscale to the field level. Such approach leads however to the increasing uncertainty, because the results are disconnected from spatial and temporal heterogeneity in substrate availability and redox potential in fields. So, the measurements of field AOM potential is very highly demanded.
The approach of $^{13}CH_4$-labeling by silicone tubes (study 1 and 2) should be standardized for the field conditions to target the underground CH_4 cycling. Dorodnikov et al., (manuscript in prep.) utilized passive diffusion chambers (PDC, porous silicone tubes) for the delivery of ^{13}C-labeled CH_4 belowground for the in *situ* determination of the net CH_4 oxidation potential in peatlands. Similar to the laboratory set-up, the silicone tubes there were used for the belowground isotope labeling and sampling of CO_2 as product of CH_4 oxidation. The applicability of the belowground labeling for the CH_4 turnover was approved and the *in-situ* occurrence of deep peat CH_4 oxidation was verified. However, much higher risk of oxygen contamination as compared to the laboratory conditions confirmed the need to apply additional measurements of oxygen concentrations at trace amounts inside silicone tubes. Nonetheless, this makes field AOM potential measurements a step forward towards realistic natural conditions.

1.6.2 Multiple environmental factors effect on AOM

The controlled microcosms always have the standard conditions, which overlook multiple climatic factors, e.g. temperature, the fluctuation of water table, salinity and pH conditions, etc. occurring simultaneously. Although individual or even multiple climatic factors can be manipulated, it is impossible to create fully natural conditions in the laboratory. From another side, there are parameters, such as microbial community structure and activity, which so far cannot be followed *in-situ*. Therefore, scientific studies should apply both filed- and laboratory methods to fully cover research topics. ANME-2d and NC10 were related to nitrate/nitrite-dependent AOM, they were most enriched at 25-35 ^{o}C (Bai et al., 2019; Ettwig et al., 2010; Raghoebarsing et al., 2006). He et al., (2015) observed that the microbial activity of nitrate/nitrite-dependent AOM was highest at 35 ^{o}C, the activity would be inhibited with further temperature increase (>35 ^{o}C). However, to the best of our knowledge, the temperature sensitivity of the AOM process is still not quantified yet in any of ecosystems. The optimal concentration of each AEA for the microorganisms conducting AOM also stays a large gap of knowledge. Thus, Hu et al., (2011) observed that nitrite caused toxic effects on *M.oxyfera* at a concentration of 1 mmol NO_2^--N l^{-1}, but Ettwig et al., (2009) used similar nitrite concentration for substrate to enrich the microbial cultures, and did not observe the inhibition of the NC10 enrichment including *M. oxyfera*. Sulfate is the major electron acceptor for marine AOM (Knittel and Boetius, 2009), but addition of sulfate in paddy soil completely inhibited AOM activity (study 3). This indicated that specific ecosystems with different alternative electron acceptors play a role in

determining preferential AOM pathways. Gauthier et al., (2015) and Gupta et al., (2013) also found soil types and geographical location would lead to significantly different AOM rates. Altogether, there is a necessity to investigate AOM in different ecosystems widely and specifically to quantify the realistic ecological benefits of AOM.

1.6.3 Role of humic substances as electron acceptors for AOM

Humic substances (humic acids) can accelerate dissimilatory Fe^{3+} reduction by electron shuttling between microorganisms and poorly soluble iron (III) (hydr)oxides (Wolf et al., 2009), thus they have the potential to be terminal electron acceptors for AOM. However, the functional microbes and electron transfer mechanisms as well as benefited humic chemical structures during humic acids-dependent AOM are still poorly understood. For example, Bai et al., (2019) reported the highest AOM rate after three-cycle (23 days) incubation with humic acids in a denitrifying anaerobic methane oxidation reactor, and proposed humic acids as electron acceptors for AOM driven by ANME-2d linked with *Geobacter* via interspecies electron transferring. In line with our results (study 3), we observed a distinct temporal delay (~56 days) of AOM under humic acids amendment. Humic acids in all above studies seem cannot be readily available AEAs for AOM, they must undergo decomposition before the intermediate decomposition products could serve as AEAs for AOM. If so, the AOM rate will depend on the humic acids decomposition rate. The redox potentials of intermediates are different depending on humics decomposed. Quinones are the most important shuttle compounds in the redox reactions. Scheller et al., (2016) observed that the artificial quinones oxidants (anthraquinone-2,6-disulfonic acid, AQDS) and AQDS isomers decoupled ANME from their syntrophic sulfate reducing bacteria (SRB) partners, and served as AEAs for AOM. But the quinones studied by Wolf et al., (2009) performed differently: Some had strong accelerating effects, whereas others showed only small effects, no effects, or even inhibitory effects on the kinetics of iron reduction. Therefore, the question of which intermediate decomposition products and structures are the favorable chemical groups is not fully answered.

Organic fertilizers, such as biochar and livestock manure which contained abundant humic acids, are a common agricultural management in paddy soil. Biochar is evaluated globally as a mean of soil amendment to improve soil fertility and to mitigate climate change (e.g. decreasing CH_4 emission) (Lehmann et al., 2011). Zhang et al., (2019) reported that biochar can stimulate AOM by ANME-2d, and proposed biochar amendment for CH_4 mitigation in anaerobic environments. However, in our results (study 3) we did not observe a higher AOM rate under biochar treatment as compared with the control. The contradictory results between studies may be caused by the following reasons. In the short term, fresh biochar can release a variety of organic molecules, the dissolved organic compounds from biochar can serve as electron shuttle under the different redox potential. Explicitly, AOM mediated by electron shuttles of biochar is mainly controlled by thermodynamic properties of organic compounds. But in the long term, biochar is ageing and losing such internal capability (of transferring electrons?). In the future, research on CH_4 mitigation by biochar must include a systematic analysis of different biochar types and measurement of the redox potential of biochar.

1.6.4 Lipids and carbon assimilation

Genomic approaches are widely applied for the detection of AOM-related microorganisms (e.g. NC10 of *M. oxyfera*, Archaea of *M. nitroreducens* and *M. ferrireducens*) and their functional genes (methane monooxygenase, *pmo*A, and *mcr*A) (Cai et al., 2018; Ettwig et al., 2010; Shen et al., 2019). But specific primers of genomic sequencing may capture only a selection of organisms potentially contributing to AOM, and most of such studies carried out *in-vitro*. Knowledge of the lipid biomarkers profile of AOM-related microorganisms would potentially facilitate their environmental detections, especially in combination with stable carbon isotope signatures. The setup to obtain solid evidence for incorporation of methane into bacterial and archaeal biomarkers is seemingly straightforward: incubation with $^{13}CH_4$ as the sole electron donor for an extended period of time to allow for sufficient

incorporation of labeled carbon into microbial biomass. Indeed, incorporation of methane into the bacterial and archaeal biomarkers have been detected several times (Raghoebarsing et al., 2006; Segarra et al., 2015). But individual study showed distinct patterns of biomarkers and the results were somehow difficult to interpret. Substantial amounts of methane-derived carbon were incorporated in only few lipids. For example, Raghoebarsing et al., (2006) detected a single archaeal and ten bacterial biomarkers by analyzing the membrane lipids of the enrichment culture. Segarra et al., (2015) observed two bacterial and five archaeal lipids involved in AOM, both of them were sampled from freshwater sediments. In our results (study 4), we found 16 bacterial lipids showed substantial ^{13}C incorporation after $^{13}CH_4$ addition relative to the natural abundance control. Moreover, Raghoebarsing et al., (2006) found the bacterial biomarkers were labeled more rapidly and substantially than the archaeal biomarker. Similarly, Blumenberg et al., (2005) reported that there was substantial incorporation of ^{13}C from methane in the lipids of SRB, but there was minor ^{13}C incorporation in archaeal lipids only after prolonged incubation (>300 days).

Kool et al., (2012) proposed that the typical branch fatty acids 10MeC16:0 (~46%) and 10MeC16:1Δ7 (~10%) are key and characteristic components of the lipid profile of *M. oxyfera*. However, 10Me16:0 is also a major constituent of the total lipids of SRB (Rütters et al., 2002). It is also sometimes attributed to Actinobacteria (González et al., 2005), in anammox bacteria and other planctomycetes (Sinninghe Damsté et al., 2005), and in *Geobacter* species (Zhang et al., 2003). Therefore, future experiments could target specific enrichment cultures under the supply of labeled methane to elucidate the pathways of carbon assimilation in AOM.

1.6.5 Stoichiometry of AOM process

We revealed three AOM pathways according to the electron transfer methods (study 4). I.e., **(1)** archaea independently conduct "reverse methanogenesis" pathway associated with reduction of (i) NO_3^- to NO_2^- by *M. nitroreducens* of ANME-2d, (ii) Fe^{3+} to Fe^{2+} by *M. ferrireducens* of ANME-2d. **(2)** Bacteria independently conduct "intra-aerobic denitrification" pathway by NC10 *M. oxyfera*, where O_2 is derived from intracellular NO_2^- dismutation. **(3)** Interspecies-extracellular electron transferring "reverse methanogenesis" pathway by archaea and associated syntrophic bacteria via the putative reduction of (i) Fe^{3+} and (ii) humic substances by consortia of ANME with *Geobacter*, and (iii) reduction of SO_4^{2-} by consortia of ANME with sulfate reducing bacteria. The theoretical stoichiometry between methane and electron acceptors is different because of the different thermodynamic parameters of AEAs. In the future experiments, more attention should be payed to the stoichiometry, when different electron acceptors are tested for the AOM potential in a batch experiment and under different environmental conditions.

i. NO_3^- and Fe^{3+} in reverse methanogenesis pathway

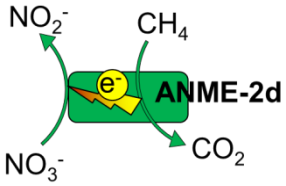

$$CH_4 + 4NO_3^- = CO_2 + 4NO_2^- + 2H_2O$$

($\Delta G^{0'}$ = -503 kJ mol^{-1} CH_4) (Haroon et al., 2013)

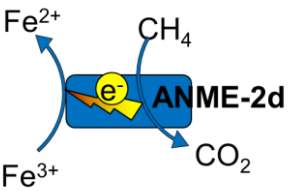

$$CH_4 + 8Fe^{3+} + 2H_2O = CO_2 + 8Fe^{2+} + 8H^+$$

($\Delta G^{0'}$ = -454 kJ mol^{-1} CH_4) (Cai et al., 2018)

ii. NO_2^- in 'intra-aerobic' pathway

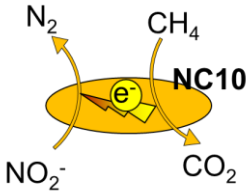

$3CH_4 + 8NO_2^- + 8H^+ = 3CO_2 + 4N_2 + 10H_2O$

($\Delta G^{0'}$ = -928 kJ mol^{-1} CH_4) (Ettwig et al., 2010)

iii. Fe^{3+}, SO_4^{2-} and humic acids in interspecies e^- transferring pathway

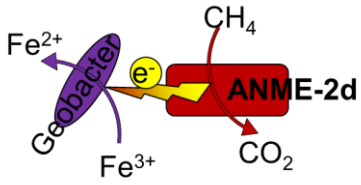

$CH_4 + 8Fe^{3+} + 2H_2O = CO_2 + 8Fe^{2+} + 8H^+$

($\Delta G^{0'}$ = -454 kJ mol^{-1} CH_4) (Cai et al., 2018)

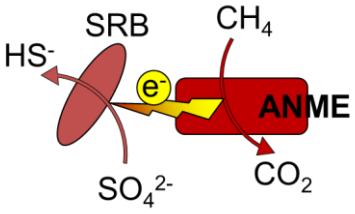

$CH_4 + SO_4^{2-} = HCO_3^- + HS^- + H_2O$

($\Delta G^{0'}$ = -17 kJ mol^{-1} CH_4) (Scheller et al., 2016)

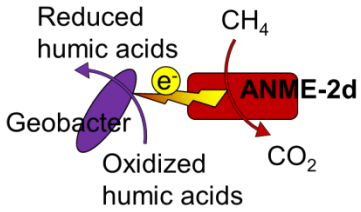

$CH_4 + 4AQDS + 3H_2O = HCO_3^- + 4AQH_2DS + H^+$

($\Delta G^{0'}$ = -41 kJ mol^{-1} CH_4) (Scheller et al., 2016)

1.6.6 Applicability of nitrate/nitrite-dependent AOM

The microbial mechanisms of nitrate/nitrite-dependent AOM metabolism are more clear than that via reverse methanogenesis pathway and 'intra-aerobic' pathway, due to increasing number of studies with enrichment cultures of related microorganisms (e.g. *M. oxyfera*, *M. oxyfera* like bacteria, and *M. nitroreducens*) (Ettwig et al., 2009; Vaksmaa et al., 2017; Wang et al., 2018). The ecological benefits of AOM process is overlooked, and it is less included in process-based models of the terrestrial C cycle. For example, as a methane sink, Gupta et al., (2013) estimated that northern peatland could anaerobically consume 24 Tg of CH_4 annually, Hu et al., (2014) estimated that nitrite-dependent AOM has the potential to consume ~4.1–6.1 Tg of CH_4 on average each year in wetland, and our estimation (study 3) proposed nitrate-induced AOM together with manure fertilization has the potential to recycle ~3.9 Tg C–CH_4 annually, which represents a roughly ~10–20% offset of global net CH_4 emissions from rice paddies.

Another interesting and advantageous point of nitrate/nitrite-dependent AOM is that it can remove nitrogen and mitigate methane emission from wastewater treatment, as an engineering approach. For

example, Zhang et al., (2020) demonstrated that nitrite-dependent AOM could be adopted in tidal flow constructed wetlands to remove nitrite, which is an effective approach to treat contaminated river. But the biggest challenge of that is the slow enrichment rate of related microbial biomass and biomass retention. For example, Ettwig et al., (2009) required 6 months to enrich NC10 as dominating in the microbial population in a bioreactor with a constant supply of methane and nitrite. Vaksmaa et al., (2017) enriched *M. nitroreducens* and NC10 in a reactor and after 2 years of operation the 16S rRNA gene copies were increased by 1.2 and 4.2 times, respectively.

Nie et al., (2019) reported that the co-cultures of nitrate-dependent AOM microorganisms (i.e. *M. nitroreducens*) and Anammox (anaerobic ammonium oxidation, which is a reaction that oxidizes ammonium to dinitrogen gas using nitrite as the electron acceptor under anoxic conditions) microorganisms could enrich within 25 days in a novel lab-scale membrane-aerated-membrane bioreactor. Nie et al., (2019) proposed that the membrane-aerated-membrane bioreactor is a practical technology for application of anammox and nitrite-dependent AOM processes through combining membrane aeration for efficient methane supply, and membrane filtration for complete separating the slow-growing microorganisms from the mixed liquor. Such progressive approaches are promising for the practical application of nitrate/nitrite-dependent AOM and/or Anammox in municipal wastewater treatment.

1.7 References

Apostel, C., Herschbach, J., Bore, E.K., Spielvogel, S., Kuzyakov, Y., Dippold, M.A., 2018. Food for microorganisms: Position-specific ^{13}C labeling and ^{13}C-PLFA analysis reveals preferences for sorbed or necromass C. Geoderma 312, 86-94.

Bai, Y., Wang, X., Wu, J., Lu, Y., Fu, L., Zhang, F., Lau, T., Zeng, R.J., 2019. Humic substances as electron acceptors for anaerobic oxidation of methane driven by ANME-2d. Water Research 164, 114935.

Barberán A, Bates ST, Casamayor EO, Fierer N. Using network analysis to explore co-occurrence patterns in soil microbial communities. The ISME Journal. 2012; 6:343-351.

Barnes, R.O., Goldberg, E.D., 1976. Methane production and consumption in anoxic marine sediments. Geology 4, 297.

Beal, E.J., House, C.H., Orphan, V.J., 2009. Manganese-and iron-dependent marine methane oxidation. Science 325, 184-187.

Berry D, Widder S. Deciphering microbial interactions and detecting keystone species with co-occurrence networks. Frontiers in Microbiology. 2014; 5:219.

Blazewicz, S.J., Petersen, D.G., Waldrop, M.P., Firestone, M.K., 2012. Anaerobic oxidation of methane in tropical and boreal soils: Ecological significance in terrestrial methane cycling. Journal of Geophysical Research: Biogeosciences 117.

Blodau, C., Roulet, N.T., Heitmann, T., Stewart, H., Beer, J., Lafleur, P., Moore, T.R., 2007. Belowground carbon turnover in a temperate ombrotrophic bog. Global Biogeochemical Cycles 21.

Blumenberg, M., Seifert, R., Nauhaus, K., Pape, T., Michaelis, W., 2005. *In vitro* study of lipid biosynthesis in an anaerobically methane-oxidizing microbial mat. Applied and Environmental Microbiology 71, 4345-4351.

Bousquet, P., Ciais, P., Miller, J.B., Dlugokencky, E.J., Hauglustaine, D.A., Prigent, C., Van der Werf, G.R., Peylin, P., Brunke, E.G., Carouge, C., Langenfelds, R.L., Lathière, J., Papa, F., Ramonet, M., Schmidt, M., Steele, L.P., Tyler, S.C., White, J., 2006. Contribution of anthropogenic and natural sources to atmospheric methane variability. Nature 443, 439.

Cai, C., Leu, A.O., Xie, G., Guo, J., Feng, Y., Zhao, J., Tyson, G.W., Yuan, Z., Hu, S., 2018. A methanotrophic archaeon couples anaerobic oxidation of methane to Fe(III) reduction. The ISME journal 12, 1929-1939.

Cai, Z.C., Mosier, A.R., 2000. Effect of NH_4Cl addition on methane oxidation by paddy soils. Soil Biology & Biochemistry 32, 1537-1545.

Callahan, B.J., McMurdie, P.J., Holmes, S.P., 2017. Exact sequence variants should replace operational taxonomic units in marker-gene data analysis. The ISME Journal 11, 2639-2643.

Conrad, R., Rothfuss, F., 1991. Methane oxidation in the soil surface layer of a flooded rice field and the effect of ammonium. Biology and Fertility of Soils 12, 28-32.

Cui, M., Ma, A., Qi, H., Zhuang, X., Zhuang, G., 2015. Anaerobic oxidation of methane: an "active" microbial process. MicrobiologyOpen 4, 1-11.

Deutzmann, J.S., Schink, B., 2011. Anaerobic oxidation of methane in sediments of lake constance, an oligotrophic freshwater lake. Applied and Environmental Microbiology 77, 4429-4436.

Ettwig, K.F., Butler, M.K., Le Paslier, D., Pelletier, E., Mangenot, S., Kuypers, M.M.M., Schreiber, F., Dutilh, B.E., Zedelius, J., de Beer, D., Gloerich, J., Wessels, H.J.C.T., van Alen, T., Luesken, F., Wu, M.L., van de Pas-Schoonen, K.T., Op Den Camp, H.J.M., Janssen-Megens, E.M., Francoijs, K., Stunnenberg, H., Weissenbach, J., Jetten, M.S.M., Strous, M., 2010. Nitrite-driven anaerobic methane oxidation by oxygenic bacteria. Nature 464, 543-548.

Ettwig, K.F., van Alen, T., van de Pas-Schoonen, K.T., Jetten, M.S.M., Strous, M., 2009. Enrichment and molecular detection of denitrifying methanotrophic bacteria of the NC10 phylum. Applied and Environmental Microbiology 75, 3656-3662.

Ettwig, K.F., Zhu, B., Speth, D., Keltjens, J.T., Jetten, M.S., Kartal, B., 2016. Archaea catalyze iron-dependent anaerobic oxidation of methane. Proceedings of the National Academy of Sciences 113, 12792-12796.

Forster, P., Ramaswamy, V., Artaxo, P., Berntsen, T., Betts, R., Fahey, D.W., Haywood, J., Lean, J., Lowe, D.C., Myhre, G., 2007. Changes in atmospheric constituents and in radiative forcing. Chapter 2, Climate Change 2007. The Physical Science Basis.

Gauthier, M., Bradley, R.L., Šimek, M., 2015. More evidence that anaerobic oxidation of methane is prevalent in soils: Is it time to upgrade our biogeochemical models? Soil Biology & Biochemistry 80, 167-174.

González, I., Ayuso-Sacido, A., Anderson, A., Genilloud, O., 2005. Actinomycetes isolated from lichens: Evaluation of their diversity and detection of biosynthetic gene sequences. FEMS Microbiology Ecology 54, 401-415.

Gunina, A., Dippold, M.A., Glaser, B., Kuzyakov, Y., 2014. Fate of low molecular weight organic substances in an arable soil: From microbial uptake to utilisation and stabilisation. Soil Biology & Biochemistry 77, 304-313.

Guo, J., Song, Z., Zhu, Y., Wei, W., Li, S., Yu, Y., 2017. The characteristics of yield-scaled methane emission from paddy field in recent 35-year in China: A meta-analysis. Journal of Cleaner Production 10, 1044-1050.

Gupta, V., Smemo, K.A., Yavitt, J.B., Fowle, D., Branfireun, B., Basiliko, N., 2013. Stable isotopes reveal widespread anaerobic methane oxidation across latitude and peatland type. Environmental Science &

Technology, 265198755.

Haroon, M.F., Hu, S., Shi, Y., Imelfort, M., Keller, J., Hugenholtz, P., Yuan, Z., Tyson, G.W., 2013. Anaerobic oxidation of methane coupled to nitrate reduction in a novel archaeal lineage. Nature 500, 567-570.

He, Z., Geng, S., Shen, L., Lou, L., Zheng, P., Xu, X., Hu, B., 2015. The short- and long-term effects of environmental conditions on anaerobic methane oxidation coupled to nitrite reduction. Water Research 68, 554-562.

Heitmann, T., Goldhammer, T., Beer, J., Blodau, C., 2007. Electron transfer of dissolved organic matter and its potential significance for anaerobic respiration in a northern bog. Global Change Biology 13, 1771-1785.

Hu, B.L., Shen, L.D., Lian, X., Zhu, Q., Liu, S., Huang, Q., He, Z.F., Geng, S., Cheng, D.Q., Lou, L.P., Xu, X.Y., Zheng, P., He, Y.F., 2014. Evidence for nitrite-dependent anaerobic methane oxidation as a previously overlooked microbial methane sink in wetlands. Proceedings of the National Academy of Sciences 111, 4495-4500.

Hu, S., Zeng, R.J., Keller, J., Lant, P.A., Yuan, Z., 2011. Effect of nitrate and nitrite on the selection of microorganisms in the denitrifying anaerobic methane oxidation process. Environmental Microbiology Reports 3, 315-319.

Joergensen, R.G., 1996. The fumigation-extraction method to estimate soil microbial biomass: Calibration of the kEC value. Soil Biology & Biochemistry 28, 25-31.

Kammann, C., Grünhage, L., Jäger, H.J., 2001. A new sampling technique to monitor concentrations of CH_4, N_2O and CO_2 in air at well-defined depths in soils with varied water potential. European Journal of Soil Science 52, 297-303.

Keppler, F., Hamilton, J.T., Braß, M., Röckmann, T., 2006. Methane emissions from terrestrial plants under aerobic conditions. Nature 439, 187.

Khalil, M.I., Baggs, E.M., 2005. CH4 oxidation and N_2O emissions at varied soil water-filled pore spaces and headspace CH4 concentrations. Soil Biology & Biochemistry 37, 1785-1794.

Knittel, K., Boetius, A., 2009. Anaerobic oxidation of methane: Progress with an unknown process. Annual Review of Microbiology 63, 311-334.

Kögel-Knabner, I., Amelung, W., Cao, Z., Fiedler, S., Frenzel, P., Jahn, R., Kalbitz, K., Kölbl, A., Schloter, M., 2010. Biogeochemistry of paddy soils. Geoderma 157, 1-14.

Kool, D.M., Zhu, B., Rijpstra, W.I.C., Jetten, M.S.M., Ettwig, K.F., Sinninghe Damsté, J.S., 2012. Rare branched fatty acids characterize the lipid composition of the intra-aerobic methane oxidizer 'Candidatus Methylomirabilis oxyfera'. Applied and Environmental Microbiology 78, 8650-8656.

Krüger, M., Frenzel, P., 2003. Effects of N-fertilisation on CH4 oxidation and production, and consequences for CH4 emissions from microcosms and rice fields. Global Change Biology 9, 773-784.

Lai, D.Y.F., 2009. Methane dynamics in northern peatlands: A review. Pedosphere 19, 409-421.

Lehmann, J., Rillig, M.C., Thies, J., Masiello, C.A., Hockaday, W.C., Crowley, D., 2011. Biochar effects on soil biota – A review. Soil Biology & Biochemistry 43, 1812-1836.

Liu, P., Conrad, R., 2017. Syntrophobacteraceae-affiliated species are major propionate-degrading sulfate reducers in paddy soil. Environmental Microbiology 19, 1669-1686.

McAnulty, M.J., G. Poosarla, V., Kim, K., Jasso-Chávez, R., Logan, B.E., Wood, T.K., 2017. Electricity from methane by reversing methanogenesis. Nature Communications 8.

Mohanty, S.R., Bandeppa, G.S., Dubey, G., Ahirwar, U., Patra, A.K., Bharati, K., 2017. Methane oxidation in response to iron reduction-oxidation metabolism in tropical soils. European Journal of Soil Biology 78, 75-81.

Nayak, D.R., Babu, Y.J., Datta, A., Adhya, T.K., 2007. Methane oxidation in an intensively cropped tropical rice field soil under long-term application of organic and mineral fertilizers. Journal of Environmental Quality 36, 1577-1584.

Nie, W., Xie, G., Ding, J., Lu, Y., Liu, B., Xing, D., Wang, Q., Han, H., Yuan, Z., Ren, N., 2019. High performance nitrogen removal through integrating denitrifying anaerobic methane oxidation and Anammox: from enrichment to application. Environment International 132, 105107.

Nisbet, E.G., Dlugokencky, E.J., Manning, M.R., Lowry, D., Fisher, R.E., France, J.L., Michel, S.E., Miller, J.B., White, J.W.C., Vaughn, B., Bousquet, P., Pyle, J.A., Warwick, N.J., Cain, M., Brownlow, R., Zazzeri, G., Lanoiselle, M., Manning, A.C., Gloor, E., Worthy, D.E.J., Brunke, E.G., Labuschagne, C., Wolff, E.W., Ganesan, A.L., 2016. Rising atmospheric methane: 2007-2014 growth and isotopic shift. Global Biogeochemical Cycles 30, 1356-1370.

Orcutt, B., Boetius, A., Elvert, M., Samarkin, V., Joye, S.B., 2005. Molecular biogeochemistry of sulfate reduction, methanogenesis and the anaerobic oxidation of methane at Gulf of Mexico cold seeps. Geochimica et Cosmochimica Acta 69, 4267-4281.

Pan, G., Li, L., Wu, L., Zhang, X., 2004. Storage and sequestration potential of topsoil organic carbon in China's paddy soils. Global Change Biology 10, 79-92.

Pausch, J., Kuzyakov, Y., 2012. Soil organic carbon decomposition from recently added and older sources estimated by $\delta^{13}C$ values of CO_2 and organic matter. Soil Biology & Biochemistry 55, 40-47.

Pozdnyakov, L.A., Stepanov, A.L., Manucharova, N.A., 2011. Anaerobic methane oxidation in soils and water ecosystems. Moscow University soil science bulletin 66, 24-31.
Putkinen, A., Tuittila, E., Siljanen, H.M.P., Bodrossy, L., Fritze, H., 2018. Recovery of methane turnover and the associated microbial communities in restored cutover peatlands is strongly linked with increasing Sphagnum abundance. Soil Biology & Biochemistry 116, 110-119.
Raghoebarsing, A.A., Pol, A., van de Pas-Schoonen, K.T., Smolders, A.J.P., Ettwig, K.F., Rijpstra, W.I.C., Schouten, S., Damsté, J.S.S., Op Den Camp, H.J.M., Jetten, M.S.M., Strous, M., 2006. A microbial consortium couples anaerobic methane oxidation to denitrification. Nature 440, 918-921.
Reeburgh, W.S., 2007. Oceanic methane biogeochemistry. Chemical Reviews 107, 486-513.
Roden, E.E., Kappler, A., Bauer, I., Jiang, J., Paul, A., Stoesser, R., Konishi, H., Xu, H., 2010. Extracellular electron transfer through microbial reduction of solid-phase humic substances. Nature Geoscience 3, 417.
Roland, F.A.E., Darchambeau, F., Morana, C., Bouillon, S., Borges, A.V., 2017. Emission and oxidation of methane in a meromictic, eutrophic and temperate lake (Dendre, Belgium). Chemosphere 168, 756-764.
Rütters, H., Sass, H., Cypionka, H., Rullkötter, J., 2002. Phospholipid analysis as a tool to study complex microbial communities in marine sediments. Journal of Microbiological Methods 48, 149-160.
Sass, R.L., Fisher Jr, F.M., Ding, A., Huang, Y., 1999. Exchange of methane from rice fields: national, regional, and global budgets. Journal of Geophysical Research: Atmospheres 104, 26943-26951.
Saunois, M., Bousquet, P., Poulter, B., Peregon, A., Ciais, P., Canadell, J.G., Dlugokencky, E.J., Etiope, G., Bastviken, D., Houweling, S., 2016. The global methane budget 2000-2012. Earth System Science Data 8, 697.
Scheller, S., Yu, H., Chadwick, G.L., McGlynn, S.E., Orphan, V.J., 2016. Artificial electron acceptors decouple archaeal methane oxidation from sulfate reduction. Science 351, 703-707.
Segarra, K.E.A., Schubotz, F., Samarkin, V., Yoshinaga, M.Y., Hinrichs, K., Joye, S.B., 2015. High rates of anaerobic methane oxidation in freshwater wetlands reduce potential atmospheric methane emissions. Nature Communications 6, 7477.
Serrano-Silva, N., Sarria-Guzmán, Y., Dendooven, L., & Luna-Guido, M., 2014. Methanogenesis and methanotrophy in soil: A review. Pedosphere 24, 291-307.
Shen, L., Ouyang, L., Zhu, Y., Trimmer, M., 2019. Active pathways of anaerobic methane oxidation across contrasting riverbeds. The ISME Journal 13, 752-766.
Shen, L.D., Liu, S., Huang, Q., Lian, X., He, Z.F., Geng, S., Jin, R.C., He, Y.F., Lou, L.P., Xu, X.Y., Zheng, P., Hu, B.L., 2014. Evidence for the cooccurrence of nitrite-dependent anaerobic ammonium and methane oxidation processes in a flooded paddy field. Applied and Environmental Microbiology 80, 7611-7619.
Shi, Y., Wang, Z., He, C., Zhang, X., Sheng, L., Ren, X., 2017. Using 13C isotopes to explore denitrification-dependent anaerobic methane oxidation in a paddy-peatland. Scientific Reports 7, 40848.
Sinninghe Damsté, J.S., Rijpstra, W.I.C., Geenevasen, J.A., Strous, M., Jetten, M.S.M., 2005. Structural identification of ladderane and other membrane lipids of planctomycetes capable of anaerobic ammonium oxidation (anammox). The FEBS journal 272, 4270-4283.
Smemo, K.A., Yavitt, J.B., 2007. Evidence for anaerobic CH4 oxidation in freshwater peatlands. Geomicrobiology Journal 24, 583-597.
Smemo, K.A., Yavitt, J.B., 2011. Anaerobic oxidation of methane: an underappreciated aspect of methane cycling in peatland ecosystems? Biogeosciences 8, 779-793.
Tate, K.R., 2015. Soil methane oxidation and land-use change – from process to mitigation. Soil Biology & Biochemistry 80, 260-272.
Templeton, A.S., Chu, K., Alvarez-Cohen, L., Conrad, M.E., 2006. Variable carbon isotope fractionation expressed by aerobic CH4-oxidizing bacteria. Geochimica et Cosmochimica Acta 70, 1739-1752.
Vaksmaa, A., Guerrero-Cruz, S., van Alen, T.A., Cremers, G., Ettwig, K.F., Lüke, C., Jetten, M.S.M., 2017. Enrichment of anaerobic nitrate-dependent methanotrophic 'Candidatus Methanoperedens nitroreducens' archaea from an Italian paddy field soil. Applied Microbiology and Biotechnology 101, 7075-7084.
Vaksmaa, A., Lüke, C., van Alen, T., Valè, G., Lupotto, E., Jetten, M.S.M., Ettwig, K.F., 2016. Distribution and activity of the anaerobic methanotrophic community in a nitrogen-fertilized Italian paddy soil. FEMS Microbiology Ecology 92, w181.
Valentine, D.L., 2002. Biogeochemistry and microbial ecology of methane oxidation in anoxic environments: a review. Antonie van Leeuwenhoek 81, 271-282.
Valenzuela, E.I., Avendaño, K.A., Balagurusamy, N., Arriaga, S., Nieto-Delgado, C., Thalasso, F., Cervantes, F.J., 2019. Electron shuttling mediated by humic substances fuels anaerobic methane oxidation and carbon burial in wetland sediments. Science of the Total Environment 650, 2674-2684.
Voordeckers, J.W., Kim, B.C., Izallalen, M., Lovley, D.R., 2010. Role of Geobacter sulfurreducens uuter surface c-Type cytochromes in reduction of soil humic acid and Anthraquinone-2,6-Disulfonate. Applied and Environmental Microbiology 76, 2371-2375.
Wang, J., Cai, C., Li, Y., Hua, M., Wang, J., Yang, H., Zheng, P., Hu, B., 2018. Denitrifying anaerobic methane oxidation: A previously overlooked methane sink in intertidal zone. Environmental Science & Technology 53, 203-212.

Weber, H.S., Thamdrup, B., Habicht, K.S., 2016. High sulfur isotope fractionation associated with anaerobic oxidation of methane in a low-sulfate, iron-rich environment. Frontiers in Earth Science 4, 61.

Whalen, S.C., Reeburgh, W.S., Sandbeck, K.A., 1990. Rapid methane oxidation in a landfill cover soil. Applied and Environmental Microbiology 56, 3405-3411.

Wolf, M., Kappler, A., Jiang, J., Meckenstock, R.U., 2009. Effects of humic substances and quinones at low concentrations on ferrihydrite reduction by Geobacter metallireducens. Environmental Science & Technology 43, 5679-5685.

Yu, Z., Peiffer, S., Göttlicher, J., Knorr, K., 2015. Electron transfer budgets and kinetics of abiotic oxidation and incorporation of aqueous sulfide by dissolved organic matter. Environmental Science & Technology 49, 5441-5449.

Zhang, C.L., Li, Y., Ye, Q., Fong, J., Peacock, A.D., Blunt, E., Fang, J., Lovley, D.R., White, D.C., 2003. Carbon isotope signatures of fatty acids in Geobacter metallireducens and Shewanella algae. Chemical Geology 195, 17-28.

Zhang, M., Huang, J., Sun, S., Rehman, M.M.U., He, S., 2020. Depth-specific distribution and significance of nitrite-dependent anaerobic methane oxidation process in tidal flow constructed wetlands used for treating river water. Science of the Total Environment, 137054.

Zhang, X., Xia, J., Pu, J., Cai, C., Tyson, G.W., Yuan, Z., Hu, S., 2019. Biochar-mediated anaerobic oxidation of methane. Environmental Science & Technology 53, 6660-6668.

Zhou, L., Wang, Y., Long, X., Guo, J., Zhu, G., 2014. High abundance and diversity of nitrite-dependent anaerobic methane-oxidizing bacteria in a paddy field profile. FEMS Microbiology Letters 360, 33-41

1.8 Contributions to the included manuscripts

The PhD. thesis comprises publications and manuscripts which were elaborated in cooperation with various coauthors. The coauthors listed in these publications and manuscripts contributed as follows:

Study 1 To shake or not to shake: Silicone tube approach for incubation studies on CH_4 oxidation in submerged soils

Status: Published in *Science of The Total Environment* (2019)

Lichao Fan	experimental design and execution, data preparation and interpretation, manuscript preparation
Muhammad Shahbaz	discussion of experimental design; comments to improve the manuscript
Tida Ge	discussion of results, comments to improve the manuscript
Jinshui Wu	discussion of results, comments to improve the manuscript
Yakov Kuzyakov	discussion of results, comments to improve the manuscript
Maxim Dorodnikov	experimental design, data interpretation, discussion of results, comments to improve the manuscript

Study 2 To shake or not to shake: ^{13}C-based evidence on anaerobic methane oxidation in paddy soil

Status: Published in *Soil Biology & Biochemistry* (2019)

Lichao Fan	experimental design and execution, data preparation and interpretation, manuscript preparation
Muhammad Shahbaz	discussion of experimental design; comments to improve the manuscript
Tida Ge	discussion of results, comments to improve the manuscript
Jinshui Wu	discussion of results, comments to improve the manuscript
Volker Thiel	discussion of results, comments to improve the manuscript
Yakov Kuzyakov	discussion of results, comments to improve the manuscript
Maxim Dorodnikov	experimental design, data interpretation, discussion of results, comments to improve the manuscript

Study 3 Anaerobic oxidation of methane in paddy soil: Role of electron acceptors and fertilization in mitigating CH_4 fluxes

Status: Published in *Soil Biology & Biochemistry* (2020)

Lichao Fan	experimental design and execution, data preparation and interpretation, manuscript preparation
Michaela A. Dippold	discussion of results, comments to improve the manuscript
Tida Ge	discussion of results, comments to improve the manuscript
Jinshui Wu	discussion of results, comments to improve the manuscript
Volker Thiel	discussion of results, comments to improve the manuscript
Yakov Kuzyakov	discussion of results, comments to improve the manuscript
Maxim Dorodnikov	experimental design, data interpretation, discussion of

	results, comments to improve the manuscript

Study 4 Anaerobic methane oxidation: Active pathways and functioning of the microbial community network in paddy soils

Status: *submitted*

Lichao Fan	experimental design and execution, data preparation and interpretation, manuscript preparation
Dominik Schneider	data interpretation, discussion of results, comments to improve the manuscript
Michaela A. Dippold	discussion of results, comments to improve the manuscript
Weichao Wu	discussion of results, comments to improve the manuscript
Heng Gui	discussion of results, comments to improve the manuscript
Tida Ge	discussion of results, comments to improve the manuscript
Jinshui Wu	discussion of results, comments to improve the manuscript
Volker Thiel	discussion of results, comments to improve the manuscript
Yakov Kuzyakov	discussion of results, comments to improve the manuscript
Maxim Dorodnikov	experimental design, data interpretation, discussion of results, comments to improve the manuscript

2. Manuscripts

Study 1 To shake or not to shake: Silicone tube approach for incubation studies on CH_4 oxidation in submerged soils

Lichao Fan[a,*], Muhammad Shahbaz[b], Tida Ge[c], Jinshui Wu[c], Yakov Kuzyakov[a,d,e], Maxim Dorodnikov[a]

[a] Department of Soil Science of Temperate Ecosystems, University of Göttingen, 37077, Göttingen, Germany

[b] Department of Soil and Environment, Swedish University of Agricultural Sciences, Box 7014, 75007 Uppsala, Sweden

[c] Key Laboratory of Agro-ecological Processes in Subtropical Region & Changsha Research Station for Agricultural and Environmental Monitoring, Institute of Subtropical Agriculture, Chinese Academy of Sciences, 410125 Hunan, China

[d] Department of Agricultural Soil Science, University of Göttingen, 37077 Göttingen, Germany

[e] Institute of Environmental Sciences, Kazan Federal University, 420049 Kazan, Russia

Status: Published in Science of The Total Environment

Fan, L., Shahbaz, M., Ge, T., Wu, J., Kuzyakov, Y., Dorodnikov, M., 2019. To shake or not to shake: Silicone tube approach for incubation studies on CH4 oxidation in submerged soils. Science of The Total Environment 657, 893-901.

*** Corresponding Author**: Lichao Fan, lfan@gwdg.de

Abstract:
Incubation experiments are the most common approach to measure methane (CH_4) oxidation potential in soils from various ecosystems and land-use practices. However, the commonly used headspace CH_4 injection into microcosms and the shaking of the soil slurry during incubation fully removes CH_4 (soil-born) and O_2 (air-born) gradients common in *situ*, and may also induce various errors and disturbances. As an alternative, we propose CH_4 input into microcosm soils via a silicone tube located within the slurry. We hypothesized that (i) poor CH_4 diffusion in slurry will be compensated by direct CH_4 delivery into the slurry via a silicone tube and, consequently, (ii) shaking of microcosms can be substituted with the soil silicone tube CH_4 injection.
During a 29-day submerged paddy soil incubation, the highest net CH_4 oxidation rate was 1.6 μg C g^{-1} dry soil h^{-1}, measured between the 3rd and 7th day after injecting $^{13}CH_4$ into the slurry via a silicone tube without shaking. This rate was 1.5-2.5 times faster than the respective CH_4 oxidation after headspace injection without shaking (1st hypothesis supported). As expected, shaking accelerated CH_4 oxidation regardless of injection methods by 3.2-3.7 times (most intensively on days 3-7) compared to headspace injection without shaking. Nonetheless, the rates were similar between silicone tube injection without shaking and headspace injection with shaking. This supports the hypothesized potential of silicone tubes to substitute the common shaking method (2nd hypothesis). Furthermore, shaking increased the incorporation of ^{13}C from CH_4 into soil organic matter and microbial biomass by 1.8-2.7 times compared with CH_4 injection into tubes and the static control without tubes. This reflects an overestimation of CH_4 oxidation due to shaking. We conclude that direct soil CH_4 injection via silicone tubes is advantageous in incubation experiments because gas concentration gradients are maintained and thereby more realistically reflect natural soil conditions.

Keywords: $^{13}CH_4$; methane oxidation; paddy soil; slurry; shaking; silicone tube

1. Introduction

Methane (CH_4) is an important greenhouse gas with a 28-fold greater global warming potential compared to carbon dioxide (CO_2) (Forster et al., 2007). Importantly, the global CH_4 concentrations in the atmosphere have increased ~ 2.5-3.0 times since the industrial revolution (Keppler et al., 2006). CH_4 is anaerobically produced by methanogens, and most is oxidized to CO_2 by methanotrophs under aerobic conditions. Submerged paddy fields are hotspots for methanogenesis and, given that the global paddy field area is 164 million hectares (FAO, 2017), they are one of the largest human-related sources of CH_4, contributing 10-20% to global anthropogenic atmospheric CH_4 (Guo et al., 2017; Huang et al., 2014; Nayak et al., 2007; Win et al., 2016). CH_4 along with the availability of oxygen (O_2) at the soil-atmosphere interface as well as in the rhizosphere of rice plants (Le Mer and Roger, 2001) provides a high potential for CH_4 oxidation even in submerged paddy soils. Nonetheless, substantial uncertainties about CH_4 oxidation rates remain because of the large temporal and spatial variability of *in situ* CH_4 oxidation (Guo et al., 2017). The uncertainties associated with the current methods of CH_4 oxidation measurements under controlled conditions compound the problem.
A common approach to standardize measurements of CH_4 oxidation potential is based on controlled incubation experiments. Almost all laboratory CH_4 oxidation experiments on submerged soils use incubation microcosms with CH_4 injection into the microcosms' headspace and subsequent shaking of soil as slurry (Khalil and Baggs, 2005; Nayak et al., 2007). Because aerobic CH_4 oxidation is controlled by the availability of O_2 and CH_4 (Le Mer and Roger, 2001; Serrano-Silva et al., 2014), their diffusion from the headspace into the slurry is the "bottle neck" in measuring CH_4 oxidation rates (Le Mer and Roger, 2001; Castaldi et al., 2006). In contrast to O_2, however, which is two times more soluble in water than CH_4 (Sander, 2015), the CH_4 diffusion rate in water is four orders of magnitude lower than in air (Bender and Conrad, 1995). Accordingly, the transition of CH_4 from air to water is a limiting factor for the CH_4 oxidation process (Templeton et al., 2006). This entails a strong risk of

underestimating CH_4 oxidation in the incubation microcosms compared to natural submerged soils; in the latter, CH_4 produced in anaerobic zones is oxidized in the aerobic zones within the soil profile. To compensate for the low CH_4 solubility, the common microcosm approach requires continuous shaking of the slurry during incubation. Shaking, however, completely removes the *in situ* CH_4 and O_2 gradients. Other studies have demonstrated that dissolved O_2 is depleted within the top 3.5 mm surface layer of flooded rice bulk soil (without plants) under static conditions. Moreover, the CH_4 oxidation rate strongly decreases as the O_2 concentration drops with soil depth (Frenzel et al., 1992). Shaking also induces forced mixing of the gases (CH_4 and O_2) with the slurry, and the high headspace CH_4 concentration maintains a high rate of CH_4 oxidation (Cai and Mosier, 2000). More C-CH_4 is therefore expected to be incorporated into soil organic matter (SOM) and microbial biomass than under static conditions. The result is a strong overestimation of CH_4 oxidation. Finally, shaking also affects various other processes in soil (e.g. CO_2 efflux, pH gradients, substrate localization). Shaking inhibits methanogenesis: the cumulative anaerobic CH_4 oxidation with shaking was 33-80% lower than under static conditions (Fan et al., submitted).

Thus, in contrast to pulse headspace injection with shaking, the relatively slow CH_4 delivery belowground and O_2 diffusion from the headspace into soil should better mimic the common *in situ* gas gradients. This would mitigate the above-mentioned shortcomings in measuring the soil CH_4 oxidation potential. CH_4 can be continuously delivered into the soil slurry by using a silicone tube approach. This approach is commonly used for belowground gas sampling under field conditions (Kammann et al., 2001; Pausch and Kuzyakov, 2012). The porous silicone material allows exclusively gas to diffuse through the tube walls from the zone of high to low concentration, thereby promoting continuous release of CH_4.

The main goal of the study was to compare two approaches for estimating the potential CH_4 oxidation in submerged soils – the conventional headspace CH_4 injection with simultaneous shaking of the microcosms versus the novel direct soil CH_4 injection via silicone tubes under static conditions. We followed the incorporation of ^{13}C-labeled CH_4 into CO_2, microbial biomass and SOM (Lozanovska et al., 2016) of a paddy soil (as slurry), either with/without silicone tube or with/without shaking according to a full-factorial design. We hypothesized that (i) poor CH_4 diffusion in water (soil slurry) would be compensated for by directly delivering CH_4 into the soil through a silicone tube, yielding a faster CH_4 oxidation rate without shaking and, consequently, (ii) that shaking of microcosms can be efficiently substituted with the soil CH_4 silicone tube injection approach because the latter better reflects the common *in situ* gas gradients.

2. Materials and methods

2.1. Site description and soil collection

Soil samples were collected from a double rice cropping paddy field with early rice grown from late April to mid-July and late rice grown from late July to late October near Jinjing town, Changsha county of Hunan province in China (28°33′04″N, 113°19′52″E, 80 m above sea level). The paddy field has a tillage history of more than 1000 years of rice cultivation. The field has been plowed every time before rice seedlings transplanting and then flooded during the whole two rice growing periods starting from April to October. The soil (classified as a *Stagnic Anthrosol*) was sampled from the three replicated field plots under NPK additions. N was applied as urea (120-150 kg N ha^{-1}), P as $Ca(H_2PO_4)_2$ (18 kg P ha^{-1}) and K as K_2SO_4 (83 kg K ha^{-1}) (Shen et al., 2014). The soil texture was 26.7% clay, 29.2% silt, and 44.2% sand; the SOM content was 13.2 g C kg^{-1}, total nitrogen content 1.5 g kg^{-1}, soil microbial biomass carbon (MBC) 607 mg kg^{-1}, and pH 5.2. At each of the three replicated plots, four soil cores were collected from 10-20-cm depth (middle layer of a plough horizon 0-30 cm) using a soil auger. These cores were mixed and homogenized to form one composite sample per plot. There were no large stones in the paddy soil and the plant remnants were carefully removed before incubation. Soil samples were not sieved due to thorough regular ploughing and also to avoid un-

natural overexposure of soil to air. Field-moist samples were sealed and stored at 4 ℃ until needed for the experiment. For a detailed description of the area's climate and the experimental site, refer to Shen et al. (2014).

2.2. Experimental design and layout

To test the new approach of soil CH_4 injection by silicone tubes in a lab incubation experiment, we developed a microcosm with a silicone tube inside the soil (Fig. 1). A silicone tube (Carl Roth GmbH + Co. KG, Germany, inner diameter: 4 mm, wall thickness: 1 mm, surface area: 18.8 cm^2, volume: 1.2 ml) was fixed around a plastic cap and tied in place with stainless steel wires (Fig. 2). Both ends of the tube were sealed with silicone rubber septa, and one end was connected with a needle as a sampling port, sealed with a 3-way stopcock. During installation, care was taken to ensure that the silicone tubes were buried below the soil slurry: no parts of a tube had direct contact to the atmosphere, avoiding a "chimney effect".

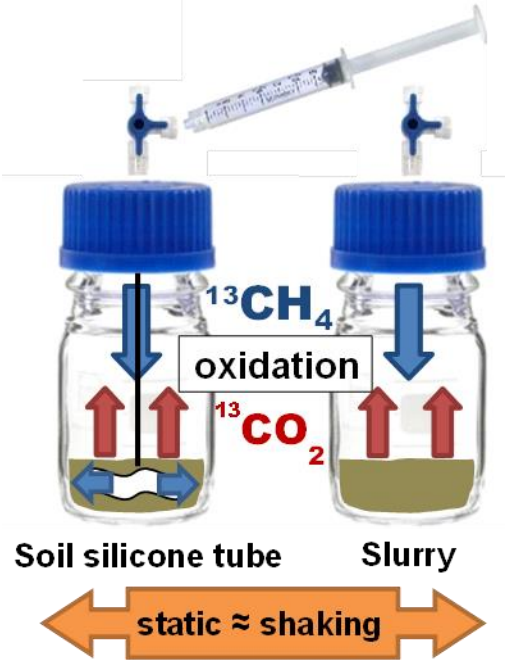

Fig. 1 Schematic diagram of the incubation experiment set-up with and without soil silicone tube (white color on the left), and with and without shaking. To estimate CH_4 oxidation potential, ^{13}C-labeled CH_4 was applied. Controls without CH_4 injection are not shown here.

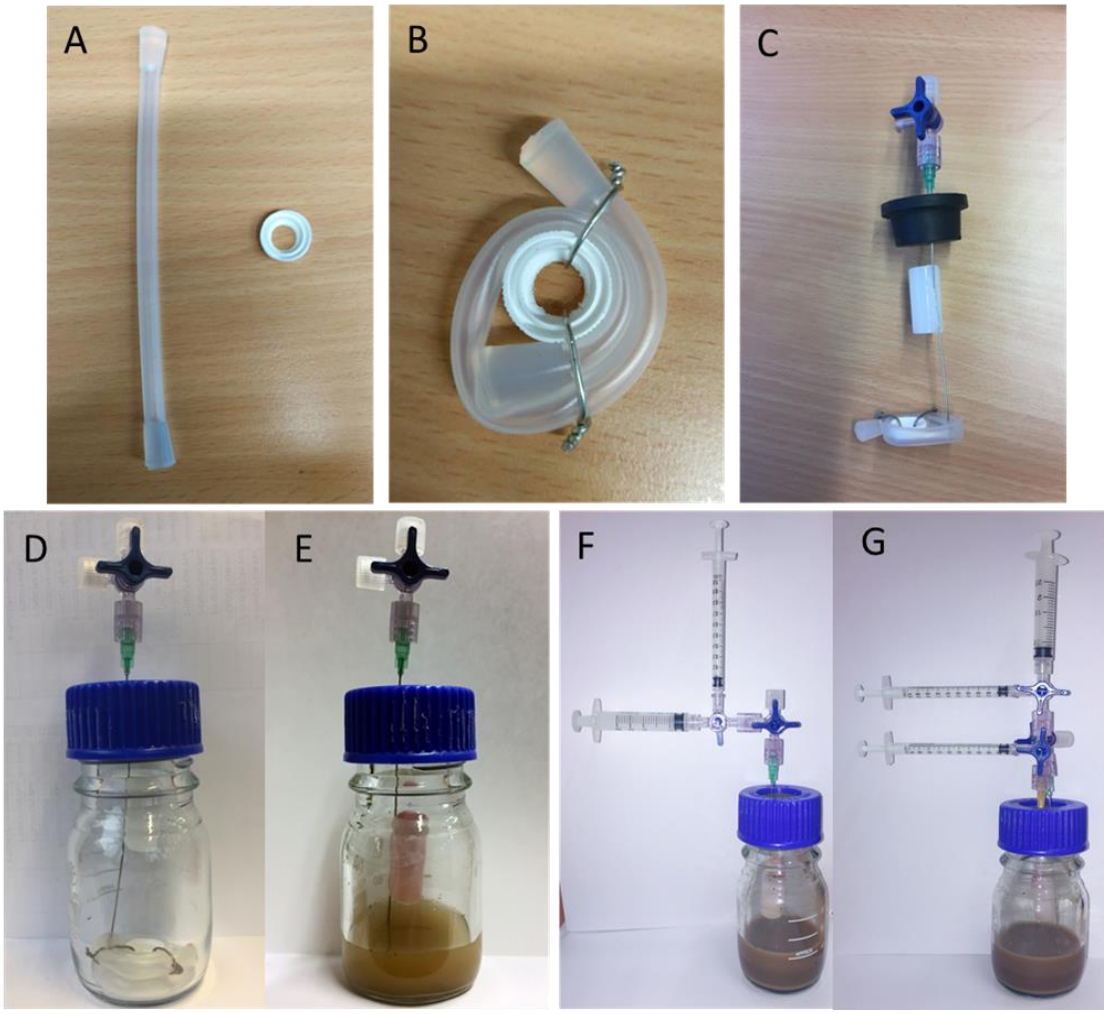

Fig. 2 The design of the soil silicone tube and its parameters (a, b), a set-up with a needle (c), an assembled incubation jar (d), the microcosm with slurry (e), the set-up for sampling with simultaneous N_2 replacement from silicone tube (f) and headspace (g). A plastic holder on a needle (c) is a site for an anaerobic indicator to control availability of O_2 in the headspace during incubation. S, the outside surface area of silicone tube.

The incubation experiment included four treatments – with/without soil silicone tube and with/without shaking (100 r min^{-1} during incubation, stopped for ca. 30 min for every gas sampling). We also included treatments testing the location of CH_4 injection – into the headspace (with/without tube) or into the soil (with tube). Altogether, five treatments including controls were prepared (Fig. S1): (1) CH_4 injection into the headspace and gas sampling from the headspace (I-headspace-headspace) and from the soil silicone tube simultaneously (I-headspace-tube), (2) injection via the silicone tube – sampling from the headspace (II-tube-headspace), (3) injection into the headspace – sampling from the headspace without silicone tube (III-headspace-headspace-no-tube), (4) control of CH_4 injection – sampling from the headspace (IV-control-headspace) and from the silicone tube simultaneously (IV-control-tube). To standardize gas removal, dilution due to sampling, and potential gas loss during the experiment, we set up blank jars (without soil) with silicone tubes. Thus, the last treatment (5) included a blank with CH_4 injection into the headspace and sampling from the headspace (V-blank-headspace-headspace) and from the tube simultaneously (V-blank-headspace-tube), and a blank with CH_4 injection into silicone tube – sampling from the headspace (V-blank-tube-headspace). Labeled CH_4 (4.8 ml 5 atom% ^{13}C-CH_4) was added to the headspace or to the soil silicone tube to quantify the net oxidation of $^{13}CH_4$ to $^{13}CO_2$ over time. Importantly, for the silicone tube, only CH_4 (no O_2) was injected because we aimed to mimic natural soil conditions. Under such conditions, CH_4 is produced

in the soil in an anaerobic environment and diffuses to the oxygenated surface layer, and O_2 diffuses into the soil mainly from the atmosphere. Note that we did not aim to mimic the situation with the delivery of O_2 belowground via rice plants' aerenchyma; this is because the effect of plants on CH_4 in such a case is much more complex than solely an oxidation process.

For the incubation, field-moist soil (20 g, 30% soil weight-based water content) was placed into 120 ml glass jars with wide necks, and 15 ml of deionized water was added to make a soil slurry. Visible plant debris and small stones were hand-removed prior to loading. Jars were sealed with gas-impermeable butyl rubber septa and fixed with plastic screw caps. The slurry was pre-incubated in the dark at 18℃ for 10 days to establish an equilibrium after disturbance caused by soil slurry preparation. At the end of the pre-incubation, the headspace was flushed with synthetic air (20/80% O_2/N_2) for 10 min through needles inserted in the septa. The soil silicone tubes were also flushed with synthetic air using two 25 ml syringes as input and exhaust ports switched by a three-way stopcock. Headspace and soil tube pressures were equilibrated to 101.3 *kPa*. Thereafter, gas was sampled for background values, after which 4.8 ml of 5 atom% ^{13}C-CH_4 was immediately injected into the jars designated to receive CH_4. After injection, the pressure of the headspace increased to 106.6 *kPa*, and the pressure inside the silicone tubes was 405.2 *kPa*. This allowed a gradual CH_4 release from the silicone tubes to the slurry. The pressure inside microcosms was measured with a gas pressure meter (gauge; GDH 13AN digital manometer, SMS-TORK, Istanbul, Turkey). To monitor oxygen availability after CH_4 injection, anaerobic indicators (Thermo scientific, Oxoid Ltd. Wade Road, Basingstoke, Hants, RG24 8PW, UK) were placed inside the jars and the color was regularly recorded (pink – aerobic, white – anaerobic). All indicators remained pink, i.e. the microcosms remained aerobic for the whole 29-day experiment.

During the incubation, gas samples were collected at 1, 3, 7, 12, 17, and 29 days after $^{13}CH_4$ injection. One-ml gas-tight syringes fitted with stopcocks were used to collect gas from the headspace (through septa with needles) and from soil tubes (through outlet ports). After each sampling, the equivalent volume of N_2 was injected to compensate any pressure loss and to maintain a slight overpressure. All gas samples were transferred to evacuate, N_2-flushed glass vials and diluted with N_2 (1 ml sample into 12 ml N_2). The CO_2 and CH_4 concentrations were then measured on a gas chromatograph (GC-14B, Shimadzu, Ld. Nds., Japan) equipped with a flame ionization detector (for CH_4) and an electron capture detector (for CO_2). A separate set of vials was used to determine the ^{13}C isotope composition, with a dilution of 1 ml sample into 15 ml N_2. The gas was analysed within two weeks after sampling.

2.3. Microbial biomass C and isotope analyses

The chloroform fumigation−K_2SO_4 extraction method was applied to determine post-incubation soil microbial biomass carbon (MBC). Briefly, 8 g (moist) soil from each microcosm was fumigated with ethanol-free $CHCl_3$ in an evacuated pot for 24 h in the dark at 22 ℃. Another 8 g (moist) soil was treated similarly but without $CHCl_3$ fumigation. After fumigation, samples were mixed with 32 ml of 0.05 M K_2SO_4 and shaken for 1 h. The extracts obtained were analyzed for total C content using a TOC/TIC analyzer (Multi N/ C 2100, Analytikjena, Germany). Microbial biomass C was calculated based on the difference between the extracted organic C content of the fumigated and the non-fumigated soils using k_{EC} factor = 0.45 (Joergensen, 1996).

Stable C isotopes of gas (CO_2) and solids (soil, dry K_2SO_4 extracts) were analyzed using an isotope ratio mass spectrometer (Delta plus IRMS, Thermo Fisher Scientific, Bremen, Germany). The ^{13}C values were corrected for the Vienna Peedee Belemnite (VPDB) standard and expressed as delta values ($\delta^{13}C$). For ^{13}C measurement of MBC, the K_2SO_4 extracts were freeze-dried and analyzed as solid material.

2.4. Calculations and statistics

The quantity of net $^{13}CH_4$ oxidized (*i.e.* $^{13}CO_2$ excess as an end-product of oxidation) at each time point (*i.e.* 1, 3, 7, 12, 17, and 29 days), and incorporation of CH_4-derived C into soil or microbial biomass at the end of incubation, was calculated using the following equation:

$$C_{OX} = \frac{(\delta^{13}C_{Total} - \delta^{13}C_{Control})}{(\delta^{13}C_{OX} - \delta^{13}C_{Control})} \times C_{Total} \quad (1)$$

Where C_{OX} (μg C) represents the estimated amount of net C-CH_4 oxidized based on the release of ^{13}C-CO_2, C_{Total} (μg C) represents the total amount of ^{13}C in the corresponding pool (*i.e.* CO_2, MBC, SOM), $\delta^{13}C_{Total}$ is the delta value of ^{13}C in CO_2 (or MBC and SOM) in the samples treated with $^{13}CH_4$, $\delta^{13}C_{Control}$ is the delta value of ^{13}C in CO_2 (or MBC and SOM) in the control (no $^{13}CH_4$ addition), and $\delta^{13}C_{OX}$ is the delta value of ^{13}C in CH_4 of 5 atom% (*i.e.* 3774‰). The rate of CH_4 oxidation was calculated using the differences between respective values of adjacent time points (e.g. 0^{th} vs. 1^{st} day, 1^{st} vs. 3^{rd} day, etc.). Rates are presented as C-CH_4 per gram of dry soil per hour.

Analyses of variance (ANOVA) were applied for dependent variables: ANOVA with repeated measures was used to determine the differences in CH_4 concentrations as well as the estimated CH_4 oxidation rates over 29 days incubation. The homogeneity of the residuals of the CH_4 concentrations and the CH_4 oxidation rates were tested. The Shapiro–Wilk test was used to test the normality of the CH_4 concentrations, the $\delta^{13}CO_2$ signatures, the CH_4 oxidation rates, total MBC and SOM as well as CH_4-derived MBC and SOM: all passed ($p > 0.05$) the normality test. *t*-tests were used to characterize differences with and without shaking. Standard errors were calculated using each set of three replicates from each instance of samples. All the statistical analyses were performed using SPSS software (ver. 19.0, SPSS Inc., Chicago, IL, USA) and SigmaPlot software (ver. 12.5, Systat Software, Inc, San Jose, California, USA).

3. Results

3.1. CH_4 dynamics and delta $^{13}CO_2$ signatures

Without shaking, the CH_4 was completely oxidized in 29 days of incubation when injected into and sampled from the headspace (Fig. 3 a, d, white circles). Injection into the soil via the silicone tube caused the CH_4 concentration ($[CH_4]$) in the headspace to significantly increase during the first three days of the incubation and then gradually decrease to zero by day 17 (Fig. 3 c). Injection into the headspace and sampling from the silicone tube without shaking resulted in a 3.0-7.5 times lower value compared to other injection/sampling approaches (Fig. 3 b). Both controls of CH_4 injection sampled either from the headspace or from the tube (Fig. 3 e, f) demonstrated low values with weak dynamics during the incubation period. This suggests a small contribution of newly produced CH_4 and hence negligible dilution of added CH_4.

Shaking oxidized the CH_4 5-12 days faster than without shaking, depending on the injection/sampling approaches (Fig. 3, black circles). It took the same time to complete CH_4 oxidation between shaking conditions and without shaking when injected into the soil slurry (Fig. 3 a vs. c). In total, the effects of shaking (vs. without shaking) and of the silicone tube (vs. without tube) on the $[CH_4]$ dynamics over 29 days were both significant at $p < 0.001$ (Table S1).

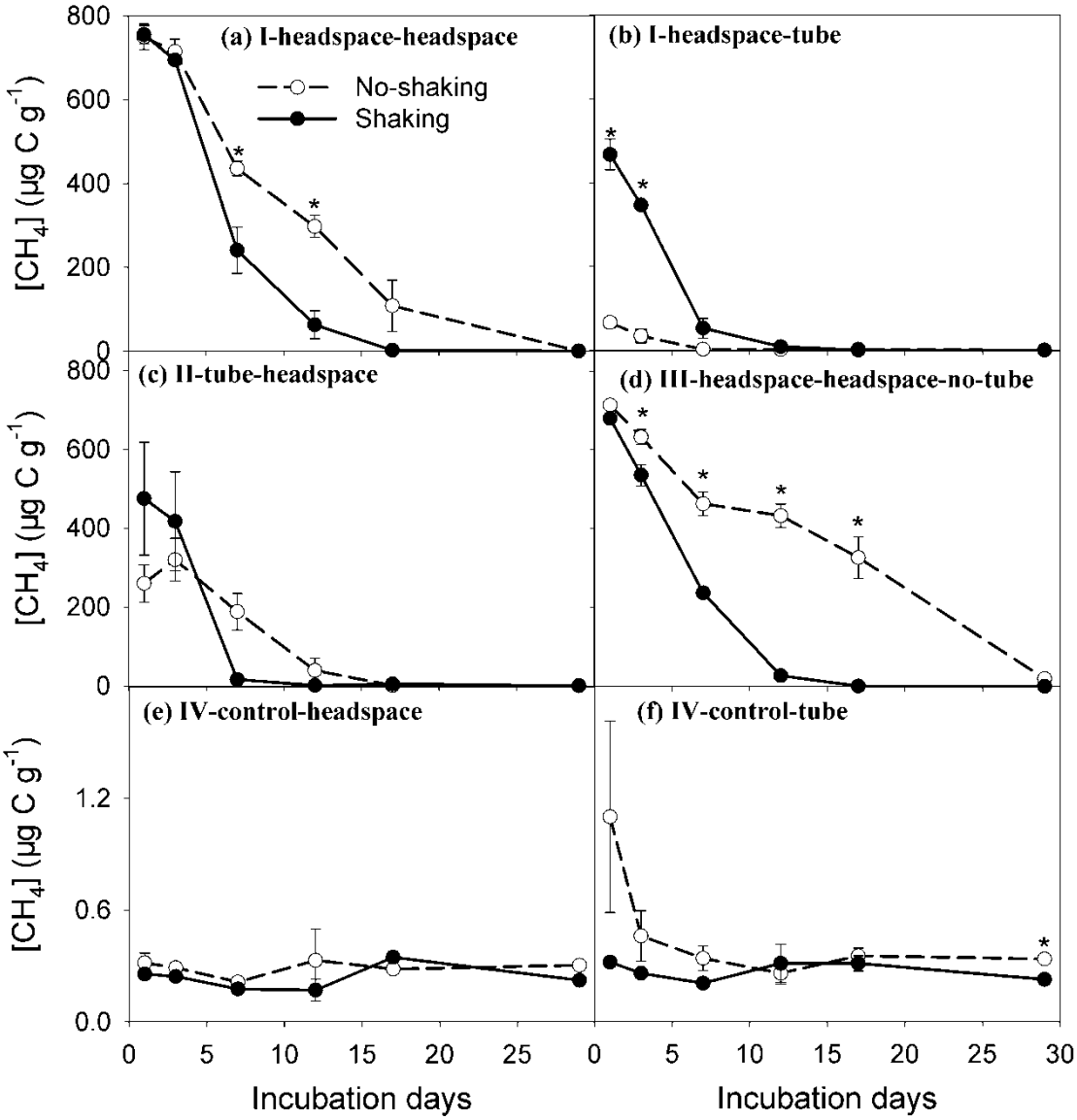

Fig. 3 Dynamics of CH_4 concentration ([CH_4]) over 29 days of incubation with and without shaking in the microcosms following headspace injection with either headspace sampling (a, I-headspace-headspace) or silicone tube sampling (b, I-headspace-tube), soil injection through silicone tube with headspace sampling (c, II-tube-headspace), and headspace injection without silicone tube with headspace sampling (d, III-headspace-headspace-no-tube), control without CH_4 injection with headspace sampling (e, IV-control-headspace) and silicone tube sampling (f, IV-control-tube). Asterisks: significant difference ($p < 0.05$) between shaking and no-shaking treatments. Error bars: standard error of means ($n = 3$).

Headspace CO_2 became ^{13}C enriched, with values of 800-1500‰ (Fig. 4) compared to controls without CH_4 injection, *i.e.* -23‰ to -29‰ (Fig. 4, $p < 0.001$). Between the injection/sampling approaches, the highest $\delta^{13}CO_2$ values without shaking were measured in the headspace after injection into the soil (Fig. 4 c). On average, $\delta^{13}C$ values of CO_2 were either similar between shaking or static conditions, or were even higher without shaking in microcosms with silicone tubes ($p < 0.05$). Shaking had a pronounced effect in soil without silicone tubes, where CO_2 had a 3-fold higher ^{13}C-enrichment compared with the static counterpart (Fig. 4d).

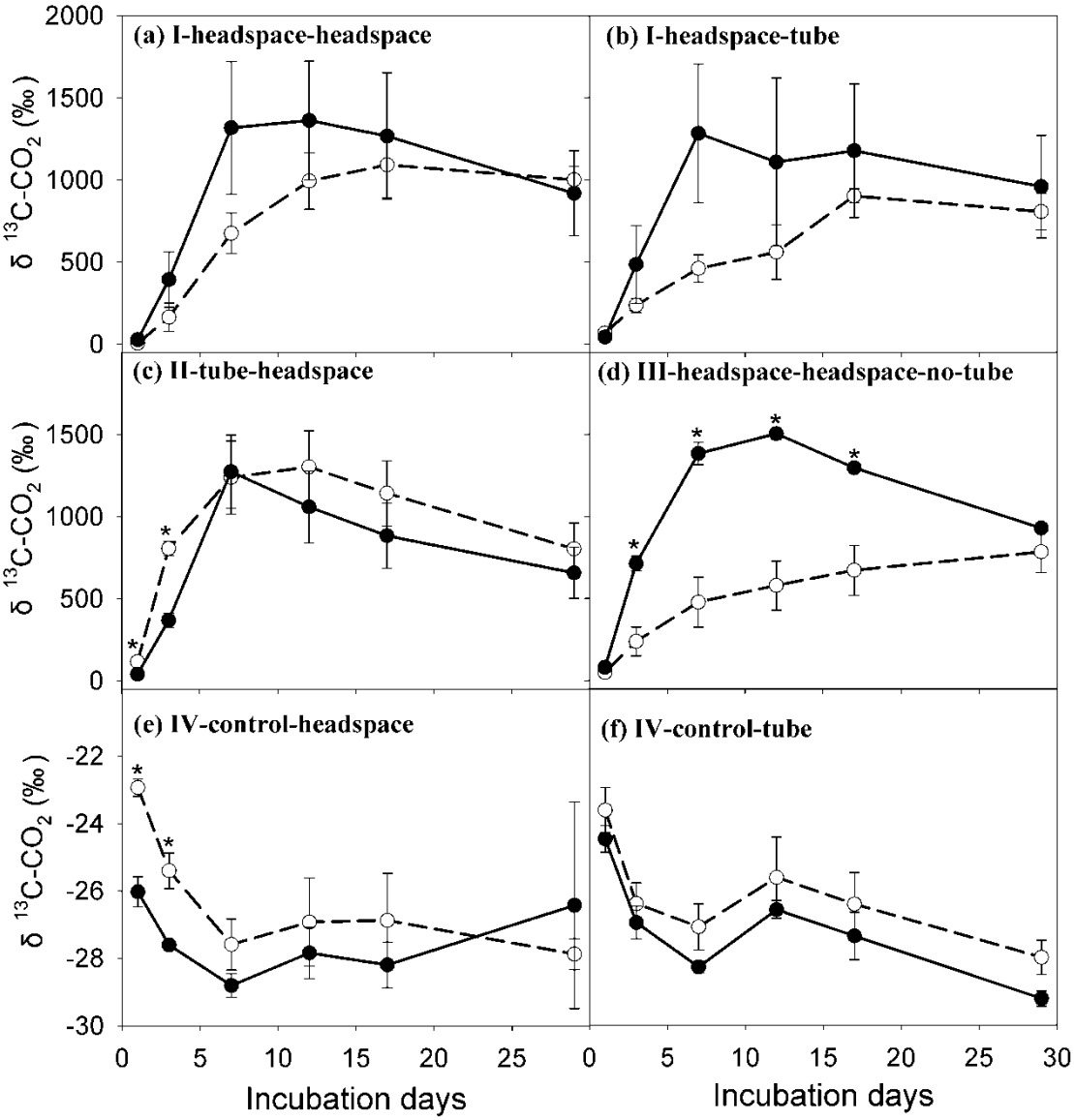

Fig. 4 Dynamics of $\delta^{13}CO_2$ signatures over 29 days with and without shaking in the microcosms subjected to the treatments (see (a)-(f) in Fig. 3). Asterisks: significant difference ($p < 0.05$) between shaking and no-shaking treatments. Error bars: standard error of means ($n = 3$).

3.2. CH_4 oxidation rate and incorporation of CH_4-derived C into SOM and MBC

Without shaking, the maximum CH_4 oxidation rate of 1.6 μg C g^{-1} soil h^{-1} was recorded during the 3rd to 7th day of incubation in microcosms in which CH_4 was injected into the soil slurry. This was faster than the other injection/sampling approaches without shaking (Fig. 5 c). Injection/sampling approaches had no effect on total SOM and MBC or on incorporation of CH_4-derived C into these pools (Fig. 6, white bars).

With shaking, the CH_4 oxidation rate increased rapidly during the first 7 days in all injection/sampling treatments, and the maximum CH_4 oxidation rates reached 1.7-2.7 μg C g^{-1} soil h^{-1} (Fig. 5, black circles). The rates were higher ($p < 0.05$) with shaking than without shaking under headspace CH_4 injection, but shaking did not affect these rates when the silicone tube was used. Overall, the effect of the tubes on CH_4 oxidation rate was significant ($p = 0.042$) without shaking, but insignificant with shaking ($p = 0.326$, Table S2).

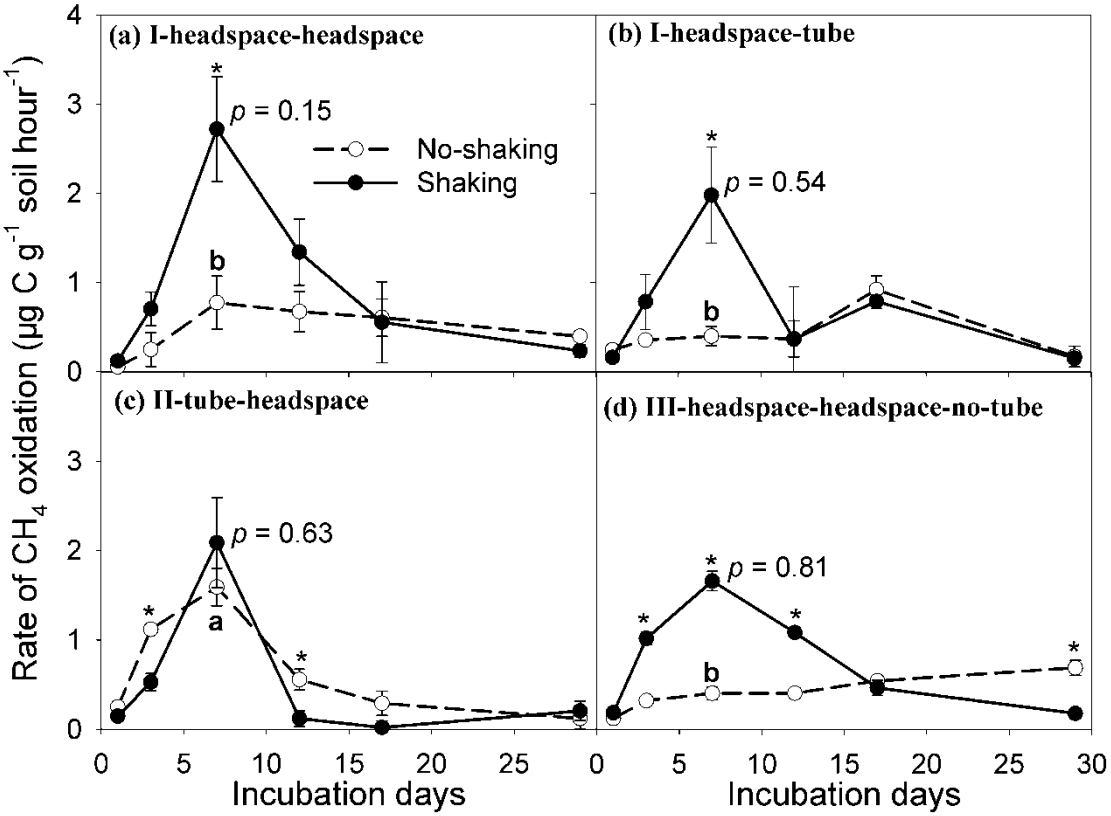

Fig. 5 CH_4 oxidation rates over 29 days of incubation with and without shaking. Estimations based on isotope mixing model (Eq. 1) for the microcosms subjected to the treatments (see (a)-(d) in Fig. 3). Lowercase letters: significant differences ($p < 0.05$) of the maximum CH_4 oxidation rates (day 7) between microcosms under no-shaking. Asterisks: significant difference ($p < 0.05$) between shaking and no-shaking at each instance of measurement. p values refer to t-test of the maximum CH_4 oxidation rates (day 7) between the soil injection without shaking (II-tube-headspace, white circles) and both injection approaches with shaking. Error bars: standard error of means ($n = 3$).

Neither SOM- nor CH_4-derived C in SOM and MBC were different between injection approaches with shaking (Fig. 6, black bars). Shaking, however, increased the incorporation of ^{13}C from CH_4 injected into the headspace to SOM and MBC by 1.8-2.7 times compared with no-shaking conditions (Fig. 6 b, d).

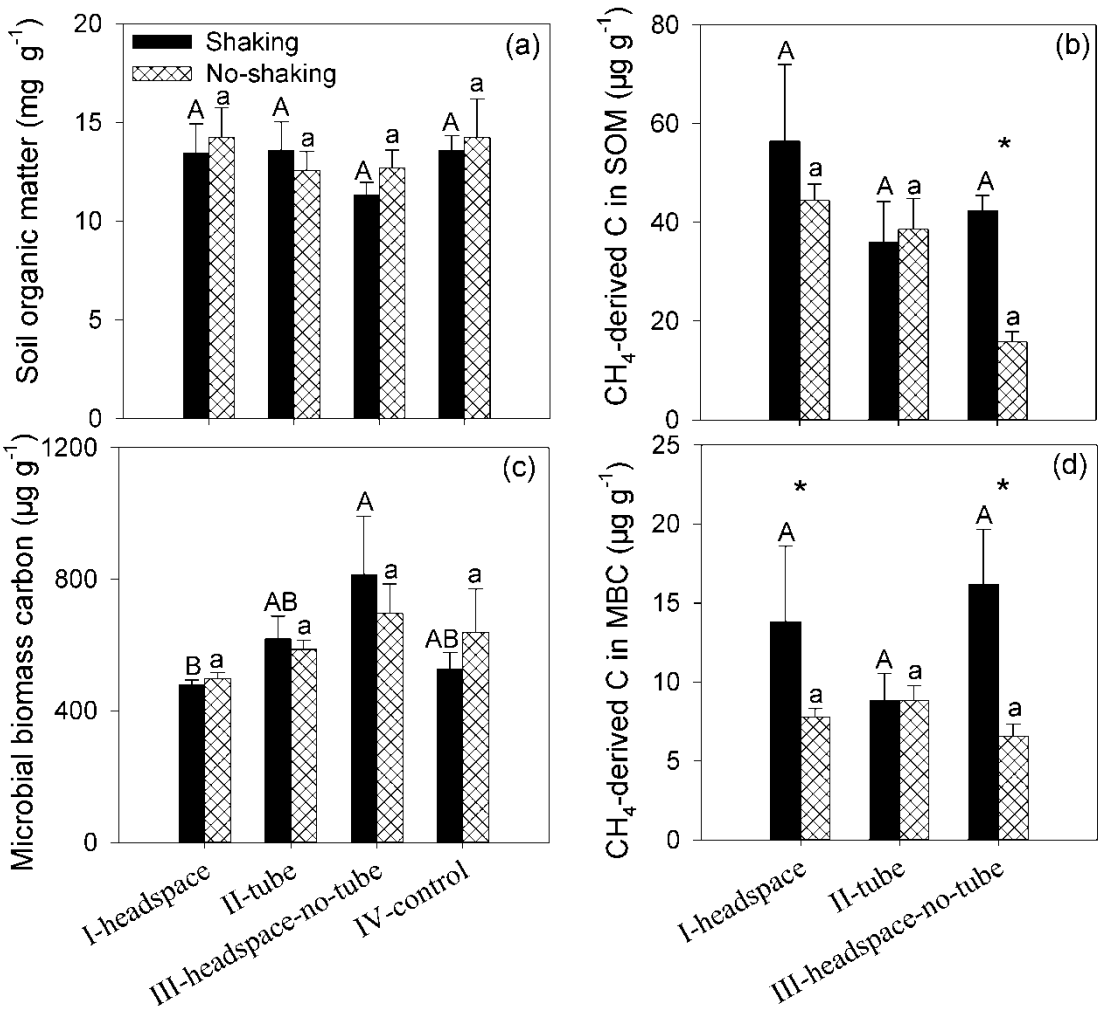

Fig. 6 Soil organic matter, SOM (a), CH_4-derived C in SOM (b), microbial biomass carbon, MBC (c) and CH_4-derived C in MBC (d) in microcosms with CH_4 injection into the headspace (I-headspace), to the silicone tube (II-tube), to the headspace without silicone tube (III-headspace-no-tube) and the control without CH_4 injection (IV-control, for SOM and MBC only) with and without shaking. Capital and lowercase letters: significant differences ($p < 0.05$) between microcosms with and without shaking, respectively. Asterisks: significant differences ($p < 0.05$) for each injection method between shaking and no-shaking.

4. Discussion

4.1. Effects of soil injection via silicone tube on CH_4 oxidation

Our tests on the soil CH_4 injection via silicone tubes on CH_4 oxidation in submerged soil are first of their kind that we know of. We assumed that the restricted CH_4 diffusion from the headspace into the soil slurry (Bender and Conrad, 1995) can be compensated by direct CH_4 delivery into the soil compared to the common shaking. Such a set-up enabled us to maintain the CH_4 and O_2 gradients typical of submerged soils, where CH_4 is produced and oxidized within the soil profile, but O_2 diffuses from the atmosphere. The soil slurry we used in the experiment partly resembles the field conditions, where intensive ploughing and simultaneous flooding completely destroys the soil structure, mixes it with water and creates slurry.

The results from microcosms without shaking confirmed the restricted CH_4 diffusion into the soil slurry. Thus, in the microcosms with CH_4 injection into the headspace and sampling from the silicone tube (I-headspace-tube), the CH_4 concentrations in soil were 5-7 times lower than with headspace injection and dropped to near zero after one week (Fig. 3 a, b, white circles). In contrast, for the CH_4 injected to the slurry through the silicone tube (II-tube-headspace) it took 2-3 days to reach the

maximum CH_4 concentration in the headspace. This demonstrates the slow, gradual release of the gas from the silicone tube through the soil where oxidation is occurring. The CH_4 oxidation rate when injected into the slurry (II-tube-headspace) was higher in the first week than for other injection/sampling approaches (Fig. 5 a, b and c). In agreement with the overall CH_4 concentration dynamics without shaking, the silicone tube approach accelerated oxidation compared to microcosms without soil tubes (Table S2). This supported our first hypothesis claiming that direct CH_4 delivery into the slurry via a silicone tube should compensate for poor CH_4 diffusion without shaking. Indeed, the continuous delivery of CH_4 into the slurry increased its availability for methanotrophs (Khalil and Baggs, 2005; Nayak et al., 2007) in contrast to CH_4 diffusion from the headspace. Finally, the silicone tube approach produced no side effects when compared to the control without the tube, either on the total SOM and MBC or on the contribution of new CH_4-derived C to SOM and MBC (Fig. 6 a-d, white bars). We did not, however, examine changes in the microbial community structure.

Accordingly, our silicone tube approach for microcosm studies coped with problems of gas diffusion and enabled gas delivery directly into soil. In a broader view, CH_4 injection to a depth of interest is promising for those experiments under field conditions designed to evaluate CH_4 oxidation and gas diffusion in various horizons. This approach would also be useful for belowground isotope labeling in water-saturated or unsaturated soils. The approach has broader applications than studies on CH_4 oxidation: it could be applied to study fluxes, diffusion and transformation of other gases, e.g. N_2O fluxes, CO_2 reduction through methanogenesis in soils, etc.

4.2. Effects of injection type and shaking on CH_4 oxidation

Shaking is a conventional method to maximize mass transfer and to enhance CH_4 equilibration during incubation experiments (Megraw et al., 1987; Van Winden et al., 2012; Whalen et al., 1990). In the context of this study, shaking accelerated CH_4 transfer from the headspace into the slurry because the initial CH_4 concentration in the silicone tube was higher with shaking than without shaking (Fig. 3 b). Faster CH_4 oxidation rates with shaking are explained by the mass transfer of reacting gases (CH_4 and O_2) into the slurry. Clearly, along with CH_4, O_2 is also a limiting factor for aerobic CH_4 oxidation in soil (Murase and Frenzel, 2007). Although we did not measure the O_2 concentration, the CH_4 was completely oxidized over 29 days, and the O_2 indicators showed no establishment of anaerobic conditions. We therefore conclude that the CH_4 concentration rather than O_2 was the limiting factor for CH_4 oxidation.

Importantly, the fastest oxidation rates in microcosms without shaking and with CH_4 injection into the soil via the silicone tube did not differ from those with shaking (Fig. 5, $p > 0.05$). We therefore conclude that the tube-based CH_4 injection facilitates gas diffusion between gas-solution-soil phases, which has a similar effect as shaking on CH_4 oxidation, as hypothesized. In contrast, shaking enhanced the incorporation of CH_4-derived C into microbial biomass and SOM compared with the static conditions (Fig. 6 b, d). This suggests that the former approach overestimates CH_4 oxidation. Accordingly, silicone tube injection can substitute shaking of microcosms. Further studies are necessary to test the approach under a variety of conditions, e.g. aerobic vs. anaerobic, slurry vs. cores, etc.

Our measured CH_4 oxidation rates agree with the respective rates for microcosms with shaking reported elsewhere. Conrad and Rothfuss (1991) and Krüger and Frenzel (2003) observed maximum rates between 1.9 and 4.7 μg C g^{-1} dry soil h^{-1} (our rates were 1.7-2.7 μg C g^{-1} dry soil h^{-1}) under continuous shaking (75-120 rpm) in slurry from paddy soils. The rates without shaking also coincided moderately well to several reported values, e.g. 0.3-0.6 μg C g^{-1} dry soil h^{-1} (Blazewicz et al., 2012) vs. 0.1-0.7 μg C g^{-1} dry soil h^{-1} in the current study (Fig. 5). The latter rates without shaking are 2-8 times slower than with shaking, even considering the diverse ecosystems and soils compared here. The CH_4 oxidation rate (1.6 μg C g^{-1} dry soil h^{-1}) via silicone tube injection was 2-4 times faster than headspace CH_4 injection without shaking and ca. 1.1 times slower (Fig. 5d, 1.7 μg C g^{-1} dry soil h^{-1}) than

conventional headspace CH_4 injection with shaking. Unfortunately, no studies have reported *in situ* CH_4 oxidation rates to compare with the silicone tube approach under controlled conditions. In summary, CH_4 injection by silicone tube is an advanced approach to measure the CH_4 oxidation potential because 1) the approach considers the CH_4 and O_2 gradients common in soils, 2) avoids underestimating CH_4 oxidation due to low CH_4 solubility and restricted diffusion – the main problem of the headspace injection approach without shaking and 3) excludes forced mixing induced by shaking.

5. Conclusions and outlook

Based on ^{13}C labeling, this study demonstrated for the first time that CH_4 injection through a silicone tube directly into the soil is an efficient approach for incubation studies on CH_4 oxidation. The direct injection through the tube compensated for poor CH_4 diffusion in water (soil slurry) and demonstrated faster CH_4 oxidation rates when compared to headspace CH_4 injection without shaking. There were no negative side-effects on gas dynamics or label incorporation into microbial biomass when compared to the control without silicone tubes. We therefore suggest that the silicone tube injection approach can be applied for many research objectives and questions (e.g. N_2O and CO_2 movement and transformation processes in soils) as well as for variety of ecosystems. This goes beyond inundated to include dry aerated environments, especially under field conditions. Finally, the silicone tube set-up is inexpensive and easy-to-build. As compared to the conventional shaking method, it demonstrated similar efficiency. This suggests that the former can substitute the latter, especially in light of the shortcomings of shaking such as the removal of gas and solute concentration gradients, microbial community disturbance, mixing of substrate sources, overestimation of label incorporation into SOM and MBC, etc. This makes direct soil CH_4 injection through silicone tubes without shaking a step forward in incubation studies towards more realistic natural soil conditions.

Acknowledgement

The authors are thankful to the China Scholarship Council (CSC) for funding to Lichao Fan in Germany, and German Research Foundation (DFG, Do 1533/2-1) and the National Natural Science Foundation of China (41761134095) for the research support. Special thanks to the Kompetenzzentrum Stabile Isotope (KOSI), Göttingen and personally to Lars Szwec and Reinhard Langel for the isotope analyses.

References:

Bender, M., Conrad, R., 1995. Effect of CH_4 concentrations and soil conditions on the induction of CH_4 oxidation activity. Soil Biology & Biochemistry 27, 1517-1527.

Blazewicz, S.J., Petersen, D.G., Waldrop, M.P, Firestone, M.K., 2012. Anaerobic oxidation of methane in tropical and boreal soils: Ecological significance in terrestrial methane cycling. Journal of Geophysical Research-Biogeosciences 117(G2).

Cai, Z.C., Mosier, A.R., 2000. Effect of NH_4Cl addition on methane oxidation by paddy soils. Soil Biology & Biochemistry 32, 1537-1545.

Castaldi, S., Ermice, A., Strumia, S., 2006. Fluxes of N_2O and CH_4 from soils of savannas and seasonally - dry ecosystems. Journal of Biogeography 33, 401-415.

Conrad, R., 2005. Quantification of methanogenic pathways using stable carbon isotopic signatures: a review and a proposal. Organic Geochemistry 36, 739-752.

Conrad, R., Rothfuss, F., 1991. Methane oxidation in the soil surface layer of a flooded rice field and the effect of ammonium. Biology and Fertility of Soils 12, 28-32.

Fan, L., Shahbaz, M., Ge, T., Wu, J., Dippold, M., Thiel, V., Kuzyakov, Y., Dorodnikov, M., (2018). To shake or not to shake: ^{13}C-based evidence on anaerobic methane oxidation in paddy soil. Soil Biology & Biochemistry, submitted.

Food and Agriculture Organizatin of the United Nations 2017. Rice market monitor. XX, 1.

Forster, P., Ramaswamy, V., Artaxo, P., Berntsen, T., Betts, R., Fahey, D. W., Haywood, J., Lean, J., Lowe, D. C., Myhre, G. 2007. Changes in atmospheric constituents and in radiative forcing. Chapter 2. in Climate Change 2007. The Physical Science Basis.

Frenzel, P., Rothfuss, F., Conrad, R., 1992. Oxygen profiles and methane turnover in a flooded rice microcosm. Biology and Fertility of Soils 14, 84-89.

Guo, J., Song, Z., Zhu, Y., Wei, W., Li, S., Yu, Y., 2017. The characteristics of yield-scaled methane emission from paddy field in recent 35-year in China: A meta-analysis. Journal of Cleaner Production 161, 1044-1050.

Huang, H. Y., Cao, J. L., Wu, H. S., Ye, X. M., Ma, Y., Yu, J. G., Shen, Q. R., Chang, Z. Z., 2014. Elevated methane emissions from a paddy field in southeast China occur after applying anaerobic digestion slurry. Global Change Biology Bioenergy 6, 465-472.

Joergensen, R.G., 1996. The fumigation-extraction method to estimate soil microbial biomass: Calibration of the k_{EC} value. Soil Biology & Biochemistry 28, 25-31.

Kammann, C., Grünhage, L., Jäger, H.J., 2001. A new sampling technique to monitor concentrations of CH_4, N_2O and CO_2 in air at well - defined depths in soils with varied water potential. European Journal of Soil Science 52, 297-303.

Keppler, F., Hamilton, J.T., Braß, M., Röckmann, T., 2006. Methane emissions from terrestrial plants under aerobic conditions. Nature 439, 187.

Khalil, M.I., Baggs, E.M., 2005. CH_4 oxidation and N_2O emissions at varied soil water-filled pore spaces and headspace CH_4 concentrations. Soil Biology & Biochemistry 37, 1785-1794.

Krüger, M., Frenzel, P., 2003. Effects of N - fertilisation on CH_4 oxidation and production, and consequences for CH_4 emissions from microcosms and rice fields. Global Change Biology 9, 773-784.

Le Mer, J., Roger, P., 2001. Production, oxidation, emission and consumption of methane by soils: A review. European Journal of Soil Science 37, 25 - 50.

Lozanovska, I., Kuzyakov Y., Krohn J., Parvin S., Dorodnikov M., 2016. Effects of nitrate and sulfate on greenhouse gas emission potentials from microform-derived peats of a boreal peatland: A ^{13}C tracer study. Soil Biology & Biochemistry 100, 182-191.

Megraw, S.R., Knowles, R., 1987. Methane production and consumption in a cultivated humisol. Biology and Fertility of Soils 5, 56-60.

Murase, J., Frenzel, P., 2007. A methane - driven microbial food web in a wetland rice soil. Environmental Microbiology 9, 3025-3034.

Nayak, D.R., Babu, Y.J., Datta, A., Adhya, T.K., 2007. Methane oxidation in an Iintensively cropped tropical rice field soil under long-term application of organic and mineral fertilizers. Journal of Environmental Quality 36, 1577-1584.

Pausch J., Kuzyakov Y. 2012. Soil organic carbon decomposition from recently added and older sources estimated by $\delta^{13}C$ values of CO_2 and organic matter. Soil Biology & Biochemistry 55, 40-47.

Sander, R., 2015. Compilation of Henry's law constants (version 4.0) for water as solvent. Atmospheric Chemistry and Physics 15, 4399-4981.

Serrano-Silva, N., Sarria-Guzmán, Y., Dendooven, L., Luna-Guido, M., 2014. Methanogenesis and methanotrophy in soil: a review. Pedosphere 24, 291-307.

Shen, L. D., Liu, S., Huang, Q., Lian, X., He, Z. F., Geng, S., Jin, R. C., He, Y. F., Lou, L. P., Xu, X. Y., Zheng, P., Hu, B. L., 2014. Contrasting effects of straw and straw-derived biochar amendments on greenhouse gas emissions within double rice cropping systems. Agriculture, Ecosystems & Environment 188, 264-274.

Templeton, A.S., Chu, K., Alvarez-Cohen, L., Conrad, M.E., 2006. Variable carbon isotope fractionation expressed by aerobic CH_4-oxidizing bacteria. Geochimica et Cosmochimica Acta 70, 1739-1752.

Tyler, S.C., Crill, P.M., Brailsford, G.W., 1994. $^{13}C^{12}C$ Fractionation of methane during oxidation in a temperate forested soil. Geochimica et Cosmochimica Acta 58, 1625-1633.

van Winden, J. F., Talbot, H. M., De Vleeschouwer, F., Reichart, G., Sinninghe Damsté, J. S., 2012. Bacteriohopanepolyol signatures as markers for methanotrophic bacteria in peat moss. Geochimica et Cosmochimica Acta 77, 52-61.

Whalen, S.C., Reeburgh, W.S., Sandbeck, K.A., 1990. Rapid methane oxidation in a landfill cover soil. Applied and Environmental Microbiology 56, 3405-3411.

Win, A. T., Toyota, K., Ito, D., Chikamatsu, S., Motobayashi, T., Takahashi, N., Ookawa, T., Hirasawa, T., 2016. Effect of two whole-crop rice (*Oryza sativa L.*) cultivars on methane emission and Cu and Zn uptake in a paddy field fertilized with biogas slurry. Journal of Soil Science and Plant Nutrition 62, 99-105.

Yan, X., H. Akiyama, K. Yagi, H. Akimoto. 2009. Global estimations of the inventory and mitigation potential of methane emissions from rice cultivation conducted using the 2006 Intergovernmental Panel on Climate Change Guidelines. Global Biogeochemical Cycles 23, GB2002.

Supporting Information for study 1

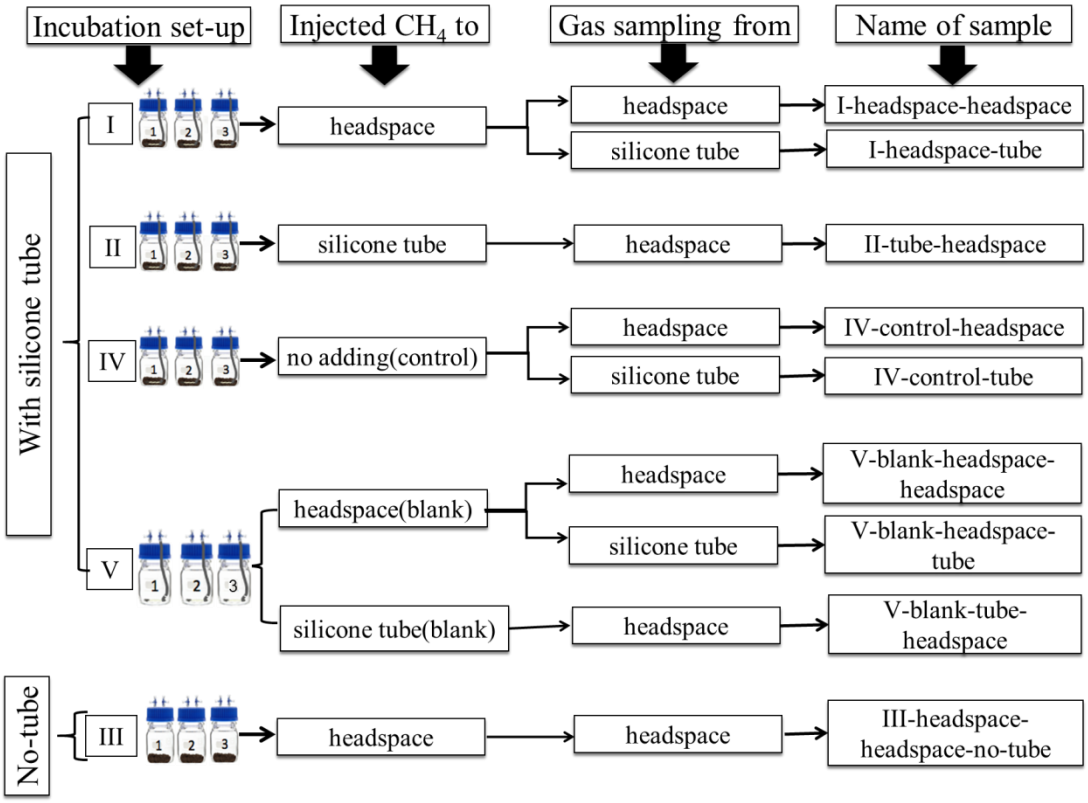

Fig. S1 Conceptual diagram of incubation experimental design and sample codes.

Table S1 Summary table for two-way ANOVA repeated measures reflecting the significance of the effects of soil silicone tube, duration of incubation (29 days) and their interactions on CH_4 concentration with and without shaking.

Source of Variation	Degree of freedom	Sum of Squares	Mean Square	F	*p*
		Shaking			
Inner soil tube	5	1332755	266551	36.4	< 0.001
Subject (inner soil tube)	12	87782	7315		
Time	5	2863109	572622	195	< 0.001
Inner soil tube × time	25	1684342	67374	22.9	< 0.001
Residual	60	176400	2940		
Total	107	6144388	57424		
		No-shaking			
Inner soil tube	5	2874464	574893	170	< 0.001
Subject (inner soil tube)	12	40550	3379		
Time	5	1548558	309712	454	< 0.001
Inner soil tube × time	25	1809452	72378	106	< 0.001
Residual	60	40928	682		
Total	107	6313952	59009		

Table S2 Summary table for two-way ANOVA repeated measures reflecting the significance of the effects of soil silicone tube, duration of incubation (29 days) and their interactions on rate of CH_4 oxidation with and without shaking.

Source of Variation	Degree of freedom	Sum of Squares	Mean Square	F	*p*
		Shaking			
Inner soil tube	3	2.40	0.80	1.32	0.335
Subject (inner soil tube)	8	4.85	0.61		
Time	5	46.7	9.35	41.1	< 0.001
Inner soil tube × time	15	5.18	0.35	1.52	0.144
Residual	40	9.09	0.23		
Total	71	68.3	0.96		
		No-shaking			
Inner soil tube	3	0.93	0.31	4.74	0.035
Subject (inner soil tube)	8	0.52	0.07		
Time	5	4.64	0.93	24.4	< 0.001
Inner soil tube × time	15	4.92	0.33	8.64	< 0.001
Residual	40	1.52	0.04		
Total	71	12.5	0.18		

Study 2 To shake or not to shake: ^{13}C-based evidence on anaerobic methane oxidation in paddy soil

Lichao Fan[a,*], Muhammad Shahbaz[b], Tida Ge[c], Jinshui Wu[c], Michaela Dippold[d], Volker Thiel[e], Yakov Kuzyakov[a,f,g], Maxim Dorodnikov[a]

[a] Department of Soil Science of Temperate Ecosystems, Georg August University of Göttingen, 37077, Göttingen, Germany

[b] Department of Soil and Environment, Swedish University of Agricultural Sciences, 75007 Uppsala, Sweden

[c] Key Laboratory of Agro-ecological Processes in Subtropical Region & Changsha Research Station for Agricultural and Environmental Monitoring, Institute of Subtropical Agriculture, Chinese Academy of Sciences, Hunan 410125, China

[d] Biogeochemistry of Agroecosystems, Department of Crop Sciences, Georg August University of Göttingen, 37077 Göttingen, Germany

[e] Geobiology, Geoscience Center, Georg August University of Göttingen, 37077 Göttingen, Germany

[f] Department of Agricultural Soil Science, Georg August University of Göttingen, 37077 Göttingen, Germany

[g] Institute of Environmental Sciences, Kazan Federal University, 420049 Kazan, Russia

Status: Published in Soil Biology & Biochemistry

Fan, L., Shahbaz, M., Ge, T., Wu, J., Dippold, M., Thiel, V., Kuzyakov, Y., Dorodnikov, M., 2019. To shake or not to shake: ^{13}C-based evidence on anaerobic methane oxidation in paddy soil. Soil Biology & Biochemistry 133, 146-154.

*** Corresponding Author**: Lichao Fan, lfan@gwdg.de

Abstract
The anaerobic oxidation of methane (AOM) removes most of the biologically produced methane (CH_4) from marine ecosystems before it enters the atmosphere and thus mitigates greenhouse gas emissions. As compared to marine environments, surprisingly little is known about the role of AOM in terrestrial ecosystems. Particularly, how AOM controls the CH_4 budget of paddy soils is unexplored, partly reflecting analytical difficulties in analyzing CH_4 turnover. To date, the most commonly used method to study AOM in soils is *in vitro* incubation of microcosms with CH_4 injection into the headspace with/without shaking of slurry. Shaking, however, introduces various errors and disturbances. Here we measured AOM in rice paddy soil using a new alternative approach that introduced ^{13}C-labelled CH_4 directly into soil slurry via a silicone tube without shaking. The results were compared to those obtained by the classical approaches (i.e., with and without tubes and/or shaking). In all batches, ^{13}C enrichment of CO_2 after $^{13}CH_4$ injection clearly confirmed the occurrence of AOM in paddy soil. The cumulative AOM during 59 days reached 0.16-0.24 μg C g^{-1} dry soil without shaking, but it was 33-80% lower with shaking. Unexpectedly, the effect of silicone tubes on AOM was insignificant either with or without shaking, suggesting that the CH_4 concentration in water (slurry) was not the main limiting factor for AOM. Without shaking, the controls without CH_4 addition revealed a steady increase of CH_4 in the headspace/tube, whereas the CH_4 concentration in jars with shaking was constantly low during 59 days. This suggests that shaking inhibited methanogenesis. There was a strong linear correlation between the amount of CH_4 oxidized and CH_4 produced with shaking (R^2 = 0.91), whereas without shaking this relationship followed a power growth regression. Based on the current and reported AOM rates, rough upscale to paddy soils in China showed recycling of ca. 2.0 Tg C of CH_4 each year, making AOM a crucial terrestrial CH_4 sink.

Key words: AOM; CH_4 oxidation; ^{13}C-CH_4; paddy soil; rice cultivation, greenhouse gas emissions, incubation methods

1 Introduction

Investigations of the biogeochemical cycle of methane (CH_4) in terrestrial ecosystems have focused mainly on methanogenesis and aerobic CH_4 oxidation (Lai, 2009; Luna-Guido, 2014; Tate, 2015), whereas another global process, the anaerobic oxidation of methane (AOM), has been underappreciated. For marine environments, ample studies have demonstrated that AOM, mainly linked to sulfate reduction, consumes up to 80% of CH_4 produced in sediments and is therefore critically important for the global carbon (C) cycle (see Valentine, 2002 and Knittel & Boetius, 2009 for reviews). Studies on freshwater sediments have also reported high rates of AOM in limnic ecosystems (Deutzmann et al., 2014; Segarra et al., 2015; Weber et al., 2016). AOM in terrestrial ecosystems, in contrast, receives rare but increasing attention. Smemo and Yavitt (2007) were among the first to conclusively prove the occurrence of AOM in several peatlands. Gupta et al. (2013) and Gauthier et al. (2015) revealed widespread AOM over a wide range of peatland types and soil management practices. The process, however, is still not included in most process-based biogeochemical models (Gauthier et al., 2015). Accordingly, there is a strong need to study AOM occurrence, ecological relevance and underlying mechanisms in various terrestrial environments to deepen our current understanding of global CH_4 cycling.

Wetlands and submerged agricultural soils such as paddy fields are the primary sources of the increasing biogenic CH_4 concentrations in the atmosphere (Nisbet et al., 2016; Saunois et al., 2016). Paddy soils have specific physical and chemical properties compared to natural wetlands due to rice field management practices including fertilizer application (Kögel-Knabner et al., 2010; Ge et al., 2017; Wei et al., 2018). Depending on the intensity of the process, AOM may regulate the net CH_4 efflux from these agroecosystems.

AOM measurements in *situ* are still challenging to conduct and rarely reported (Roland et al., 2016) due to the dynamics of the physicochemical conditions in deeper soil layers and problems in separating gross and net processes of CH_4 cycling (Smemo and Yavitt, 2011). Current studies on AOM in terrestrial ecosystems are largely based on microcosm incubations with headspace CH_4 injection with or without shaking (Gupta et al., 2013; He et al., 2015; Hu et al., 2015). Shaking enhances the gas equilibration between gas-liquid phases (Megraw and Knowles, 1987; Whalen et al., 1990; Van Winden et al., 2012). Mechanical disturbances however, introduce various errors: unrealistically low/high rates of AOM, large variation between replicates, accelerated redox-processes, etc. Without shaking, on the other hand, there is a strong risk of systematically underestimating CH_4 oxidation due to relatively low CH_4 solubility (as compared to e.g. CO_2) and its restricted diffusion through water (Bender and Conrad, 1995).

We hypothesized that the shortcomings of headspace CH_4 injection into microcosm can be overcome with an approach that partly mimics *in situ* conditions: the belowground injection of ^{13}C-labelled CH_4 via silicone tubes directly to the slurry simulates the expected natural release via methanogenesis and diffusion throughout the soil profile (Fan et al., 2019). We then observed the fate of the ^{13}C-label from CH_4 into CO_2 in a paddy soil, microbial biomass and dissolved organic carbon with/without silicone tubes and with/without shaking to answer the following research questions:

(i) Does AOM occur in submerged paddy soil and at which rates?

(ii) Does CH_4 injection via silicone tubes enhance AOM as compared with the traditional headspace injection?

(iii) Does shaking disturb AOM as compared with the static slurry?

2 Materials and methods

2.1 Site description and soil collection

The study region is located near Jinjing town, Changsha county of Hunan province in China (28°33′04″N, 113°19′52″E), which is characterized by a subtropical humid monsoon climate with a mean annual precipitation of 1330 mm and annual air temperature of 17.5°C. Soils were obtained from a batch of samples described in Fan et al. (2019). Briefly, these samples were collected from a double rice cropping paddy field (with early rice grown in late April to mid-July and late rice grown in mid-July to late October). The paddy field has a tillage history of more than 1000 years of rice production. The field has been plowed every time prior to the transplanting of rice seedlings and remained continuously flooded during the two rice growing periods starting from April to October. The soil at the experimental field is classified as *Stagnic Anthrosol* developed from red granite parental material (Shen et al., 2014a; Huang et al., 2018). The soil texture was 26.7% clay, 29.2% silt, and 44.2% sand; the soil organic carbon (SOC) content was 13.2 g kg^{-1}, total nitrogen content was 1.5 g kg^{-1}, soil microbial biomass carbon (MBC) was 607 mg kg^{-1}, and pH was 5.2. The soil was sampled from three replicated field plots under NPK treatment. N was applied as urea (120-150 kg N ha^{-1}), P as $Ca(H_2PO_4)_2$ (18 kg P ha^{-1}) and K as K_2SO_4 (83 kg K ha^{-1}) (Shen et al., 2014a). At each of the three replicated plots, we collected four soil cores from 10-20 cm depth (middle layer of a plow horizon 0-30 cm) with a soil auger. The samples were mixed and homogenized to form one composite sample per plot, and immediately sealed in plastic bags. There were no large stones in the paddy soil and the plant remnants were carefully removed before incubation. Soil samples were not sieved due to originally thorough regular plowing and also to avoid un-natural overexposure of soil to air. The air in the bags was evicted to minimize exposure to atmospheric oxygen (O_2). Soil samples were transported to the University of Göttingen, Germany, where they were stored in a cooling room (4 °C) until incubation start.

2.2. Experimental setup

The silicone tube approach for the direct CH_4 delivery into the soil (Fan et al., 2019) consisted of a silicone tube (inner diameter: 0.4 cm, wall thickness: 0.1 cm, volume: 1.2 ml, surface area: 18.8 cm^2) which was fixed around a plastic cap and tied in place with stainless steel wires. Both tube ends were sealed with silicone rubber septa. One end was connected with a needle sealed with a 3-way stopcock that served as a sampling port (Fig. S1).

To determine the potential for AOM in paddy soils and the effects of silicone tube injection and shaking, anaerobic laboratory incubations with or without silicone tube and with or without shaking (100 rounds min^{-1}) were conducted. The incubation experiment included CH_4 injection both into the headspace (with and without tube) or into the soil (with tube).

Altogether, five treatments including controls were prepared (Fig. S2): (I) CH_4 injection into the headspace and gas sampling from the headspace (headspace-headspace) and from the soil silicone tube simultaneously (headspace-tube), (II) CH_4 injection into the silicone tube and gas sampling from the headspace (tube-headspace), (III) control with no CH_4 injection and gas sampling from the headspace (control-headspace) and from the silicone tube simultaneously (control-tube). To consider the gas removal, dilution due to sampling and potential gas loss during the experiment, we set up blank jars (without soil) with silicone tubes. Thus, treatment (IV) involved a blank with CH_4 injection into the headspace and gas sampling from the headspace (blank-headspace-headspace) and from the tube simultaneously (blank-headspace-tube), as well as a blank with CH_4 injection into the silicone tube and gas sampling from the headspace (blank-tube-headspace). (V) CH_4 injection into the headspace and gas sampling from the headspace without silicone tube (headspace-headspace-no-tube).

For the incubations, 100-ml Kimble KIMAX borosilicate laboratory glass jars (GL 45, Kimble Chase Life Science and Research Products, LLC., Meiningen, Germany) with wide necks were filled with 20 g field-moist soil (30% soil weight-based water content) and 15 ml deionized water were added to make the soil slurry. Visible plant debris and small stones were hand-removed prior to loading. During silicone tube installation, care was taken to ensure that the silicone tubes were buried below the soil slurry surface. Gas-impermeable black butyl rubber septa and plastic screw caps were used to seal the jars. All jars and septa were autoclaved at 121 ℃ for 20 min before incubation. To create anaerobic conditions in the microcosms, the headspace was evacuated with a vacuum pump (Ilmvac MP 301 Vp, Ilmvac GmbH, Ilmenau, Germany) for 5 min by vacuuming down to -95 kPa and then back-flushed 8 times with high purity N_2 to over-pressure up to 95 kPa. The soil silicone tubes were also flushed 8 times with N_2 using two 25 ml syringes as input and exhaust ports switched by a three-way stopcock. On final filling, the N_2 pressure in the headspace and the soil silicone tubes was then equilibrated to 101.3 *kPa*. To confirm that anaerobic conditions prevailed in the microcosms throughout the experiments, O_2 (anaerobic) indicators (Thermo Scientific, Oxoid Ltd., Basingstoke, Hampshire, UK) were placed inside the jars and the color was regularly recorded (pink – aerobic, white – anaerobic). The slurry was pre-incubated in the dark at 18 ℃ for 10 days to allow the equilibrium to establish and consume any O_2 remaining in the microcosms. At the end of pre-incubation, the headspace and silicone tubes were re-flushed with N_2 5 times as described above to purify the gas in the headspace and silicone tubes, and the N_2-pressure was equilibrated to 101.3 *kPa*. Thereafter, gas was sampled for background values, and labeled CH_4 (4.8 ml 5 atom% ^{13}C-CH_4) was added to the headspace and to the soil silicone tube to quantify the net anaerobic oxidation of $^{13}CH_4$ to $^{13}CO_2$ over time. After injection, the headspace pressure increased to 106.6 *kPa*, whereas the pressure inside the silicone tubes was 405.2 *kPa*, thereby allowing the gradual CH_4 release from the silicone tube to the slurry. All treatments were carried out with three independent (field) replicates. All O_2 indicators remained white (i.e., anaerobic) over the whole 59 days of the experiment.

During the incubation, gas samples were collected at 1, 3, 7, 12, 17, 29 and 59 days after $^{13}CH_4$ injection. One-ml gas-tight syringes fitted with stopcocks were used to collect gas from the headspace (through septa with needles) and from soil tubes (through outlet ports) (Fig. S1 e, f). After each sampling, the equivalent volume of N_2 was injected into the headspace of incubation jars and the

silicone tubes to compensate for any pressure loss and in order to maintain slight overpressure. All gas samples were transferred to evacuated N_2-flushed glass vials, diluted with N_2 (1 ml sample into 12 ml N_2). The CO_2, N_2O and CH_4 concentrations were then measured on a gas chromatograph (GC-14B, Shimadzu, Ld. Nds., Japan) equipped with a flame ionization detector (for CH_4) and electron capture detector (for CO_2 and N_2O) according to an established protocol (Loftfield et al., 1997). A separate set of vials was measured for stable C isotope composition, with a dilution of 1 ml sample into 15 ml N_2 (see below). Gas analyses were done within two weeks after sampling. All transfers, additions, and gas samplings were done using gas-tight syringes fitted with stopcocks and N_2-flushed.

2.3. Microbial biomass and dissolved organic C

A chloroform fumigation−K_2SO_4 extraction method (as described in Fan and Han, 2018; Wei et al., 2019) was applied to determine post-incubation soil microbial biomass carbon (MBC). The extracts obtained were analyzed for total C content using a TOC/TIC analyzer (Multi N/ C 2100, Analytik Jena, Germany). MBC was calculated based on the difference between the extracted organic C content of fumigated and non-fumigated soils using k_{EC} factor = 0.45 (Joergensen, 1996). Dissolved organic carbon (DOC) was measured from the extracts of the non-fumigated samples.

2.4. Isotopic analysis

Stable C isotope analysis of gas (CO_2) and solids (dry K_2SO_4 extracts of MBC and DOC) was conducted using an isotope ratio mass spectrometer (Delta plus IRMS, Thermo Fisher Scientific, Bremen, Germany) at the Centre for Stable Isotope Research and Analysis, University of Goettingen, Germany. Data are reported as $\delta^{13}C$-values relative to the Vienna Pee Dee Belemnite (VPDB) standard. For ^{13}C measurement of MBC and DOC, the relative K_2SO_4 extracts were freeze-dried and analyzed as solid material.

2.5. Calculations and statistics

The quantity of net anaerobic $^{13}CH_4$ oxidized (i.e. ^{13}C-CO_2 excess as an end-product of oxidation) at each time point (i.e. 1, 3, 7, 12, 17, 29 and 59 days), and incorporations of CH_4-derived C into MBC and DOC at the end of incubation were calculated using the following equation (as described in Fan et al., 2019):

$$C_{OX} = \frac{(\delta^{13}C_{Total} - \delta^{13}C_{Control})}{(\delta^{13}C_{OX} - \delta^{13}C_{Control})} \times C_{Total}, \quad (1),$$

Where C_{OX} (μg C) represents the amount of net C-CH_4 oxidized estimated based on the release of ^{13}C-CO_2, C_{Total} (μg C) represents the total amount of ^{13}C in the corresponding pool (i.e. CO_2, MBC, DOC), $\delta^{13}C_{Total}$ is the delta value of ^{13}C in CO_2 (or MBC and DOC) in the samples treated with $^{13}CH_4$, $\delta^{13}C_{Control}$ is the delta value of ^{13}C in CO_2 (or MBC and DOC) in the control (no $^{13}CH_4$ addition), and $\delta^{13}C_{OX}$ is the delta value of ^{13}C in CH_4 of 5 atom% (i.e. 3774‰). Gross CH_4 production was calculated as the net AOM (as determined from the different injection/sampling approaches) plus net CH_4 production (as determined from the control without CH_4 added). AOM rates are presented per gram of dry soil per hour.

A two-way ANOVA (analysis of variance) with repeated measures was used to determine the effects of silicone tube and shaking treatments on cumulative AOM over 59 days of incubation. One-way ANOVA was used to determine differences in MBC and DOC as well as in CH_4-derived MBC and DOC. The normality of the residuals and homogeneity of the variances of the cumulative AOM, MBC and DOC as well as CH_4-derived MBC and DOC were tested. *t*-tests were used to characterize the differences in the CH_4 concentrations, the cumulative AOM, and the rates of AOM over time between shaking and static treatments. The Shapiro–Wilk test was used to test the normality of the CH_4 concentrations, the cumulative AOM, and the rates of AOM. Standard errors were calculated by using each set of three replicates from each sampling time. All statistical analyses were performed using

SPSS software (ver. 19.0, SPSS Inc., Chicago, IL, USA) and SigmaPlot software (ver. 12.5, Systat Software, Inc, San Jose, California, USA).

3 Results

3.1. CH_4 dynamics and $\delta^{13}C$-CO_2 signatures

Without shaking, when CH_4 was injected into the headspace, the CH_4 concentration ($[CH_4]$) in headspace decreased slowly but gradually over the 59 days of incubation (Fig. 1 a, d, white circles). When CH_4 was injected into the silicone tube, the $[CH_4]$ in the headspace was low at the beginning but significantly increased during the first week of incubation (Fig. 1 c, white circles). Injecting CH_4 into the headspace and sampling from the silicone tube showed a similar result (Fig. 1 b). The controls (without CH_4 injection) revealed a steady increase in $[CH_4]$ in the headspace and in the tube starting after about one week of incubation (Fig. 1 e, f).

With continuous shaking (100 rounds min^{-1}) over 59 days, the $[CH_4]$ slowly decreased over time irrespective of injection/sampling approaches (Fig. 1, black circles). The controls sampled either from the headspace or from the tube demonstrated a constantly low $[CH_4]$ during the 59 days (Fig. 1 a, b), suggesting a small contribution of newly produced CH_4. At the end of the experiment the $[CH_4]$ in each treatment was not different between shaking and static conditions.

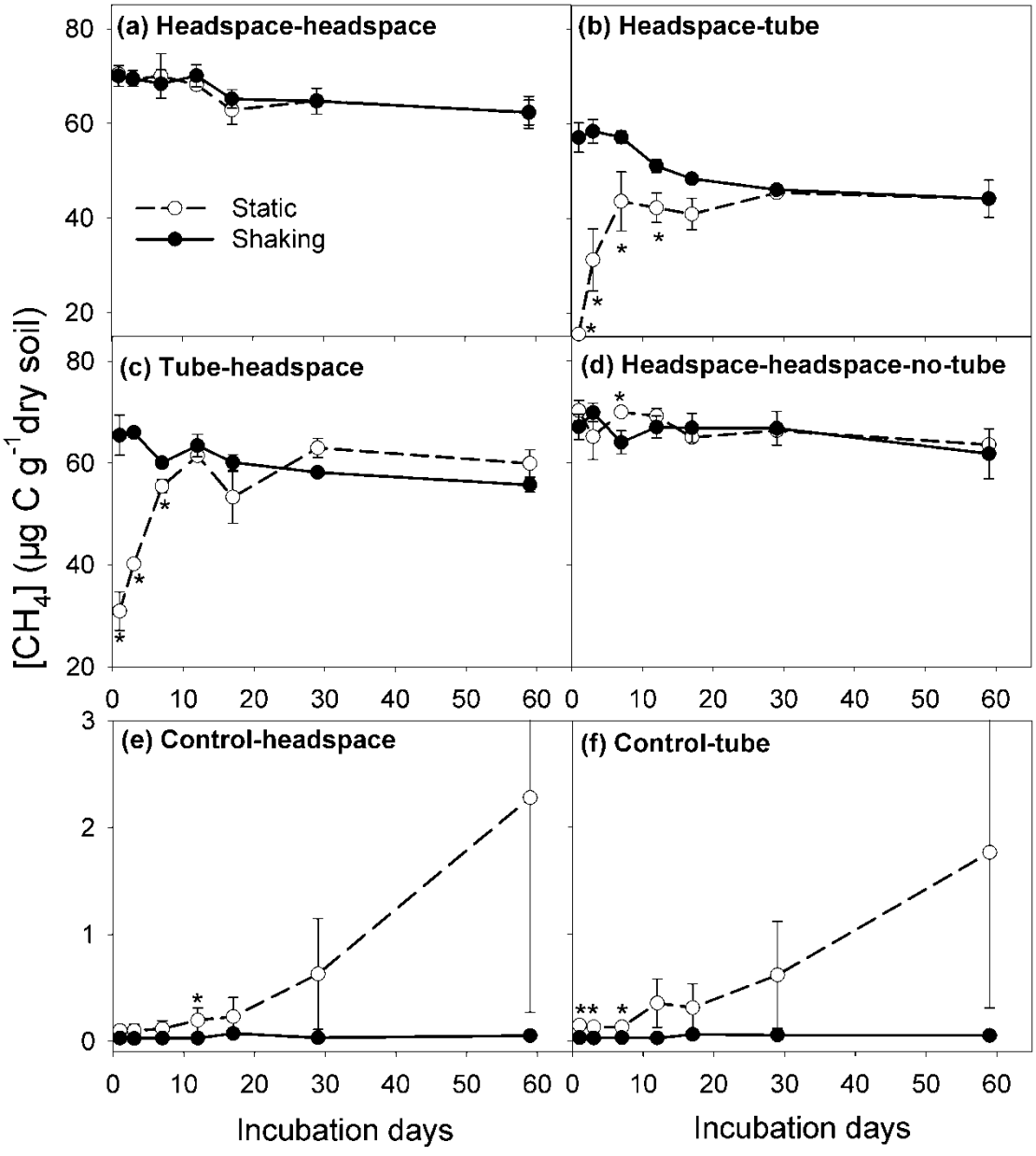

Fig. 1 Dynamics of CH_4 concentration ([CH_4]) over 59 days of incubation with and without shaking in the microcosms subjected to (a) headspace injection with sampling from headspace (headspace-headspace) and (b) silicone tube (headspace-tube), (c) injection to soil slurry through silicone tube with sampling from headspace (tube-headspace), (d) headspace injection and sampling without silicone tube (headspace-headspace-no-tube), (e) control without CH_4 injection with headspace sampling (control-headspace) and (f) silicone tube sampling (control-tube). Asterisks: significant difference ($p < 0.05$) between shaking and static treatments. Error bars: standard error of means ($n = 3$).

CO_2 sampled from the headspace or silicone tube became considerably more ^{13}C enriched in slurries treated with $^{13}CH_4$ as compared to the controls without CH_4 injection in both shaking and static conditions (Fig. 2). This demonstrated that there was actual CH_4 oxidation to CO_2 (i.e. AOM) in the anaerobic environment. Over 59 days of incubation, the ^{13}C enrichment of CO_2 after CH_4 injection was higher in static conditions (i.e. -10 ‰) than with shaking (i.e. -17 ‰), whereas in the control, the ^{13}C natural abundance of CO_2 did not exceed -20 ‰ (Fig. 2 e, f).

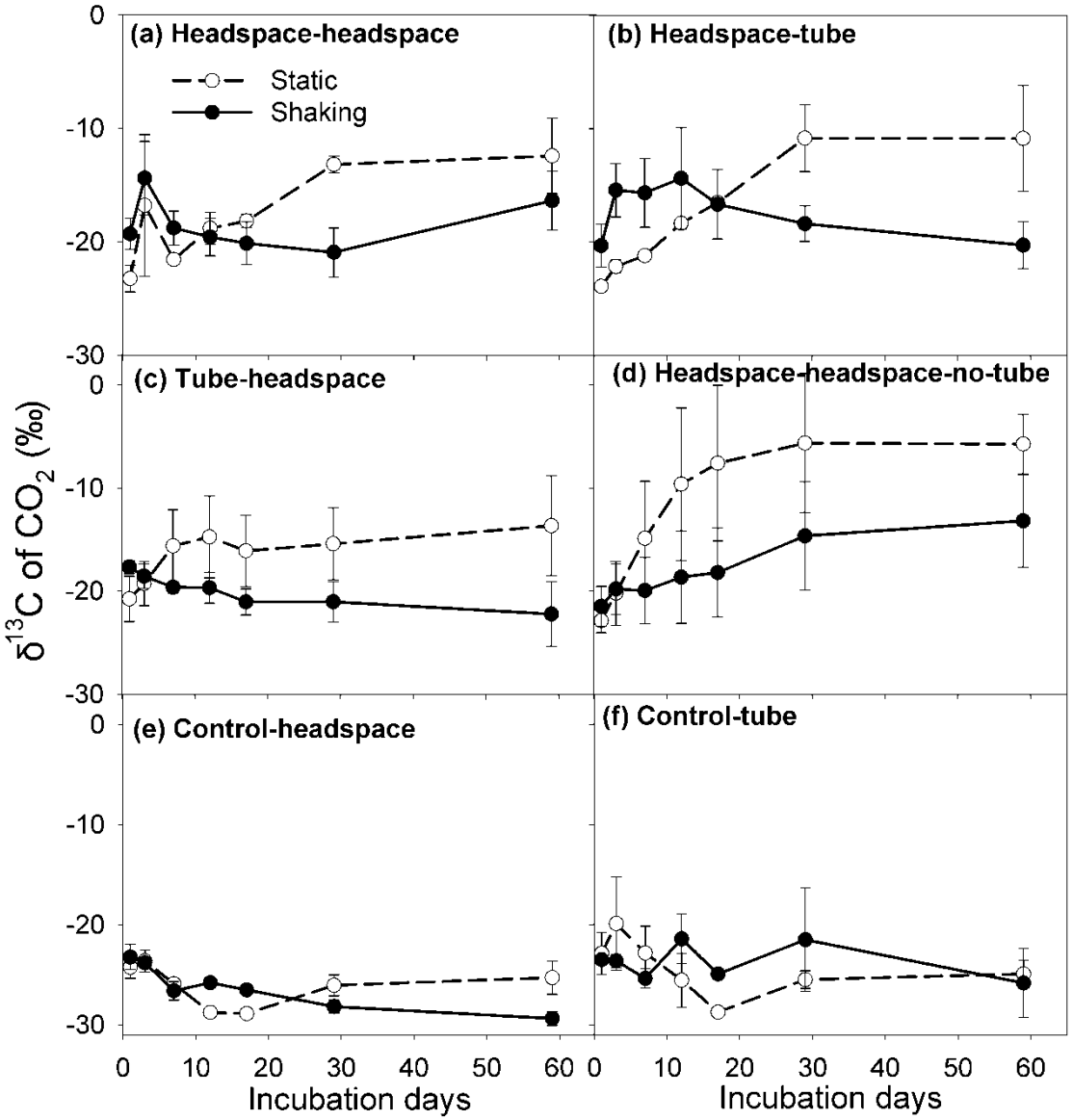

Fig. 2 Dynamics of $\delta^{13}C$ of CO_2 over 59 days of incubation with and without shaking in the microcosms subjected to 6 treatments (see (a)-(f) in Fig. 1). Error bars: standard error of means ($n = 3$).

3.2. Rate of CH_4 oxidation and cumulative AOM

Without shaking, the rate of CH_4 oxidation peaked (0.21-0.44 ng C g^{-1} dry soil h^{-1}) during the first two weeks and then gradually decreased (Fig. 3, white circles). The cumulative AOM (CH_4-derived CO_2) reached 0.16-0.24 μg C g^{-1} dry soil during 59 days depending on the injection/sampling approaches (Fig. 4, white circles). The cumulative AOM did not differ much between injection/sampling approaches, and the effect of the silicone tubes on CH_4 oxidation was not significant (p = 0.200, Table S1). There was a linear correlation between the amount of oxidized and gross produced CH_4 when the CH_4 production was relatively low (Fig. 5 a, dashed line, R^2 = 0.68, p < 0.001). With high CH_4 production, this relationship followed a strong nonlinear power growth, regardless of injection/sampling approaches during incubation (Fig. 5 a, R^2 = 0.78, p < 0.001).

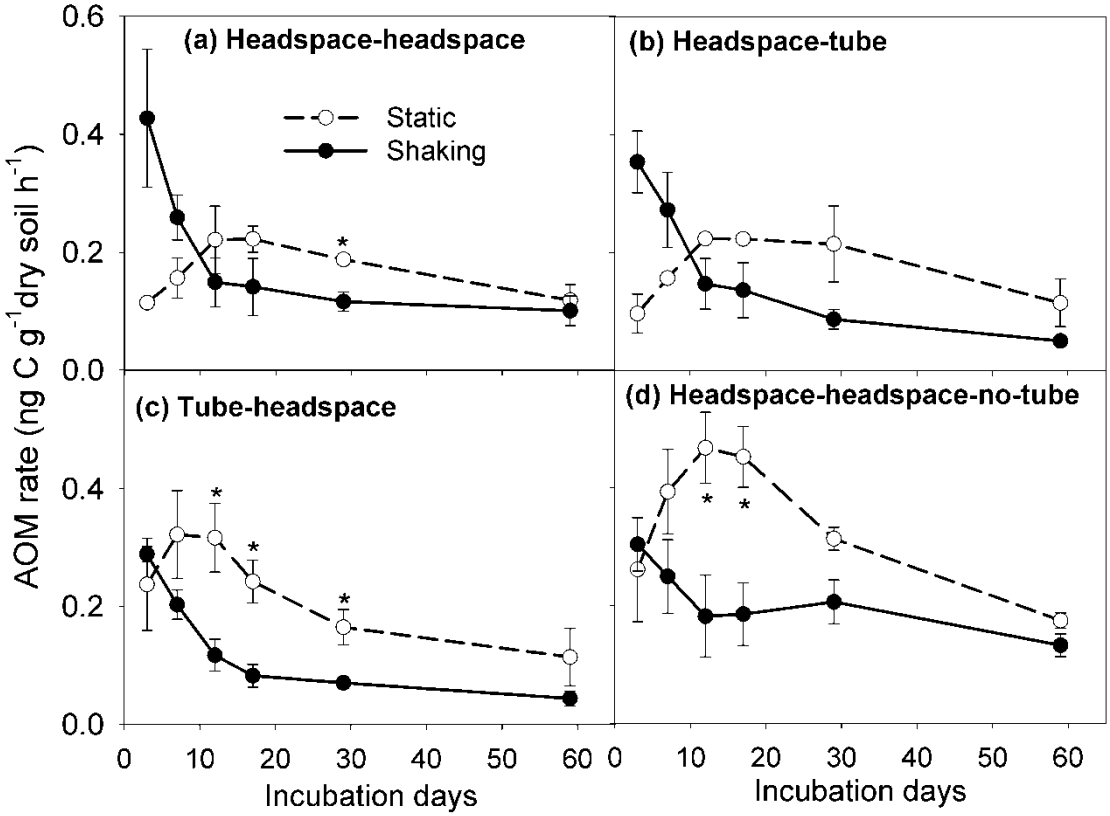

Fig. 3 Anaerobic CH_4 oxidation (AOM) rates over 59 days of incubation with and without shaking in the microcosms subjected to 6 treatments (see (a)-(f) in Fig. 1). Asterisks: significant difference (p < 0.05) between shaking and static treatments at each measurement day . Error bars: standard error of means (n = 3).

With shaking, the maximal AOM rate was observed solely in the very beginning of incubation (0.22-0.51 ng C g^{-1} dry soil h^{-1}), and after the first two weeks it sharply decreased to the end of incubation (Fig. 3, black circles). The cumulative AOM was 1.2-3.0 times lower (0.06-0.18 μg C g^{-1} dry soil) as compared with static slurry (Fig. 4, black circles, p = 0.010, Table S2). The cumulative AOM was similar between injection/sampling approaches, and the effect of the soil silicone tubes on CH_4 oxidation was similar to that with shaking (p = 0.205, Table S1). There was a strong linear correlation between the amount of cumulative AOM and gross CH_4 production, regardless of injection/sampling approaches (Fig. 5 b, R^2 = 0.91, p < 0.001).

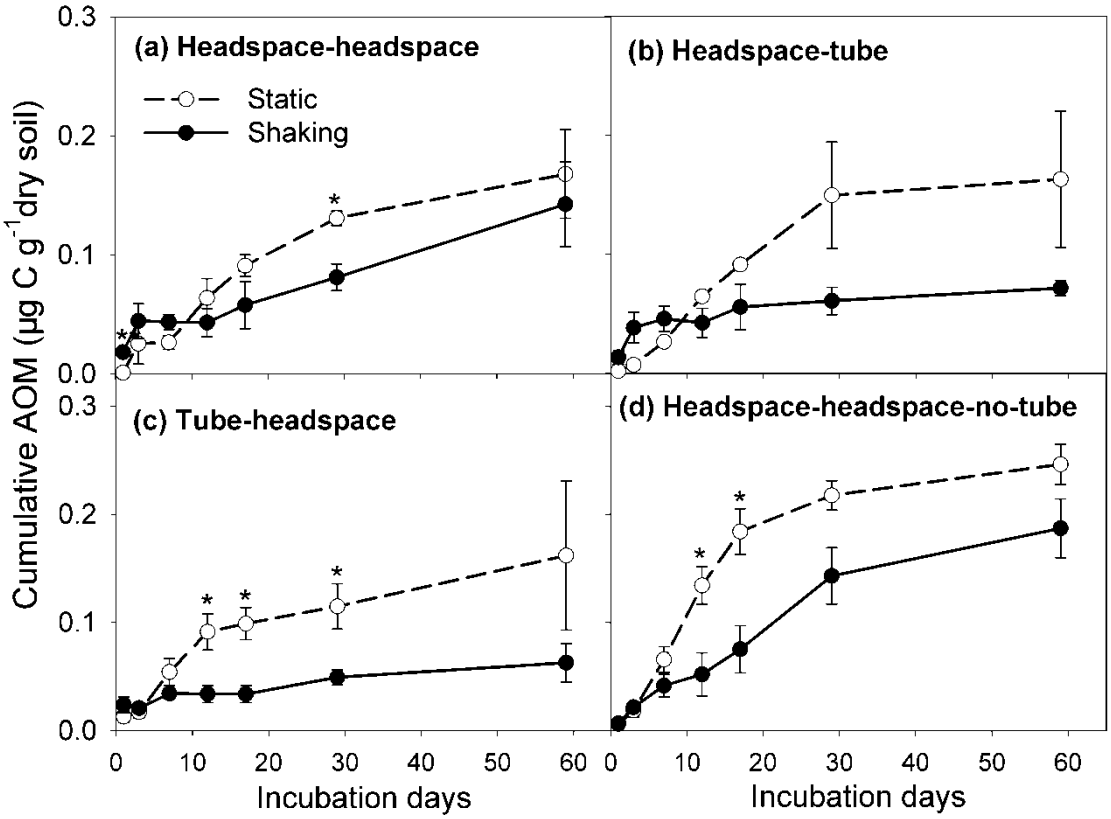

Fig. 4 Cumulative anaerobic CH_4 oxidation (AOM, CH_4-derived CO_2) over 59 days of incubation with and without shaking. Estimations based on isotope mixing model (Eq. 1) for the microcosms subjected to 6 treatments (see (a)-(f) in Fig. 1). Asterisks: significant difference ($p < 0.05$) between shaking and static treatments at each day of measurements. Error bars: standard error of means ($n = 3$).

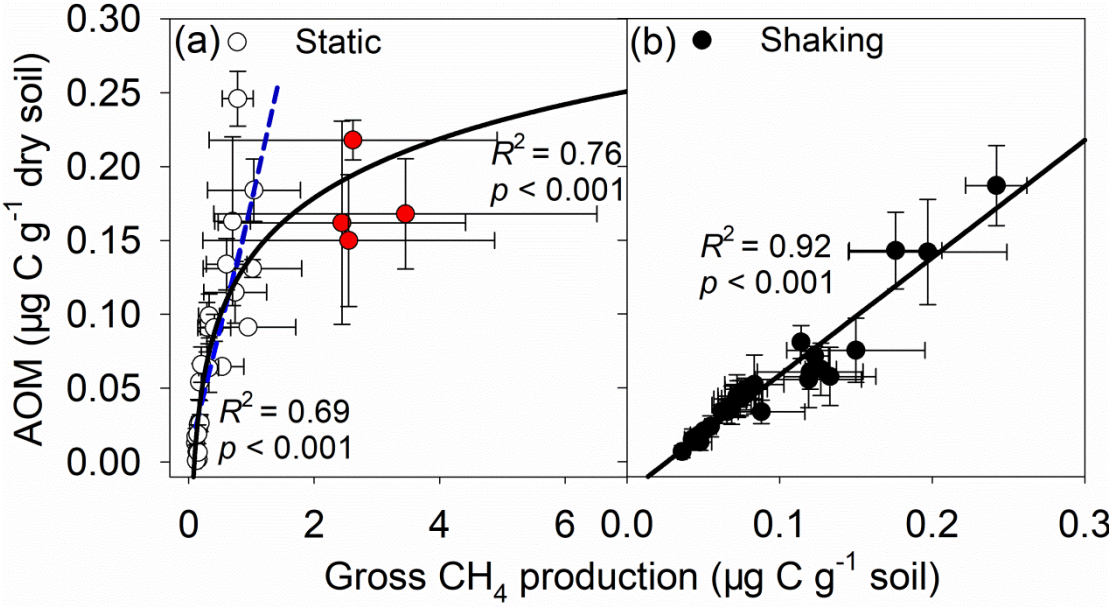

Fig. 5 Relationships between gross CH_4 production and anaerobic CH_4 oxidation (AOM) with and without shaking. Solid lines are regressions of all data measured (a) under static conditions ($y = 246x^{(2.34\times10^{-4})} - 246$) and (b) with shaking ($y = 0.79x - 0.021$). Dashed blue line is a regression of data ($y = 0.17x + 0.004$) excluding the highest CH_4 production rates (the red circles). Gross CH_4 production was calculated as the sum of net CH_4 oxidation (from different injection/sampling approaches) plus net CH_4 production (from control without added CH_4). Vertical error bars: standard error of AOM means ($n = 3$); horizontal error bars: standard error of gross CH_4 production means ($n = 3$).

3.3. Incorporation of CH_4-derived C into MBC and DOC

Shaking and injection/sampling approaches had no effect on total DOC or MBC content (Fig. S3 a, c). CH_4-derived C in MBC and DOC also showed no difference between injection approaches or between shaking and static conditions (Fig. S3 b, d).

4. Discussion

A ^{13}C excess in CO_2 occurred under anaerobic conditions in soil after ^{13}C-CH_4 addition (as compared to the control without CH_4 injection), irrespective of shaking and injection/sampling approaches (Fig. 2). We therefore demonstrated that AOM takes place in submerged paddy soil (see the first research question and discussion below). Regarding the approach of direct belowground delivery of CH_4 into slurry via silicone tubes and shaking/static conditions, for the first time we obtained the important information that static condition but not shaking is favorable for AOM process.

CH_4 injection into silicone tubes resulted in a [CH_4] increase in the headspace (Fig. 1 c, white circles, tube-headspace). The same occurred when CH_4 was injected into the headspace and sampled from the silicone tubes (Fig. 1 b, white circles, and headspace-tube). This means that the silicone tubes gradually released the CH_4 from tubes to slurry as expected. During the 59-day incubation, however, the effect of the silicone tubes on AOM was not significant either with (p = 0.21) or without shaking (p = 0.20, Table S2). This is because the amount of CH_4 dissolved in water (slurry) was 2 orders of magnitude higher than the cumulative AOM (500 μg vs. 1.0-3.9 μg CH_4 per jar). Continuous production of CH_4 in anaerobic microcosms as demonstrated with the control (Fig. 1 e, f, white circles) suggests that the gross methanogenesis masked the methanotrophic activity. Therefore, we conclude that the [CH_4] in water (slurry) was not the main limiting factor for the AOM. Instead, the quantity and activity of the anaerobic methanotrophic organisms and the concentration of the alternative electron acceptors may be the limiting factors for the AOM process.

Advantageously, silicone material had no side effect either on total MBC and DOC or on the contribution of new CH_4-derived C to MBC and DOC because the CH_4-derived C in MBC and DOC was similar between injection approaches (Fig. S3). The reason for the silicone tube approach is to compensate for poor CH_4 solubility and the restricted diffusion between gas-liquid phases. Nonetheless, this approach does not appear useful for the AOM process as long as methanogenesis is not inhibited and is saturating the slurry with CH_4 (thereby answering our second research question). In situations when the CH_4 concentration is limiting and/or the rate of oxidation is high, however, the silicone tube approach could be much more important (Fan et al., 2019).

Shaking is supposed to enhance CH_4 equilibration and accelerate CH_4 mixing from the headspace into the slurry. Accordingly, it substitutes the effect of silicone tubes on CH_4 diffusion. Indeed, with shaking, the [CH_4] in the headspace and the silicone tubes was higher than without shaking early in the incubation (Fig. 1 b, c, headspace-tube, tube-headspace). Thus, the AOM rate peaked in shaken microcosms shortly after the CH_4 addition, but was more intensive in static microcosms during the second week (Fig. 3).

The cumulative AOM was lower (p = 0.01, Table S2) under shaking vs. static conditions (Fig. 4), demonstrating the overall negative effect of shaking on AOM and answering our third research question. The following mechanisms may be responsible for the negative effects of shaking:

1. AOM is controlled by CH_4 production, and one of the pathways is carried out by methanogens via "reverse methanogenesis" (Smemo and Yavitt, 2007; Smemo and Yavitt, 2011; Blazewicz et al., 2012; Gauthier et al., 2015). In the experiment, CH_4 oxidation was dependent on gross CH_4 production with shaking, and also without shaking when the CH_4 production was low (Fig. 5 a, dashed fitting line, and b, solid line), indicating that AOM is related to methanogenic activity. Methanogens are able to oxidize CH_4 without using exogenous electron acceptors under anaerobic conditions (Moran et al., 2005, 2007). The gross CH_4 production, however, was on average 11 times lower (Fig. 1 e, f), and the

cumulative AOM was 1.2-2.6 times slower with shaking versus static conditions (Fig. 4). One possible reason for the negative effect of shaking could be a mechanical disturbance of microbial communities (e.g. syntrophic bacteria, Liu and Conrad, 2017), thus preventing them from organizing in a way that stimulates CH_4 production and/or oxidation. So, although AOM was detected in submerged paddy soil in microcosms with shaking, the shaking strongly inhibited methanogenic activity.

In contrast to the linear relationship of AOM at lower rates of methanogenesis, as CH_4 production increased, AOM slowed down (Fig. 5 a, power growth regression). This suggests that "reverse methanogenesis" was not the only (dominating) process, and that unidentified electron acceptors drive AOM in submerged paddy soil.

2. Electron acceptors other than oxygen ultimately control redox processes under anaerobic conditions, including AOM (reviewed in Smemo and Yavitt, 2011). Several potential alternative electron acceptors have been described, such as NO_3^- (Raghoebarsing et al., 2006; Deutzmann et al., 2014), Fe^{3+} (Ettwig et al., 2016; Mohanty et al., 2017), manganese in different oxidation states (Beal et al., 2009), SO_4^{2-} (Weber et al., 2016), humic acids (Blodau and Deppe, 2012). Shaking can maximize mass transfer and equilibration; it thereby increases the probability of interactions between methanotrophs and electron acceptors, so the maximal AOM rate occurred in the early incubation phase. In static systems, the interactions would be much less probable, especially initially when the relevant microbial populations are likely to be less active. Accordingly, it took two weeks to reach the peak AOM rate that optimally co-localized the electron acceptors and the methane oxidizers. As the AOM proceeds, the concentration of electron acceptors decreases, triggering a reduction in the AOM rate. Shaking, which destroys gradients and moments of co-localization, leads to lower AOM rates (Fig. 6). This suggests that AOM was limited by the amount of available electron acceptors. Unfortunately, the current experimental setup was not designed to measure key electron acceptors. This knowledge gap should be closed in future experiments. Previously, NO_3^- was suggested as the most feasible electron acceptor for paddy soil systems, and the nitrite-dependent anaerobic methane oxidation (n-damo) is a recently discovered process of CH_4 oxidation (Raghoebarsing et al., 2006; Shen et al., 2014b). Indeed, long-term fertilization of paddy fields increased the NO_3^- concentration in soil solution (Zhao et al., 2009). However, the available NO_3^- participates in a range of other biochemical processes beyond AOM. Above all, it is involved in denitrification, which is energetically more favorable than AOM (Smemo, and Yavitt, 2011; Lan et al., 2015). Based on this and our results on N_2O production (which is a side product of denitrification), the cumulative N_2O was higher with shaking than under static conditions (Fig. S4). This suggests that denitrification is more intense under shaking, thereby outcompeting AOM. This may explain the higher AOM in static slurry.

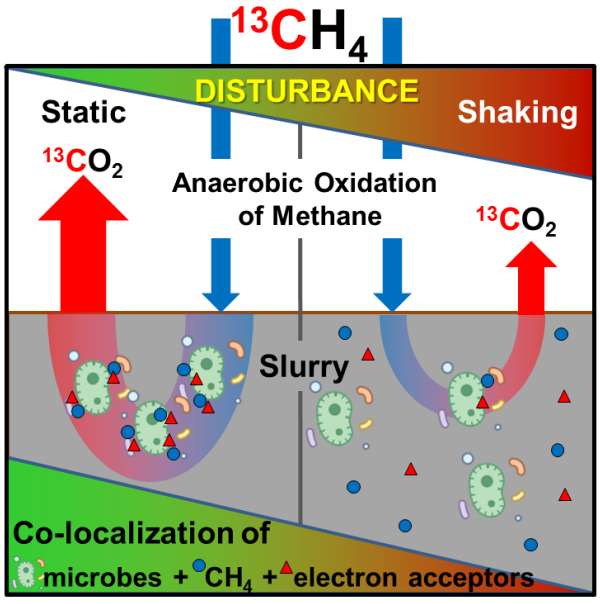

Fig. 6 Conceptual scheme demonstrating the effects of shaking vs. static conditions on anaerobic oxidation of methane (AOM) estimated based on the ^{13}C-labelled CH_4 (blue arrows). The colour gradient from green to red and shape of triangles mean the increasing disturbance on AOM due to shaking, and the decreasing co-localization of substrate (CH_4, blue circles), electron acceptors (red circles) and microorganisms from shaking vs. static conditions.

Notably, the AOM rates reported here are among the lowest found in studies on paddy soil (Hu et al., 2014, Shen et al., 2014b, Zhou et al., 2014, Shi et al., 2017), where, however, the conventional headspace injection approach was used (Fig. 7). Apart from paddy soils, similar AOM rates were reported for tropical and boreal soils (Blazewicz et al. 2012) and wetlands (Shen et al. 2015). In summary, the AOM rates were ca. 1 order of magnitude slower in paddy soils than in peatlands (Gupta et al., 2013), and the average across-terrestrial-ecosystems AOM rate was considerably slower than the rate of aerobic CH_4 oxidation (Fig. 7). The difference in AOM rates between the current study and several other studies can be related, first of all, to the complexity of the environmental factors controlling the AOM (soil properties, agricultural management etc.) but also to the specific conditions of the experiments (slurries vs. soil cores, temperature, concentration of added CH_4 etc.). Therefore, with the unified experimental protocol, next steps in research should be devoted to factors controlling the AOM, e.g. temperature, available electron acceptors, carbon sources, microbial communities, soil structure and texture, etc.

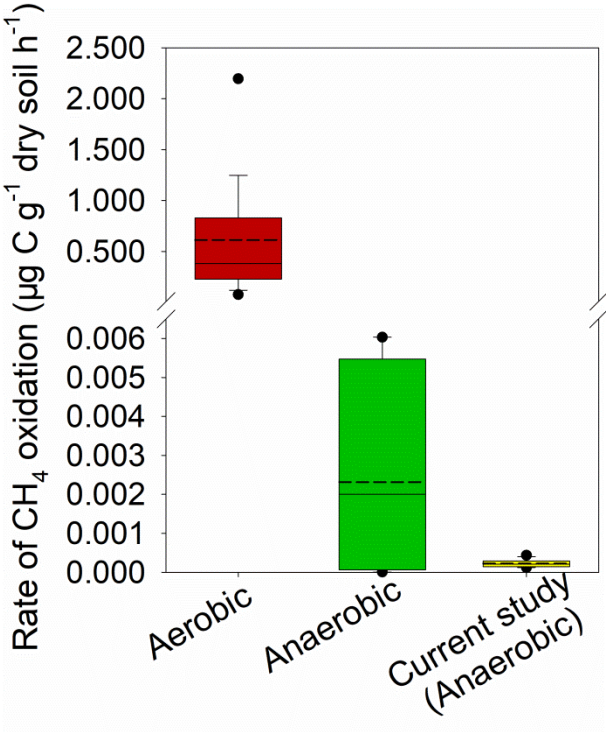

Fig. 7 Box plots of aerobic and anaerobic CH_4 oxidation rates in paddy soils. The upper bar is a maximum observation, the lower bar is a minimum observation, the top of the box is the third quartile, the bottom of the box is the first quartile, the middle thin horizontal line is the median value, the dashed line is the mean, and the circles beyond the 5-95% confidence interval are outliers. The data on aerobic (n = 66) and anaerobic (n = 36) CH_4 oxidation were taken from Conrad and Rothfuss, 1991; Cai and Mosier, 2000; Chan and Parkin, 2001; Krüger and Frenzel, 2003; Mohanty et al., 2014; Shen et al., 2014b; Shi et al., 2017; Fan et al., 2019. Only the data obtained under the static conditions (no continuous shaking) and without chemical amendments (e.g. electron acceptors, inhibitors etc.) were considered.

Even though aerobic CH_4 oxidation is the main driver of total terrestrial CH_4 recycling, increasing evidence has verified that AOM is ubiquitous in soils (Smemo and Yavitt, 2011; Gupta et al., 2013; Gauthier et al., 2015). The current ^{13}C-based study demonstrated AOM to be a valuable CH_4 sink despite slow rates in paddy soil. Based on the total paddy area in China (3.0×10^7 ha, Chinese Ministry of Agriculture, 2017), on the average soil bulk density (1.3 g cm^{-3}, Pan et al., 2004), on the plow layer (25.5 cm, Pen et al., 2004) and on the average AOM rate in paddy soils (2.3 ng C-CH_4 g^{-1} soil h^{-1}, Fig. 7, green box) we assess that paddy soils in China could anaerobically consume ~ 2.0 Tg of C-CH_4 annually. At an average CH_4 emission rate of ~36 g C m^{-2} (Cai et al., 2000), ca. 9.5 Tg C y^{-1} net CH_4 is released to the atmosphere. Consequently, AOM is potentially responsible for a ca. 20% reduction of the net CH_4 emission to the atmosphere (assuming constant rates of aerobic CH_4 oxidation) (Fig. 7). Similarly, Gupta et al. (2013) estimated that the northern peatlands could anaerobically consume 18 Tg C y^{-1} net CH_4. Segarra et al. (2015) calculated that AOM in global freshwater wetlands may offset the net CH_4 by ca. 150 Tg C y^{-1}. Given the strong role of AOM in reduction of global CH_4 emissions, it is crucial to understand the mechanisms controlling AOM in terrestrial ecosystems in order to predict the future global C cycle. Importantly, terrestrial AOM must be added to marine AOM to complete the estimations and models on global CH_4 turnover.

Conclusions

The AOM experimental data highlighted the occurrence of AOM in submerged paddy soil. Based on the low AOM rates, and on the lack of advantages of the silicone tube approach versus the conventional headspace CH_4 injection, we conclude that the CH_4 concentration in slurry is not the main limiting factor for AOM. A static setup is superior to shaking when estimating AOM due to lesser disturbance and/or a lower level of competition with other processes (i.e. anaerobic respiration based on the same electron acceptors). Based on the measured rates of CH_4 production and oxidation as well as on previously published data, we estimate that AOM has the potential to sink ca. 2.0 Tg C of CH_4 annually, which is roughly 20% of total net CH_4 emission from paddy fields in China. As paddy soils are one of the major sources of global CH_4 emissions, the AOM in paddy soils is an important yet underappreciated process of the global CH_4 sink.

Acknowledgement

The authors are thankful to the China Scholarship Council (CSC) for funding Lichao Fan in Germany, and to the German Research Foundation (DFG, Do 1533/2-1) and the National Natural Science Foundation of China (41761134095; 41430860; 41671253), Innovation Groups of National Natural Science Foundation of Hunan Province (2019JJ10003), Youth Innovation Team Project of ISA, CAS (2017QNCXTD_GTD) and Hunan Province Base for Scientific and Technological Innovation Cooperation (2018WK4012) for the invaluable support. The work is performed according to the Government Program of Competitive Growth of Kazan Federal University. Special thanks to the Kompetenzzentrum Stabile Isotope (KOSI), University of Goettingen, and personally to Lars Szwec and Reinhard Langel for the isotope analyses.

References:

Beal, E.J., House, C.H., Orphan, V.J., 2009. Manganese-and iron-dependent marine methane oxidation. Science 325, 184-187.

Bender, M., Conrad, R., 1995. Effect of CH_4 concentrations and soil conditions on the induction of CH_4 oxidation activity. Soil Biology & Biochemistry 27, 1517-1527.

Blazewicz, S.J., Petersen, D.G., Waldrop, M.P., Firestone, M.K., 2012. Anaerobic oxidation of methane in tropical and boreal soils: Ecological significance in terrestrial methane cycling. Journal of Geophysical Research: Biogeosciences 117.

Blodau, C., Deppe, M., 2012. Humic acid addition lowers methane release in peats of the Mer Bleue bog, Canada. Soil Biology & Biochemistry 52, 96-98.

Cai, Z.C., Mosier, A.R., 2000. Effect of NH_4Cl addition on methane oxidation by paddy soils. Soil Biology & Biochemistry 32, 1537-1545.

Cai, Z.C., Tsuruta, H., Minami, K., 2000. Methane emission from rice fields in China: measurements and influencing factors. Journal of Geophysical Research: Atmospheres 105, 17231-17242.

Chan, A., Parkin, T.B., 2001. Methane oxidation and production activity in soils from natural and agricultural ecosystems. Journal of Environmental Quality 30, 1896-1903.

Chinese Ministry of Agriculture 2017. Chinese Agricultural Yearbook 2016, China Agriculture Press, Beijing.

Conrad, R., Rothfuss, F., 1991. Methane oxidation in the soil surface layer of a flooded rice field and the effect of ammonium. Biology and Fertility of Soils 12, 28-32.

Deutzmann, J.S., Stief, P., Brandes, J., Schink, B., 2014. Anaerobic methane oxidation coupled to denitrification is the dominant methane sink in a deep lake. Proceedings of the National Academy of Sciences 111, 18273-18278.

Ettwig, K.F., Zhu, B., Speth, D., Keltjens, J.T., Jetten, M.S., Kartal, B., 2016. Archaea catalyze iron-dependent anaerobic oxidation of methane. Proceedings of the National Academy of Sciences 113, 12792-12796.

Fan, L.C., Han, W.Y., 2018. Soil respiration in Chinese tea gardens: autotrophic and heterotrophic respiration. European Journal of Soil Science 69, 675-684.

Fan, L.C, Shahbaz, M., Ge, T., Wu, J., Kuzyakov, Y., Dorodnikov, M., 2019. To shake or not to shake: Silicone tube approach for incubation studies on CH_4 oxidation in submerged soils. Science of the Total Environment 657, 893-901.

Gauthier, M., Bradley, R.L., Šimek, M., 2015. More evidence that anaerobic oxidation of methane is prevalent in soils: Is it time to upgrade our biogeochemical models? Soil Biology & Biochemistry 80, 167-174.

Ge, T.D., Li, B.Z., Zhu, Z.K., Hu, Y.J., Yuan, H.Z., Dorodnikov, M., Jones, D.L., Wu, J.S., Kuzyakov, Y., 2017. Rice rhizodeposition and its utilization by microbial groups depends on N fertilization. Biology and Fertility of Soils 53, 37-48.

Gupta, V., Smemo, K.A., Yavitt, J.B., Fowle, D., Branfireun, B., Basiliko, N., 2013. Stable isotopes reveal widespread anaerobic methane oxidation across latitude and peatland type. Environmental Science & Technology, 265198755.

He, Z., Geng, S., Shen, L., Lou, L., Zheng, P., Xu, X., Hu, B., 2015. The short- and long-term effects of environmental conditions on anaerobic methane oxidation coupled to nitrite reduction. Water Research 68, 554-562.

Hu, B.L., Shen, L.D., Lian, X., Zhu, Q., Liu, S., Huang, Q., He, Z.F., Geng, S., Cheng, D.Q., Lou, L.P., Xu, X.Y., Zheng, P., He, Y.F., 2014. Evidence for nitrite-dependent anaerobic methane oxidation as a previously overlooked microbial methane sink in wetlands. Proceedings of the National Academy of Sciences 111, 4495-4500.

Hu, S., Zeng, R.J., Haroon, M.F., Keller, J., Lant, P.A., Tyson, G.W., Yuan, Z., 2015. A laboratory investigation of interactions between denitrifying anaerobic methane oxidation (DAMO) and anammox processes in anoxic environments. Scientific Reports 5.

Huang, X.Z, Wang, C., Liu, Q., Zhu, Z.K., Lynn, T.M., Shen, J.L., Whiteley, A.S., Kumaresan, D., Ge, T.D., Wu, J.S. 2018. Abundance of microbial CO_2-fixing genes during the late rice season in long-term management paddy field amended with straw and straw-derived biochar. Canadian Journal of Soil Science 98, 306-316.

Joergensen, R.G., 1996. The fumigation-extraction method to estimate soil microbial biomass: Calibration of the k_{EC} value. Soil Biology & Biochemistry 28, 25-31.

Knittel, K., & Boetius, A., 2009. Anaerobic oxidation of methane: progress with an unknown process. Annual review of microbiology 63, 311-334.

Kögel-Knabner, I., Amelung, W., Cao, Z., Fiedler, S., Frenzel, P., Jahn, R., Kalbitz, K., Kölbl, A., Schloter, M., 2010. Biogeochemistry of paddy soils. Geoderma 157, 1-14.

Krüger, M., Frenzel, P., 2003. Effects of N-fertilisation on CH_4 oxidation and production, and consequences for CH_4 emissions from microcosms and rice fields. Global Change Biology 9, 773-784.

Lai, D.Y.F., 2009. Methane Dynamics in Northern Peatlands: A Review. Pedosphere 19, 409-421.

Lan, T., Han, Y., Cai, Z., 2015. Denitrification and its product composition in typical Chinese paddy soils. Biology and Fertility of Soils 51, 89-98.

Liu, P., Conrad, R., 2017. Syntrophobacteraceae‐affiliated species are major propionate‐degrading sulfate reducers in paddy soil. Environmental Microbiology 19, 1669-1686.
Loftfield, N., Flessa, H., Augustin, J., Beese, F., 1997. Automated gas chromatographic system for rapid analysis of the atmospheric trace gases methane, carbon dioxide, and nitrous oxide. Journal of Environmental Quality 26, 560-564
Luna-Guido, N.S.Y.S., 2014. Methanogenesis and Methanotrophy in Soil： A Review. Pedosphere 24, 291-307.
Megraw, S.R., Knowles, R., 1987. Methane production and consumption in a cultivated humisol. Biology and Fertility of Soils 5, 56-60.
Mohanty, S.R., Bandeppa, G.S., Dubey, G., Ahirwar, U., Patra, A.K., Bharati, K., 2017. Methane oxidation in response to iron reduction-oxidation metabolism in tropical soils. European Journal of Soil Biology 78, 75-81.
Mohanty, S.R., Kollah, B., Sharma, V.K., Singh, A.B., Singh, M., Rao, A.S., 2014. Methane oxidation and methane driven redox process during sequential reduction of a flooded soil ecosystem. Annals of Microbiology 64, 65-74.
Moran, J.J., House, C.H., Freeman, K.H., Ferry, J.G., 2005. Trace methane oxidation studied in several Euryarchaeota under diverse conditions. Archaea 1, 303-309.
Moran, J.J., House, C.H., Thomas, B., Freeman, K.H., 2007. Products of trace methane oxidation during nonmethyltrophic growth by Methanosarcina. Journal of Geophysical Research 112, G02011.
Nisbet, E.G., Dlugokencky, E.J., Manning, M.R., Lowry, D., Fisher, R.E., France, J.L., Michel, S.E., Miller, J.B., White, J.W.C., Vaughn, B., Bousquet, P., Pyle, J.A., Warwick, N.J., Cain, M., Brownlow, R., Zazzeri, G., Lanoiselléé, M., Manning, A.C., Gloor, E., Worthy, D.E.J., Brunke, E.G., Labuschagne, C., Wolff, E.W., Ganesan, A.L., 2016. Rising atmospheric methane: 2007-2014 growth and isotopic shift. Global Biogeochemical Cycles 30, 1356-1370.
Pan, G., Li, L., Wu, L., Zhang, X., 2004. Storage and sequestration potential of topsoil organic carbon in China's paddy soils. Global Change Biology 10, 79-92.
Raghoebarsing, A.A., Pol, A., van de Pas-Schoonen, K.T., Smolders, A.J.P., Ettwig, K.F., Rijpstra, W.I.C., Schouten, S., Damste, J.S.S., Op Den Camp, H.J.M., Jetten, M.S.M., Strous, M., 2006. A microbial consortium couples anaerobic methane oxidation to denitrification. Nature 440, 918-921.
Roland, F.A., Darchambeau, F., Morana, C., Crowe, S.A., Thamdrup, B., Borges, A.V., 2016. Anaerobic methane oxidation in an East African great lake (Lake Kivu). Biogeosciences Discuss.
Saunois, M., Bousquet, P., Poulter, B., Peregon, A., Ciais, P., Canadell, J.G., Dlugokencky, E.J., Etiope, G., Bastviken, D., Houweling, S., 2016. The global methane budget 2000-2012. Earth System Science Data 8, 697.
Segarra, K.E.A., Schubotz, F., Samarkin, V., Yoshinaga, M.Y., Hinrichs, K., Joye, S.B., 2015. High rates of anaerobic methane oxidation in freshwater wetlands reduce potential atmospheric methane emissions. Nature Communications 6, 7477.
Serrano-Silva, N., Sarria-Guzmán, Y., Dendooven, L., Luna-Guido, M., 2014. Methanogenesis and methanotrophy in soil: a review. Pedosphere 24, 291-307.
Shen, J., Tang, H., Liu, J., Wang, C., Li, Y., Ge, T., Jones, D.L., Wu, J., 2014a. Contrasting effects of straw and straw-derived biochar amendments on greenhouse gas emissions within double rice cropping systems. Agriculture, ecosystems & environment 188, 264-274.
Shen, L.D., Liu, S., Huang, Q., Lian, X., He, Z.F., Geng, S., Jin, R.C., He, Y.F., Lou, L.P., Xu, X.Y., Zheng, P., Hu, B.L., 2014b. Evidence for the cooccurrence of nitrite-dependent anaerobic ammonium and methane oxidation processes in a flooded paddy field. Applied and Environmental microbiology 80, 7611-7619.
Shen, L., Huang, Q., He, Z., Lian, X., Liu, S., He, Y., Lou, L., Xu, X., Zheng, P., Hu, B., 2015. Vertical distribution of nitrite-dependent anaerobic methane-oxidising bacteria in natural freshwater wetland soils. Applied Microbiology and Biotechnology 99, 349-357.
Shi, Y., Wang, Z., He, C., Zhang, X., Sheng, L., Ren, X., 2017. Using ^{13}C isotopes to explore denitrification-dependent anaerobic methane oxidation in a paddy-peatland. Scientific Reports 7, 40848.
Smemo, K.A., Yavitt, J.B., 2007. Evidence for anaerobic CH_4 oxidation in freshwater peatlands. Geomicrobiology Journal 24, 583-597.
Smemo, K.A., Yavitt, J.B., 2011. Anaerobic oxidation of methane: an underappreciated aspect of methane cycling in peatland ecosystems? Biogeosciences 8, 779-793.
Tate, K.R., 2015. Soil methane oxidation and land-use change – from process to mitigation. Soil Biology & Biochemistry 80, 260-272.
Valentine, D.L., 2002. Biogeochemistry and microbial ecology of methane oxidation in anoxic environments: a review. Antonie van Leeuwenhoek 81, 271-282.
Van Winden, J.F., Talbot, H.M., Kip, N., Reichart, G., Pol, A., McNamara, N.P., Jetten, M.S., den Camp, H.J.O., Damstéé, J.S.S., 2012. Bacteriohopanepolyol signatures as markers for methanotrophic bacteria in peat moss. Geochimica et Cosmochimica Acta 77, 52-61.
Weber, H.S., Thamdrup, B., Habicht, K.S., 2016. High sulfur isotope fractionation associated with anaerobic oxidation of methane in a low-sulfate, iron-rich environment. Frontiers in Earth Science 4, 61.

Wei, X.M., Ge, T.D., Zhu, Z.K., Hu, Y.J., Liu, S.L., Wu, J.S., Razavi, B.S., 2018. Expansion of rice enzymatic rhizosphere: temporal dynamics in response to phosphorus and cellulose application Plant Soil 1-13.

Wei, X.M., Hu, Y.J., Razavi, B.S., Zhou, J., Shen, J.L., Liu, S.L., Nannipieri, P., Wu, J.S., Ge, T.D. 2019. Rare taxa of alkaline phosphomonoesterase-harboring microorganisms mediate soil phosphorus mineralization. Soil Biology & Biochemistry 131: 62-70

Whalen, S.C., Reeburgh, W.S., Sandbeck, K.A., 1990. Rapid methane oxidation in a landfill cover soil. Applied and Environmental Microbiology 56, 3405-3411.

Zhao, X., Xie, Y., Xiong, Z., Yan, X., Xing, G., & Zhu, Z. 2009. Nitrogen fate and environmental consequence in paddy soil under rice-wheat rotation in the Taihu lake region, China. Plant and Soil, 319, 225-234.

Zhou, L., Wang, Y., Long, X., Guo, J., Zhu, G., 2014. High abundance and diversity of nitrite-dependent anaerobic methane-oxidizing bacteria in a paddy field profile. FEMS Microbiology Letters 360, 33-41.

Supporting Information for study 2

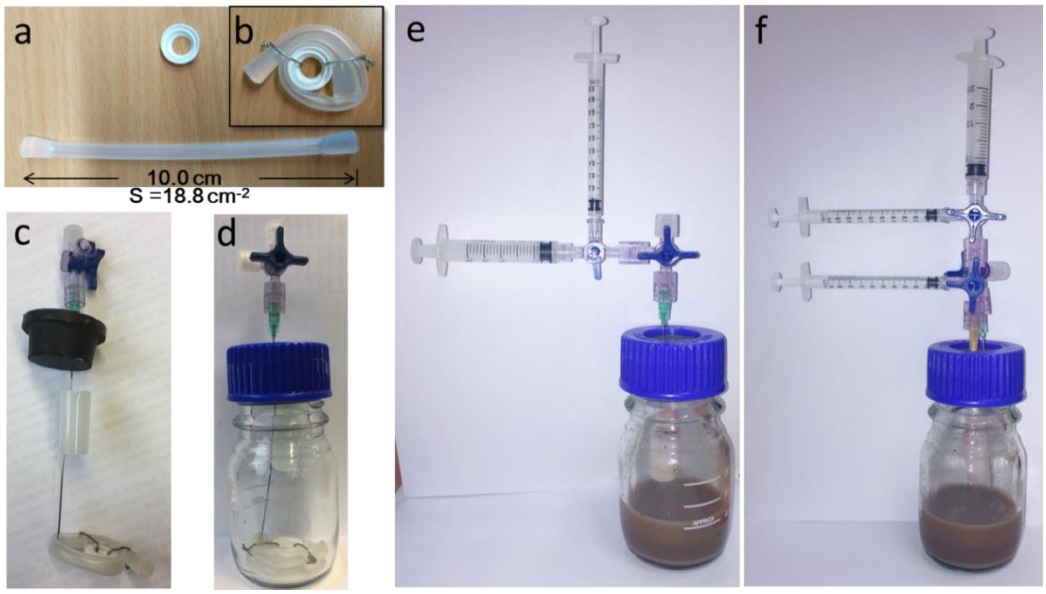

Fig. S1 The design of the soil silicone tube and its parameters (a, b), a set-up with a needle (c), an assembled incubation jar (d), the set-up for sampling with simultaneous N_2 replacement from silicone tube (e) and headspace (f). A plastic holder on a needle (c) is a site for an anaerobic indicator to control availability of O_2 in the headspace during incubation. S, outside surface area of silicone tube.

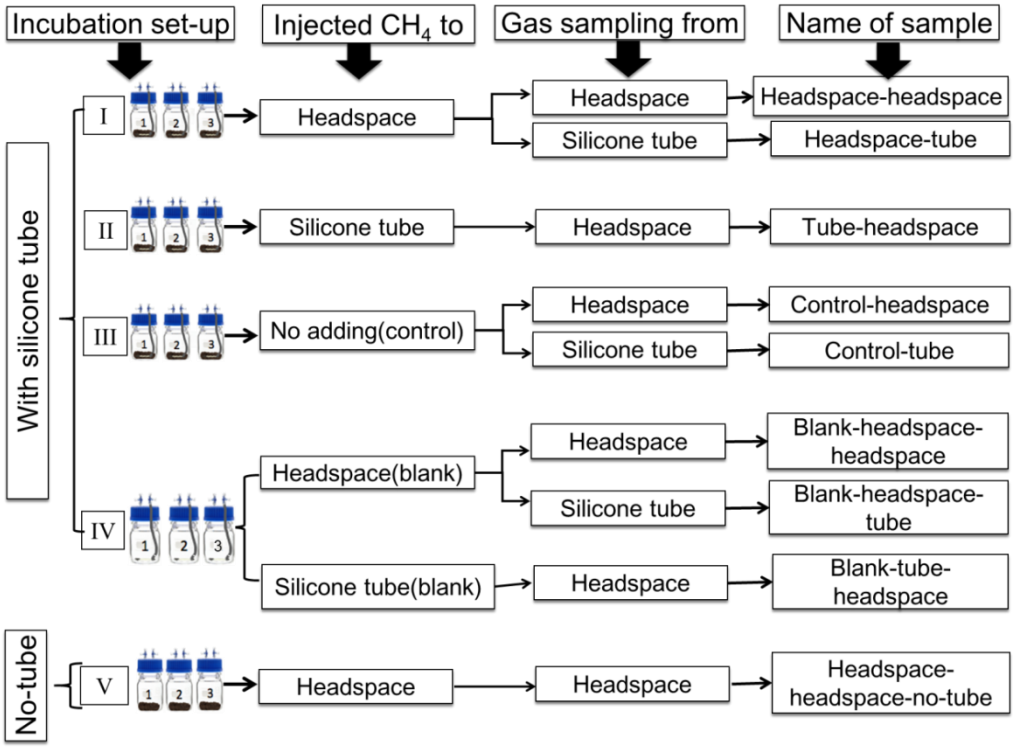

Fig. S2 Conceptual diagram of incubation experimental design and sample codes

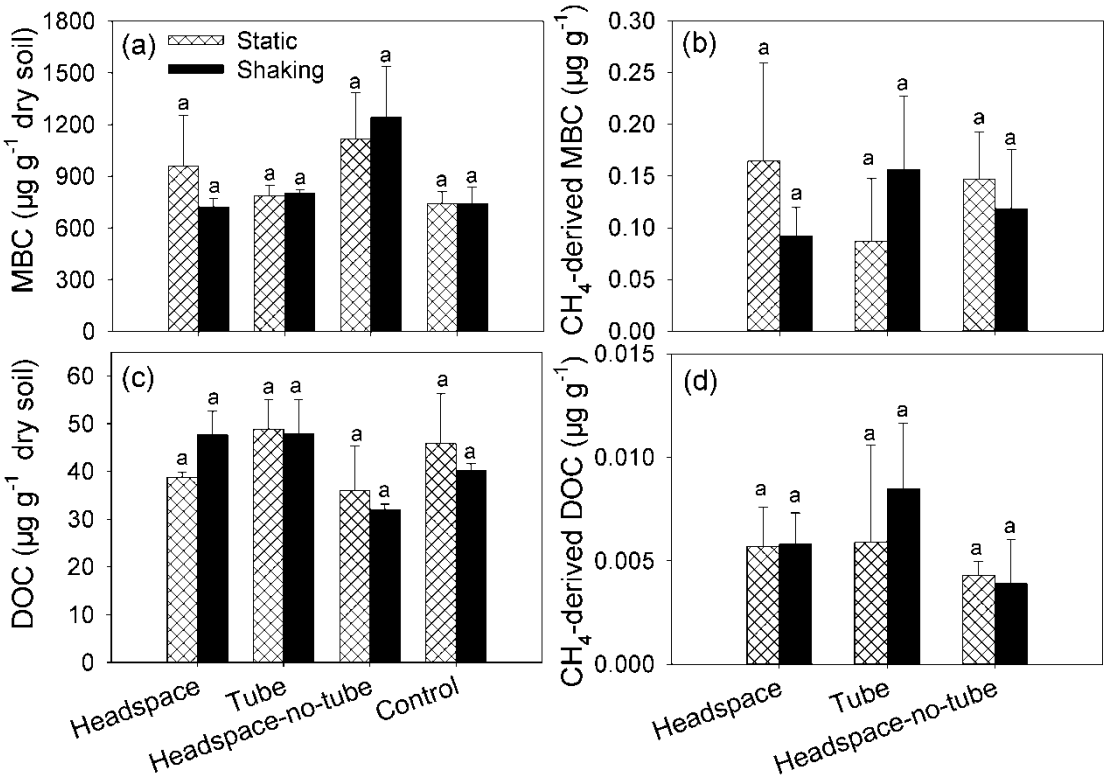

Fig. S3 Soil microbial biomass carbon, MBC (a) and CH_4-derived C in MBC (b), dissolved organic carbon, DOC (c), and CH_4-derived C in DOC (d) in microcosms with CH_4 injection into the headspace (Headspace), into the silicone tube (Tube), into the headspace without silicone tube (Headspace-no-tube) and the control without CH_4 injection (Control, for DOC and MBC only) with and without shaking. Letters: significant differences ($p < 0.05$) between microcosms with and without shaking.

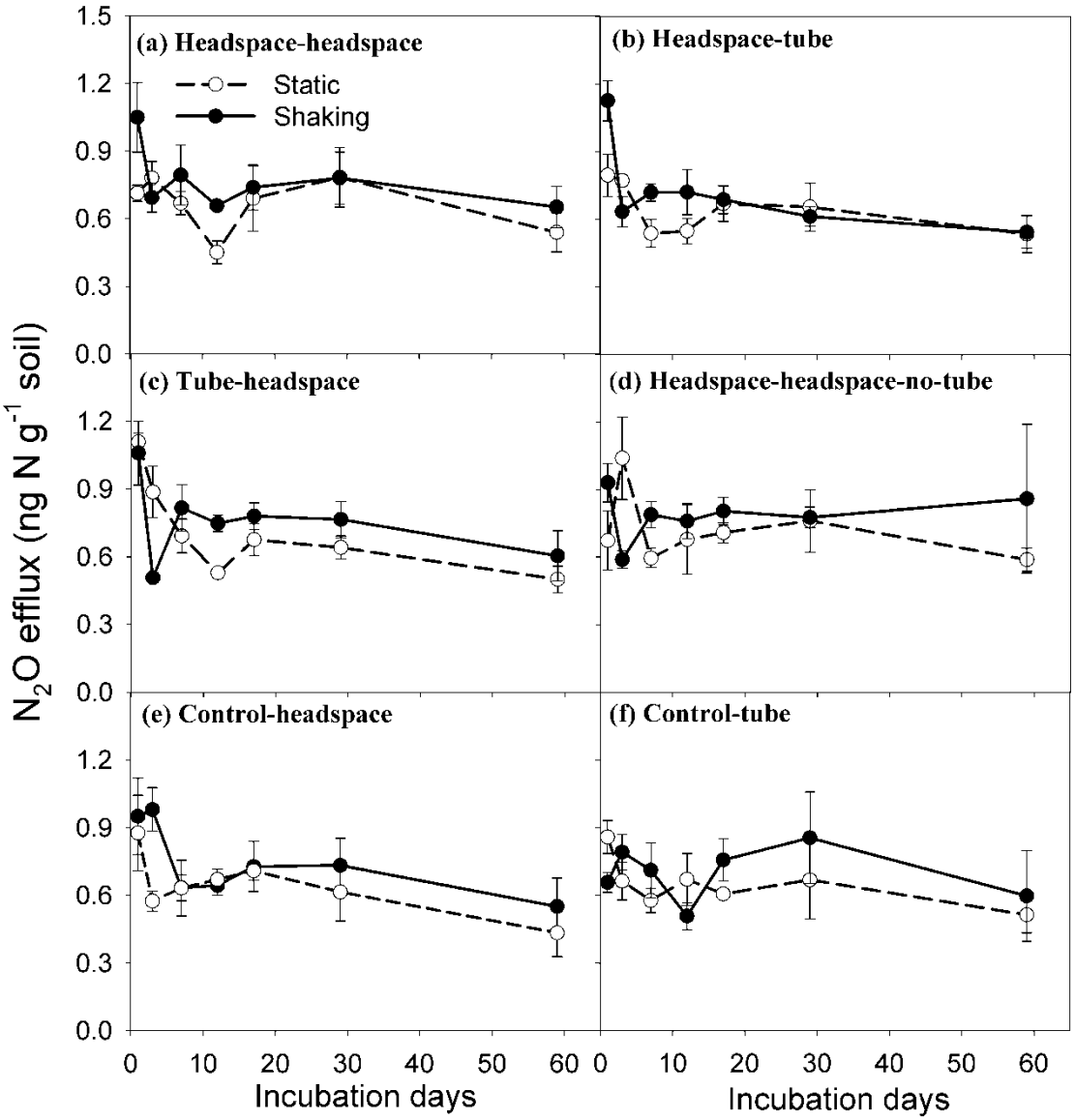

Fig. S4 N_2O production over 59 days of incubation with and without shaking in the microcosms subjected to (a) headspace injection with sampling from headspace (headspace-headspace) and (b) silicone tube (headspace-tube), (c) injection to soil slurry through silicone tube with sampling from headspace (tube-headspace) and (d) headspace injection and sampling without silicone tube (headspace-headspace-no-tube), (e) control without CH_4 injection with headspace sampling (control-headspace) and (f) silicone tube sampling (control-tube). Error bars: standard error of means (n = 3).

Table S1 Summary table for two-way ANOVA with repeated measures reflecting the significance of the effects of soil silicone tube, duration of incubation (59 days) and their interactions on cumulative CH_4 oxidation with and without shaking.

Source of Variation	Degree of freedom	Sum of Squares	Mean Square	F	*p*
		Shaking			
Silicone tube	3	0.015	0.005	2.24	0.171
Subject (silicone tube)	7	0.015	0.002		
Time	6	0.075	0.013	26.8	<0.001
Silicone tube × time	18	0.033	0.002	3.93	<0.001
Residual	42	0.020	0.000		
Total	76	0.169	0.002		
		Static			
Silicone tube	3	0.028	0.009	2.69	0.157
Subject (silicone tube)	5	0.017	0.003		
Time	6	0.247	0.041	34.2	<0.001
Silicone tube × time	18	0.019	0.001	0.88	0.609
Residual	30	0.036	0.001		
Total	62	0.341	0.006		

Table S2 Summary table for two-way ANOVA with repeated measures reflecting the significance of the effects of shaking treatments (static and shaking), duration of incubation (59 days) and their interactions on cumulative CH_4 oxidation.

Source of Variation	Degree of freedom	Sum of Squares	Mean Square	F	*p*
Shaking treatments	1	0.030	0.030	7.23	0.015
Subject (shaking treatments)	18	0.075	0.004		
Time	6	0.309	0.051	51.5	<0.001
Shaking treatments × time	6	0.035	0.006	5.9	<0.001
Residual	108	0.108	0.001		
Total	139	0.541	0.004		

Study 3 Anaerobic oxidation of methane in paddy soil: Role of electron acceptors and fertilization in mitigating CH_4 fluxes

Lichao Fan[a,*], Michaela A. Dippold[b], Tida Ge[c,*], Jinshui Wu[c], Volker Thiel[d], Yakov Kuzyakov[a,e,f], Maxim Dorodnikov[a]

[a] Department of Soil Science of Temperate Ecosystems, University of Göttingen, 37077 Göttingen, Germany

[b] Department of Biogeochemistry of Agroecosystems, University of Göttingen, 37077 Göttingen, Germany

[c] Key Laboratory of Agro-ecological Processes in Subtropical Region & Changsha Research Station for Agricultural and Environmental Monitoring, Institute of Subtropical Agriculture, Chinese Academy of Sciences, 410125 Hunan, China

[d] Geobiology, Geoscience Center, University of Göttingen, 37077 Göttingen, Germany

[e] Department of Agricultural Soil Science, University of Göttingen, 37077 Göttingen, Germany

[f] Agro-Technological Institute, RUDN University, 117198 Moscow, Russia

Status: Published in Soil Biology & Biochemistry

Fan, L., Dippold, M.A., Ge, T., Wu, J., Thiel, V., Kuzyakov, Y., Dorodnikov, M., 2020. Anaerobic oxidation of methane in paddy soil: Role of electron acceptors and fertilization in mitigating CH_4 fluxes. Soil Biology & Biochemistry 141, 107685.

*** Corresponding Authors**: Lichao Fan, lfan@gwdg.de; Tida Ge, gtd@isa.ac.cn

Abstract
The anaerobic oxidation of methane (AOM) in marine ecosystems is ubiquitous and largely coupled to sulfate reduction. In contrast, the role of AOM in terrestrial environments and the dominant electron acceptors driving terrestrial AOM needs deeper understanding. Submerged rice paddies with intensive CH_4 production have a high potential for AOM, which can be important for greenhouse gas mitigation strategies. Here, we used $^{13}CH_4$ to quantify the AOM rates in paddy soils under organic (Pig manure, Biochar) and mineral (NPK) fertilization. Alternative-to-oxygen electron acceptors for CH_4 oxidation, including Fe^{3+}, NO_3^-, SO_4^{2-}, and humic acids, were examined and their potential for CH_4 mitigation from rice paddies was assessed by $^{13}CH_4$ oxidation to $^{13}CO_2$ under anoxic conditions.
During 84 days of anaerobic incubation, the cumulative AOM ($^{13}CH_4$-derived CO_2) reached 0.15-1.3 μg C g^{-1} dry soil depending on fertilization. NO_3^- was the most effective electron acceptor, yielding an AOM rate of 0.80 ng C g^{-1} dry soil h^{-1} under Pig manure. The role of Fe^{3+} in AOM remained unclear, whereas SO_4^{2-} inhibited AOM but strongly stimulated the production of unlabeled CO_2, indicating intensive sulfate-induced decomposition of organic matter. Humic acids were the second most effective electron acceptor for AOM, but increased methanogenesis by 5-6 times in all fertilization treatments. We demonstrated for the first time that organic electron acceptors (humic acids) are among the key AOM drivers and are crucial in paddy soils. The most pronounced AOM in paddy soils occurred under Pig manure, followed by Control and NPK, while AOM was the lowest under Biochar. We estimate that nitrate (nitrite)-dependent AOM in paddy fields globally consumes ~3.9 Tg C-CH_4 yr^{-1}, thereby offsetting the global CH_4 emissions by ~10-20%. Thus, from a broader agroecological perspective, the organic and mineral fertilizers control an important CH_4 sink under anaerobic conditions in submerged ecosystems. Appropriate adjustments of soil fertilization management strategies would therefore help to decrease the net CH_4 flux to the atmosphere and hence the global warming.

Key words: anaerobic oxidation of methane; paddy soil; electron acceptors; fertilization; humic acids; CH_4 mitigation

1 Introduction

The anaerobic oxidation of methane (AOM) in marine ecosystems is a globally important biogeochemical process. In marine sediments, AOM is mainly linked to microbial sulfate reduction and consumes 20-300 Tg CH_4 yr^{-1} – equivalent to as much as 80% of the CH_4 produced by methanogenesis (Valentine, 2002). This makes AOM crucial for the global CH_4 balance and represents a potential constraint on climate change (Segarra et al., 2015; Hu et al., 2014). Due to the global significance in marine ecosystems, the exact mechanisms (potential electron acceptors, optimal biochemical conditions, etc.) and relevance of AOM in terrestrial ecosystems have received increasing attention (Bai et al., 2019; Shen et al., 2019). However, the evidence on AOM in terrestrial ecosystems is sporadic and cannot be directly compared to available information from the marine environment (Reeburgh, 2007). The process has therefore not been considered in most process-based biogeochemical models (Gauthier et al., 2015). This calls for studying the specific mechanisms of terrestrial AOM and for estimating the relevance for CH_4 consumption in oxygen-free environments, especially in ecosystems exposed to prolonged anaerobic conditions such as peatlands, rice paddies, and freshwater sediments.
AOM depends strongly on the availability of alternative-to-oxygen electron acceptors (AEAs) (Serrano-Silva et al., 2014; Cui et al., 2015). Previous studies have reported the occurrence of AOM in freshwater sediments (Beal et al., 2009; Deutzmann et al., 2014; Segarra et al., 2015), peatlands (Gupta et al., 2013; Putkinen et al., 2018), rice paddies (Fan et al., 2019b; Shen et al., 2014b; Shi et al., 2017), as well as in boreal and tropical soils (Blazewicz et al., 2012; Mohanty et al., 2017). Despite the increasing recognition of AOM in these environments, no systematic studies are available on the role

of potential AEAs, whose identification will be a key to elucidating the driving factors behind terrestrial AOM.

In marine environments, SO_4^{2-} is the most common and dominant alternative electron acceptor (AEA), and microbial sulfate reduction is intimately linked to AOM (Knittel and Boetius, 2009). In contrast, available information on AEAs for AOM in terrestrial ecosystems is elusive. Several potential predominately inorganic AEAs have been suggested, including sulfate (SO_4^{2-}), nitrate (NO_3^-), nitrite (NO_2^-), and ferric iron (Fe^{3+}) but with conflicting results. Gauthier et al. (2015) demonstrated that adding SO_4^{2-} suppressed methanogenesis rather than enhancing AOM in soils. This is because of SO_4^{2-} concentrations in terrestrial ecosystems are typically too low (~0.01-0.2 mM in freshwater vs. 28 mM in sea water; Canfield and Farquhar, 2009; Shen et al., 2019). On the other hand, Gupta et al. (2013) suggested that SO_4^{2-} served as the AEA accelerating AOM rates in a fen peat, where SO_4^{2-} concentrations were higher. Likewise, NO_3^- application in peatland soils revealed both positive (Pozdnyakov et al., 2011) and negative effects (Gupta et al., 2013) on AOM. So far there are only a few enrichment culture studies that have demonstrated the direct potential of *Candidatus 'Methanoperedens nitroreducens' (M. nitroreducens)* and *Candidatus* '*Methylomirabilis oxyfera'* (*M. oxyfera*) to oxidize CH_4 anaerobically with nitrate/nitrite as electron acceptors (Vaksmaa et al., 2016; 2017). Nonetheless recent studies revealed nitrate/nitrite-dependent AOM is becoming a significant important CH_4 sink globally, since the anthropogenic N inputs are increasing rapidly into marine (e.g. river runoff and N deposition) and terrestrial ecosystems (e.g. agricultural N fertilization, municipal waste) (Hu et al., 2014). Regarding microorganisms driving AOM, sulfate-dependent AOM is performed by methanotrophic archaea of the ANME-1, ANME-2 (subgroups -a, b, c) and ANME-3 clades forming consortia with sulfate reducing bacteria (Knittel and Boetius, 2009). Nitrate-dependent AOM is performed by *M. nitroreducens* of the ANME-2d clade within the family *Candidatus 'Methanoperedenaceae'* (Haroon et al., 2013), whereas nitrite-dependent AOM is driven by *M. oxyfera* of the NC10 phylum bacteria (Ettwig et al., 2010). Iron (III)-dependent AOM is reported to be performed by *Candidatus 'Methanoperedens ferrireducens'* (*M. ferrireducens*) which belongs to a novel genus within the family *Candidatus 'Methanoperedenaceae'* (Cai et al., 2018).

In tropical soils, AOM is linked to iron reduction-oxidation (Mohanty et al. (2017), the possible mechanism of providing energy for AOM being similar to microbial sulfate reduction (Smemo and Yavitt, 2011). In addition to inorganic AEAs, there is also evidence that organic AEAs such as humic acids (HA) and humic substances actively participate in redox processes driving AOM (Blodau and Deppe, 2012). Humic substances can act as direct AEAs for AOM driven by ANME-2d (Bai et al., 2019), or as indirect AEAs via the re-oxidation of other AEAs (e.g. Fe^{2+}) (Valenzuela et al., 2019) or intermediate sulfur species (Yu et al., 2015). As yet, however, the specific role of organic substances as AEAs for AOM remains largely unclear.

Submerged rice paddies with active methanogenesis provide ideal habitats for AOM microbes. Globally there are 167 million hectares of rice paddies (FAO, 2018) generating 31 million tons of CH_4 per year (Keppler et al., 2006). This represents one of the largest human-related sources of atmospheric CH_4 (Chen et al., 2013; Huang et al., 2002; Zhang et al., 2011). To increase rice yield and maintain paddy soil fertility, organic (*e.g.* livestock manure, biochar) and mineral (NPK) fertilizers are routinely applied. This leads to a high availability of humifying organic matter and nutrients and would further argue for the presence of an ecologically relevant AOM process in paddy soils. Indeed, AOM occurs in rice paddies and has been shown to be performed by nitrite-dependent anaerobic methane-oxidizing bacteria (Hu et al., 2014; Shen et al., 2014b). However, the role of other AEAs, including organic compounds, and the intensity of the process in offsetting of CH_4 fluxes from rice paddies remain unclear. This calls for narrowing the knowledge gap on the relevance and factors controlling AOM in these submerged agro-ecosystems.

Here, we used ^{13}C-labelled CH_4 to examine the occurrence and rates of AOM in paddy soils under the addition of various potential AEAs: NO_3^-, Fe^{3+}, SO_4^{2-}, and HA. Three paddy soils under long-term

application of pig manure, biochar, and NPK fertilizers were tested and compared with the low-fertilized control to gain a better sustainable paddy field management in terms of CH_4 mitigation. Based on the above, we hypothesized that (i) NO_3^- is the most preferential AEA for AOM in paddy soils because it is present in high amounts and has a higher energy release by reduction compared to other AEAs. In comparison, Fe^{3+} and SO_4^{2-} could both be relevant but less effective than NO_3^-. Further, (ii) pig manure and NPK fertilization should induce the highest AOM rate due to larger availability of organic and inorganic AEAs as compared with the low-fertilized control and biochar addition. Beyond testing these hypotheses, we verified whether HA serve as an AEA for AOM in paddy soil. Finally, we assessed the potential offset in CH_4 efflux from paddy soils due to AOM, and demonstrated the relevance of AOM in these agroecosystems for CH_4 mitigation.

2 Materials and methods

2.1 Site description and soil collection

The sampling site was located near Jinjing town, Changsha county of Hunan province in China (28°33′04″N, 113°19′52″E), which is characterized by a subtropical humid monsoon climate. The mean annual air temperature of the region is 17.5 °C and the mean annual precipitation is 1330 mm. The typical paddy field has a tillage history of more than 1000 years of rice production (double cropping, with early rice grown season in late April to mid-July and late rice grown season in mid-July to late October). The soil at the experimental field is classified as Hydragric Anthrosol developed from red granite parental material (Driessen et al., 2000). It has a bulk density of 1.26 g cm^{-3} and shows a sandy loam soil texture (as referred to USDA soil taxonomy) consisting of 27% clay, 29% silt, and 44% sand. The soil pH is 5.2 (Shen et al., 2014a).

Soil samples were collected from the ongoing field experiment under four fertilization treatments: (i) Control with conventional fertilization (60 kg N ha^{-1} yr^{-1} as urea, 18 kg P ha^{-1} as $Ca(H_2PO_4)_2$, and 83 kg K ha^{-1} were applied before the seedling transplanting in each of the rice seasons), (ii) Pig manure (60 Mg ha^{-1} yr^{-1}, half of which was applied before transplanting in the early and another half in the late rice season; containing 250 g C kg^{-1}, 16.8 g N kg^{-1}, 5.3 g P kg^{-1}, 2.5 g K kg^{-1}; pH 8.0) with conventional fertilization, (iii) Biochar (24,000 kg ha^{-1} applied in spring 2016; biochar was pyrolyzed from wheat straw at 500 °C by Sanli New Energy Ltd. (Shangqiu, Henan Province, China); containing 418 g C kg^{-1}, 2.8 g N kg^{-1}; pH 9.8) with conventional fertilization, and (iv) NPK (240 kg N ha^{-1} yr^{-1} as urea, 120 kg N ha^{-1} in the early rice season and the rest in the late rice season; 18 kg P ha^{-1} as $Ca(H_2PO_4)_2$ and 83 kg K ha^{-1} were applied before the seedling transplanting in each of the rice seasons as basal fertilizer). Each plot was flooded for one week before the early rice transplanting, and through the whole growing season till rice harvesting when water was drained from the rice field. Each of these fertilization treatments was applied independently on three field plot replicates (35 m^2 per plot), and the rice cultivars *Oryza sativa* L. 'Xiangzaoxian No. 45' for the early rice season, and *Oryza sativa* L. 'T-you 207' for the late grown season as well as management were similar.

Soil samples were collected after the late season rice harvesting in December 2016, when the plots were field-moist but not over-flooded. The soil sampling method is described in Fan et al. (2019a, b). Briefly, from each of the plots, we collected four soil cores from 10-30 cm depth (bottom layer of a plow horizon 0-30 cm) with a soil auger. We omitted the top 10 cm layer due to periodic aerobic conditions and potentially higher aerobic vs. anaerobic CH_4 oxidation potential; soil samples from 20-30 cm depth were used for the current study as most potent for AOM. The core samples were mixed and homogenized to form one composite sample per plot. There were no large stones in the paddy soil and un-decomposed plant remnants were carefully removed before incubation. All soil samples (ca. 30% soil weight-based water content) were immediately sealed in plastic bags. The air in the bags was evicted to minimize exposure to atmospheric oxygen (O_2). Soil samples for laboratory incubation were not sieved because the paddy field has been thoroughly and regularly plowed for more than 1000 years, and also to avoid un-natural overexposure to air and minimize unfavorable effects on the anaerobic

processes studied. Soil samples were transported from China to the University of Göttingen, Germany, at room temperature during one day; thereafter they were stored in a cooling room (4 °C) until the incubation experiment. Soil subsamples (~ 10 g) were air-dried, passed through a 1-mm sieve to exclude any occasional stone incorporation, and ground to powder for soil organic carbon (SOC) content, total nitrogen (N) content and elements analysis. SOC and total N were determined with a Vario Max CN Analyzer (Elementar Analysensysteme GmbH, Langenselbold, Germany). Other elements (*i.e.* S, Fe) in the soils were determined using inductively coupled plasma optical emission spectroscopy (ICP-OES; iCAP 6000 series, ASX-520 Auto-Sampler, Thermo Scientific, COUNTRY). Soil microbial biomass carbon (MBC), NH_4^+, and NO_3^- contents were measured from un-sieved field-moist soil. MBC was determined by a chloroform fumigation K_2SO_4 extraction method (10 g soil was extracted by 40 ml 0.05 M K_2SO_4), and calculated based on the difference between extracted organic C content of fumigated and non-fumigated soils by using a k_{EC} factor = 0.45 after Joergensen (1996). Extractable dissolved organic carbon (eDOC) was determined from the extracts of the non-fumigated samples. The extracts obtained were analyzed for total C content using a TOC/TIC analyzer (Multi N/C 2100, Analytik Jena, Germany). NH_4^+ and NO_3^- were extracted with 0.05 M K_2SO_4 and measured using continuous flow injection colorimetry (SEAL Analytical AA3, SEAL Analytical GmbH, Norderstedt, Germany). All measured basic biochemical properties of the soil are given in Table S1.

2.2 Experimental setup

The anaerobic incubation experiment was designed to test paddy soils under different fertilization treatments (see 2.1) for AOM induced by addition of several AEAs, *i.e.* Fe^{3+}, NO_3^-, SO_4^{2-}, and humic acids (Sigma Aldrich, Chemie GmbH, Steinheim, Germany).

To prepare the microcosms, 15 g field-moist soil was loaded into 100-ml Kimble KIMAX borosilicate laboratory glass jars with wide necks (GL 45, Kimble Chase Life Science and Research Products, LLC., Meiningen, Germany). The jars were sealed by gas-impermeable black butyl rubber septa and fixed by blue plastic screw caps. All jars and septa were autoclaved twice at 121 °C for 20 min before loading soil into jars. To reduce the remaining O_2 in the microcosms, the headspace was evacuated 8 times with a vacuum pump for 5 min and then back-flushed with high-purity N_2, then the N_2-flushed microcosms were left overnight to allow for consumption of any remaining O_2. To exclude further contamination with atmospheric O_2, all manipulations with soils were conducted in a glovebox (N_2/H_2, 97/3%) under fully controlled anaerobic conditions. Inside the glovebox, the jars were opened and 20 ml deionized sterile water or chemical solutions (see below) were added to make the soil slurries. To ensure that anaerobic conditions prevailed in the microcosms throughout the experiments, oxygen indicators (Thermo Scientific, Oxoid Ltd., Basingstoke, Hampshire, UK) were placed inside the jars before closing septa and caps, and the color was regularly recorded during the experiment (pink – aerobic, white – anaerobic). To quantify the anaerobic oxidation of $^{13}CH_4$ to $^{13}CO_2$ over time, labeled CH_4 (5 ml 5 atom% $^{13}CH_4$) was injected into the headspace of the microcosms, resulting in an initial average headspace CH_4 concentration of 3.1%. Along with CH_4 injection, we produced references using the same volume of N_2 instead of CH_4 to determine the methanogenesis potential. The microcosms were moved out of the glovebox and incubated with continuous shaking (100 rounds min^{-1}) in the dark at 18 °C over 84 days. All O_2 indicators remained white (*i.e.* anaerobic) over the whole 84 days of the experiment.

2.3 AEA addition and gas sampling

Anaerobic soil samples were amended with AEAs and an additional set was left as a non-amended control (reference) soil. The added AEA amounts corresponded to the upper limits of the respective concentration ranges measured in the soil (Table S1). NO_3^- (22.3 μg g^{-1}) was added as $NaNO_3$, SO_4^{2-} (12.7 mg g^{-1}) was added as Na_2SO_4, and HA (1.25 mg g^{-1}, obtained from Sigma-Aldrich Chemie GmbH, Kappelweg 1, D-91625 Schnelldorf, Germany) were added as solution dissolved in deionized

sterile water with help of sonication (RK 100H, Bandelin Sonorex, Heinrichstr. 3-4, 12207 Berlin, Germany). Fe^{3+} was added as Fe_2O_3 (23.3 mg Fe g^{-1}) powder. To prepare the powder, Fe_2O_3 was dehydrated from crystalline $Fe(OH)_3$. $Fe(OH)_3$ was synthesized by neutralizing a solution of $FeCl_3 \cdot 6H_2O$ with NaOH. To remove chloride ions and to obtain the crystalline $Fe(OH)_3$, an excessive NaOH amount was added to the $FeCl_3 \cdot 6H_2O$ solution (Blazewicz et al., 2012). The reaction mixture was centrifuged at 2000 r min^{-1} for 5 min and the supernatant discarded. The resulting pellet was washed four times with deionized water using vortexing and centrifugation of the solution. After each washing the supernatant was discarded. The crystalline $Fe(OH)_3$ was dehydrated in an oven at 105 ± 2 ℃ (24 h), and the Fe_2O_3 obtained was mechanically ground by ball milling (Retsch MM200, Haan, Germany) and stored dry in tightly closed glass bottles until use. Deionized water and solutions were purged with N_2 in glass volumetric bottles at 135 kPa for 30 min to remove dissolved O_2. The glass volumetric bottles and water were autoclaved twice at 121 ℃ for 20 min before using.

During the incubations, gas samples were collected at 2, 7, 14, 21, 28, 42, 56 and 84 days after $^{13}CH_4$ injection. Two 1-ml and one 2.5-ml gas-tight N_2-flushed plastic syringes (Thermo Scientific™) fitted with stopcocks were used: two 1-ml syringes to collect gas from the headspace (through septa with needles) and one 2.5-ml syringe with 2 ml N_2 to immediately compensate the equivalent volume of N_2 to maintain slight overpressure (ca. +100-150 mbar from the ambient). All gas samples were transferred to evacuated N_2-flushed glass vials. Thereafter, one separate set of gas samples was diluted with N_2 (1 ml sample into 15 ml N_2) and the CO_2 and CH_4 concentrations were measured on a gas chromatograph (GC-14B, Shimadzu, Ld. Nds., Japan) equipped with a flame ionization detector (for CH_4) and electron capture detector (for CO_2) according to an established protocol (Loftfield et al., 1997). Another separate set of gas samples was analysed for stable C isotope composition of CO_2, with a dilution of 1 ml sample into 12 ml N_2. Gas analyses were done within two weeks after sampling.

2.4 Isotope analysis

Stable C isotope analysis of gas (CO_2) was conducted using an isotope ratio mass spectrometer (Delta plus IRMS, Thermo Fisher Scientific, Bremen, Germany) at the Centre for Stable Isotope Research and Analysis (KOSI), University of Goettingen, Germany. Data are reported as $\delta^{13}C$-values relative to the Vienna Peedee Belemnite (VPDB) standard.

2.5. Calculations and statistics

The quantity of $^{13}CH_4$ oxidized anaerobically, as expressed by the amount of $^{13}CO_2$ generated as the end-product of oxidation, was calculated for each time point (*i.e.* 2, 7, 14, 21, 28, 42, 56 and 84 days) using the following equation:

$$C_{OX} = \frac{(\delta^{13}C_{Total} - \delta^{13}C_{Control})}{(\delta^{13}C_{OX} - \delta^{13}C_{Control})} \times C_{Total} \quad (1)$$

where C_{OX} (μg) represents the amount of $^{13}CH_4$ oxidized based on the released $^{13}CO_2$, C_{Total} represents the total amount of C in the corresponding pool (*i.e.* CO_2,), $\delta^{13}C_{Total}$ is the delta value of $^{13}CO_2$ in the samples treated with $^{13}CH_4$, $\delta^{13}C_{Control}$ is the delta value of $^{13}CO_2$ in the reference (no $^{13}CH_4$ addition), and $\delta^{13}C_{OX}$ is the delta value of $^{13}CH_4$ with 5 atom% enrichment. The rate of AOM was calculated from the differences between the respective values of adjacent time points (*e.g.* 0 vs. 2nd day). The cumulative AOM was calculated from the sum of these differences over the entire experiment. Gross CH_4 production was calculated as the AOM plus the net CH_4 emission (as determined from references without CH_4 added, assuming similar AOM rates in CH_4-added and reference microcosms).

A two-way ANOVA (analysis of variance) with repeated measures was used to determine the effects of AEA addition on $\delta^{13}CO_2$, and the effects of fertilization treatments on cumulative AOM over the 84 days of incubation. One-way ANOVA was used to determine differences in AOM rates between fertilization treatments and different AEA amendments. The normality and homogeneity of the

residuals of the resulting $\delta^{13}CO_2$, AOM rates, and cumulative AOM were tested. *t*-tests were used to characterize the differences in $\delta^{13}CO_2$ at each time point between reference and AEAs. The Shapiro–Wilk test was used to test the normality of the data sets. Standard errors of measurements are based on three replicates from each sampling time. All statistical analyses were performed using SPSS software (ver. 19.0, SPSS Inc., Chicago, IL, USA) and SigmaPlot software (ver. 12.5, Systat Software, Inc, San Jose, California, USA).

3 Results

3.1 CH_4 dynamics

In microcosms without $^{13}CH_4$ injection (Fig. 1, left column), the CH_4 concentration after HA amendment ([CH4]) continuously increased by 4.3 to ~ 20.2 times as compared to the reference without AEAs amendments. This increase occurred irrespective of the fertilizer type applied. Adding NO_3^- did not significantly affect [CH_4] in any of the soils. Adding Fe^{3+} to soil under NPK resulted in [CH_4] 2.0 times lower than the reference, whereas soils under other fertilizations were not affected. The [CH_4] decreased by 3.4 to ~ 5.5 times after SO_4^{2-} amendment in all soils except Pig manure, where [CH_4] kept similar to the reference.

In microcosms with $^{13}CH_4$ injection (Fig. 1, right column), the [CH_4] again increased most significantly in HA amended soils under all fertilizers. A moderate [CH_4] increase, similar to the reference, was observed in soils amended with Fe^{3+} and NO_3^-. In soils amended with SO_4^{2-}, [CH_4] remained stable over the entire 84 days of the experiment, independent of fertilization.

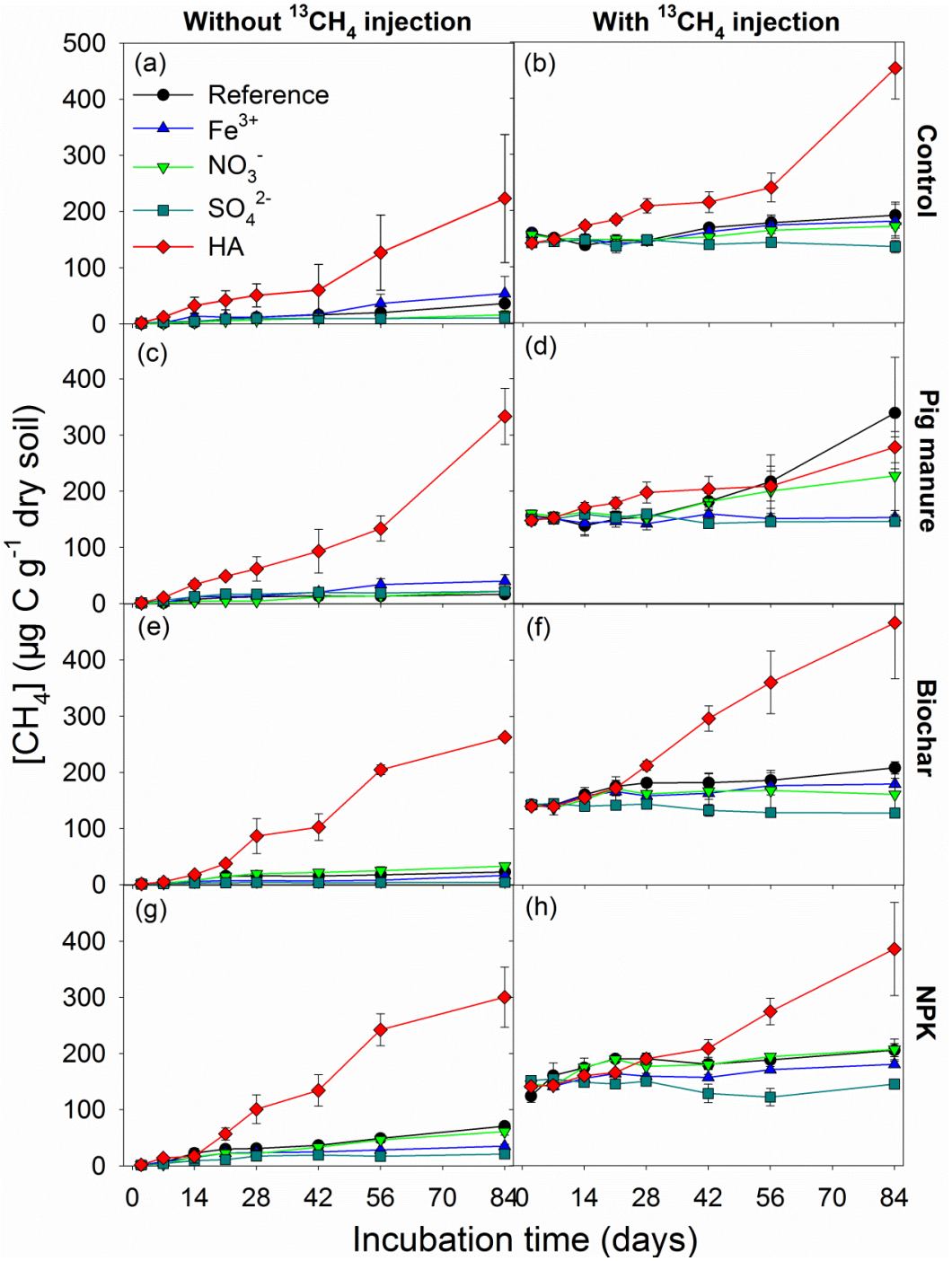

Fig. 1 Dynamics of CH_4 concentration ($[CH_4]$) in the headspace of microcosms from three field fertilization treatments (Pig manure, Biochar, NPK) and the low-fertilized Control over 84 days of incubation without (a, c, e, g) and with (b, d, f, h) $^{13}CH_4$ injection and with Fe^{3+} (as Fe_2O_3), NO_3^- (as $NaNO_3$), SO_4^{2-} (as Na_2SO_4), and HA (humic acids) amendment as well as non-amended Reference. Error bars: standard error of mean (n=3).

3.2 $\delta^{13}CO_2$ signatures

As compared to the ^{13}C natural abundance (Fig. 2, dashed lines), the highest $^{13}CO_2$ enrichment occurred with NO_3^- amendment, followed by the reference, and the Fe^{3+} amendment soil ($P < 0.05$, Table S2). The above pattern was most pronounced under Pig manure, followed by Control and NPK, and was the lowest under Biochar (Fig. 2). No significant $^{13}CO_2$ enrichment was recorded after SO_4^{2-} amendment under all fertilizations (Fig. 2 m, n, o, p). With HA amendment, $^{13}CO_2$ enrichment occurred at the beginning and at the end of the 84 days under Control, Biochar and NPK (Fig. 2 q, s, t).

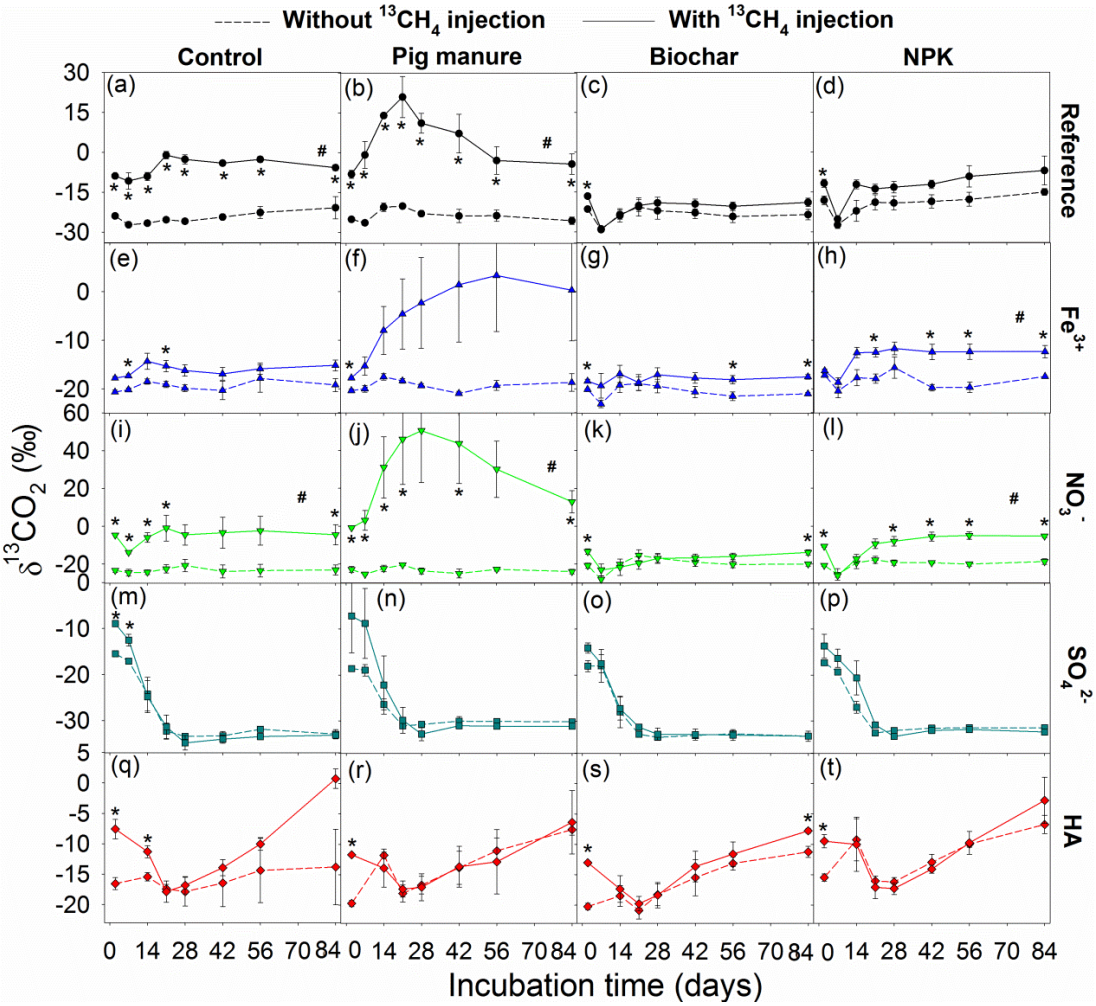

Fig. 2 Dynamics of $\delta^{13}CO_2$ signatures over 84 days of incubation without and with $^{13}CH_4$ injection nested with electron acceptors ((Fe^{3+} (as Fe_2O_3), e-h; NO_3^- (as $NaNO_3$), i-l; SO_4^{2-} (as Na_2SO_4), m-p; HA (humic acids), q-t) amendments and the non-amended Reference (a-d) under field fertilization treatments (Control, Pig manure, Biochar, and NPK). HA: humic acids. Asterisks *: significant difference ($P < 0.05$) between microcosms with added $^{13}CH_4$ and natural abundance counterparts at each day of measurements. Dash symbol (#): significant difference ($P < 0.05$) between $^{13}CH_4$ and natural abundance over period of incubation (Table S2). Error bars: standard error of mean (n=3).

3.3 Rate of AOM

The 84 days' average AOM rates increased by 20-90% after NO_3^- amendment under all fertilizations except for Biochar, where it was 30% lower than the reference. The maximal average AOM rate (0.80 ng C g^{-1} dry soil h^{-1}) for NO_3^- amended soil was recorded under Pig manure (Fig. 3b) followed by Control, NPK, and Biochar (Fig. 3). Fe^{3+} addition did not affect the average AOM rates under Biochar and NPK, whereas a decrease was observed in Control and under Pig manure (Fig. 3a, b). SO_4^{2-} amendment reduced the average AOM rates by 5-51 times under all fertilizations except for Biochar, where it was similar to the reference. Likewise, HA decreased the average AOM rates by 25-256% under all fertilizations except for Biochar, where it was 50% higher than in the reference (Fig. 3). There was a close correlation between the average AOM rate and the MBC in reference among all the fertilization treatments (Fig. S2, $R^2 = 0.89$, $P = 0.036$).

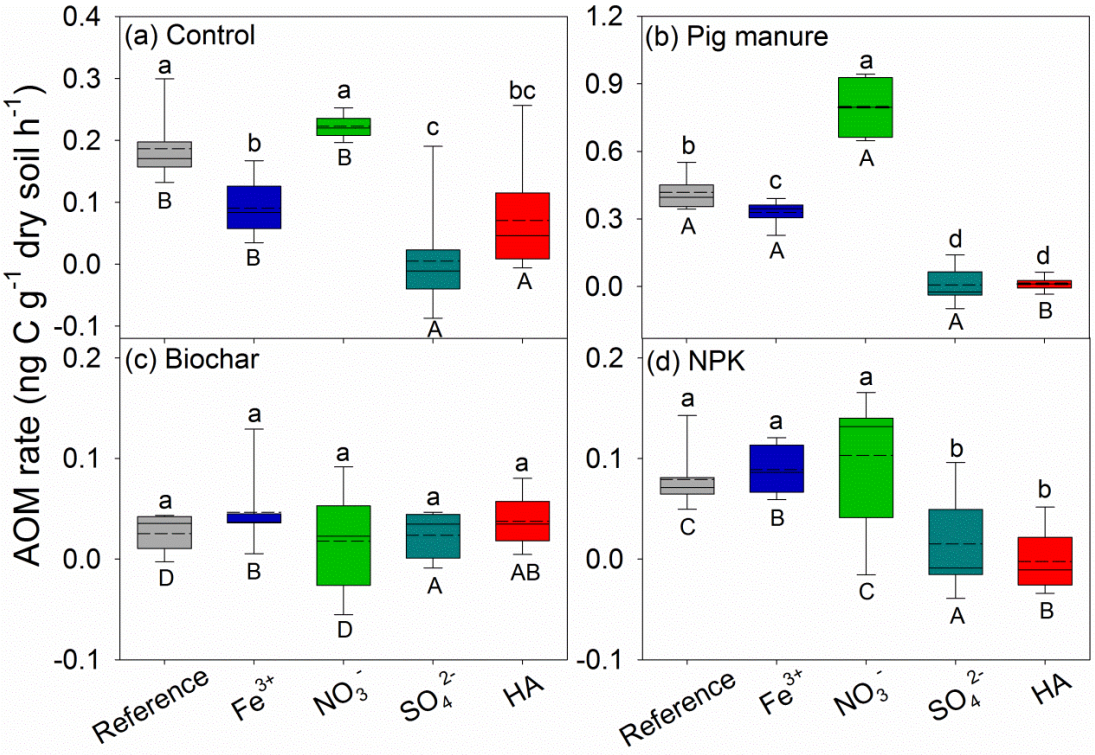

Fig. 3 Box plots of the average rates of anaerobic oxidation of methane (AOM) over 84 days of incubation under field fertilization treatments: Control (a), Pig manure (b), Biochar (c) and NPK (d). Upper and lower bars: maximum and minimum observations, respectively; top and bottom of boxes: third and first quartiles; thin horizontal solid lines in boxes: median values; dashed lines: mean values (without outliers). HA: humic acids. Lowercase letters: significant differences ($P < 0.05$) between electron acceptors for each soil fertilization treatment. Captial letters: significant differences ($P < 0.05$) between soil fertilization treatments for each electron acceptor

3.4 Cumulative AOM

The cumulative AOM over the 84-day period varied between 0.15-1.3 µg C g^{-1} dry soil depending on the fertilization. The cumulative AOM after 84 days was 1.3 to ~ 2.0 times higher after NO_3^- amendment to soils under all fertilization (Fig. 4, green line). Fe^{3+} addition had no effect on the cumulative AOM, independent of fertilization ($P > 0.05$) (Fig. 4, blue line). After HA addition, the cumulative AOM was lower than that of the reference during the first 54 days; then it increased rapidly and even exceeded that of the reference under Biochar and Control but not under Pig manure and NPK (Fig. 4, red line). SO_4^{2-} amendment inhibited AOM throughout the incubation (Fig. 4, cyan line). Overall, the field fertilization had a significant effect ($P < 0.001$, Table S3) on the cumulative AOM. There was a linear correlation between the amount of gross produced and oxidized CH_4 under all fertilization treatments (Fig. 5, $R^2 = 0.55 \sim 0.93$, $P < 0.05$).

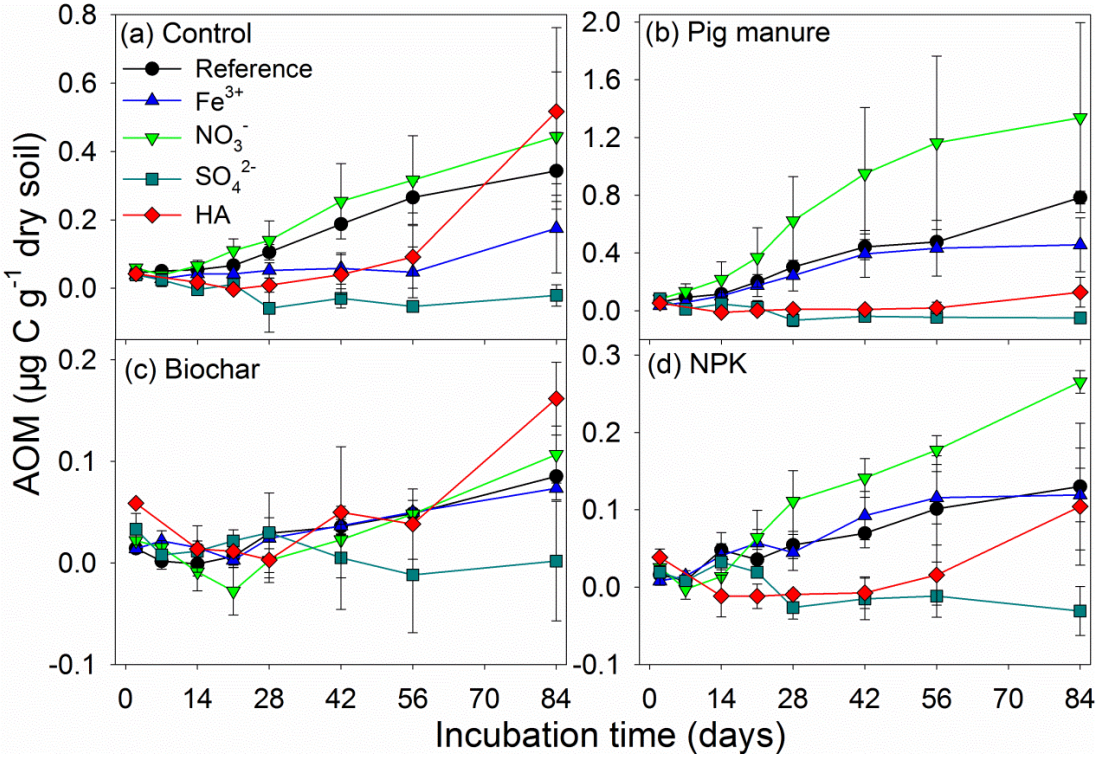

Fig. 4 Cumulative anaerobic oxidation of methane (AOM) over 84 days' incubation under field fertilization treatments (Control (a), Pig manure (b), Biochar (c), NPK (d)) and electron acceptor amendments (NO_3^-, Fe^{3+}, SO_4^{2-}, and humic acids (HA)). Error bars: standard error of mean (n=3).

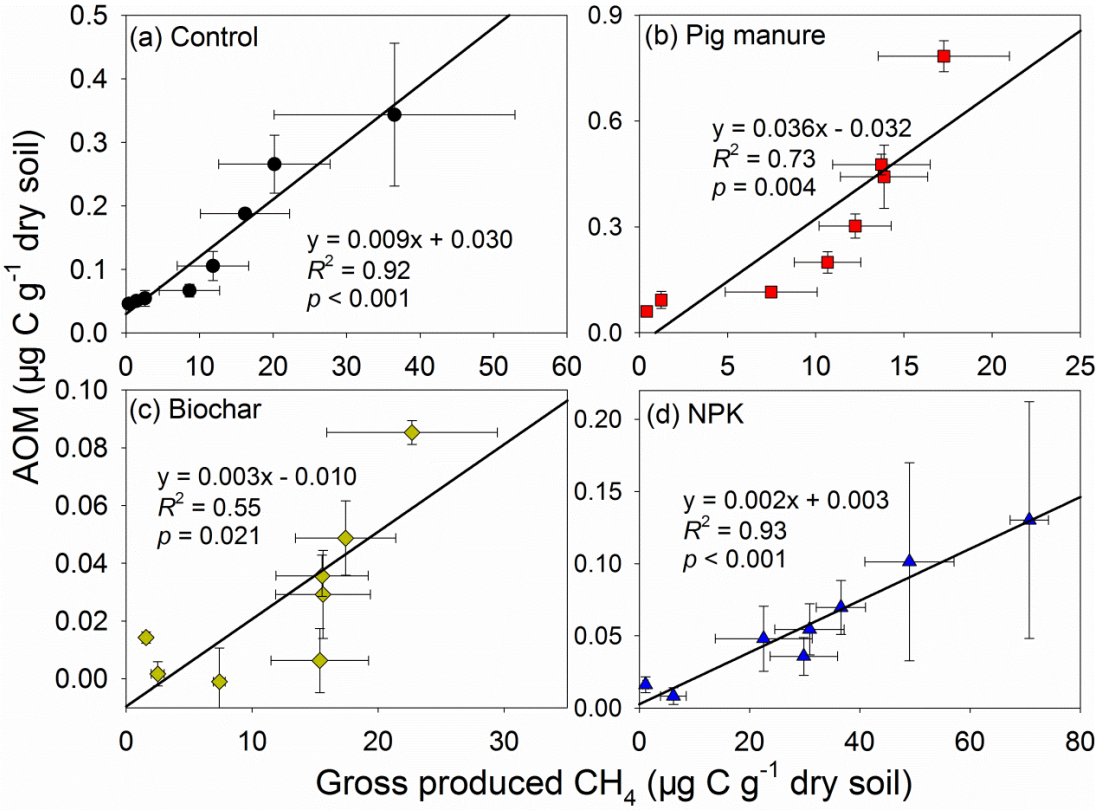

Fig. 5 Relationships between the amounts of gross CH_4 production (net + AOM) and anaerobic oxidation of methane (AOM) in reference soils without electron acceptor amendments: Control (a), Pig manure (b), Biochar (c) and NPK (d). Error bars: standard error of mean (n=3).

4 Discussion

4.1 AOM rates and the hypothesis of "reverse methanogenesis"

The ^{13}C excess in the headspace CO_2 under strictly controlled anaerobic conditions (Fig. 2) enabled us to confirm the earlier reported occurrence of AOM in submerged paddy soils (Fan et al., 2019b; Hu et al., 2014; Shi et al., 2017). We demonstrated for the first time how AOM depends on the type of AEA and the fertilization (Fig. 6). Average AOM rates measured (~ 0.80 ng C g^{-1} dry soil h^{-1} over 84 days, Fig. 3) were similar to those earlier reported for paddy soils at a similar soil depth (Hu et al., 2014, 0.15-1.02 ng C g^{-1} dry soil h^{-1}; Shen et al., 2014b, 0.11-1.05 ng C g^{-1} dry soil h^{-1}). These AOM rates were also comparable to those documented in wetlands (Shen et al., 2015; 0.1-0.5 ng C g^{-1} dry soil h^{-1} at 20-30 cm depth) and tropical mineral soils (Blazewicz et al., 2012; 1.45 ng C g^{-1} dry soil h^{-1} at 10-15 cm depth). Interestingly, the observed rates are 1 to ~2 orders of magnitude lower than in peatlands (Gupta et al., 2013; 8.3-255.3 ng C g^{-1} dry peat h^{-1} at 15-45 cm depth), freshwater sediments (Shen et al., 2019; 10-30.5 ng C g^{-1} dry sediments h^{-1}), and marine systems (Orcutt et al., 2005; 15-80 ng C g^{-1} dry sediments h^{-1}). Therefore, the mechanisms controlling AOM may strongly differ in various ecosystems.

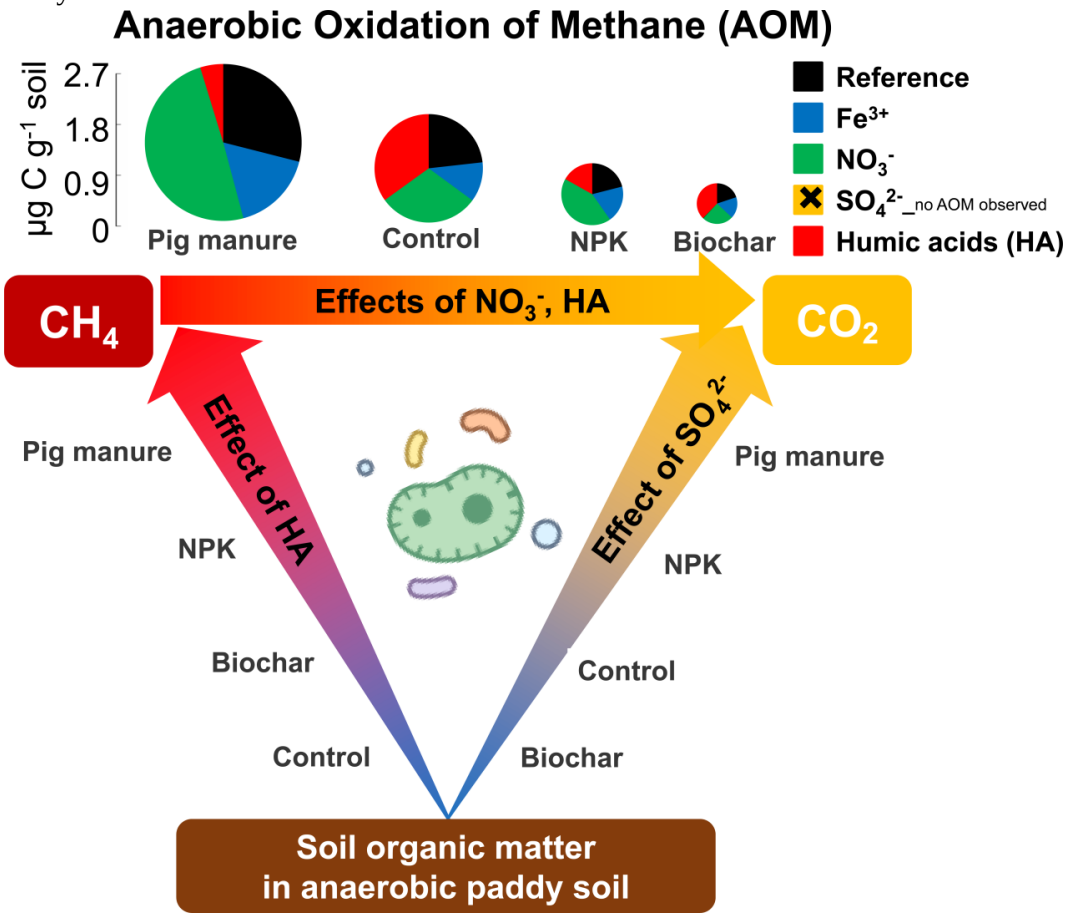

Fig. 6 Conceptual scheme demonstrating the effects of alternative electron acceptors (*i.e.* NO_3^-, Fe^{3+}, SO_4^{2-}, and humic acids (HA)) on anaerobic oxidation of methane (AOM) and anaerobic soil organic matter (SOM) decomposition. The field fertilization treatments included Control, Pig manure, Biochar, and NPK. Pie size reflects the amount of cumulative AOM during the 84-day incubation, and pie sectors correspond to the contribution of tested electron acceptors to cumulative AOM. Colour gradients: an increasing effect of (i) HA on CH_4 production (blue to red), (ii) SO_4^{2-} on CO_2 production (blue to yellow) and (iii) NO_3^- and HA on AOM (red to yellow).

Among all fertilization treatments, average AOM rates were closely related to the MBC (Fig. S2, R^2 = 0.89, P = 0.036). This may suggest that the AOM rate increases with the microbial population. However, this relationship must be treated with care, since the MBC is also affected by various biogeochemical soil properties (e.g. pH) (Pietri and Brookes, 2009). Moreover, we found a positive linear correlation between the amount of gross produced and AOM oxidized CH_4 in each of

fertilizations (Fig. 5, R^2 = 0.55 ~ 0.93, P < 0.05). This indicates that terrestrial AOM is not only correlated with microbial biomass (which can be accidental), but is also affected by CH_4 production. The link between AOM and methanogenesis, where CH_4 oxidation is correlated with CH_4 production, was mechanistically described as a process of "reverse methanogenesis" (Hallam et al., 2004). It was found that CH_4 was oxidized only when CH_4 was simultaneously produced, and adding terminal AEAs (NO_3^-, SO_4^{2-}, Fe^{3+}) inhibited both the AOM and methanogenesis (Blazewicz et al., 2012). Our present results, however, demonstrate inconsistent effects of the AEAs. HA effectively stimulated methanogenesis from the beginning of incubation (Fig. 1) but delayed AOM irrespective of fertilization (Fig. 4). SO_4^{2-} only partially suppressed methanogenesis (Fig. 1, cyan line) but totally inhibited AOM (Fig. 4, cyan line). This apparent decoupling of CH_4 production from the AOM process suggests that "reverse methanogenesis" was not the dominant mechanism. Rather, it appears that CH_4 production and oxidation are separated temporally and mediated by different enzymes.

4.2 The effects of inorganic electron acceptors on AOM

4.2.1 Nitrate

The $^{13}CO_2$ enrichment (Fig. 2) and the AOM rate (Fig. 3) were dependent on AEA amendments. NO_3^- was the most effective AEA in the paddy soil and probably fueled the nitrate/nitrite-dependent AOM, particularly under Pig manure. This finding verified our first hypothesis on NO_3^- as the most preferential AEA for the AOM process. Indeed, NO_3^- is most favorable thermodynamically to fuel ATP generation because the Gibb's Free Energy of nitrate-dependent AOM process is one order of magnitude higher than that of other AEAs (*e.g.* SO_4^{2-}) (reviewed in Smemo and Yavitt, 2011). Nitrite-dependent AOM mediated by *M. oxyfera* (Deutzmann et al., 2014; Hanson and Madsen, 2015; Hu et al., 2014) oxidizes CH_4 by nitrite reduction and nitric oxide dismutation without any syntrophic partner through an intra-aerobic methane oxidation pathway (Ettwig et al., 2010). The nitrate-driven AOM can also be conducted by anaerobic methanotrophic archaea (ANME-2d, *M. nitroreducens*). These organisms are capable of independent AOM through reverse methanogenesis using nitrate as the terminal electron acceptor and have been detected in a mixture of freshwater sediments and anaerobic wastewater sludge (Haroon et al., 2013), and also in paddy soil (Vaksmaa et al., 2017).

Among the fertilization types, Pig manure demonstrated the highest AOM potential (Fig. 6) as compared to other organic/inorganic fertilizers and Control. This only partly confirms our second hypothesis because NPK (which was expected to demonstrate a high AOM rate due to larger availability of inorganic AEAs) resulted in lower AOM compared to Control. Apart from insignificant differences between fertilizations due to high natural variability (Table S1), the NO_3^- content was almost 2 times higher under Pig manure than NPK and about 4 times higher than Control. Thus, long-term fertilization with pig manure increased the amount of NO_3^- in paddy soil, thereby providing a suitable environment for AOM-performing microorganisms such as *M. oxyfera*, *M. oxyfera*-like bacteria - *Candidatus Methylomirabilis sinica* (NC10 phylum, He et al., 2016) and/or anaerobic methanotrophic archaea.

4.2.2 Sulfate

The coupling of sulfate reduction and AOM has been clearly demonstrated for marine environments where it is performed by ANME-1, ANME-2 subgroups -2a, -2b, and 2c, and ANME-3 clades in consortia with sulfate reducing bacteria (Knittel and Boetius, 2009). On the other hand, current evidence on the role of this process for terrestrial AOM is contradictory. SO_4^{2-} amendment yielded close-to-zero AOM rates (and even inhibited AOM), independent of fertilization (Fig. 2). This fully rejects our hypothesis of SO_4^{2-} being a relevant AEA for AOM in paddy soils. The current results are consistent with those of Hu et al., (2014) who reported that no significant accumulation of $^{13}CO_2$ in incubations amended with SO_4^{2-} in paddy soils and wetlands. In contrast, Segarra et al. (2015) found a significant correlation between the rates of sulfate reduction and AOM (r = 0.85, P < 0.01); and Gupta

et al. (2013) suggested that SO_4^{2-} may act as an AEA in fen peat only at high SO_4^{2-} concentrations. However, along with the positive effect of SO_4^{2-} on AOM, Gupta et al. (2013) also observed a negative relationship in 20 hydromorphic surface soil samples. This calls for a separate study to determine a threshold SO_4^{2-} concentration for the potential onset of sulfate-dependent AOM in paddy soils. On average, unlabeled CO_2 increased by 140% (Fig. S1) and methanogenesis was suppressed by 50% after SO_4^{2-} amendment, independent of fertilization (Fig. 1). This stimulation of CO_2 release suggests that sulfate-induced anaerobic organic matter degradation was thermodynamically more favorable than AOM in the examined paddy soils (Fig. 6).

4.2.3 Iron (III)

Amendment with Fe^{3+} did not significantly support AOM (Fig. 4, blue lines) and even partially suppressed the AOM rates in Control and Pig manure (Fig. 3 a, b). This contradicts the hypothesized relevance of Fe^{3+} for AOM in paddy soil. Iron(III)-dependent AOM has been reported in tropical soils, freshwater and brackish wetland sediments, and marine sediments (Mohanty et al., 2017, Ettwig et al., 2016, Segarra et al., 2013, and Beal et al., 2009). Recently, Cai et al. (2018) reported iron (III)-dependent AOM can be performed by *M. ferrireducens*. In contrast, other studies found negative effects of iron addition on AOM in peatlands as well as tropical and boreal soils (Gupta et al., 2013; Blazewicz et al., 2012). After Fe^{3+} amendment, we did not observe a significant CO_2 release and CH_4 production. This result was similar to findings by Smemo and Yavitt (2007), who reported no effect on CH_4 dynamics and CO_2 production after Fe^{3+} addition to *Carex*-derived peat. These authors also recorded that the Fe^{3+} added (50 mM) was almost fully reduced to Fe^{2+} in porewater over the 96 h of incubation. The Fe^{3+} reduction may not directly be related to microbial activity, *i.e.* iron-reducing bacteria, but also to chemical reduction by inorganic (*e.g.* NO_2^-) or organic compounds with higher reducing capacity (Ionescu et al., 2015).

4.3 The effects of organic electron acceptors on AOM

HA stimulated methanogenesis in paddy soil under all fertilizations (Fig. 1, red lines). This result was inconsistent with findings made by Blodau and Deppe (2012) who reported that HA strongly suppressed CH_4 flux from peats of the Mer Bleue bog in Canada. These conflicting observations suggest that HA is playing a complex role – it may either serve as an electron donor and/or as a precursor for substrate (e.g. acetate) formation in paddy soils (as shown by higher CH_4 production after HA amendment compared with reference and other AEAs in all fertilizer treatments, Fig. 1), or as an AEA in peatlands (Keller et al., 2009; Roden et al., 2010). Such contrasting behavior of HA can be related to the specific intrinsic soil conditions, *i.e.* carbon-rich peats poor in inorganic AEAs vs. more carbon-limited paddy soils rich in inorganic AEAs (such as NO_3^-, Fe^{3+}).

We demonstrated a distinct temporal delay of AOM under HA amendment as compared with *e.g.* NO_3^-, which was especially strong in DOC-depleted paddy soils under Biochar and Control (Table S1, Fig. 4 a, c). Two mechanisms may explain this: (i) unlike NO_3^- which is readily available for AOM, HA must undergo decomposition and be partly re-utilized for methanogenesis (as acetate) before the intermediate decomposition products could serve as AEAs for AOM. If so, the AOM rate will depend on the HA decomposition rate. This scenario is consistent with Bai et al. (2019), who reported that highest AOM after three-cycle (23 days) incubation with HA in a denitrifying anaerobic methane oxidation reactor. The artificial substitutes of HA decomposition intermediates (i.e. anthraquinone-2,6-disulfonic acid and anthraquinone-2-sulfonic acid) were identified as electron acceptors for AOM in a process driven by ANME-2d archaea (Bai et al., 2019; Scheller et al., 2016). (ii) AOM may be driven by different microbial groups – with lower and higher affinity to CH_4. Raghoebarsing et al. (2006) reported that the affinity of sulfate-dependent AOM for methane is four orders of magnitude lower than nitrite-dependent AOM. In two of our setups with HA amendments – paddy soil under Biochar and Control: AOM was detected at CH_4 concentrations exceeding 400 μg C-CH_4 (Fig. 1), but paddy

soil under Pig manure: AOM was stressed at CH_4 concentrations below 220 µg C-CH_4. This indicates that HA could stimulate low-affinity methanotrophs. Whereas further research is needed to explain the exact mechanism, our findings positively answered the research question whether HA could serve as AEA for AOM. The role of HA in AOM appears to be particularly important in DOC-depleted paddy soils or when [CH_4] is high enough for low-affinity methanotrophs (Fig. 6).

4.4 Paddy soil fertilization management for CH_4 mitigation strategies

Paddy fields are a significant source of CH_4, accounting for ~10-20% of global CH_4 emissions (Conrad, 2009). Management practices and especially fertilization have important effects on the CH_4 emission (Kruger and Frenzel, 2003). Thus, N fertilizers increased CH_4 emissions in 98 of 155 meta-data pairs of N fertilization amendments and control in rice soils (Banger et al., 2012). Livestock manure typically increases soil C and greenhouse gas emission in the short-term, but long-term manure application demonstrated a decrease in greenhouse gas emission (Owen et al., 2015). In our study, NPK fertilization led to a 3.2-times higher CH_4 production rate, whereas the Pig manure and Biochar had similar production rates compared to the low-fertilized Control (Fig. S3). With the background AEAs available in the paddy soil (*i.e.* non-amended reference), the AOM rate was the highest under Pig manure (Fig. 3). Therefore, the long-term application of livestock manure should be considered vs. other fertilization practices in the sustainable management of rice paddy fields, as it would help to reduce CH_4 emissions due to lower CH_4 production and higher AOM (Fig. 3, Fig. S3).
This positive effect on CH_4 mitigation will be even stronger when NO_3^- availability fuels AOM. Assuming that the physical parameters of our paddy soils are representative of those globally (namely a bulk density of 1.3 g cm^{-3} and plow layer of 25.5 cm; Pan et al., 2004), and considering the AOM rate observed for manure-fertilized NO_3^--amended paddy soil (0.80 ng C g^{-1} soil h^{-1}, Fig. 3), then the AOM has the potential to recycle ~3.9 Tg C-CH_4 yr^{-1}. This is roughly 10-20% of the global CH_4 emissions from paddy fields (comprising 19.5-37.5 Tg C yr^{-1}; Keppler et al., 2006; Sass et al., 1999) and in line with our earlier estimations for rice paddies in China (Fan et al., 2019b). Undoubtedly, the rough upscaling of *in vitro* data is associated with a very large uncertainty and more studies are required to determine the quantitative importance of AOM as a CH_4 sink in variety of paddy fields, but we still consider such estimations as a valuable basis for future studies. Our results clearly point at the impact of fertilization management on AOM in submerged agroecosystems, and its key role to decrease the net CH_4 flux to the atmosphere and hence the potential global warming.

Conclusions

The anaerobic oxidation of methane (AOM) in paddy soils depends strongly on the type of electron acceptors (AEAs) alternative to oxygen and the type of fertilization. We confirmed NO_3^- as the most effective AEA, suggesting nitrate-induced AOM as the main underlying mechanism offsetting net CH_4 efflux. Iron (III) had no effect and SO_4^{2-} negatively affected AOM, indicating that both are not relevant AEAs in paddy soils, at least not at the concentrations tested. Humic acids (HA) obviously played a dual role, *i.e.* as a substrate for methanogenesis and as an AEA for AOM in DOC-depleted paddy soils. Alternatively, HA might stimulate low-affinity methanotrophs to conduct AOM – an issue that clearly deserves more attention. The most pronounced AOM in paddy soils occurred under Pig manure, followed by Control and NPK, while AOM was the lowest under Biochar. On a larger scale, nitrate-induced AOM together with manure fertilization has the potential to recycle ~3.9 Tg C-CH_4 annually, which represents a roughly ~10–20% offset of global net CH_4 emissions from rice paddies. Consequently, from a broader ecological perspective, organic and mineral fertilization are important controls of the CH_4 sink under anaerobic conditions in submerged agricultural ecosystems.

Acknowledgement

The authors are thankful to the China Scholarship Council (CSC) for funding Lichao Fan in Germany, and to the German Research Foundation (DFG, Do 1533/2-1) and the National Natural Science Foundation of China (41761134095; 41430860; 41671253), Youth Innovation Team Project of ISA, CAS (2017QNCXTD_GTD) and Hunan Province Base for Scientific and Technological Innovation Cooperation (2018WK4012) for the invaluable support. The work is performed according to the Government Program of Competitive Growth of Kazan Federal University. Special thanks to the Kompetenzzentrum Stabile Isotope (KOSI), University of Goettingen, and personally to Lars Szwec and Reinhard Langel for the isotope analyses. We are also greatly thankful to two anonymous expert reviewers for the constructive suggestions and valuable recommendations for the improvement of this manuscript.

References:

Banger, K., Tian, H., Lu, C. 2012., Do nitrogen fertilizers stimulate or inhibit methane emissions from rice fields? Global Change Biology, 1810, 3259-3267.

Bai, Y., Wang, X., Wu, J., Lu, Y., Fu, L., Zhang, F., Lau, T., Zeng, R.J., 2019. Humic substances as electron acceptors for anaerobic oxidation of methane driven by ANME-2d. Water Research 164, 114935.

Beal, E.J., House, C.H., Orphan, V.J., 2009. Manganese-and iron-dependent marine methane oxidation. Science 3255937, 184-187.

Blazewicz, S.J., Petersen, D.G., Waldrop, M.P., Firestone, M.K., 2012. Anaerobic oxidation of methane in tropical and boreal soils: Ecological significance in terrestrial methane cycling. Journal of Geophysical Research 117, G02033. doi: 10.1029/2011JG001864

Blodau, C., Deppe, M., 2012. Humic acid addition lowers methane release in peats of the Mer Bleue bog, Canada. Soil Biology & Biochemistry 52, 96-98.

Canfield, D. E., Farquhar, J., 2009. Animal evolution, bioturbation, and the sulfate concentration of the oceans. Proceedings of the National Academy of Sciences 10620, 8123-8127.

Cai, C., Leu, A.O., Xie, G., Guo, J., Feng, Y., Zhao, J., Tyson, G.W., Yuan, Z., Hu, S., 2018. A methanotrophic archaeon couples anaerobic oxidation of methane to Fe(III) reduction. The ISME journal 12, 1929-1939.

Chen, H., Zhu, Q., Peng, C., Wu, N., Wang, Y., Fang, X., Jiang, H., Xiang, W., Chang, J., Deng, X., Yu, G., 2013. Methane emissions from rice paddies natural wetlands, lakes in China: synthesis new estimate. Global Change Biology 191, 19-32.

Conrad, R. 2009., The global methane cycle: recent advances in understanding the microbial processes involved. Environmental Microbiology Reports 15, 285-292.

Cui, M., Ma, A., Qi, H., Zhuang, X., Zhuang, G., 2015. Anaerobic oxidation of methane: an “active” microbial process. MicrobiologyOpen 41, 1-11.

Deutzmann, J.S., Stief, P., Brandes, J., Schink, B., 2014. Anaerobic methane oxidation coupled to denitrification is the dominant methane sink in a deep lake. Proceedings of the National Academy of Sciences 11151, 18273-18278.

Ettwig, K.F., Butler, M.K., Le Paslier, D., Pelletier, E., Mangenot, S., Kuypers, M.M.M., Schreiber, F., Dutilh, B.E., Zedelius, J., de Beer, D., Gloerich, J., Wessels, H.J.C.T., van Alen, T., Luesken, F., Wu, M.L., van de Pas-Schoonen, K.T., Op Den Camp, H.J.M., Janssen-Megens, E.M., Francoijs, K., Stunnenberg, H., Weissenbach, J., Jetten, M.S.M., Strous, M., 2010. Nitrite-driven anaerobic methane oxidation by oxygenic bacteria. Nature 4647288, 543-548.

Ettwig, K.F., Zhu, B., Speth, D., Keltjens, J.T., Jetten, M.S., Kartal, B., 2016. Archaea catalyze iron-dependent anaerobic oxidation of methane. Proceedings of the National Academy of Sciences 11345, 12792-12796.

Fan, L.C., Shahbaz, M., Ge, T., Wu, J., Kuzyakov, Y., Dorodnikov, M., 2019a. To shake or not to shake: Silicone tube approach for incubation studies on CH_4 oxidation in submerged soils. Science of the Total Environment 657, 893-901.

Fan, L.C, Shahbaz, M., Ge, T., Wu, J., Dippold, M., Thiel, V., Kuzyakov, Y., Dorodnikov, M., 2019b. To shake or not to shake: ^{13}C-based evidence on anaerobic methane oxidation in paddy soil. Soil Biology & Biochemistry 133, 146-154.

Driessen, P., Deckers, J., Spaargaren, O., Nachtergaele, F., 2000. Lecture notes on the major soils of the world (No. 94). Food and Agriculture Organization (FAO).

Gauthier, M., Bradley, R.L., Šimek, M. , 2015. More evidence that anaerobic oxidation of methane is prevalent in soils: Is it time to upgrade our biogeochemical models? Soil Biology & Biochemistry 80, 167-174.

Gupta, V., Smemo, K.A., Yavitt, J.B., Fowle, D., Branfireun, B., Basiliko, N., 2013. Stable Isotopes Reveal Widespread Anaerobic Methane Oxidation Across Latitude and Peatland Type. Environmental Science & Technology 4715, 8273-8279.

Hallam, S.J., Putnam, N., Preston, C.M., Detter, J.C., Rokhsar, D., Richardson, P.M., DeLong, E.F., 2004. Reverse methanogenesis: testing the hypothesis with environmental genomics. Science 3055689, 1457-1462.

Hanson, B.T., Madsen, E.L., 2015. In situ expression of nitrite-dependent anaerobic methane oxidation proteins by Candidatus Methylomirabilis oxyfera co-occurring with expressed anammox proteins in a contaminated aquifer. Environmental Microbiology Reports 72, 252-264.

Haroon M.F., Hu S., Shi Y., Imelfort M., Keller J., Hugenholtz P., Yuan Z., Tyson G.W., 2013. Anaerobic oxidation of methane coupled to nitrate reduction in a novel archaeal lineage. Nature 5007464, 567-570.

He, Z., Cai, C., Wang, J., Xu, X., Zheng, P., Jetten, M.S., Hu, B., 2016. A novel denitrifying methanotroph of the NC10 phylum and its microcolony. Scientific Reports 6, 32241.

Hu, B.L., Shen, L.D., Lian, X., Zhu, Q., Liu, S., Huang, Q., He, Z.F., Geng, S., Cheng, D.Q., Lou, L.P., Xu, X.Y., Zheng, P., He, Y.F., 2014. Evidence for nitrite-dependent anaerobic methane oxidation as a previously overlooked microbial methane sink in wetlands. Proceedings of the National Academy of Sciences 11112, 4495-4500.

Huang, Y., Sass, R.L., Fisher, J.F.M., 2002. A semi-empirical model of methane emission from flooded rice paddy soils. Global Change Biology 48, 809-821.

Ionescu, D., Heim, C., Polerecky, L., Thiel, V., de Beer, D., 2015. Biotic and abiotic oxidation and reduction of iron at circumneutral pH are inseparable processes under natural conditions. Geomicrobiology Journal 32, 221-230.

Joergensen, R.G., 1996. The fumigation-extraction method to estimate soil microbial biomass: Calibration of the k_{EC} value. Soil Biology & Biochemistry 281, 25-31.

Keller, J.K., Weisenhorn, P.B., Megonigal, J.P., 2009. Humic acids as electron acceptors in wetland decomposition. Soil Biology & Biochemistry 417, 1518-1522.

Keppler, F., Hamilton, J.T., Braß, M., Röckmann, T., 2006. Methane emissions from terrestrial plants under aerobic conditions. Nature 4397073, 187-191.

Knittel, K., Boetius, A., 2009. Anaerobic oxidation of methane: progress with an unknown process. Annual Review of Microbiology 631, 311-334.

Kruger, M., Frenzel, P., 2003. Effects of N-fertilisation on CH_4 oxidation and production, and consequences for CH_4 emissions from microcosms and rice fields. Global Change Biology 9, 773-784.

Serrano-Silva, N., Sarria-Guzmán, Y., Dendooven, L. and Luna-Guido, M., 2014. Methanogenesis and methanotrophy in soil：A review. Pedosphere 243, 291-307.

Loftfield, N., Flessa, H., Augustin, J., Beese, F., 1997. Automated gas chromatographic system for rapid analysis of the atmospheric trace gases methane, carbon dioxide, and nitrous oxide. Journal of Environmental Quality 262:560-564.

Mohanty, S.R., Bandeppa, G.S., Dubey, G., Ahirwar, U., Patra, A.K., Bharati, K., 2017. Methane oxidation in response to iron reduction-oxidation metabolism in tropical soils. European Journal of Soil Biology 78, 75-81.

Orcutt, B., Boetius, A., Elvert, M., Samarkin, V., Joye, S.B., 2005. Molecular biogeochemistry of sulfate reduction, methanogenesis and the anaerobic oxidation of methane at Gulf of Mexico cold seeps. Geochimical et Cosmochimica Acta 6917, 4267-4281.

Owen, J.J., Parton, W.J., Silver, W.L., 2015. Long-term impacts of manure amendments on carbon and greenhouse gas dynamics of rangelands. Global Change Biology 21, 4533-4547.

Pan, G., Li, L., Wu, L., Zhang, X., 2004. Storage and sequestration potential of topsoil organic carbon in China's paddy soils. Global Change Biology 101, 79-92.

Pietri, J.A., Brookes, P.C., 2009. Substrate inputs and pH as factors controlling microbial biomass, activity and community structure in an arable soil. Soil Biology & Biochemistry 41, 1396-1405.

Pozdnyakov, L.A., Stepanov, A.L., Manucharova, N.A., 2011. Anaerobic methane oxidation in soils and water ecosystems. Moscow University soil science bulletin 661, 24-31.

Putkinen, A., Tuittila, E., Siljanen, H.M.P., Bodrossy, L., Fritze, H., 2018. Recovery of methane turnover and the associated microbial communities in restored cutover peatlands is strongly linked with increasing *Sphagnum* abundance. Soil Biology & Biochemistry 116, 110-119.

Raghoebarsing, A.A., Pol, A., van de Pas-Schoonen, K.T., Smolders, A.J.P., Ettwig, K.F., Rijpstra, W.I.C., Schouten, S., Damsté, J.S.S., Op Den Camp, H.J.M., Jetten, M.S.M., Strous, M., 2006. A microbial consortium couples anaerobic methane oxidation to denitrification. Nature 440, 918-921.

Reeburgh, W.S., 2007. Oceanic methane biogeochemistry. Chemical Reviews 1072, 486-513.

Roden, E.E., Kappler, A., Bauer, I., Jiang, J., Paul, A., Stoesser, R., Konishi, H., Xu, H., 2010. Extracellular electron transfer through microbial reduction of solid-phase humic substances. Nature Geoscience 36, 417.

Sass, R.L., Fisher, F.M., Ding, A., Huang, Y., 1999. Exchange of methane from rice fields: National, regional, and global budgets. Journal of Geophysical Research: Atmospheres 104D21, 26943-26951.

Scheller, S., Yu, H., Chadwick, G.L., McGlynn, S.E., Orphan, V.J., 2016. Artificial electron acceptors decouple archaeal methane oxidation from sulfate reduction. Science 351, 703-707.

Segarra, K.E.A., Comerford, C., Slaughter, J., Joye, S.B., 2013. Impact of electron acceptor availability on the anaerobic oxidation of methane in coastal freshwater and brackish wetland sediments. Geochimical et Cosmochimica Acta 115, 15-30.

Segarra, K.E.A., Schubotz, F., Samarkin, V., Yoshinaga, M.Y., Hinrichs, K., Joye, S.B., 2015. High rates of anaerobic methane oxidation in freshwater wetlands reduce potential atmospheric methane emissions. Nature Communications 61, 7477.

Shen, J., Tang, H., Liu, J., Wang, C., Li, Y., Ge, T., Jones, D.L., Wu, J., 2014a. Contrasting effects of straw and straw-derived biochar amendments on greenhouse gas emissions within double rice cropping systems. Agriculture, ecosystems & environment 188, 264-274.

Shen, L., Huang, Q., He, Z., Lian, X., Liu, S., He, Y., Lou, L., Xu, X., Zheng, P., Hu, B., 2015. Vertical distribution of nitrite-dependent anaerobic methane-oxidising bacteria in natural freshwater wetland soils. Applied and Environmental Microbiology 991, 349-357.

Shen, L.D., Liu, S., Huang, Q., Lian, X., He, Z.F., Geng, S., Jin, R.C., He, Y.F., Lou, L.P., Xu, X.Y., Zheng, P., Hu, B.L., 2014b. Evidence for the Cooccurrence of Nitrite-Dependent Anaerobic Ammonium and Methane Oxidation Processes in a Flooded Paddy Field. Applied and Environmental Microbiology 8024, 7611-7619.

Shen, L., Ouyang, L., Zhu, Y., Trimmer, M., 2019. Active pathways of anaerobic methane oxidation across contrasting riverbeds. The ISME Journal 133, 752-766.

Shi, Y., Wang, Z., He, C., Zhang, X., Sheng, L., Ren, X., 2017. Using ^{13}C isotopes to explore denitrification-dependent anaerobic methane oxidation in a paddy-peatland. Scientific Reports 71, 40848.

Smemo, K.A., Yavitt, J.B., 2007. Evidence for anaerobic CH_4 oxidation in freshwater peatlands. Geomicrobiology Journal 247-8, 583-597.

Smemo, K.A., Yavitt, J.B., 2011. Anaerobic oxidation of methane: an underappreciated aspect of methane cycling in peatland ecosystems? Biogeosciences 83, 779-793.

Vaksmaa, A., Lüke, C., van Alen, T., Valè, G., Lupotto, E., Jetten, M.S.M., Ettwig, K.F., 2016. Distribution and activity of the anaerobic methanotrophic community in a nitrogen-fertilized Italian paddy soil. FEMS Microbiology Ecology 92, w181.

Vaksmaa, A., Guerrero-Cruz, S., van Alen, T.A., Cremers, G., Ettwig, K.F., Lüke, C., Jetten, M.S.M., 2017. Enrichment of anaerobic nitrate-dependent methanotrophic 'Candidatus *Methanoperedens nitroreducens*' archaea from an Italian paddy field soil. Applied Microbiology and Biotechnology 10118, 7075-7084.

Valentine, D.L., 2002. Biogeochemistry and microbial ecology of methane oxidation in anoxic environments: a review. Antonie van Leeuwenhoek 811, 271-282.

Valenzuela, E.I., Avendaño, K.A., Balagurusamy, N., Arriaga, S., Nieto-Delgado, C., Thalasso, F., Cervantes, F.J., 2019. Electron shuttling mediated by humic substances fuels anaerobic methane oxidation and carbon burial in wetland sediments. Science of the Total Environment 650, 2674-2684.

Yu, Z., Peiffer, S., Göttlicher, J., Knorr, K., 2015. Electron transfer budgets and kinetics of abiotic oxidation and incorporation of aqueous sulfide by dissolved organic matter. Environmental Science & Technology 499, 5441-5449.

Zhang, W., Yu, Y., Huang, Y., Li, T., Wang, P., 2011. Modeling methane emissions from irrigated rice cultivation in China from 1960 to 2050. Global Change Biology 1712, 3511-3523.

Supporting Information for study 3

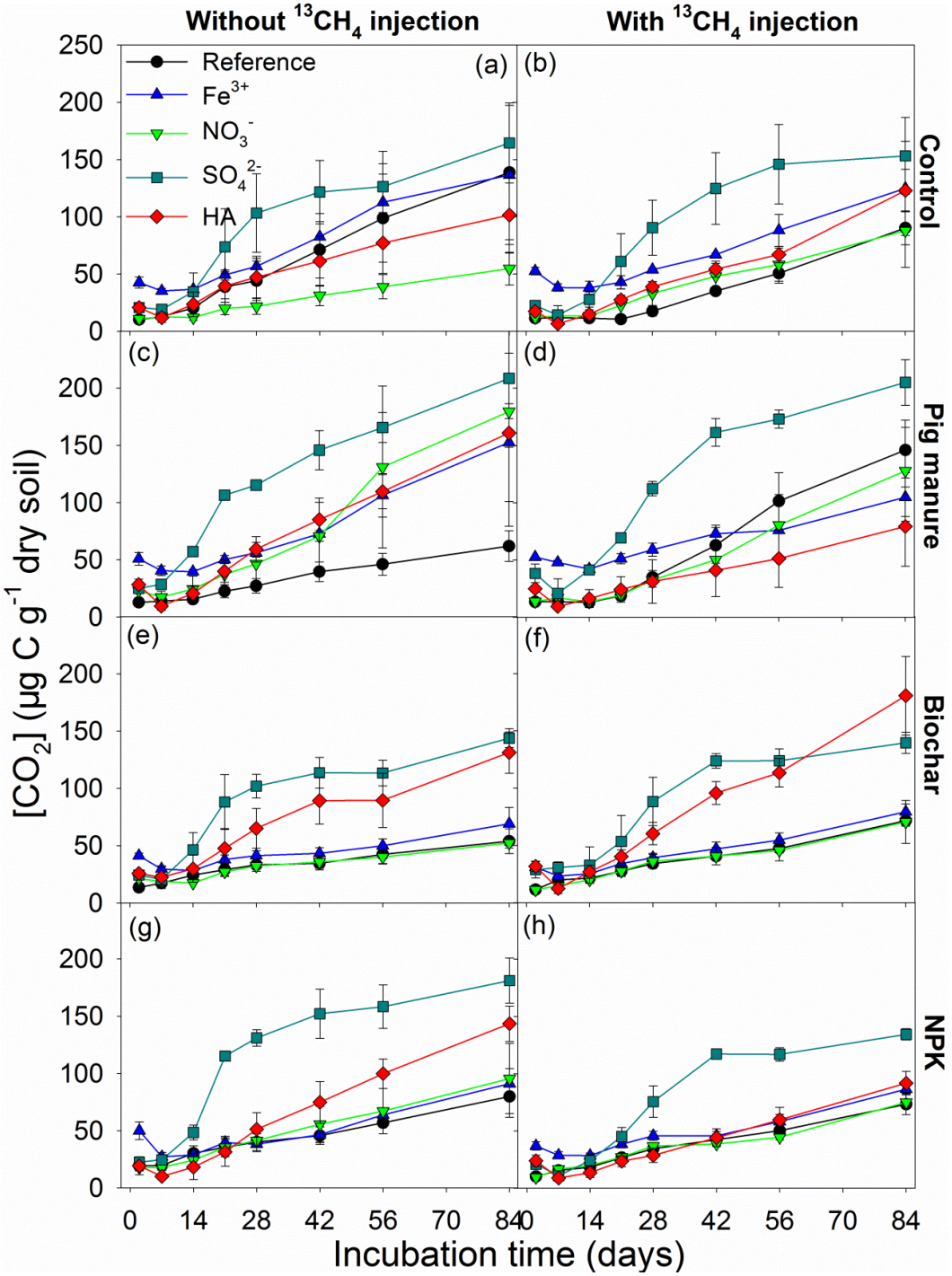

Fig. S1 Dynamics of CO_2 concentration ($[CO_2]$) in headspace of microcosms from three field fertilization treatments (Pig manure, Biochar, NPK) and the low-fertilized Control over 84 days of incubation without (a, c, e, g) and with (b, d, f, h) $^{13}CH_4$ injection and with Fe^{3+} (as Fe_2O_3), NO_3^- (as $NaNO_3$), SO_4^{2-} (as Na_2SO_4), and HA (humic acids) amendment as well as non-amended Reference. Error bars: standard error of mean (n=3).

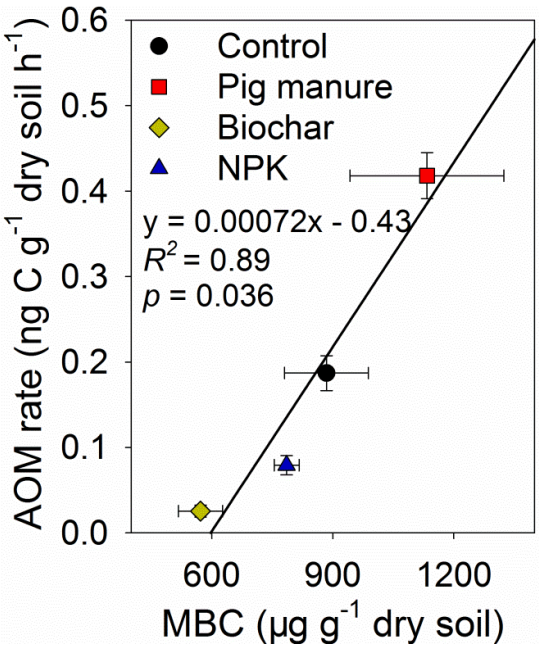

Fig. S2 Relationship between rate of anaerobic oxidation of methane (AOM) and microbial biomass carbon (MBC) in reference soil without electron acceptor amendments. Error bars: standard error of mean (n=3).

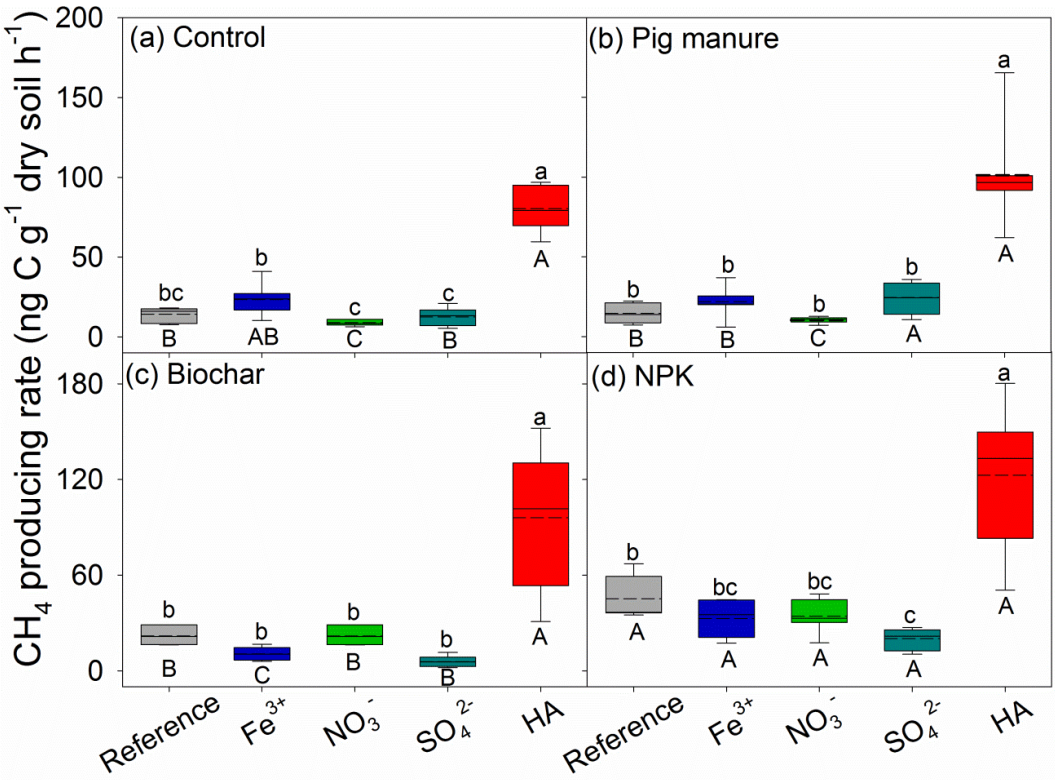

Fig. S3 Box plots of the average gross rates of CH_4 production (net + AOM) over 84 days of incubation under field fertilization treatments: Control (a), Pig manure (b), Biochar (c) and NPK (d). Upper and lower bars: maximum and minimum observations, respectively; top and bottom of boxes: third and first quartiles; thin horizontal solid lines in boxes: median values; dashed lines: mean values (without outliers). HA: humic acids. Lowercase letters: significant differences ($P < 0.05$) between electron acceptors for each soil fertilization treatment. Captial letters: significant differences ($P < 0.05$) between soil fertilization treatments for each electron acceptor.

Table S1 Soil basic physicochemical properties

Soil treatments	SOC mg g^{-1}	Total N mg g^{-1}	MBC μg g^{-1}	eDOC μg g^{-1}	NO_3^- μg g^{-1}	NH_4^+ μg g^{-1}	S μg g^{-1}	Fe mg g^{-1}
Control	11.7 ± 0.3b	1.35 ± 0.05a	884.1 ± 104a	62.4 ± 2.4a	2.73 ± 0.0a	1.77 ± 0.2a	359.2 ± 100a	19.4 ± 0.2a
Pig manure	15.7 ± 1.2b	1.85 ± 0.25a	1133.3 ± 191a	63.4 ± 2.2a	10.0 ± 6.9a	2.13 ± 0.2a	407.8 ± 51.1a	21.3 ± 4.5a
Biochar	28.5 ± 6.0a	1.75 ± 0.05a	571.6 ± 54.8b	60.7 ± 7.0a	6.84 ± 3.5a	1.79 ± 0.1a	458.1 ± 40.7a	16.9 ± 1.4a
NPK	13.7 ± 0.5b	1.55 ± 0.05a	785.2 ± 30.9ab	66.0 ± 4.4a	5.13 ± 4.2a	1.97 ± 0.1a	419.7 ± 13.5a	17.7 ± 0.6a

Note: SOC, soil organic carbon; total N, total nitrogen content; MBC, soil microbial biomass carbon; eDOC, extractable dissolved organic carbon; S, sulfur; Fe, iron. Different letters mean significant differences ($P < 0.05$) between soil fertilization treatments. Values represent means ± standard error.

Table S2 Summary table for two-way ANOVA with repeated measures reflect the significance of the $^{13}CH_4$ labeling, duration of incubation (84 days) and their interactions on ^{13}C enrichments under different elector acceptors amendments and fertilization $^{13}CH_4$ labeling.

Source of Variation	Degree of freedom	Sum of Squares	Mean Square	F	P
Control					
Reference					
$^{13}CH_4$ labeling	1	4331.1	4331.1	178.3	<0.001
subject ($^{13}CH_4$ labeling)	4	97.2	24.3		
Time	7	232.9	33.3	5.2	<0.001
$^{13}CH_4$ labeling x Time	7	133.2	19.0	3.0	0.019
Residual	28	180.1	6.4		
Total	47	4974.5	105.8		
Fe^{3+}					
$^{13}CH_4$ labeling	1	134.4	134.4	7.3	0.054
subject ($^{13}CH_4$ labeling)	4	73.4	18.4		
Time	7	43.4	6.2	2.3	0.054
$^{13}CH_4$ labeling x Time	7	5.6	0.8	0.30	0.95
Residual	28	75.2	2.7		
Total	47	332.0	7.1		
NO_3^-					
$^{13}CH_4$ labeling	1	3979.6	3979.6	13.1	0.022
subject ($^{13}CH_4$ labeling)	4	1212.6	303.1		
Time	7	217.2	31.0	1.7	0.142
$^{13}CH_4$ labeling x Time	7	125.7	18.0	1.0	0.45
Residual	28	501.4	18.0		
Total	47	6036.5	128.4		
SO_4^{2-}					
$^{13}CH_4$ labeling	1	10.8	10.8	0.9	0.396
subject ($^{13}CH_4$ labeling)	4	48.1	12.0		
Time	7	3370.7	481.5	62.9	<0.001
$^{13}CH_4$ labeling x Time	7	95.2	13.6	1.8	0.132
Residual	28	214.3	7.7		
Total	47	3739.1	79.6		
Humic acids					
$^{13}CH_4$ labeling	1	264.2	264.2	2.9	0.162
subject ($^{13}CH_4$ labeling)	4	360.1	90.0		
Time	6	521.5	86.9	8.1	<0.001
$^{13}CH_4$ labeling x Time	6	238.4	39.7	3.7	0.01
Residual	24	258.6	10.8		
Total	41	1642.8	40.1		
Pig manure					
Reference					
$^{13}CH_4$ labeling	1	9483.4	9483.4	820.4	<0.001
subject ($^{13}CH_4$ labeling)	4	46.2	11.6		
Time	7	1574.9	225.0	5.1	<0.001
$^{13}CH_4$ labeling x Time	7	721.9	103.1	2.3	0.052

Residual	28	1239.3	44.3		
Total	47	13065.8	278.0		
		Fe^{3+}			
$^{13}CH_4$ labeling	1	2334.0	2334.0	3.8	0.122
subject ($^{13}CH_4$ labeling)	4	2444.4	611.1		
Time	7	671.7	95.9	3.1	0.016
$^{13}CH_4$ labeling x Time	7	621.1	88.7	2.8	0.023
Residual	28	873.	31.2		
Total	47	6944.1	147.8		
		NO_3^-			
$^{13}CH_4$ labeling	1	30431.4	30431.4	12.8	0.023
subject ($^{13}CH_4$ labeling)	4	9484.4	2371.1		
Time	7	4381.8	626.0	3.9	0.004
$^{13}CH_4$ labeling x Time	7	3952.9	564.7	3.6	0.007
Residual	28	4453.9	159.1		
Total	47	52704.4	1121.4		
		SO_4^{2-}			
$^{13}CH_4$ labeling	1	90.5	90.5	1.9	0.239
subject ($^{13}CH_4$ labeling)	4	189.1	47.3		
Time	7	2623.7	374.8	12.1	<0.001
$^{13}CH_4$ labeling x Time	7	300.4	42.9	1.4	0.252
Residual	28	869.8	31.1		
Total	47	4073.4	86.7		
		Humic acids			
$^{13}CH_4$ labeling	1	7.3	7.3	0.1	0.777
subject ($^{13}CH_4$ labeling)	4	317.5	79.4		
Time	6	476.1	79.4	6.7	<0.001
$^{13}CH_4$ labeling x Time	6	103.9	17.3	1.5	0.236
Residual	24	286.0	11.9		
Total	41	1190.7	29.0		
		Biochar			
		Reference			
$^{13}CH_4$ labeling	1	74.9	74.9	1.3	0.325
subject ($^{13}CH_4$ labeling)	4	238.3	59.6		
Time	7	403.1	57.6	11.1	<0.001
$^{13}CH_4$ labeling x Time	7	44.8	6.4	1.2	0.316
Residual	28	144.9	5.2		
Total	47	906.1	19.3		
		Fe^{3+}			
$^{13}CH_4$ labeling	1	75.2	75.2	3.0	0.159
subject ($^{13}CH_4$ labeling)	4	100.7	25.2		
Time	7	40.9	5.9	3.0	0.017
$^{13}CH_4$ labeling x Time	7	14.1	2.0	1.0	0.425
Residual	28	54.3	1.9		
Total	47	285.4	6.1		
		NO_3^-			
$^{13}CH_4$ labeling	1	68.7	68.7	1.4	0.307

subject ($^{13}CH_4$ labeling)	4	200.8	50.2		
Time	7	382.1	54.6	4.9	0.001
$^{13}CH_4$ labeling x Time	7	173.2	24.7	2.3	0.064
Residual	28	312.8	11.2		
Total	47	1137.6	24.2		
		SO_4^{2-}			
$^{13}CH_4$ labeling	1	9.9	9.9	1.0	0.381
subject ($^{13}CH_4$ labeling)	4	41.1	10.3		
Time	7	2204.	314.9	39.2	<0.001
$^{13}CH_4$ labeling x Time	7	18.8	2.7	0.3	0.931
Residual	28	225.2	8.0		
Total	47	2499.7	53.2		
		Humic acids			
$^{13}CH_4$ labeling	1	56.2	56.2	2.6	0.182
subject ($^{13}CH_4$ labeling)	4	86.2	21.6		
Time	6	507.8	84.6	13.0	<0.001
$^{13}CH_4$ labeling x Time	6	52.1	8.7	1.3	0.283
Residual	24	156.8	6.5		
Total	41	859.0	21.0		
		NPK			
		Reference			
$^{13}CH_4$ labeling	1	520.2	520.2	5.6	0.077
subject ($^{13}CH_4$ labeling)	4	370.1	92.5		
Time	7	837.6	119.7	11.3	<0.001
$^{13}CH_4$ labeling x Time	7	60.5	8.6	0.8	0.584
Residual	28	297.2	10.6		
Total	47	2085.6	44.4		
		Fe^{3+}			
$^{13}CH_4$ labeling	1	256.6	256.6	16.2	0.016
subject ($^{13}CH_4$ labeling)	4	63.5	15.9		
Time	7	126.8	18.1	6.4	<0.001
$^{13}CH_4$ labeling x Time	7	57.6	8.2	2.9	0.021
Residual	28	79.5	2.8		
Total	47	583.8	12.4		
		NO_3^-			
$^{13}CH_4$ labeling	1	1020.1	1020.1	27.0	0.007
subject ($^{13}CH_4$ labeling)	4	151.0	37.7		
Time	7	917.3	131.0	19.2	<0.001
$^{13}CH_4$ labeling x Time	7	341.7	48.8	7.1	<0.001
Residual	28	191.4	6.8		
Total	47	2621.4	55.8		
		SO_4^{2-}			
$^{13}CH_4$ labeling	1	25.5	25.5	2.0	0.231
subject ($^{13}CH_4$ labeling)	4	51.3	12.8		
Time	7	2096.3	299.5	69.2	<0.001
$^{13}CH_4$ labeling x Time	7	77.3	11.0	2.6	0.036
Residual	28	121.2	4.3		

Total	47	2371.5	50.5		
Humic acids					
$^{13}CH_4$ labeling	1	8.1	8.1	0.5	0.506
subject ($^{13}CH_4$ labeling)	4	60.5	15.1		
Time	6	649.6	108.3	8.5	<0.001
$^{13}CH_4$ labeling x Time	6	75.4	12.6	1.0	0.454
Residual	24	304.6	12.7		
Total	41	1098.2	26.8		

Table S3 Summary table for two-way ANOVA with repeated measures reflect the significance of the effects of fertilization treatments, duration of incubation (84 days) and their interactions on cumulative anaerobic CH_4 oxidation.

Source of Variation	Degree of freedom	Sum of Squares	Mean Square	F	P
Fertilization treatments	3	1.15	0.38	39.8	<0.001
Subject (Fertilization treatments)	8	0.08	0.01		
Time	7	0.96	0.14	42.6	<0.001
Fertilization treatments x Time	21	0.65	0.03	9.67	<0.001
Residual	56	0.18	0.003		
Total	95	3.02	0.03		

Study 4 Active metabolic pathways of anaerobic methane oxidation in paddy soil

Lichao Fan[a*], Dominik Schneider[b], Michaela A. Dippold[c], Anja Poehlein[b], Weichao Wu[c,d], Heng Gui[e], Tida Ge[f], Jinshui Wu[f], Volker Thiel[g], Yakov Kuzyakov[a,h,i], Maxim Dorodnikov[a,c]

[a] Department of Soil Science of Temperate Ecosystems, University of Göttingen, Göttingen 37077, Germany

[b] Institute for Microbiology and Genetics, University of Göttingen, Göttingen 37077, Germany

[c] Department of Biogeochemistry of Agroecosystems, University of Göttingen, Göttingen 37077, Germany

[d] Department of Environmental Science and Analytical Chemistry, Stockholm University, Stockholm 10691, Sweden

[e] Key laboratory for Plant Diversity and Biogeography of East Asia, Kunming Institute of Botany, Chinese Academy of Sciences, Kunming 650201, China

[f] Key Laboratory of Agro-ecological Processes in Subtropical Region & Changsha Research Station for Agricultural and Environmental Monitoring, Institute of Subtropical Agriculture, Chinese Academy of Sciences, Hunan 410125, China

[g] Geobiology, Geoscience Center, University of Göttingen, Göttingen 37077, Germany

[h] Department of Agricultural Soil Science, University of Göttingen, Göttingen 37077, Germany

[i] Agro-Technological Institute, RUDN University, Moscow 117198, Russia

Status: Submitted

***Correspondence:** Lichao Fan, lfan@gwdg.de

Department of Soil Science of Temperate Ecosystems, University of Göttingen, Büsgenweg 2, Göttingen 37077, Germany

Abstract
Anaerobic oxidation of methane (AOM) is a globally important CH_4 sink. However, the AOM pathways in paddy soils, the largest agricultural source of methane emissions (31 Mio tons per year) are not yet well described. Here, a combination of ^{13}C isotope tracer, phospholipid fatty acids (PLFA) analyses, and microbial community analysis was used to identify AOM pathways in fertilized (pig manure, biochar, NPK, and the control) paddy soils amended with alternative electron acceptors (AEAs) (NO_3^-, Fe^{3+}, SO_4^{2-}, humic acids, and the reference). After 84 days of anaerobic incubation, the microbial co-occurrence network got tightened and more complex relative to unincubated samples. Fertilization and addition of AEAs led to a strong divergence of the microbial community structure as indicated by abundances of AOM-related microbiota and ^{13}C incorporation into microbial PLFA, thus suggesting an environmental niche differentiation of AOM-involved microorganisms. Comparative analyses revealed a set of major and minor AOM pathways with synergistic relations to complementary anaerobic microbial groups. Members of candidate group ANME-2d catalyzed NO_3^--driven AOM was the major AOM pathway co-existing with minor pathways involving NO_2^- reduction by NC10, reduction of humic acids and Fe^{3+} by *Geobacter* species, and SO_4^{2-} reduction by sulfate-reducing bacteria linked with anaerobic methanotrophs. From a broader ecological perspective, as global nitrogen pollution increases, nitrogen-driven AOM will be a more important methane sink in the future.

Keywords: Anaerobic oxidation of methane; lipid biomarker; CH_4 cycle; co-occurrence network; fertilization; paddy soil; greenhouse gas emission

1. Introduction

Soil microbial communities play an indispensable role in ecological functions, and their biomass, composition, activity and diversity are sensitive to variation of biotic and abiotic factors (Delgado-Baquerizo et al., 2016; Torsvik and Øvreås, 2002; Zelles, 1999). Microbial metabolism in oxic and anoxic environments influences the Earth's biogeochemistry. Importantly, both groups of metabolic pathways – anaerobic and aerobic – differ fundamentally different in their energetics, e.g., the energy yields of glucose oxidation under anaerobic conditions accounts for only ~14% of that from aerobic glucose oxidation (Megonigal et al., 2004). Anaerobic microbial metabolism is highly dependent on the availability of alternatives to oxygen as terminal electron acceptor, i.e., so-called alternative electron acceptors (AEAs) such as nitrate (NO_3^-), nitrite (NO_2^-), oxidized metals (Mn^{4+}, Fe^{3+}), sulfate (SO_4^{2-}), and organic substances (e.g., quinones, humic substances). Using AEAs, microorganisms under anoxic conditions can oxidize organic substrates, including methane (CH_4), the terminal product of anaerobic organic carbon reduction (Megonigal et al., 2004). However, CH_4 can be used by only a few specialized groups of archaea and bacteria that are able to overcome the high activation energy for the respective reactions (SERRANO-SILVA et al., 2014). Generally, CH_4 oxidation has been studied extensively under oxic conditions (Conrad, 2009) and in anoxic marine sediments (Beal et al., 2009; Reeburgh, 2007), but not in anoxic conditions in soils.

Anaerobic oxidation of methane (AOM) was first observed in the 1970s as a process coupled to SO_4^{2-} reduction in marine sediments (Barnes and Goldberg, 1976; Martens and Berner, 1974; Reeburgh, 1976). There, AOM is a major CH_4 sink, which consumes up to 90% of the produced CH_4 before it reaches the atmosphere (Knittel and Boetius, 2009; Valentine, 2002). In marine sediments, AOM is performed by anaerobic methanotrophic archaea (in the orders *Methanosarcinales* and *Methanomicrobiales*) linked with sulfate-reducing bacteria (Knittel and Boetius, 2009). SO_4^{2-}-dependent AOM was also reported for several terrestrial ecosystems such as peatlands (Gupta et al., 2013), riverbeds (Shen et al., 2019), lake sediments (Weber et al., 2016), landfills (Grossman et al., 2002), aquifers (Wolfe and Wilkin, 2017), and mud volcanoes (Ren et al., 2018). Still, the quantitative measures of SO_4^{2-}-dependent AOM in terrestrial ecosystems remained questionable. Although AOM

in soils has gained increasing attention, evidence on its ecological relevance remains sporadic and it has not included in most modern process-based models of the terrestrial C cycle (Gauthier et al., 2015; Smemo and Yavitt, 2011). Undoubtedly, AOM is an underappreciated CH_4 sink in terrestrial ecosystems (Hu et al., 2014; Segarra et al., 2015; Smemo and Yavitt, 2011).

Besides SO_4^{2-}, AOM was found to be linked to other terminal electron acceptors such as metal oxides (Fe^{3+} and Mn^{4+}) (Beal et al., 2009), NO_2^- (Ettwig et al., 2010), NO_3^- (Haroon et al., 2013), and humic substances (Bai et al., 2019; Scheller et al., 2016). The archaeon *Candidatus* 'Methanoperedens ferrireducens' (*M. ferrireducens*) can perform Fe^{3+}-dependent AOM via "reverse methanogenesis" and putative extracellular electron transfer pathways (Cai et al., 2018; McAnulty et al., 2017). Likewise, *Candidatus* 'Methanoperedens nitroreducens' (*M. nitroreducens*)-like archaea may anaerobically oxidize CH_4 using Fe^{3+} (Ettwig et al., 2016) similar to SO_4^{2-}-dependent AOM. AOM can also be driven by *Candidatus* 'Methylomirabilis oxyfera' (*M. oxyfera*) of the bacterial phylum NC10 via the "intra-aerobic denitrification" pathway. In the latter, oxygen used to consume CH_4 is derived from splitting of NO_2^- (Ettwig et al., 2010). NO_3^--dependent AOM is performed by *M. nitroreducens* via "reverse methanogenesis" involving the reduction of NO_3^- to NO_2^-. *M. nitroreducens* thrive either in co-existence with *M. oxyfera* and/or in a syntrophic relationship with anaerobic ammonium-oxidizing bacteria (Haroon et al., 2013).

Due to the extensive anthropogenic nitrogen inputs into marine (e.g., by river runoff and N deposition) and terrestrial ecosystems (e.g., by agricultural N fertilization and municipal waste), the contribution of NO_3^-- and NO_2^--dependent AOM to global CH_4 sink is strongly increasing. Humic substances are biochemically feasible organic AEAs (Blodau and Deppe, 2012; Lovley et al., 1996) and were recently reported to fuel AOM performed by consortia of anaerobic methanotrophic archaea (subgroup-2d, the family of *Methanoperedens*) with *Geobacter* species (Bai et al., 2019). Humic substances may act as direct AEAs for humic substances-reducing bacteria (Heitmann et al., 2007; Roden et al., 2010), or indirectly via the re-oxidation of mineral electron acceptors (Kappler et al., 2004; Valenzuela et al., 2019).

Given their typically low energy yield, anaerobic metabolisms are particularly sensitive to the concentrations of substrates and AEAs. Fluctuations in the chemical environment can therefore substantially reshape microbial interactions and thus biogeochemical fluxes. Multiple AOM pathways may be expected under various environmental conditions depending on the AEAs availability, which in turn leads to shifts in dominant microbial groups driving AOM. An effective tool to reveal interactions in complex microbial communities is the co-occurrence network analysis (Barberán et al., 2012; Berry and Widder, 2014; Weiss et al., 2016). This technique helps to understand the cooperation network of microorganisms to overcome energy barriers and supply essential nutrients. For example, syntrophic bacteria (e.g., families *Syntrophaceae* and *Syntrophorhabdaceae*) can provide essential substrates (e.g., H_2 and formate) for CH_4 production by methanogenic archaea (Edwards et al., 2015; McInerney et al., 2009).

Rice paddies are hotspots of methanogenesis (Keppler et al., 2006), generating 31 million tons of CH_4 per year and, thus, 9% of the total anthropogenic contribution to atmospheric methane (Bousquet et al., 2006). In paddy soils, organic (e.g., livestock manure, biochar) and mineral (NPK) fertilizers routinely supply ample nutrients, which are available as electron donors and acceptors in redox reactions, including AOM. The concentrations and stoichiometry of various AEA in fertilized soils modify the abundance, activity, and composition of microbial communities (Geisseler and Scow, 2014). The redox potential decreases after flooding as O_2 becomes depleted, but only there where the availability of AEAs is restricted. Such conditions are especially stable in the subsoil of paddy fields (at 20 cm and deeper). The low redox potential in the subsoil becomes favorable for methanogenesis. When produced, CH_4 diffuses to the upper soil, which is characterized by high AEA availability due to fertilization. Such conditions argue for an ecologically relevant AOM in paddy soils. To date, only

NO_3^-/NO_2^--dependent AOM has been observed in paddy soils (Hu et al., 2014; Vaksmaa et al., 2016). The role of other AEAs, especially organic electron acceptors, remains largely unclear.

Here we tested the effects of different *in-situ* fertilization treatments (pig manure, biochar, NPK fertilizers, and the control with background fertilization) and *in-vitro* AEA amendments (NO_3^-, Fe^{3+}, SO_4^{2-}, humic acids, and the reference without AEA addition) on microbial community structure. This involved using 16S rRNA gene sequencing in paddy soils with ongoing AOM. The community structure in paddy soil under oxic and anoxic conditions without AEA addition was also analyzed. To reveal the preferential AOM pathway depending on mineral and organic fertilization, we chased the ^{13}C transfer from $^{13}CH_4$ into CO_2 and phospholipid fatty acids (PLFA), and combined the results with a microbial co-occurrence network analysis. The current study was designed to answer the following research questions:

i. How do anaerobic incubation, fertilization type, and various AEA affect the microbial community structure?
ii. Is there a linkage between specific AOM pathways and the co-occurrence of distinctive microbial groups?
iii. Are there other AOM pathways co-occurring with known NO_3^-/NO_2^--dependent AOM in paddy soils?

2. Material and methods

2.1. Site description and soil collection

Soil sampling site is located near Jinjing town, Changsha county of Hunan province in China (28°33′04″N, 113°19′52″E). Soil samples were collected from an ongoing field experiment under four long-term fertilization treatments (see Fan et al., 2019, 2020, for details) as follows: (i) the control representing conventional fertilization (60 kg N ha^{-1} yr^{-1} as urea, 18 kg P ha^{-1} as $Ca(H_2PO_4)_2$, and 83 kg K ha^{-1} were applied before the seedling transplanting in each of the rice seasons), (ii) pig manure fertilization (60 Mg ha^{-1} yr^{-1}, half of which was applied before transplanting in the early and another half in the late rice season; containing 250 g C kg^{-1}, 16.8 g N kg^{-1}, 5.3 g P kg^{-1}, 2.5 g K kg^{-1}; pH 8.0) with conventional fertilization, (iii) biochar application (24 Mg ha^{-1} applied once in spring 2016; biochar was pyrolyzed from wheat straw at 500 °C by Sanli New Energy Ltd. (Shangqiu, Henan Province, China); containing 418 g C kg^{-1}, 2.8 g N kg^{-1}; pH 9.8) with conventional fertilization, and (iv) NPK (240 kg N ha^{-1} yr^{-1} as urea, half of which was applied in the early and the rest in the late rice season; further, 18 kg P ha^{-1} as $Ca(H_2PO_4)_2$ and 83 kg K ha^{-1} were applied before seedling transplantation in each of the rice seasons as basal fertilizer). Each of these fertilization treatments was established independently on three randomly replicated field plots (35 m^2). The rice cultivars and field managements (e.g., flooding and weeding) were similar. We collected four soil cores from 20-30 cm depth (bottom layer of a plow horizon 0-30 cm) with a soil auger (core length: 10 cm, diameter: 4.5 cm) from each of those plots. We targeted this soil horizon as the one with sustained anaerobic conditions and therefore presumably higher AOM potential as compared with the top 20 cm.

2.2. Experimental design and post-incubation soil sampling

The anaerobic incubation experiment (Fig. S1) was designed to test AOM potential in paddy soils under four fertilization treatments (see above) as induced by the addition of the most common inorganic (Fe^{3+}, NO_3^-, SO_4^{2-}) or organic (humic acids) AEAs. The following compounds and concentrations were used: NO_3^- (22.3 μg g^{-1} soil) was added as $NaNO_3$, SO_4^{2-} (12.7 mg g^{-1}) was added as Na_2SO_4, and humic acids (1.25 mg g^{-1}, obtained from Sigma-Aldrich Chemie GmbH, Germany) were added as solutions dissolved in sterile deionized water using sonication (RK 100H, Bandelin Sonorex, Berlin, Germany). Fe^{3+} was added as freshly prepared Fe_2O_3 (23.3 mg Fe g^{-1}) powder. All concentrations were set based on literature sources (Hu et al., 2014; Shen et al., 2014) and own preliminary testing. Very detailed information about experimental operation (e.g. gas sampling) can be found in the Supplementary file. The dynamics of AOM rate during 84 days' incubation can be found

in Fan et al., (2020), and the relevant results were summarized in 3.2. For further analyses of post-incubated soil samples, at the end of 84 days' incubation, the jars were opened inside an anaerobic glovebox to collect the soil samples into the sealed plastic bags; thereafter all the soil samples were stored at -80 ℃.

Finally, 84 soil samples were chosen for further sequencing and PLFA analysis. These were: 12 original, non-incubated soil samples (the control, pig manure, biochar and NPK fertilization × 3 field replicates each), 12 incubated reference soil samples without electron acceptor amendments and without $^{13}CH_4$ addition, and 60 samples after incubation with four electron acceptor amendments (NO_3^-, SO_4^{2-}, Fe^{3+}, humic acids) and the reference, all with $^{13}CH_4$ addition (see Fig. S1).

2.3. PLFA analyses

Microbial biomass was characterized by PLFA analysis after the modified Bligh and Dyer extraction method (Gunina et al., 2014). Briefly, total lipids were extracted from 6 g freeze-dried soil with a methanol-chloroform-citrate buffer mixture (pH 4, 2:1:0.8, v/v/v). To each of the samples, 25 µL of a first internal standard (1 µg μL^{-1}, phosphatidylcholinedinonadecanoic acid), which served as recovery standard, were added. Phospholipids were purified by liquid-liquid followed by solid-phase extraction and eluted with methanol from an activated silica gel column after removal of neutral lipids and glycolipids with chloroform and acetone. Phospholipids were subjected to an alkaline methanolysis followed by BF_3-catalyzed methylation to form fatty acid methyl esters. Prior to analysis, a second internal standard (*n*-tridecanoate methyl ester) was added, and fatty acid methyl esters were quantified using coupled gas chromatography-mass spectrometry (GC-MS) using a GC7890B and a MSD 5977B (both from Agilent, Waldbronn, Germany). The resulting PLFA dataset was subjected to factor analysis and varimax rotation for grouping (Apostel et al., 2013; Dippold & Kuzyakov, 2016). Based on the loading values (Table S1) and literature references (Zelles, 1999), PLFA with similar group behavior were assigned into one microbial group. Four microbial groups were determined: (i) Gram-negative ($Gram^-$) group, a15:0, i15:0, 16:1ω5c, 16:1ω7c, i16:0, 18:1ω7c, 18:1ω9c, and cy19:0; (ii) Gram-positive ($Gram^+$) group, i14:0, a16:0, a17:0, cy17:0, and i17:0; (iii) Actinobacteria, 10Me16:0, 10Me18:0 (Frostegård et al., 1991); (iv) Fungi, 18:2ω6,9. Total PLFA were calculated by summing up the abundance of individual fatty acids, and bacterial PLFA were calculated as the sum of (i) to (iii), and expressed as ng PLFA g^{-1} dry soil.

The $\delta^{13}C$ values of the specific fatty acids were determined by GC-combustion-isotope ratio mass spectrometry (GC-C-IRMS; Delta PlusTM, Thermo Fisher Scientific, Bremen, Germany) at the Centre for Stable Isotope Research and Analysis (KOSI), University of Göttingen, Germany. The $\delta^{13}C$ values of fatty acid methyl esters were processed on ISODAT 2.0 software and are reported relative to the Vienna Peedee Belemnite (VPDB) standard. The standard deviation of $\delta^{13}C$ values of FAME standards was 0.7‰.

2.4. DNA extraction and PCR amplification

Total DNA was extracted using the DNeasy PowerSoil DNA isolation kit (100) (QIAGEN GmbH, 40724 Hilden, Germany). 0.3 g of soil from each sample soil was transferred into bead-beating tubes supplied by the manufacturer. Cell disruption was achieved using FastPrep (MP Biomedicals, Eschwege, Germany) at 6.5 m/s for 20 s. DNA was then extracted accorded to manufacturer's instructions. The V3-4 regions of the 16S rRNA gene were amplified using fusion primers S-D-Bact-0341-b-S-17 (5'-CCTACGGGNGGCWGCAG-3') and S-D-Bact-0785-a-A-21 (5'-GACTACHVGGGTATCTAATCC-3') to targeted bacteria and archaea (Klindworth et al., 2013). S-D-Bact-0785-a-A-21 is a universal bacterial and archaeal primer, while S-D-Bact-0341-b-S-17 was expected to amplify the archaeal taxa examined *in silico* when one mismatch was allowed (Klindworth et al., 2013). The polymerase chain reaction (PCR) amplification mixture was prepared with the Phusion High-Fidelity DNA Polymerase kit (Thermo Scientific): 5 µL purified DNA template (25 ng), 10 µL 5 × Phusion GC Buffer, 0.2 µL $MgCl_2$, 1 µL 10 mM deoxyribonucleotide triphosphate (dNTP), 1 µL of each primer (1:10), 0.5 µL 2U/µL Phusion HF DNA Polymerase, and sterile Milli-Q water

were mixed to a final volume of 50 μL. All the reactions were carried out in a SensoQuest Thermalcycler (Labcycler, Göttingen, Germany) with both positive (1 μL GeneRuler (1kb, Thermo Scientific) instead of DNA template) and negative (5 μL control milli-Q water instead of DNA template) templates. The PCR cycles included a 1-min initial denaturation at 98 ℃, followed by 25 cycles of denaturation at 98 ℃ for 1 min, annealing at 55 ℃ for 30 s, extension at 72 ℃ for 1 min, and a 5-min final extension step at 72 ℃, and the reactions were held at 10 ℃. An aliquot of 5 μl of each PCR product was used for the quality control on agarose gel (0.8%, v/w) to ensure successful amplification. The triplicates were pooled in equal amounts in order to avoid amplification bias; thus 40 μL PCR product of each sample were concentrated and purified with MagSi-NGS^{Prep} magnetic beads as recommended by the manufacturer (Steinbrenner, Wiesenbach, Germany).

2.5. 16S rRNA gene sequencing and processing

Sequencing was performed on an Illumina MiSeq platform (Illumina, San Diego, CA, USA) as described by Schneider et al. (2017). Demultiplexing and clipping of adapter sequences from the raw amplicon sequences were performed with the CASAVA software (Illumina). Quality filtering was performed with fastp (v0.19.4) with a minimum phred score of 20, a minimum length of 50 basepairs, and a sliding window size of four bases, read correction by overlap and adapter removal of the Illumina Nextera primers. Paired-end reverse reads were merged with PEAR v.0.9.11 (Zhang et al., 2014) with default settings. Additionally, reverse and forward primer sequences were removed with cutadapt (v1.16) (Martin, 2011). Denoising was performed with the UNOISE3 module of vsearch and a set minsize of 8 reads. Chimeric sequences were excluded with the UCHIME3 module of vsearch. This included de novo chimera and reference-based chimera removal against the SILVA SSU 132 NR database (Quast et al., 2012). Sequences were mapped to Amplicon Sequence Variants (ASVs) (Callahan et al., 2017) by vsearch by with a set identity of 100%. Taxonomy assignments were performed with BLASTn (version 2.7.1) against the SILVA SSU 132 NR database with minimum identity threshold of 90 %.

2.6. Calculation

The quantity of $^{13}CH_4$ oxidized and incorporated into PLFA was expressed as the amount of ^{13}C-PFLA, using the equation:

$$C_{OX} = \frac{(\delta^{13}C_{Total} - \delta^{13}C_{Control})}{(\delta^{13}C_{OX} - \delta^{13}C_{Control})} \times C_{Total} \quad (1)$$

Where C_{OX} (ng g^{-1} dry soil) represents the amount of $^{13}CH_4$ converted into ^{13}C-PFLA, C_{Total} represents the total amount of C in the corresponding pool (PLFA), $\delta^{13}C_{Total}$ is the delta value of ^{13}C-PFLA in the samples treated with $^{13}CH_4$, $\delta^{13}C_{Control}$ is the delta value of PLFA in the control without $^{13}CH_4$ addition, and $\delta^{13}C_{OX}$ is the delta value of 5 AT% $^{13}CH_4$. Due to the standard deviation of 0.7‰ for PLFA, the difference between $\delta^{13}C_{Total}$ and $\delta^{13}C_{Control}$ above 1.4‰ was considered as valid ^{13}C tracer incorporation into PLFA. Differences below 1.4‰ were considered as no ^{13}C incorporation and C_{OX} was taken as zero.

2.7. Statistical analyses

A *t*-test was used to determine the effects of anaerobic incubation on the diversity and abundances of AOM-related microorganisms (methanogens, ANME-2d, NC10, *Geobacter*, SRB (sulfate-reducing bacteria), and SBM (syntrophic bacteria with methanogens)), and amount of PLFA. A one-way analysis of variance (ANOVA) was used to determine the effects of fertilization treatments or AEA amendments on the diversity and abundance of specific microbiota, PLFA, gases (CO_2 and CH_4), AOM, and ^{13}C-PLFA. Two-way ANOVA was used to test the effects of fertilization treatments and AEA amendments on the compositions of ^{13}C-PLFA. ^{13}C-PLFA was $\log_{10}(x+1)$ transformed if it failed the normality test ($p>0.05$, Shapiro-Wilk), where x in the equation represents the amount of each specific ^{13}C-PLFA. The homogeneity of the residuals of the dependent variables was also tested; when

equal variances were assumed we used the least significant difference, otherwise the Games-Howell post hoc test in SPSS 19.0 software (SPSS, Chicago, IL, USA).

Spearman correlations between the observed variables reflecting $^{13}CH_4$ metabolism (i.e., the measured AOM intensity, CH_4 production, CO_2 production, and ^{13}C-enriched in PLFA of bacteria, Gram-negative, Gram-positive and Actinobacteria) were analyzed using the *corrplot* package in R (v3.5.3). The *vegan* and *dplyr* packages were used to evaluate their Mantel associations (999 permutations) with relative abundance of taxonomic composition of AOM-related microorganisms. Principal component analyses (PCA) were employed to ordinate AEA amendments according to the relative abundance of AOM-related microorganisms by the *vegan* package. Those relative abundances were logarithmically transformed, centralized by minus means value, and normalized by standard deviation dividing.

The ASV table was rarefied for alpha and beta diversity calculations. Differential abundance analysis was performed on an ASV table filtered. Based on the analysis, we excluded two soil samples under NPK: one unincubated soil and one humic acid-amended soil. The alpha (α-) diversity of soil bacterial communities was estimated based on the ASV as Chao1, Abundance-based Coverage Estimator metric, and Faith's Phylogenetic Diversity. Unweighted UniFrac distance (Lozupone et al., 2011) was calculated and Principal Coordinate Analysis (PCoA) projections were visualized using the *ampvis2* package in R. Differential ASV abundance was analyzed using a generalized linear model with p value <0.01 in the BioConductor package *EdgeR* (Zhang et al., 2018). BugBase (Ward et al., 2017) is an algorithm that predicts organism-level coverage of functional pathways. This one as well as biologically interpretable phenotypes such as oxygen tolerance and Gram staining was used. Functions were inferred using FAPROTAX (Louca et al., 2016), which is a conservative algorithm currently matching 80 functions against 7600 functional annotations of 4600 prokaryotic taxa. Significance tests between treatments were performed using Permutational multivariate analysis of variance (PERMANOVA) with 999 permutations per test.

The co-occurrence patterns were constructed by calculating multiple correlations and similarities within the network, whereby the topological sub-network associated with AOM-related microorganisms (methanogens, ANME-2d, NC10, *Geobacter*, SRB, and SBM) and the observed variables reflected $^{13}CH_4$ metabolism (AOM, ^{13}C-PLFA, CH_4, CO_2). Pairwise Pearson correlations were calculated between the remaining ASVs. A valid co-occurrence was considered as a statistically robust correlation between taxa when the Pearson's correlation (r) was >0.6 and the p value was <0.01 (Barberán et al., 2012). Each node indicated individual ASV, and each edge represented the pairwise correlations between nodes standing for a significant metabolic association in the network (Barberán et al., 2012). Multiple topological properties (i.e., number of nodes and edges, average degree, average path length, network diameter, and clustering coefficient) were calculated and visualized using *igraph* package (Csardi & Nepusz, 2006). We generated 1000 Erdős–Rényi random networks with each edge having the same probability of being assigned to any node (Erdős & Rényi, 1960) to compare with the topology of the real network. All statistical analyses were performed using R (v3.5.3) unless otherwise stated.

2.8 Data deposition

The raw 16S rRNA gene sequencing reads for this study has been deposited in the National Center for Biotechnology Information Sequence Read Archive under bioproject PRJNA629535.

3. Results

3.1. Shifts in microbial community structure during anaerobic incubation

A 100% identity threshold was used to cluster sequences into Amplicon Sequence Variants (ASVs). After rarefaction to equal sequencing depth, a data set of 635,062 high-quality sequences was produced from the soil samples. 97.4% of these sequences could be classified to bacteria phyla, 1.4% of the sequences to archaeal phyla. The ASV counts per sample are shown in Table S2. 82.4% of the bacterial sequences were clustered into six dominant phyla including *Proteobacteria* (30.0%),

Chloroflexi (15.8%), *Acidobacteria* (15.4%), *Nitrospirae* (9.5%), *Planctomycetes* (6.0%), and *Bacteroidetes* (5.8%). The phylum *Euryarchaeota* (49.1%) represented the dominant archaea co-amplified with bacteria, and therein we identified four families of methanogens (*Methanobacteriacea*e, *Methanocellaceae*, *Methanosaetaceae*, *Methanoregulaceae*) and one family of anaerobic methanotrophs (*Methanoperedenaceae*, formerly known as ANME-2d) (Fig. S2).

After 84 days of strict anaerobic incubation, the within-sample diversity (α-diversity) had increased irrespective of fertilization (Fig. 1A). Bacterial communities in soil before and after incubation were clearly separated across the first principal coordinate of the Principal Coordinate Analysis (Fig. 1B, PCoA with unweighted UniFrac distance). Permutational multivariate analysis of variance (PERMANOVA) corroborates that significant changes in the microbial community had been induced by anaerobic incubation (10%, $p < 0.001$, Table S3). 207 ASVs were significantly enriched in post-incubation soil, whereas 453 were depleted (Fig. 1C, ASV counts for a differential ASV abundance analysis). Particularly *Proteobacteria*, *Bacteroidetes* and *Chloroflexi* were depleted by the anaerobic incubation (Fig. 1E, Wilcoxon test Table S4, Fig. S3).

The relative abundance of methanogens, ANME-2d, NC10, and SO_4^{2-} reducing bacteria (SRB) were similar in both pre- and post-incubation. *Geobacter* abundance increased and SBM abundance decreased after anaerobic incubation (Fig. S4). The relative abundance of anaerobic bacteria increased after anaerobic incubation (Fig. 1D, BugBase prediction). 18-34% of the ASVs were assigned to 25 microbial functional categories out of 80 functions from FAPROTAX, a functional annotations dataset. The dominant functions (>1%) across all samples were sulfate respiration (dissimilatory sulfate reduction), respiration of sulfur compounds, fermentation, and iron respiration (dissimilatory Fe^{3+} reduction) (Fig. S5). The proportions of nitrate respiration, fermentation, and iron respiration were significantly higher after anaerobic incubation.

The co-occurrence networks enabled to identify the interactions between each taxon in microbial communities, and to determine the reshaping of soil microbiome associations by anaerobic incubation. Multiple topological properties – edges, nodes, average degree, average path length, and network diameter – increased after anaerobic incubation (Fig. 1F, Table S5), indicating that microbial interactions became more tightened and complex in the anaerobic environment. *Proteobacteria* were the most abundant microorganisms contributing to the network (Fig. 1H). NC10, Fe^{3+} reducing bacteria (i.e., *Geobacter*), SRB (families *Desulfobacteraceae*, *Desulfobulbaceae*, *Desulfovibrionaceae*, *Syntrophobacteraceae*, *Thermodesulfovibrionaceae*), and SBM (families *Syntrophaceae* and *Syntrophorhabdaceae*) were color-coded in the networks (Fig. 1F) due to their potential relation to AOM. The contribution of *Geobacter* increased in post-incubation networks (Fig. 1G). This shows that *Geobacter* may play an important role in anaerobic metabolism, involving AOM.

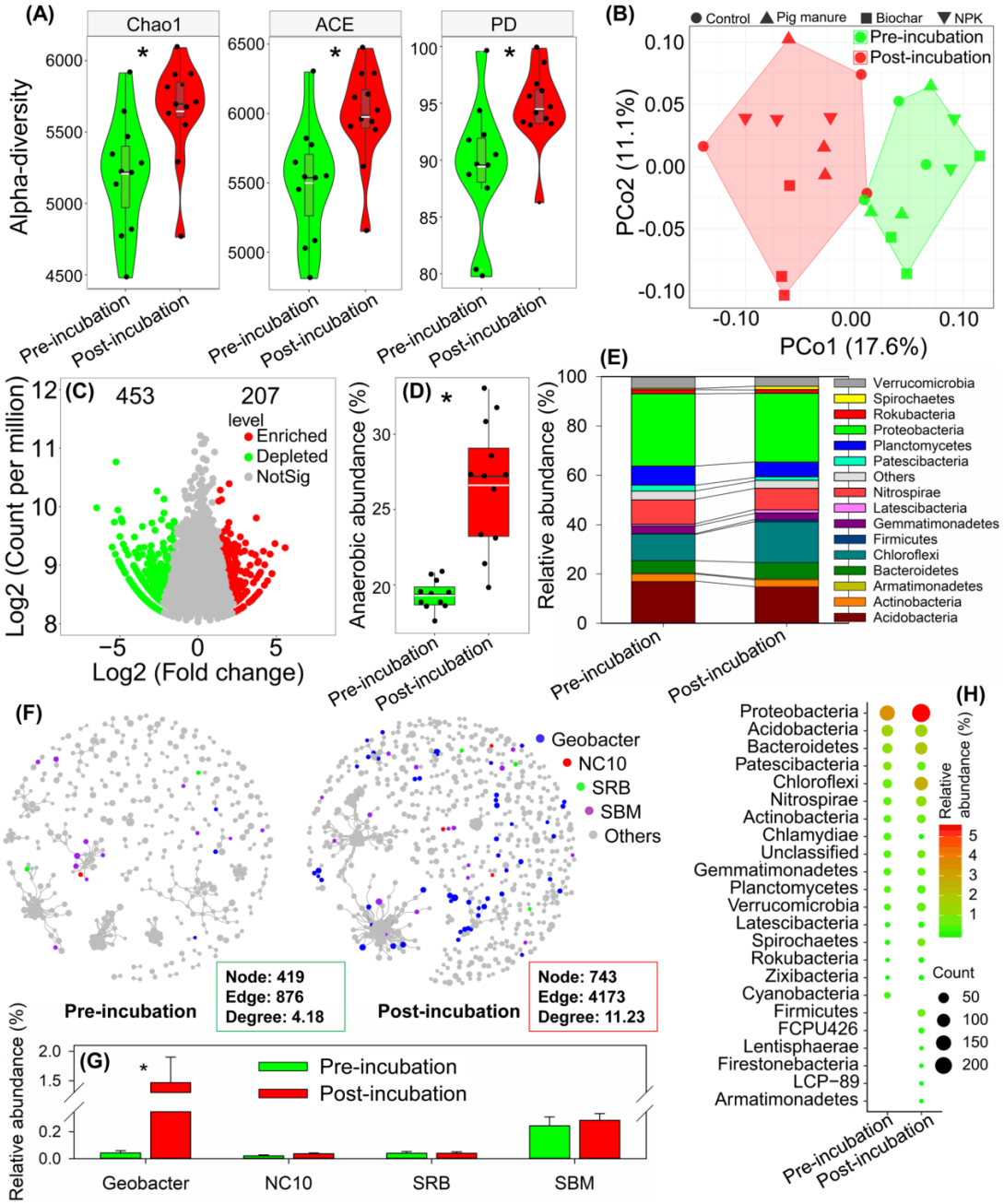

Fig. 1 Changes in bacterial communities between pre- and post-incubated paddy soils. **(A)** Alpha diversity (α-diversity) estimated as Chao1, Abundance-based Coverage Estimator metric (ACE), and Faith's Phylogenetic Diversity (PD). The horizontal black and white lines within boxes represent the median and the mean, respectively. The tops and bottoms of boxes represent 75th and 25th quartiles, respectively. The upper and lower whiskers represent a 95% confident interval. Asterisks (*) represent significance at p<0.05. **(B)** Principal Coordinates Analysis (PCoA) using the unweighted Unifrac distance metric. **(C)** Volcano plot of ASV (Amplicon Sequence Variants) count in post-incubation soils relative to pre-incubation soils. Each point refers to an individual ASV. **(D)** The relative abundance of anaerobic bacteria from BugBase prediction. **(E)** Top 15 bacterial phyla abundances in pre- and post-incubation soils. **(F)** The bacterial co-occurrence networks based on ASV correlation analysis. A connection stands for a strong (Pearson's r > 0.6) and significant (p<0.01) correlation. The size of each node is proportional to the relative abundance of each ASV. **(H)** The nodes of the co-occurrence network grouped by phyla. **(G)** Relative abundance of *Geobacter*, NC10, SRB (sulfate reducing bacteria), and SBM (syntrophic bacteria with methanogens) in the co-occurrence networks.

3.2. Effects of fertilization and electron acceptors on microbial PLFA synthesis and AOM pathways

The total amount of phospholipid fatty acids (PLFA) was highest under pig manure fertilization (49.4 μg PLFA g^{-1} soil) (p<0.05, Fig. 2A), but was independent from AEA amendments (Fig. 2C). However, the proportions of Gram-negative, Gram-positive, and Actinobacteria, as deduced from PLFA distributions, were similar between fertilizations (Fig. 2B) and AEA amendments (Fig. 2D).

We examined the uptake of $^{13}CH_4$ derived carbon into PLFA and compared it with the AOM based ^{13}C transfer into CO_2. After 84 days of incubation, 16 out of 27 individual PLFA showed substantial ^{13}C incorporation relative to the ^{13}C natural abundance. These 16 PLFA were considered as biomarkers linking distinct microbial groups to AOM (Fig. 2E, F). Total ^{13}C incorporated in PLFA (^{13}C-PLFA, calculated according to Eq. 1) ranged from 13.0-20.8 ng g^{-1} dry soil. Total and bacterial ^{13}C-PLFA was similar between fertilizations (Fig. 2C), with most ^{13}C being incorporated into Gram-negative bacteria (Fig. 2F). The cumulative AOM was highest (0.78 μg C g^{-1} soil over 84 days) under manure fertilization, and was 2.6~4.0 times lower under biochar and NPK than the control (Fig. S6A).

Among the different AEAs tested, particularly SO_4^{2-} addition increased ^{13}C-PLFA as compared to the reference (Fig. 2G). It also strongly fueled CO_2 production but completely inhibited AOM (Fig. S6). Adding NO_3^- and humic acids as AEAs did not significantly change ^{13}C-PLFA (Fig. 2G). However, NO_3^- resulted in the highest AOM (0.44 μg C g^{-1} soil), and humic acids promoted the highest cumulative CH_4 production (Fig. S6B, F). Under Fe^{3+} amendment, a minor increase in bacterial ^{13}C-PLFA was noted, but AOM was not affected compared to the reference (Fig. 2G). The partitioning of CH_4-derived ^{13}C between Gram-negative, Gram-positive and Actinobacterial PLFA was strongly affected by AEA amendments (Fig. 2H). Overall, fertilization (Fig. 2I) and AEA amendments (Fig. 2J) led to a strong divergence of microbial community structure and functions, as indicated by ^{13}C incorporation into 16 PLFA biomarkers (two-way ANOVA, p<0.001, Table S6). Multiple AOM pathways were therefore expected.

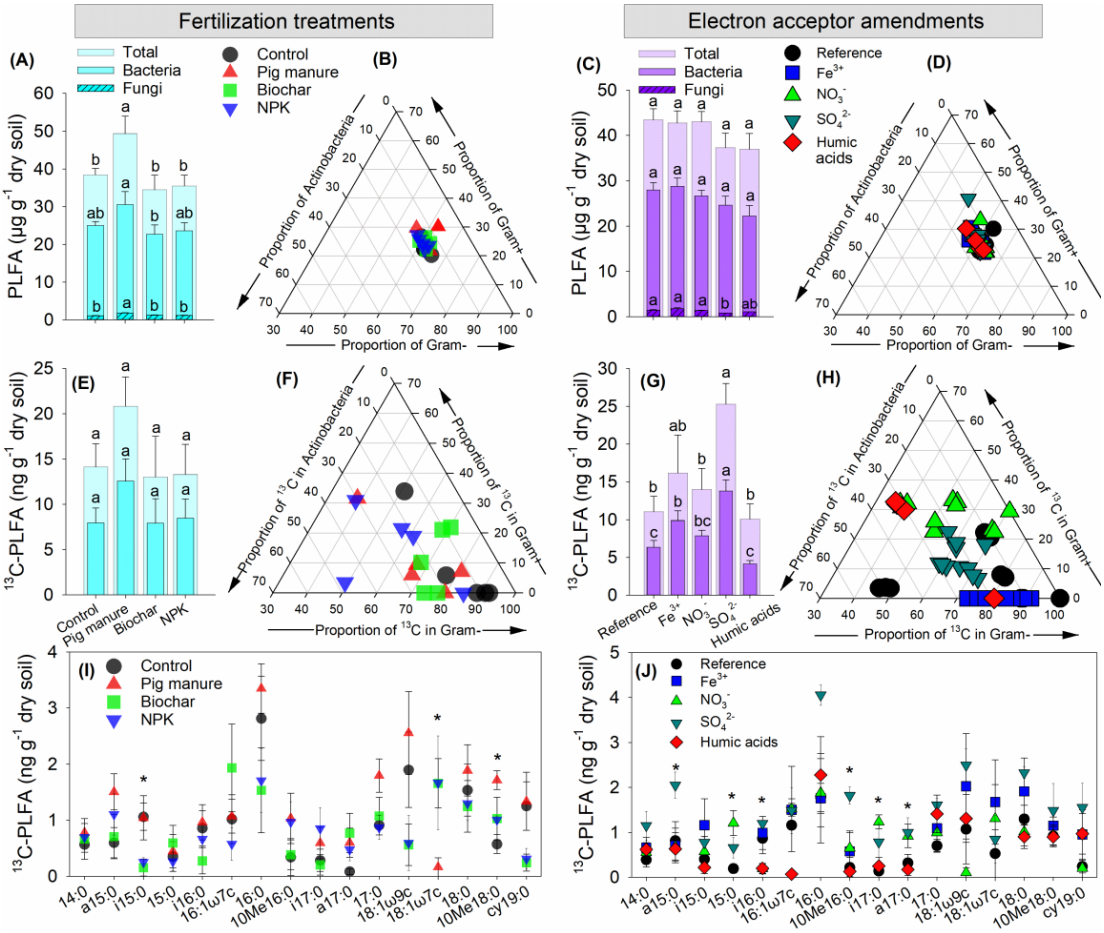

Fig. 2 Phospholipid fatty acids (PLFA) of individual microbial groups affected by fertilization and electron acceptors. (**A**) The amount of PLFA and (**B**) the proportion of Gram-negative, Gram-positive and Actinobacteria in each fertilization. (**C**) The amount of PLFA and (**D**) the proportion of individual microbial groups in each electron acceptor amendment. (**E**) CH_4-derived ^{13}C incorporation in PLFA and (**F**) proportional ^{13}C partitioning of individual microbial groups in each fertilization. (**G**) CH_4-derived ^{13}C incorporation in PLFA and (**H**) proportional ^{13}C partitioning of individual microbial groups in each electron acceptor amendment. (**I**) 16 ^{13}C-enriched PLFA in each fertilization. (**J**) 16 ^{13}C-enriched PLFA in each electron acceptor amendment. Lowercase letters: significant differences of total PLFA and ^{13}C-enriched PLFA at $p<0.05$. Asterisks (*): significant differences between individual ^{13}C-enriched PLFA at $p<0.05$.

3.3. Effects of fertilization on microbial communities and AOM pathways

We compared communities with and without $^{13}CH_4$ addition under organic and mineral fertilization in order to link methanogenesis and AOM potential on a microbiome level. Fertilization was the major source of variation within the microbiome data (17%, $p<0.001$), but not the CH_4 addition (4%, $p>0.05$, Table S7, PERMANOVA). The relative abundance of *Geobacter* was higher under biochar and NPK ($p<0.05$), but it was similar under pig manure compared to the control. NC10 abundance was higher under biochar than others, but SRB, SBM, methanogens and ANME-2d abundances were similar between all fertilizations (Fig. 3A). In the following, we focus on co-occurrence network analysis. Please refer to the Supplementary material for more data on α-diversity, beta diversity of PCoA, differential ASV abundance analysis, LEfSe analysis, phenotypes of BugBase prediction, and predicted functions based on FAPROTAX.

The co-occurrence network degree increased under pig manure and NPK fertilization vs. the control by 0.17 and 0.54 edges, respectively, but it decreased under biochar application by 0.17 edges (Fig. S7). This indicates tightening interactions of soil microbiome in response to manure and NPK

fertilization. Topological sub-networks explored the co-occurrence patterns between the variables reflecting $^{13}CH_4$ metabolism (i.e., AOM, ^{13}C-PLFA, CH_4, CO_2) and AOM-related microorganisms (i.e., methanogens, ANME-2d, *Geobacter*, NC10, SRB, SBM) (Fig. 4A). The network degree of these AOM-related sub-networks increased by 2.88 edges under biochar but decreased by 1.77-5.30 edges under manure and NPK compared to the control. Accordingly, the soil microbiome formed tighter interactions under biochar but weaker interactions under manure and NPK fertilization, where NPK had the greatest effect.

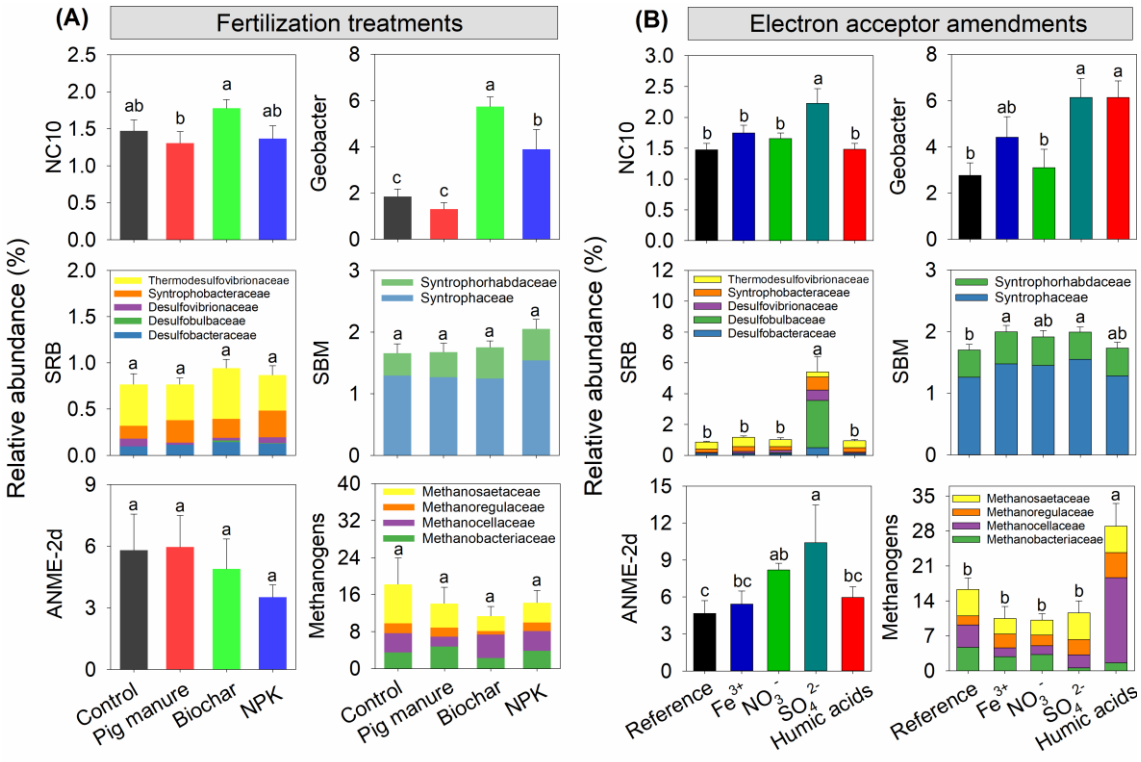

Fig. 3 Relative abundance of the AOM-related microorganisms. **(A)** AOM-related microorganisms under fertilization treatments. **(B)** AOM-related microorganisms under electron acceptor amendments. AOM-related microorganisms include NC10, *Geobacter*, SRB (sulfate-reducing bacteria), SBM (syntrophy bacteria with methanogens), ANME-2d, and methanogens. Lowercase letters represent significant differences at $p<0.05$.

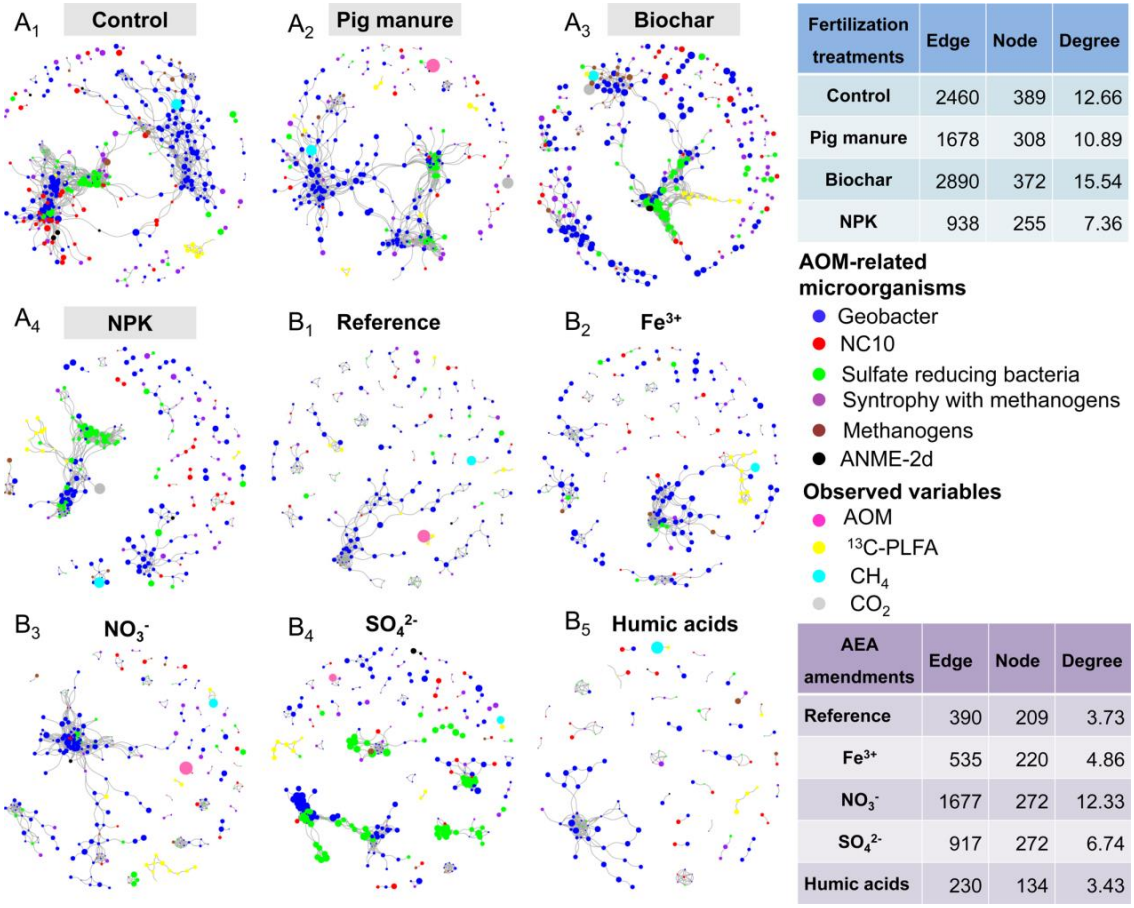

Fertilization treatments	Edge	Node	Degree
Control	2460	389	12.66
Pig manure	1678	308	10.89
Biochar	2890	372	15.54
NPK	938	255	7.36

AEA amendments	Edge	Node	Degree
Reference	390	209	3.73
Fe^{3+}	535	220	4.86
NO_3^-	1677	272	12.33
SO_4^{2-}	917	272	6.74
Humic acids	230	134	3.43

Fig. 4 The co-occurrence networks reflecting anaerobic methane oxidation (AOM) metabolism. (**$A_{1\text{-}5}$**) The co-occurrence networks under fertilization treatments. (**$B_{1\text{-}5}$**) The co-occurrence networks for each fertilization with electron acceptor amendments. The co-occurrence networks associated with AOM-related microorganisms (methanogens, ANME-2d, *Geobacter*, NC10, SRB (sulfate-reducing bacteria), and SBM (syntrophic bacteria with methanogens)) and the observed variables which reflecting $^{13}CH_4$ metabolism (AOM, ^{13}C-PLFA, CH_4, CO_2) based on Amplicon Sequence Variants correlation analysis, and a connection stands for a strong (Pearson's r>0.6) and significant (p<0.01) correlation. The size of each node is proportional to the microbial relative abundance and recorded values.

3.4. Effects of electron acceptors on microbial co-occurrence networks and AOM pathways

AEAs comprised the largest source of variation within the microbiomes (13%, p<0.001), followed by fertilization (10%, p< 0.001, Table S8, PERMANOVA). The relative abundance of NC10 and SRB were highest under SO_4^{2-}. *Geobacter* abundance increased 2.2 times after SO_4^{2-} and humic acids amendments than the reference (Fig. 3B). Methanogens abundance was 1.8-2.8 times higher after humic acids amendment than the others. However, ANME-2d abundance was highest under SO_4^{2-}, followed by NO_3^-, humic acids, and Fe^{3+}, and it was the lowest in the reference (Fig. 3B).

AEA amended soils showed a clear separation of NO_3^-, SO_4^{2-} and humic acids based on the abundance of AOM-related microorganisms (Fig. 5A, principle component analysis (PCA)). The cumulative AOM and CH_4 production correlated well with the PC2 (Fig. 5B). This indicates that AOM-related microorganisms had a strong AEA preference, underlining an environmental niche differentiation. Thus, to further identify the microbial AOM drivers, we correlated AOM-related community composition with the measured variables AOM, ^{13}C-PLFA, CH_4, and CO_2 (Fig. 5C). The abundance of taxonomic composition of ANME-2d was the only correlate to AOM, while AOM was independent from taxonomic composition of NC10, SRB, and *Geobacter*.

AEA amendments altered the topological properties of the microbial communities' networks. The network degree decreased with amendments of Fe^{3+} and humic acids, but increased with NO_3^- and

SO_4^{2-}, as compared to the reference (Fig. S8). This indicates that the soil microbiome formed tighter associations in response to NO_3^- and SO_4^{2-}, with NO_3^- having the greatest effect. The sub-network degree increased strongly by 9.60 edges under NO_3^- amendment, increased by 1.13 and 3.01 edges under Fe^{3+} and SO_4^{2-} compared to the reference, respectively, but decreased 0.3 edges after humic acids addition (Fig. 4B). Overall, the structural properties of the "real-world" network across all samples were greater than the Erdős–Rényi random networks of the clustering coefficient (Table S5). Consequently, the significance of clusters confirmed that the "real-world" microbial network consisted of highly connected microorganisms.

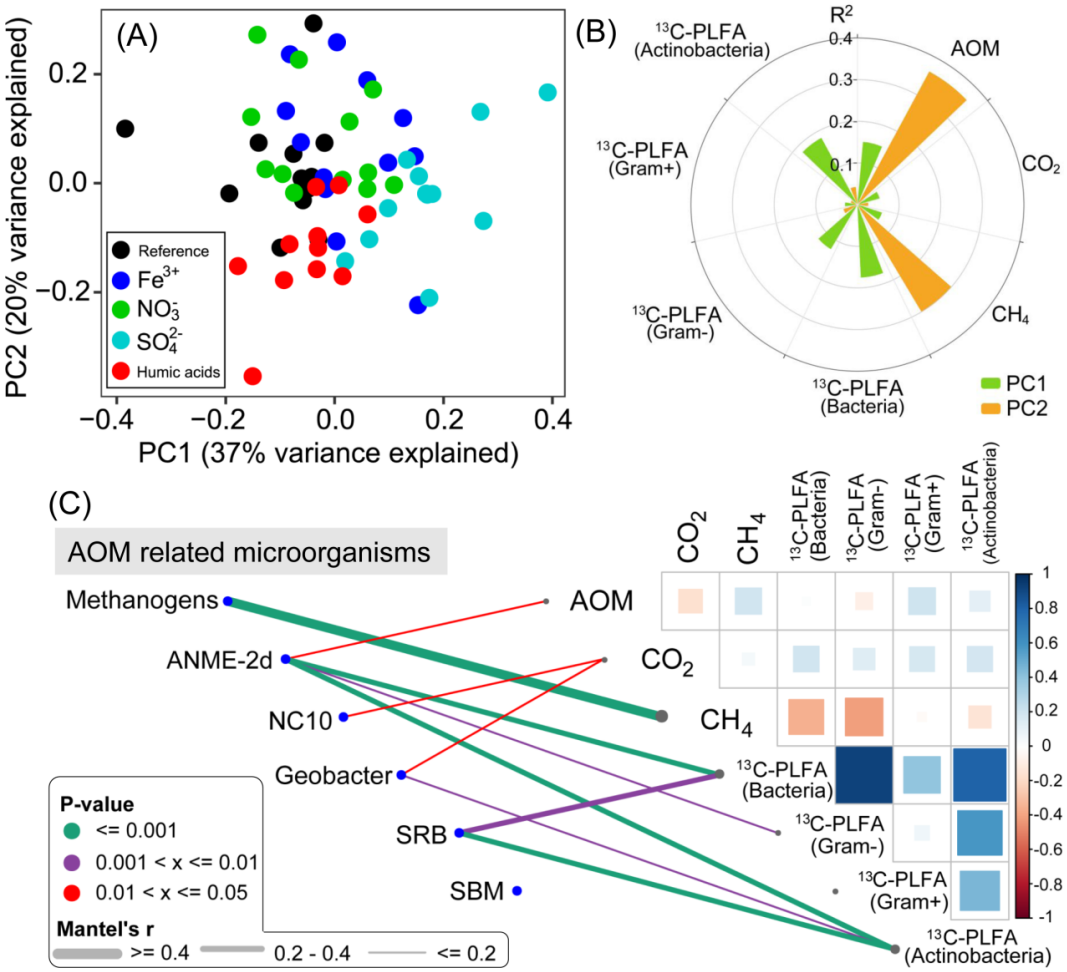

Fig. 5 Microbial drivers of anaerobic oxidation of methane (AOM). **(A)** Principal coordinate (PC) analysis of electron acceptor amendment' samples based on the relative abundance of AOM-related microorganisms (methanogens, ANME-2d, *Geobacter*, NC10, SRB (sulfate reducing bacteria), and SBM (syntrophic bacteria with methanogens)). **(B)** Correlation (R^2) between the first and second PC and the observed variables which reflecting $^{13}CH_4$ metabolism (AOM, ^{13}C-PLFA, CH_4, CO_2). **(C)** Relationships between AOM-related microorganisms and observed variables. Left, visualization of the Spearman correlation matrix of the observed variables. Right, the mantel correlations between abundance of AOM-related microorganisms (16S ASVs) and the observed variables. Edge width corresponds to the Mantel's r statistics for the corresponding correlations, and edge color denotes the statistical significance based on 999 permutations. p>0.05 was not shown.

4. Discussion

Soil microbial communities respond rapidly to environmental changes (Geisseler & Scow, 2014; Lozupone & Knight, 2007). Here we demonstrated the response of the paddy soil microbiome to (i) strict anaerobic conditions, (ii) organic and mineral fertilization, and (iii) AEA amendments.

Anaerobic incubation was the most important factor affecting the microbial community, resulting in shifts in the abundance of many ASVs (Fig. 1C) and an increased alpha-diversity (Fig. 1A). The relative increase (e.g., *Geobacter*, Fig. 1G), or decrease (e.g., *Nitrospira*) of specific microbial groups clearly reflect the adaptation of the microbial consortia to strictly anaerobic conditions (Megonigal et al., 2004). When oxygen is depleted, microorganisms turn to use AEAs for energy yield, where the highest free Gibbs energies are provided by NO_3^-, followed by humic substances, Fe^{3+}, and SO_4^{2-}. The major changes in topological properties of the co-occurrence network mirrored the alteration in microbial communities (Barberán et al., 2012). Strictly anaerobic incubation induced a more complex coupling among microorganisms which can be explained by the fact that the lower energy yield of anaerobic metabolisms requires establishing mutualistic linkages as a survival strategy (Megonigal et al., 2004).

Incorporation of ^{13}C from added $^{13}CH_4$ into CO_2 under strict anoxic conditions confirmed the occurrence of AOM irrespective of fertilization and AEA amendments (Fig. S6). At the same time, the transfer of isotope label into PLFA demonstrated the anabolic uptake of methane-derived carbon into microbial biomass (Raghoebarsing et al., 2006; Segarra et al., 2015; Fig. 2E, F). The partitioning of CH_4-derived ^{13}C between Gram-negative, Gram-positive and actinobacterial PLFA (Fig. 2F, H), and the incorporation of ^{13}C into these 16 PLFA, strongly depended on fertilization and AEA availability (p<0.001, Fig. 2). This suggests that microorganisms involved in AOM used different metabolic pathways (Segarra et al., 2015). Moreover, AOM-related microorganisms (methanogens, ANME-2d, *Geobacter*, NC10, SRB, and SBM) showed a strong AEA dependence (Fig. 5A), confirming a linkage between active AOM pathways and AEAs. Fertilization can introduce various AEAs in paddy soils and make them available for AOM. Thus, AOM potential was significant different under different fertilized paddy soils (Fig. S6), such as the highest AOM potential was reached under manure fertilization because of its high NO_3^- load (Fan et al., 2020). Biochar application resulted in a higher abundance of NC10 but lowest AOM. Under biochar and NPK fertilization, high relative abundance of *Geobacter* was recorded, but ANME-2d abundance and AOM were numerically lower relative to manure fertilization (Fig. 3A, Fig. S6). Thus, biochar application hinders the proposed pathway of extracellular electron transfer between *Geobacter* and ANME-2d, where CH_4 oxidation is coupled to the reduction of anthraquinone-2,6-disulfonate (AQDS) or humic substances (Bai et al., 2019; Scheller et al., 2016).

The AOM pathways were subsequently determined based on the thermodynamic energy yield in reactions with the main electron acceptors (NO_3^-, humic acids, Fe^{3+}, SO_4^{2-}) (Cui et al., 2015; Shen et al., 2019; Smemo & Yavitt, 2011). AOM was highest under NO_3^- amendment, with a high relative abundance of ANME-2d but NC10 abundance similar to the reference (Fig. 3B, Fig. S6), and the abundance of ANME-2d was the only correlate to AOM (Fig. 5C). In contrast, ^{13}C incorporation from CH_4 into 10Me16:0 was lowest under NO_3^-, and 10Me16:0 was identified as one of the key PLFA of "*M. oxyfera*" (Kool et al., 2012). This suggests that NO_3^-, rather than NO_2^- (which is used by NC10 *M. oxyfera*), was the dominant electron acceptor for AOM, supported by excess of NO_3^- applied with manure and N fertilization. Moreover, AOM was associated with ANME-2d in the co-occurrence network of NO_3^--amended microbial communities (Fig. $4B_3$). A plausible candidate for an AOM-performing microorganism using NO_3^- is *M. nitroreducens*, which is dominant in the ANME-2d cluster and broadly distributed in paddy soils (Vaksmaa et al., 2017, 2016). The contribution of NO_3^--dependent pathways to total AOM is strongly increasing globally following the extensive anthropogenic nitrogen inputs into marine (e.g., by river runoff and N deposition) and terrestrial ecosystems (e.g., by agricultural N fertilization and municipal waste). Besides the biogeochemical implications, NO_3^--dependent AOM can have biotechnological application for concurrent nitrogen removal and CH_4 emission mitigation from wastewater (Lee et al., 2018; Liu et al., 2020; Lu et al., 2020; Nie et al., 2019, 2020). Another AEA, namely Fe^{3+}, had a minor effect on CH_4-derived C in PLFA and demonstrated a low potential to fuel AOM.

Surprisingly, SO_4^{2-} addition increased the relative abundance of ANME-2d and NC10 (Fig. 3B), and induced higher ^{13}C incorporation into the PLFA 10Me16:0 (Fig. 2J). The measured AOM, however, was the lowest (Fig. S6B). There are several possible reasons for this observation: (i) Highest CO_2 production under SO_4^{2-} amendment (Fig. S6D) suggests that organic matter oxidation with SO_4^{2-} was thermodynamically more favorable than AOM. (ii) AOM was clustered in the co-occurrence network of SO_4^{2-}-amended microbial communities (Fig. $4B_5$), suggesting that SO_4^{2-}-dependent AOM performed by consortia of ANME-2d with SRB was one of the active AOM pathways. However, similar to NC10-derived AOM, SO_4^{2-}-dependent AOM was of minor intensity. (iii) Vigorous SO_4^{2-}-driven organic matter decomposition by *Geobacter* and SRB may have diluted the ^{13}C-label of the CH_4 by non-labeled SOM-derived CH_4, thereby masking the ongoing AOM. (iv) 10Me16:0 might be ^{13}C enriched as derived from cross-feeding of other microbial groups (e.g., *Actinobacteria*), which are also functional and can grow under these conditions. Especially for the 10Me-branched fatty acids of *Actinobacteria*, a growth based on necromass of other microbial groups incorporating $^{13}CH_4$ is very likely (Apostel et al., 2018).

Humic substances were previously acknowledged as important AEAs for organic matter decomposition (Keller et al., 2009) and AOM (Bai et al., 2019). Humic acids increased the abundance of methanogens and *Geobacter*, and led to the highest CH_4 production (Fig. 3B). Note, however, that the observed intensive methanogenesis was not connected with major AOM (Fig. 5C). Reportedly, *Geobacter* also plays a role in oxidizing acetate, and its activity is coupled to the reduction of humic acids (Voordeckers et al., 2010). A mutual linkage of *Geobacter* with methanogens is possible, whereas humic substances served as methanogenesis substrates (Voordeckers et al., 2010).

The co-occurrence patterns clearly revealed robust coupling between methanogens, ANME-2d, *Geobacter*, NC10, SRB, and SBM from one side, and AOM, ^{13}C-PLFA, CH_4, and CO_2 from another (Fig. 4). This suggests mutually beneficial relationships for energy acquisition under anaerobic conditions (Barberán et al., 2012; Berry & Widder, 2014). Accordingly, the observed clustering in the co-occurrence networks underlines (i) a tight association between methanogenesis and AOM (Newman, 2006), (ii) that ANME-2d, *Geobacter*, NC10, and SRB jointly contributed to AOM by several co-existing AOM pathways, (iii) that co-occurrence networks after individual AEA amendments demonstrated either one dominant AOM pathway or out-competition of AOM by other anaerobic metabolisms. For example, SO_4^{2-} yielded higher CO_2 production by anaerobic organic matter decomposition, and humic acids yielded the highest CH_4 production by methanogens.

Overall, *Geobacter* species (Voordeckers et al., 2010) (whose abundance increased after addition of humic acids, Fig. 3B) can be linked with methanogens when products of humic substances decomposition (e.g., acetate, formate) served as a substrate for methanogenesis. SRB (Megonigal et al., 2004) activated by SO_4^{2-} fueled organic matter oxidation, thereby breaking complex organic molecules down to simple compounds such as acetate and formate. These small molecules were used directly as precursors for methanogenesis (Serrano-Silva et al., 2014). Finally, methanogens cooperated with their syntrophic partners (e.g., SBM) to obtain substrates for CH_4 synthesis (Serrano-Silva et al., 2014). The produced CH_4 diffused to (i) anaerobic microsites in structure-less soils or the surface of a structured soil with specific AEA or, (ii) anaerobic zones inside the aggregates of a structured soil, to be simultaneously exposed to a range of microenvironments (various redox conditions, microorganisms including AOM-related microbiota, and AEAs). Therefore, the AOM pathways (summarized in Fig. 6) occur simultaneously spatially separated in each of the anaerobic microsites depending on the local redox conditions and AEA present, which suggests the differential niche of AOM-related microorganisms (pathways) in soils (Xie et al., 2020). This is the case in those conditions when sufficient CH_4 is distributed within the soil slurry. Therefore, several pathways may occur simultaneously, but the AOM intensity was limited by AEA availability. Note also that the physiological requirements of microorganisms at microenvironments are reflected by AEA variability (Parkin, 1993; Weber et al., 2017) and active AOM pathways, e.g., humic acids and Fe^{3+} can decouple

archaeal CH_4 oxidation from SO_4^{2-} reduction by SRB, and can themselves act as direct terminal electron acceptors for AOM driven by consortia of ANME-2d with *Geobacter* (Scheller et al., 2016; Bai et al., 2019; Ettwig et al., 2016) (Fig. 6). In a certain anaerobic zone, the AOM pathways progress sequentially, i.e., $NO_3^-(NO_2^-)$ → humic acids → Fe^{3+} → SO_4^{2-}. The affinity of each AOM pathway for CH_4 can also play a vital role in the preference for the specific AOM pathways due to limited CH_4 accessibility, e.g., the apparent affinity constant for CH_4 of SO_4^{2-}-dependent AOM (>16 mM) is four orders of magnitude lower than that of NO_3^-/NO_2^--dependent AOM (<0.6μM) (Raghoebarsing et al., 2006).

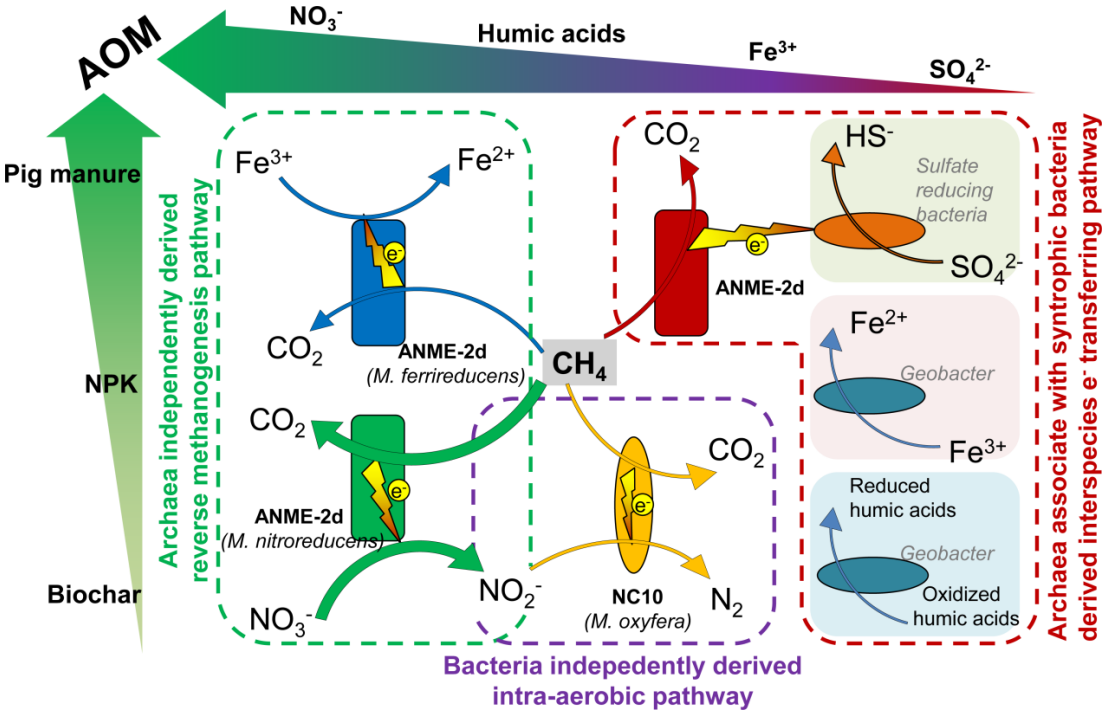

Fig. 6 Conceptual model of microbial anaerobic methane oxidation (AOM) pathways in paddy soils. **Green box,** archaea independently conduct "reverse methanogenesis" pathway associated with reduction of (i) NO_3^- to NO_2^- by *M. nitroreducens* of ANME-2D (Haroon et al., 2013), (ii) Fe^{3+} to Fe^{2+} by *M. ferrireducens* of ANME-2d (Cai et al., 2018). **Purple box,** bacteria independently conducted "intra-aerobic denitrification" pathway by NC10 *M. oxyfera*, where O_2 is derived from intracellular NO_2^- dismutation (Ettwig et al., 2010). **Red box,** interspecies-extracellular electron transferring "reverse methanogenesis" pathway by archaea and associated syntrophic bacteria (McAnulty et al., 2017), the putative reduction of (i) Fe^{3+} and (ii) humic substances by consortia of ANME with *Geobacter*, and (iii) reduction of SO_4^{2-} by consortia of ANME with sulfate reducing bacteria. Thick green arrow: the most potent AOM pathway, i.e., NO_3^--dependent AOM. Shape, direction and colour gradients of large arrows correspond to increasing effect of fertilization (biochar, NPK, pig manure) on AOM (light green to green), an increasing effect of electron acceptor amentments (SO_4^{2-}, Fe^{3+}, humic acids, NO_3^-) on AOM (red to purple to green).

5. Conclusions

The co-occurrence patterns of microbial communities in paddy soils under anaerobic conditions were strongly shaped by fertilization and electron acceptor amendments. We open new perspectives for studies on highly complex interactions of anaerobic communities in paddy soils including AOM. The latter was disentangled by jointly applying microbial community analysis and ^{13}C tracing from $^{13}CH_4$ in CO_2 and microbial PLFA. We identified AOM independently conducted by *Methanoperedenaceae* (ANME-2d) as being the major AOM pathway in paddy soils, whereby manure fertilization had greatest effect, followed by NPK, with the lowest effect after biochar application. This pathway co-

existed with the minor AOM pathways independently conducted by NC10 and with the AOM conducted by consortia of ANME-2d with *Geobacter* or sulfate-reducing bacteria. AOM is quantitatively important and must be included in modern process-based models of the terrestrial C cycle.

Acknowledgements

This research was financially supported by the German Research Foundation (DFG, Do 1533/2-1), the National Natural Science Foundation of China (41761134095; 41430860; 41671253), Youth Innovation Team Project of ISA, CAS (2017QNCXTD_GTD) and Hunan Province Base for Scientific and Technological Innovation Cooperation (2018WK4012). The authors are thankful to the China Scholarship Council (CSC) for funding Lichao Fan in Germany. Special thanks to the Kompetenzzentrum Stabile Isotope (KOSI) University of Goettingen (to Lars Szwec and Reinhard Langel for isotope analyses), Dr. Hongcui Dai for the help in Bugbase analysis, and Yuliia Ruban for the help in PLFA isolation.

References:

Apostel, C., Dippold, M., Glaser, B., Kuzyakov, Y., 2013. Biochemical pathways of amino acids in soil: Assessment by position-specific labeling and ^{13}C-PLFA analysis. Soil Biology & Biochemistry 67, 31-40.

Apostel, C., Herschbach, J., Bore, E.K., Spielvogel, S., Kuzyakov, Y., Dippold, M.A., 2018. Food for microorganisms: Position-specific ^{13}C labeling and ^{13}C-PLFA analysis reveals preferences for sorbed or necromass C. Geoderma 312, 86-94.

Bai, Y., Wang, X., Wu, J., Lu, Y., Fu, L., Zhang, F., Lau, T., Zeng, R.J., 2019. Humic substances as electron acceptors for anaerobic oxidation of methane driven by ANME-2d. Water Research 164, 114935.

Barberán, A., Bates, S.T., Casamayor, E.O., Fierer, N., 2012. Using network analysis to explore co-occurrence patterns in soil microbial communities. The ISME Journal 6, 343-351.

Barnes, R.O., Goldberg, E.D., 1976. Methane production and consumption in anoxic marine sediments. Geology 4, 297.

Beal, E.J., House, C.H., Orphan, V.J., 2009. Manganese-and iron-dependent marine methane oxidation. Science 325, 184-187.

Berry, D., Widder, S., 2014. Deciphering microbial interactions and detecting keystone species with co-occurrence networks. Frontiers in Microbiology 5, 219.

Blodau, C., Deppe, M., 2012. Humic acid addition lowers methane release in peats of the Mer Bleue bog, Canada. Soil Biology & Biochemistry 52, 96-98.

Bousquet, P., Ciais, P., Miller, J.B., Dlugokencky, E.J., Hauglustaine, D.A., Prigent, C., Van der Werf, G.R., Peylin, P., Brunke, E.G., Carouge, C., Langenfelds, R.L., Lathière, J., Papa, F., Ramonet, M., Schmidt, M., Steele, L.P., Tyler, S.C., White, J., 2006. Contribution of anthropogenic and natural sources to atmospheric methane variability. Nature 443, 439.

Cai, C., Leu, A.O., Xie, G., Guo, J., Feng, Y., Zhao, J., Tyson, G.W., Yuan, Z., Hu, S., 2018. A methanotrophic archaeon couples anaerobic oxidation of methane to Fe(III) reduction. The ISME journal 12, 1929-1939.

Callahan, B.J., McMurdie, P.J., Holmes, S.P., 2017. Exact sequence variants should replace operational taxonomic units in marker-gene data analysis. The ISME Journal 11, 2639-2643.

Conrad, R., 2009. The global methane cycle: recent advances in understanding the microbial processes involved. Environmental Microbiology Reports 1, 285-292.

Csardi, G., Nepusz, T., 2006. The igraph software package for complex network research. Inter Journal, complex systems 1695, 1-9.

Cui, M., Ma, A., Qi, H., Zhuang, X., Zhuang, G., 2015. Anaerobic oxidation of methane: an "active" microbial process. MicrobiologyOpen 4, 1-11.

Delgado-Baquerizo, M., Maestre, F.T., Reich, P.B., Jeffries, T.C., Gaitan, J.J., Encinar, D., Berdugo, M., Campbell, C.D., Singh, B.K., 2016. Microbial diversity drives multifunctionality in terrestrial ecosystems. Nature Communications 7, 10541.

Dippold, M.A., Kuzyakov, Y., 2016. Direct incorporation of fatty acids into microbial phospholipids in soils: Position-specific labeling tells the story. Geochimica et Cosmochimica Acta 174, 211-221.

Edwards, J., Johnson, C., Santos-Medellín, C., Lurie, E., Podishetty, N.K., Bhatnagar, S., Eisen, J.A., Sundaresan, V., 2015. Structure, variation, and assembly of the root-associated microbiomes of rice. Proceedings of the National Academy of Sciences 112, E911-E920.

Erdős, P., Rényi, A., 1960. On the evolution of random graphs. Publ. Math. Inst. Hung. Acad. Sci 5, 17-60.

Ettwig, K.F., Butler, M.K., Le Paslier, D., Pelletier, E., Mangenot, S., Kuypers, M.M.M., Schreiber, F., Dutilh, B.E., Zedelius, J., de Beer, D., Gloerich, J., Wessels, H.J.C.T., van Alen, T., Luesken, F., Wu, M.L., van de Pas-Schoonen, K.T., Op Den Camp, H.J.M., Janssen-Megens, E.M., Francoijs, K., Stunnenberg, H., Weissenbach, J., Jetten, M.S.M., Strous, M., 2010. Nitrite-driven anaerobic methane oxidation by oxygenic bacteria. Nature 464, 543-548.

Ettwig, K.F., Zhu, B., Speth, D., Keltjens, J.T., Jetten, M.S., Kartal, B., 2016. Archaea catalyze iron-dependent anaerobic oxidation of methane. Proceedings of the National Academy of Sciences 113, 12792-12796.

Fan, L., Dippold, M.A., Ge, T., Wu, J., Thiel, V., Kuzyakov, Y., Dorodnikov, M., 2020. Anaerobic oxidation of methane in paddy soil: Role of electron acceptors and fertilization in mitigating CH4 fluxes. Soil Biology & Biochemistry 141, 107685.

Fan, L., Shahbaz, M., Ge, T., Wu, J., Dippold, M., Thiel, V., Kuzyakov, Y., Dorodnikov, M., 2019a. To shake or not to shake: ^{13}C-based evidence on anaerobic methane oxidation in paddy soil. Soil Biology & Biochemistry 133, 146-154.

Fan, L., Shahbaz, M., Ge, T., Wu, J., Kuzyakov, Y., Dorodnikov, M., 2019b. To shake or not to shake: Silicone tube approach for incubation studies on CH4 oxidation in submerged soils. Science of The Total Environment 657, 893-901.

Frostegård, Å., Tunlid, A., Bååth, E., 1991. Microbial biomass measured as total lipid phosphate in soils of different organic content. Journal of Microbiological Methods 14, 151-163.

Gauthier, M., Bradley, R.L., Šimek, M., 2015. More evidence that anaerobic oxidation of methane is prevalent in soils: Is it time to upgrade our biogeochemical models? Soil Biology & Biochemistry 80, 167-174.

Geisseler, D., Scow, K.M., 2014. Long-term effects of mineral fertilizers on soil microorganisms–A review. Soil Biology & Biochemistry 75, 54-63.
Grossman, E.L., Cifuentes, L.A., Cozzarelli, I.M., 2002. Anaerobic methane oxidation in a landfill-leachate plume. Environmental Science & Technology 36, 2436-2442.
Gunina, A., Dippold, M.A., Glaser, B., Kuzyakov, Y., 2014. Fate of low molecular weight organic substances in an arable soil: From microbial uptake to utilisation and stabilisation. Soil Biology & Biochemistry 77, 304-313.
Gupta, V., Smemo, K.A., Yavitt, J.B., Fowle, D., Branfireun, B., Basiliko, N., 2013. Stable Isotopes Reveal Widespread Anaerobic Methane Oxidation Across Latitude and Peatland Type. Environmental Science & Technology, 265198755.
Haroon, M.F., Hu, S., Shi, Y., Imelfort, M., Keller, J., Hugenholtz, P., Yuan, Z., Tyson, G.W., 2013. Anaerobic oxidation of methane coupled to nitrate reduction in a novel archaeal lineage. Nature 500, 567-570.
Heitmann, T., Goldhammer, T., Beer, J., Blodau, C., 2007. Electron transfer of dissolved organic matter and its potential significance for anaerobic respiration in a northern bog. Global Change Biology 13, 1771-1785.
Hu, B.L., Shen, L.D., Lian, X., Zhu, Q., Liu, S., Huang, Q., He, Z.F., Geng, S., Cheng, D.Q., Lou, L.P., Xu, X.Y., Zheng, P., He, Y.F., 2014. Evidence for nitrite-dependent anaerobic methane oxidation as a previously overlooked microbial methane sink in wetlands. Proceedings of the National Academy of Sciences 111, 4495-4500.
Kappler, A., Benz, M., Schink, B., Brune, A., 2004. Electron shuttling via humic acids in microbial iron(III) reduction in a freshwater sediment. FEMS Microbiology Ecology 47, 85-92.
Keller, J.K., Weisenhorn, P.B., Megonigal, J.P., 2009. Humic acids as electron acceptors in wetland decomposition. Soil Biology & Biochemistry 41, 1518-1522.
Keppler, F., Hamilton, J.T., Braß, M., Röckmann, T., 2006. Methane emissions from terrestrial plants under aerobic conditions. Nature 439, 187.
Klindworth, A., Pruesse, E., Schweer, T., Peplies, J., Quast, C., Horn, M., Glöckner, F.O., 2013. Evaluation of general 16S ribosomal RNA gene PCR primers for classical and next-generation sequencing-based diversity studies. Nucleic Acids Research 41, e1.
Knittel, K., Boetius, A., 2009. Anaerobic Oxidation of Methane: Progress with an Unknown Process. Annual Review of Microbiology 63, 311-334.
Kool, D.M., Zhu, B., Rijpstra, W.I.C., Jetten, M.S.M., Ettwig, K.F., Sinninghe Damsté, J.S., 2012. Rare Branched Fatty Acids Characterize the Lipid Composition of the Intra-Aerobic Methane Oxidizer "Candidatus Methylomirabilis oxyfera". Applied and Environmental Microbiology 78, 8650-8656.
Louca, S., Parfrey, L.W., Doebeli, M., 2016. Decoupling function and taxonomy in the global ocean microbiome. Science 353, 1272-1277.
Lovley, D.R., Coates, J.D., Blunt-Harris, E.L., Phillips, E.J., Woodward, J.C., 1996. Humic substances as electron acceptors for microbial respiration. Nature 382, 445.
Lozupone, C., Lladser, M.E., Knights, D., Stombaugh, J., Knight, R., 2011. UniFrac: an effective distance metric for microbial community comparison. The ISME Journal 5, 169-172.
Lozupone, C.A., Knight, R., 2007. Global patterns in bacterial diversity. Proceedings of the National Academy of Sciences 104, 11436-11440.
Martens, C.S., Berner, R.A., 1974. Methane production in the interstitial waters of sulfate-depleted marine sediments. Science 185, 1167-1169.
McAnulty, M.J., G. Poosarla, V., Kim, K., Jasso-Chávez, R., Logan, B.E., Wood, T.K., 2017. Electricity from methane by reversing methanogenesis. Nature Communications 8.
McInerney, M.J., Sieber, J.R., Gunsalus, R.P., 2009. Syntrophy in anaerobic global carbon cycles. Current Opinion in Biotechnology 20, 623-632.
Megonigal, J.P., Hines, M.E., Visscher, P.T., 2004. Anaerobic metabolism: linkages to trace gases and aerobic processes. Biogeochemistry 8, 317-424.
Newman, M.E.J., 2006. Modularity and community structure in networks. Proceedings of the National Academy of Sciences 103, 8577-8582.
Parkin, T.B., 1993. Spatial variability of microbial processes in soil—a review. Journal of Environmental Quality 22, 409-417.
Raghoebarsing, A.A., Pol, A., van de Pas-Schoonen, K.T., Smolders, A.J.P., Ettwig, K.F., Rijpstra, W.I.C., Schouten, S., Damsté, J.S.S., Op Den Camp, H.J.M., Jetten, M.S.M., Strous, M., 2006. A microbial consortium couples anaerobic methane oxidation to denitrification. Nature 440, 918-921.
Reeburgh, W.S., 1976. Methane consumption in Cariaco Trench waters and sediments. Earth and Planetary Science Letters 28, 337-344.
Reeburgh, W.S., 2007. Oceanic Methane Biogeochemistry. Chemical Reviews 107, 486-513.
Ren, G., Ma, A., Zhang, Y., Deng, Y., Zheng, G., Zhuang, X., Zhuang, G., Fortin, D., 2018. Electron acceptors for anaerobic oxidation of methane drive microbial community structure and diversity in mud volcanoes. Environmental Microbiology 20, 2370-2385.

Roden, E.E., Kappler, A., Bauer, I., Jiang, J., Paul, A., Stoesser, R., Konishi, H., Xu, H., 2010. Extracellular electron transfer through microbial reduction of solid-phase humic substances. Nature Geoscience 3, 417.
Scheller, S., Yu, H., Chadwick, G.L., McGlynn, S.E., Orphan, V.J., 2016. Artificial electron acceptors decouple archaeal methane oxidation from sulfate reduction. Science 351, 703-707.
Schneider, D., Thürmer, A., Gollnow, K., Lugert, R., Gunka, K., Groß, U., Daniel, R., 2017. Gut bacterial communities of diarrheic patients with indications of Clostridioides difficile infection. Scientific Data 4, 170152.
Segarra, K.E.A., Schubotz, F., Samarkin, V., Yoshinaga, M.Y., Hinrichs, K., Joye, S.B., 2015. High rates of anaerobic methane oxidation in freshwater wetlands reduce potential atmospheric methane emissions. Nature Communications 6, 7477.
Serrano-Silva, N., Sarria-Guzmán, Y., Dendooven, L., & Luna-Guido, M. (2014). Methanogenesis and methanotrophy in soil: a review. Pedosphere, 24(3), 291-307.
Shen, L., Ouyang, L., Zhu, Y., Trimmer, M., 2019. Active pathways of anaerobic methane oxidation across contrasting riverbeds. The ISME Journal 13, 752-766.
Shen, L.D., Liu, S., Huang, Q., Lian, X., He, Z.F., Geng, S., Jin, R.C., He, Y.F., Lou, L.P., Xu, X.Y., Zheng, P., Hu, B.L., 2014. Evidence for the Cooccurrence of Nitrite-Dependent Anaerobic Ammonium and Methane Oxidation Processes in a Flooded Paddy Field. Applied and Environmental Microbiology 80, 7611-7619.
Smemo, K.A., Yavitt, J.B., 2011. Anaerobic oxidation of methane: an underappreciated aspect of methane cycling in peatland ecosystems? Biogeosciences 8, 779-793.
Torsvik, V., Øvreås, L., 2002. Microbial diversity and function in soil: from genes to ecosystems. Current Opinion in Microbiology 5, 240-245.
Vaksmaa, A., Guerrero-Cruz, S., van Alen, T.A., Cremers, G., Ettwig, K.F., Lüke, C., Jetten, M.S.M., 2017. Enrichment of anaerobic nitrate-dependent methanotrophic 'Candidatus Methanoperedens nitroreducens' archaea from an Italian paddy field soil. Applied Microbiology and Biotechnology 101, 7075-7084.
Vaksmaa, A., Lüke, C., van Alen, T., Valè, G., Lupotto, E., Jetten, M.S.M., Ettwig, K.F., 2016. Distribution and activity of the anaerobic methanotrophic community in a nitrogen-fertilized Italian paddy soil. FEMS Microbiology Ecology 92, w181.
Valentine, D.L., 2002. Biogeochemistry and microbial ecology of methane oxidation in anoxic environments: a review. Antonie van Leeuwenhoek 81, 271-282.
Valenzuela, E.I., Avendaño, K.A., Balagurusamy, N., Arriaga, S., Nieto-Delgado, C., Thalasso, F., Cervantes, F.J., 2019. Electron shuttling mediated by humic substances fuels anaerobic methane oxidation and carbon burial in wetland sediments. Science of The Total Environment 650, 2674-2684.
Voordeckers, J.W., Kim, B.C., Izallalen, M., Lovley, D.R., 2010. Role of Geobacter sulfurreducens Outer Surface c-Type Cytochromes in Reduction of Soil Humic Acid and Anthraquinone-2,6-Disulfonate. Applied Microbiology and Biotechnology 76, 2371-2375.
Ward, T., Larson, J., Meulemans, J., Hillmann, B., Lynch, J., Sidiropoulos, D., Spear, J., Caporaso, G., Blekhman, R., Knight, R., 2017. BugBase predicts organism level microbiome phenotypes. BioRxiv, 133462.
Weber, H.S., Habicht, K.S., Thamdrup, B., 2017. Anaerobic Methanotrophic Archaea of the ANME-2d Cluster Are Active in a Low-sulfate, Iron-rich Freshwater Sediment. Frontiers in Microbiology 8.
Weber, H.S., Thamdrup, B., Habicht, K.S., 2016. High Sulfur Isotope Fractionation Associated with Anaerobic Oxidation of Methane in a Low-Sulfate, Iron-Rich Environment. Frontiers in Earth Science 4.
Weiss, S., Van Treuren, W., Lozupone, C., Faust, K., Friedman, J., Deng, Y., Xia, L.C., Xu, Z.Z., Ursell, L., Alm, E.J., Birmingham, A., Cram, J.A., Fuhrman, J.A., Raes, J., Sun, F., Zhou, J., Knight, R., 2016. Correlation detection strategies in microbial data sets vary widely in sensitivity and precision. The ISME Journal 10, 1669-1681.
Wolfe, A.L., Wilkin, R.T., 2017. Evidence of Sulfate-Dependent Anaerobic Methane Oxidation within an Area Impacted by Coalbed Methane-Related Gas Migration. Environmental Science & Technology 51, 1901-1909.
Zelles, L., 1999. Fatty acid patterns of phospholipids and lipopolysaccharides in the characterisation of microbial communities in soil: a review. Biology and Fertility of Soils 29, 111-129.
Zhang, J., Zhang, N., Liu, Y., Zhang, X., Hu, B., Qin, Y., Xu, H., Wang, H., Guo, X., Qian, J., Wang, W., Zhang, P., Jin, T., Chu, C., Bai, Y., 2018. Root microbiota shift in rice correlates with resident time in the field and developmental stage. Science China Life Sciences 61, 613-621.

Supplementary Information for study 4

1. Extended material and methods

1.1. Experimental operation

To prepare the microcosms, 15 g field-moist soil was loaded into 100-ml Kimble KIMAX borosilicate laboratory glass jars with wide necks (GL 45, Kimble Chase Life Science and Research Products, LLC., Meiningen, Germany). The jars were sealed by gas-impermeable black butyl rubber septa and fixed by plastic screw caps with holes for convenient gas sampling. All jars and septa were autoclaved for 20 min twice at 121 ^{o}C before incubation. To reduce the remaining O_2 in the microcosms, the headspace was evacuated 8 times with a vacuum pump for 5 min and then back-flushed with high-purity N_2. Then the N_2-flushed microcosms were left overnight to allow for consumption of any remaining O_2. To exclude further contamination with atmospheric O_2, all manipulations with soils were conducted in a glovebox (N_2/H_2, 97/3%) under fully controlled anaerobic conditions. Inside the glovebox, the jars were opened and 20 ml sterile deionized water or chemical solutions (see above) were added to make the soil slurries. To ensure that anaerobic conditions prevailed in the microcosms throughout the experiment, oxygen indicators (Thermo Scientific, Oxoid Ltd., Basingstoke, Hampshire, UK) were placed inside the jars and the color was regularly recorded (pink – aerobic, white – anaerobic). After closing septa and cap, labeled CH_4 (5 ml 5 atom% $^{13}CH_4$) was injected into the headspace of the set of microcosms to quantify the anaerobic oxidation of $^{13}CH_4$ to $^{13}CO_2$ over time, resulting in an initial average headspace CH_4 concentration of 3.1%. Additionally, we set up a control using the same volume of N_2 instead of CH_4 to determine the methanogenesis potential and as a ^{13}C natural abundance control. The microcosms were moved out of the glovebox and incubated with continuous shaking (100 rounds min^{-1}) in the dark at 18 ℃ for 84 days. Oxygen indicators remained white during the course of incubation, demonstrating strict anaerobic conditions of microcosms. Very detailed information has been described in Fan et al., (2020).

2. Extended results and discussion

2.1. Effects of fertilization on microbial communities

The α-diversity remained similar in all fertilizations (Fig. S9A). PCoA demonstrated Biochar was separated from other fertilizations across the first principal coordinate (Fig. S9B). Biochar application had considerable depletion effect on ASVs as compared to NPK and pig manure fertilizers (117 vs. 58 and 21 ASVs, respectively; Fig. S10). In turn, fertilization treatments increased the relative abundance of Gram-negative bacteria as compared to the control (Fig. S11). LEfSe analysis revealed that 45 16S rRNA gene biomarkers affiliating with 7 phyla were sensitive to fertilization treatments (p<0.05, LDA>2.0, Fig. S12, Table S9). For instance, the genus *Geobacter* and *Anaerobacter* were more changeable to biochar and pig manure fertilization, respectively, while the family of *Syntrophaceae* (the syntrophic bacteria with methanogens) was significantly enriched under NPK. The impact on fertilization on the predicted metabolic functions is shown in Fig. S4. Pig manure fertilization showed little effect whereas biochar application stimulated iron respiration, nitrate respiration, and nitrate reduction. NPK particularly enhanced iron respiration relative to Control (Fig. S5). *Proteobacteria*, *Acidobacteria*, and *Chloroflexi* were the most important phyla that contributed to the networks (Fig. S7B). Compared to the control, biochar and NPK fertilization increased the relative abundance of *Geobacter* in the co-occurrence networks (p<0.05, Fig. S7C). Biochar application also increased the relative abundance of NC10, whereas pig manure, biochar and NPK increased the relative abundance of SRB and SBM (p<0.05, Fig. S7C).

Fertilizers applied during paddy management – especially biochar application – caused a significant source of variation in bacterial communities, which was much higher than a mere rising of the CH_4 concentration (Table S7). Soil microbiome formed more tightened microbial interactions under pig manure and NPK than in response to biochar application (Fig. S7). Because biochar has a strong sorption capacity for AEA due to its porous structure and very large surface area, it may decrease the AEA availability in contrast to pig manure and NPK, thus affects the microbial community

composition, e.g., (i) the abundance of NC10 and *Geobacter* was increased under biochar application, (ii) the genus *Geobacter*, *Anaerobacter* and *Dechloromonas* were more sensitive (changeable) to biochar application relative to other fertilizations by LEfSe analysis (p<0.05, LDA>2.0, Table S10).

2.2. Effects of electron acceptors on microbial co-occurrence networks

The α-diversity of species was highest under NO_3^- and humic acids amendments, and lowest under SO_4^{2-} (Fig. S13A). In the PCoA, SO_4^{2-} and humic acids were separated across the first principal coordinate, whereas Fe^{3+} and NO_3^- largely overlapped with the reference (Fig. S13B). Similar patterns of SO_4^{2-} separation from other AEAs were evident when each fertilization treatment was analyzed separately (Fig. S14). Furthermore, SO_4^{2-} exhibited higher enrichment and depletion effects on specific ASVs (363 vs. 209) than Fe^{3+}, NO_3^-, and humic acids (20 vs. 63, 49 vs. 36, and 91 vs. 52, respectively, Fig. S15). Similar effects of AEAs were evident when each fertilizer was analyzed separately (Fig. S16). Also, SO_4^{2-} raised the relative abundance of anaerobic bacteria (Fig. S11). LEfSe analysis revealed that 137 biomarkers affiliating with 18 phyla were sensitive to AEA amendments under different fertilizations (p<0.05, LDA>2.0, Fig. S17, Table S10). For instance, NC10 was enriched under NO_3^- and humic acids amendments (Table S10). On the functional level, the potential for iron respiration increased by 1.6 times after Fe^{3+} amendment, as expected, but it was also enhanced with humic acids addition. NO_3^- did not affect the predicted functions. SO_4^{2-} amendment increased the predicted function of sulfate respiration, sulfite respiration, respiration of sulfur compounds, fermentation, and iron respiration, but decreased nitrification (Fig. S5). *Proteobacteria*, *Chloroflexi*, *Nitrospirae*, and *Bacteroidetes* were the most important phyla that contributed to the networks (Fig. S8B). Compared to the reference, SO_4^{2-} addition increased the relative abundance of *Geobacter*, NC10, SRB and SBM, and humic acids addition increased the relative abundance of SBM (Fig. S8C).

AEA amendments always outcompeted fertilization as a source of variation in the microbiome (Table S8), and considerably changed the diversity and structure of microbial communities. The more tightened microbial associations were formed in response to the amendments of NO_3^- and SO_4^{2-}, as compared to Fe^{3+} and humic acids (Fig. S8). This suggests that AEAs play a strong role in reshaping the anaerobic microorganisms' interactions such as (i) SO_4^{2-} enhanced SRB and *Geobacter* thus accelerating anaerobic organic matter decomposition inducing highest CO_2 production (in main context Fig. 3, Fig. 5), (ii) Fe^{3+} and SO_4^{2-} amendments induced higher $^{13}CH_4$-derived C incorporation into bacterial PLFA (in main context Fig. 2G), and (iii) humic acids fueled methanogens to produce 7.6 times higher CH_4 as compared to the reference (Fig. S6). Summarizing, multiple AOM pathways are expected in fertilized paddy soils depending on AEA availability shaping specific microbial groups.

Supplementary Figures

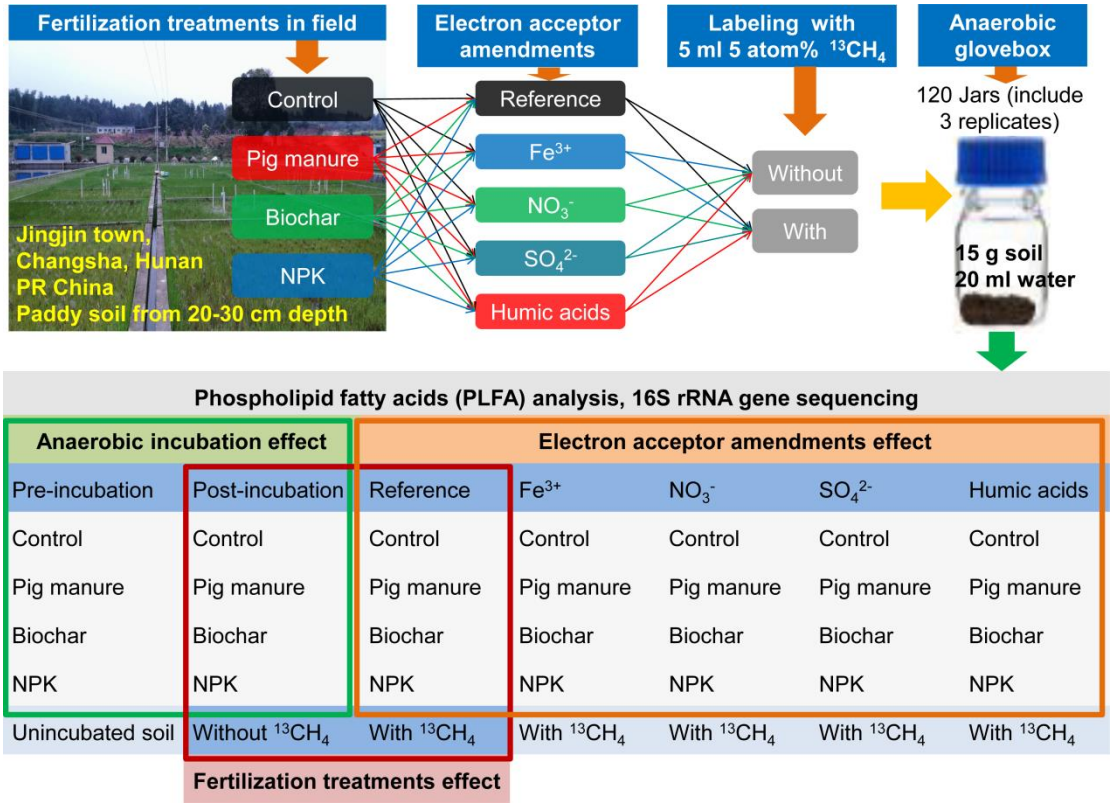

Fig. S1 Schematic diagram of the experimental design and the selected samples for downstream 16S rRNA gene sequencing. Each had three field replicates.

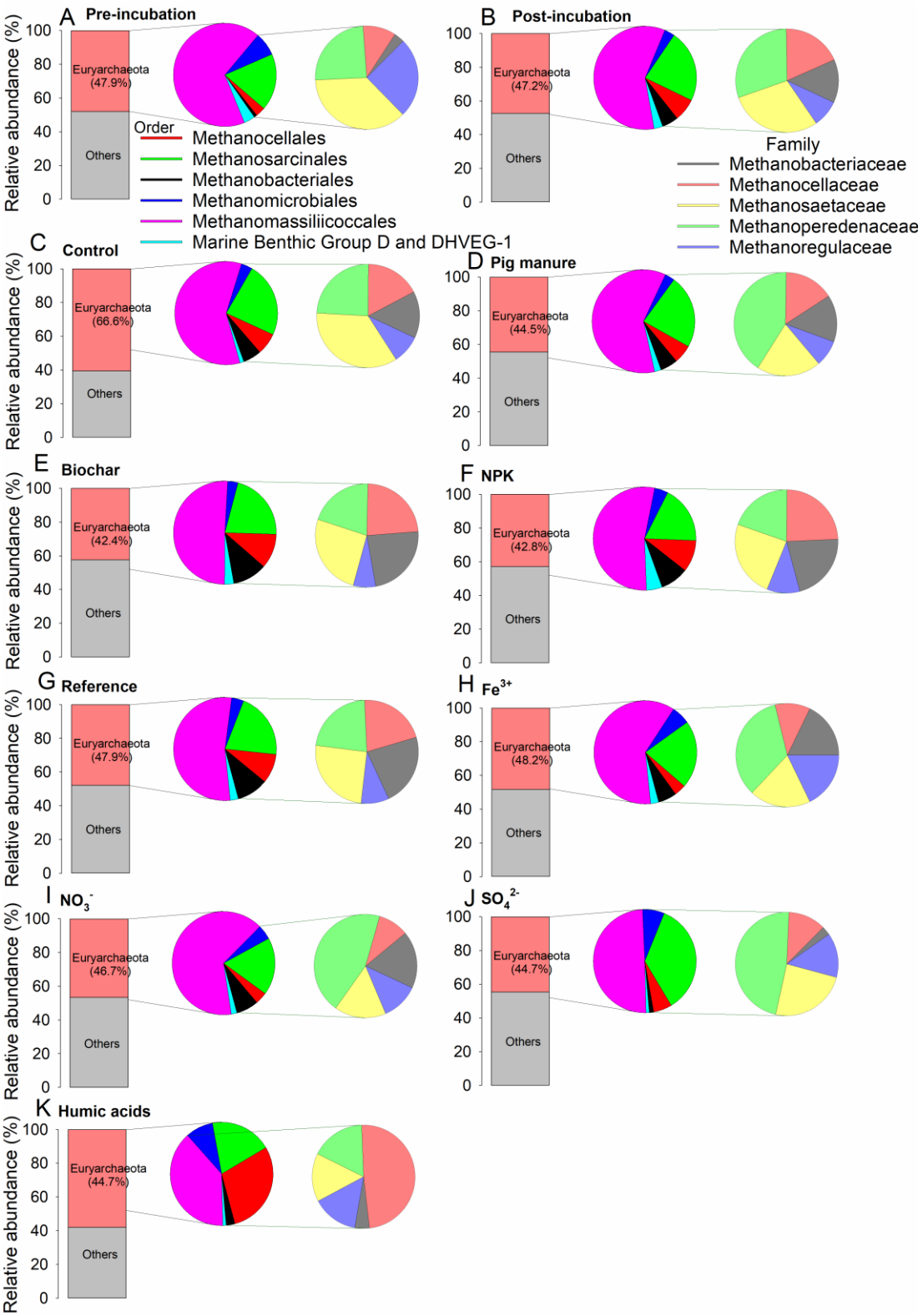

Fig. S2 Relative abundance of archaea co-amplified with bacteria. (A) Pre-incubation, (B) post-incubation, (C-F) fertilization, and (G-K) alternative electron acceptor amendments.

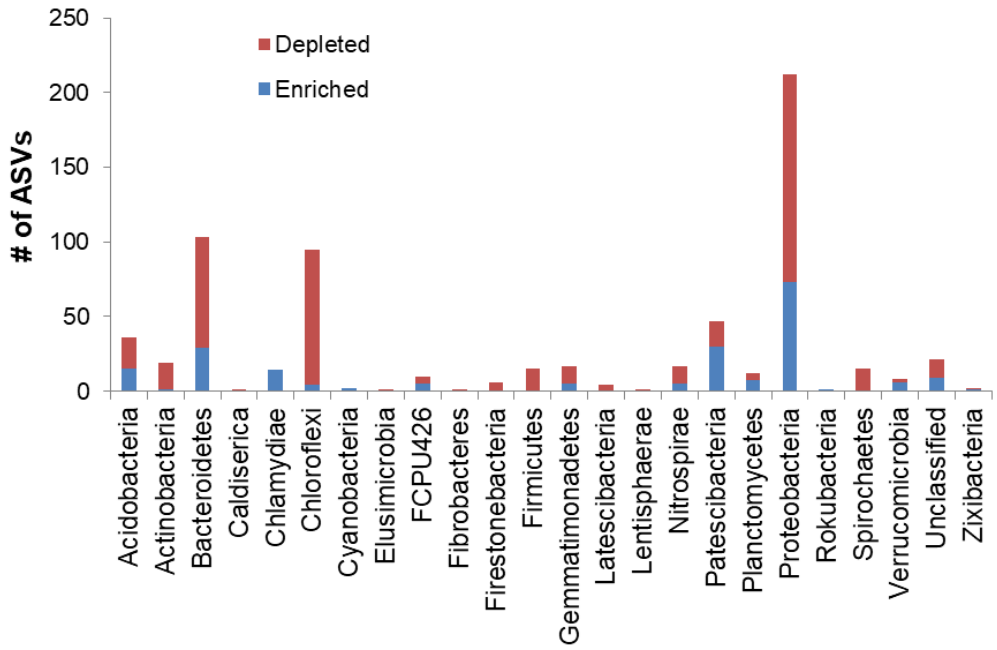

Fig. S3 Number of depleted and enriched ASV (Amplicon Sequence Variants) in post-incubation soil compared to pre-incubation.

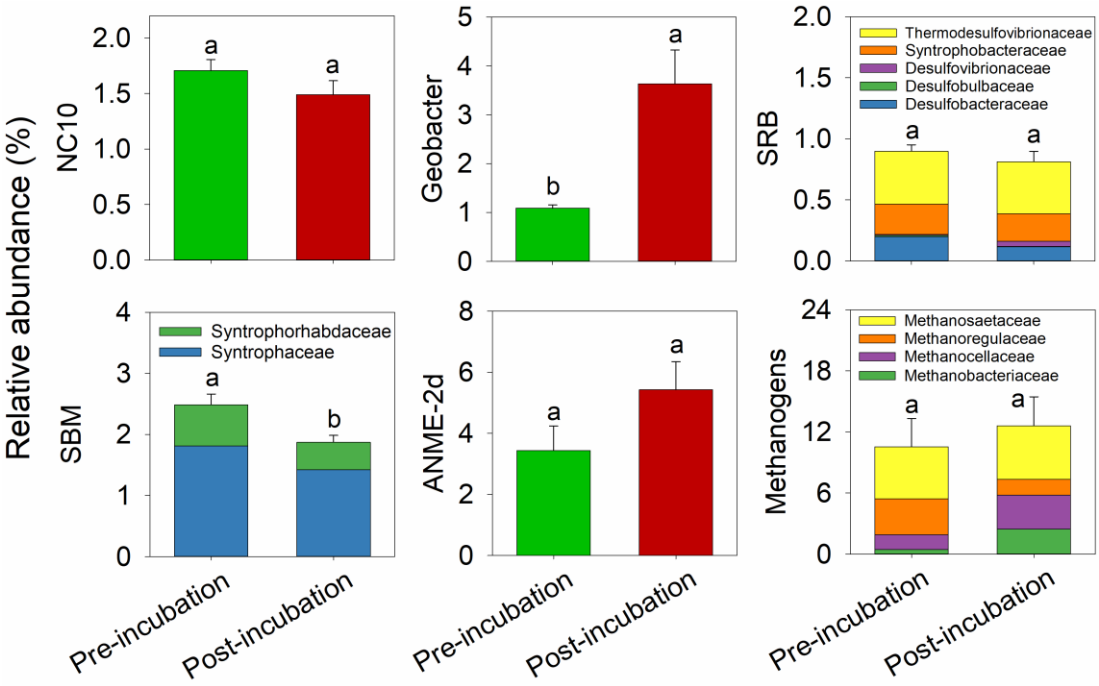

Fig. S4 Relative abundance of AOM-related microbial groups in pre- and post-anaerobic incubation. i.e. NC10, *Geobacter*, SRB (sulfate reducing bacteria), SBM (strophic bacteria with methanogens), methanogens, and ANME-2d. Lowercase letters represent significance at $p < 0.05$.

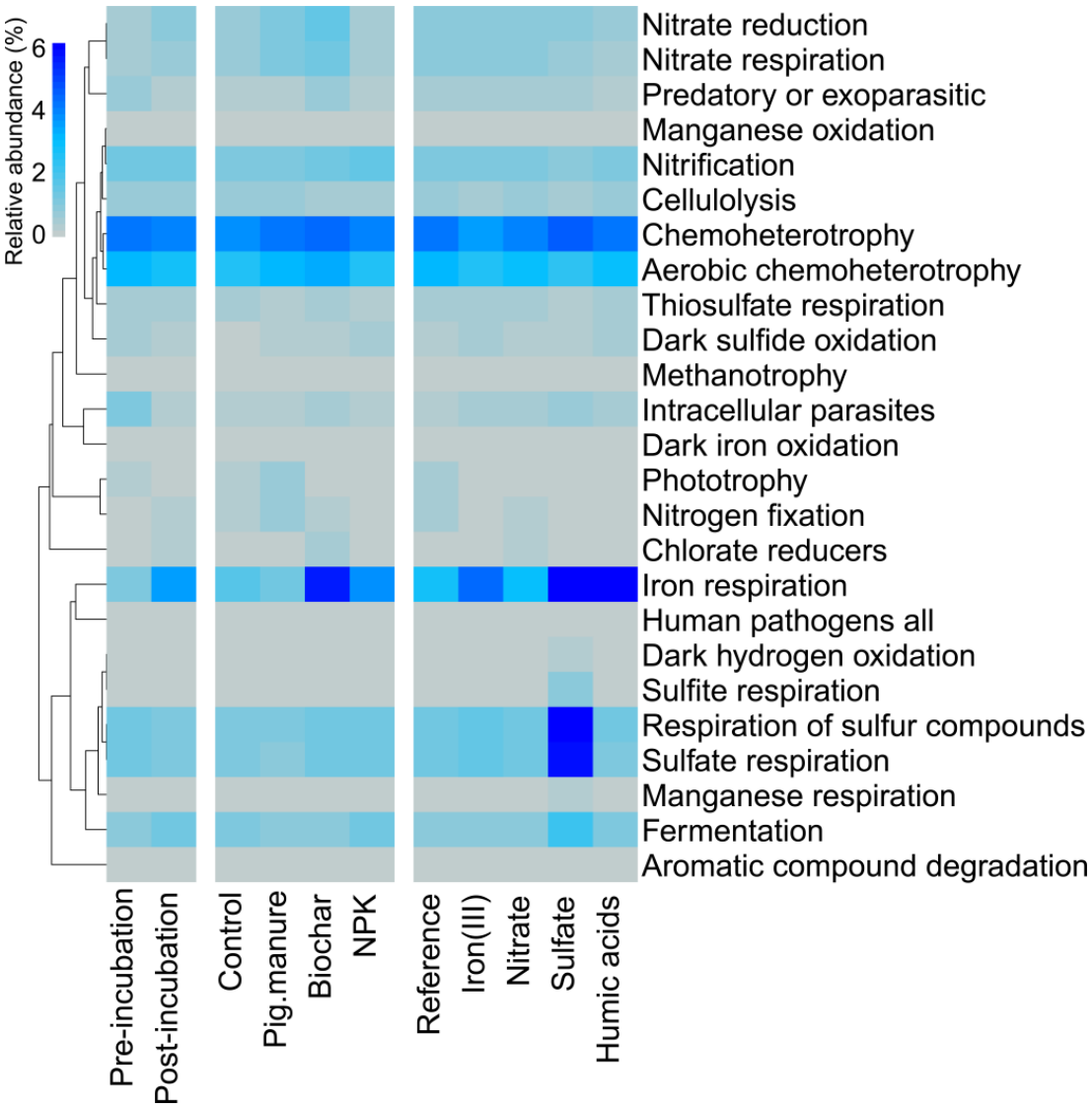

Fig. S5 Predicted functions of the bacterial communities based on FAPROTAX database.

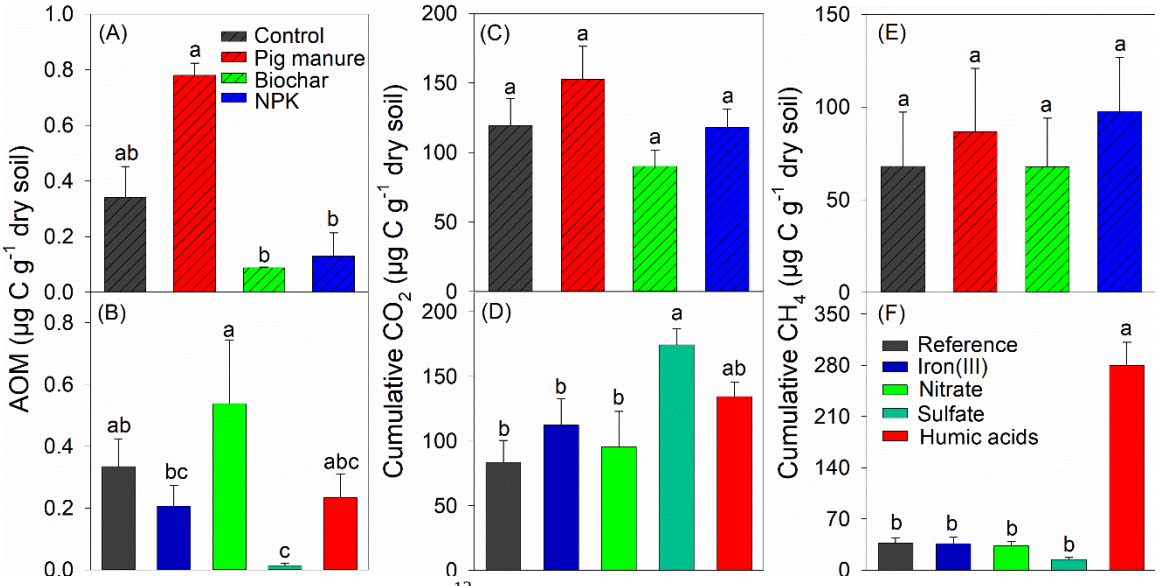

Fig. S6 The amounts of CH_4-derived ^{13}C in CO_2 (AOM) (A and B), cumulative CO_2 (C, D) and CH_4 production (E and F) in different fertilization treatments and electron acceptor amendments. Lowercase letters and asterisks (*) represent significant difference at $p<0.05$. This Figure is summarized from Fan et al. (2020).

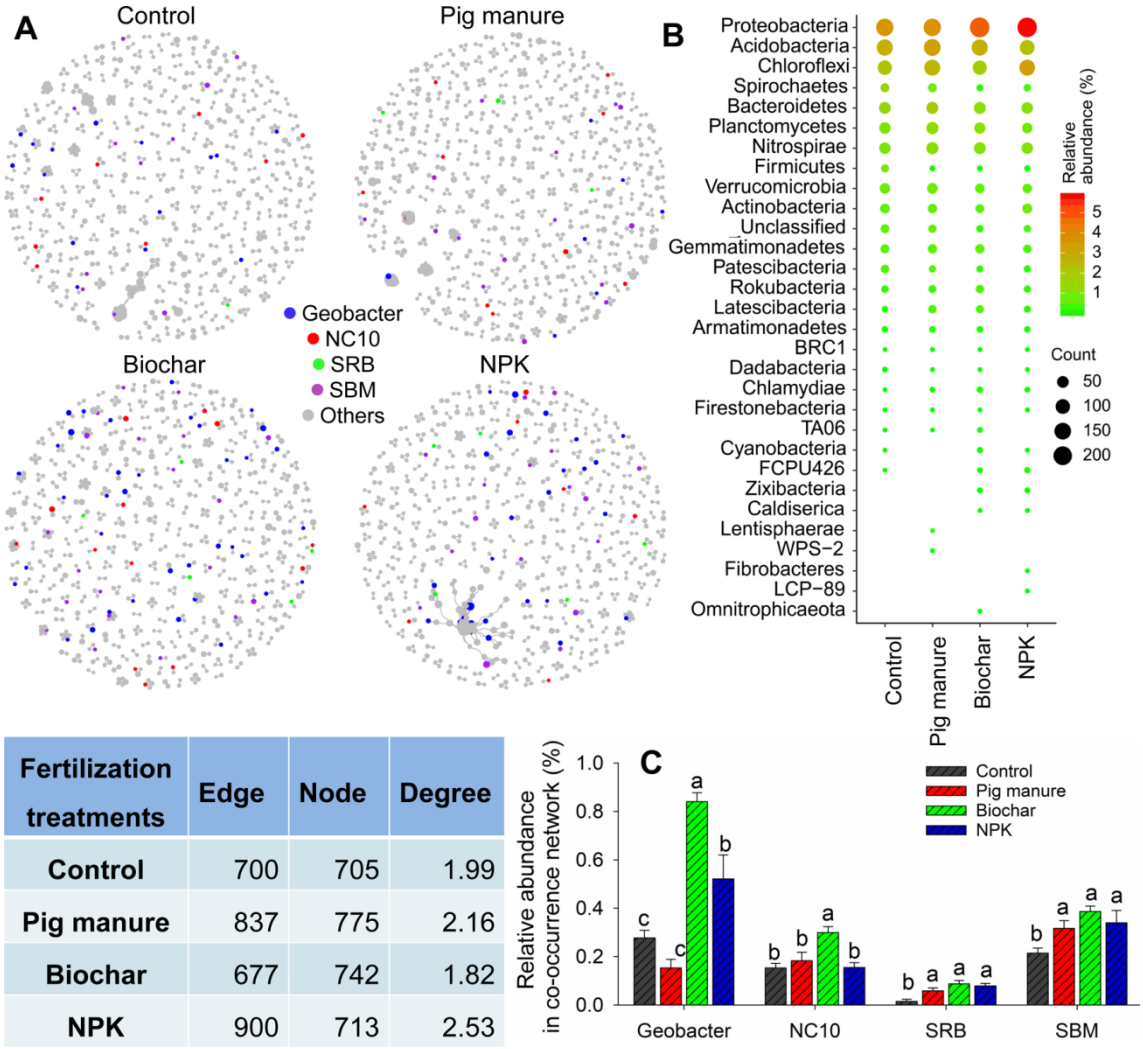

Fertilization treatments	Edge	Node	Degree
Control	700	705	1.99
Pig manure	837	775	2.16
Biochar	677	742	1.82
NPK	900	713	2.53

Fig. S7 The bacterial co-occurrence networks based on ASVs (Amplicon Sequence Variants) correlation analysis under different fertilization treatments (A). The ASV with relative abundance above 0.015% was selected. A connection stands for a strong (Pearson's r > 0.6) and significant (p<0.01) correlation. The size of each node is proportional to the relative abundance. (B) The relative abundances and amounts of nodes contributed into co-occurrence networks grouped by phyla. (C) The relative abundances and amounts of nodes of co-occurrence networks grouped by phyla. *Geobacter*, NC10, SRB (sulfate reducing bacteria), and SBM (syntrophic bacteria with methanogens) in the co-occurrence networks considered as AOM-related microorganisms in each fertilization treatment. Lowercase letters: significant difference at p<0.05 for each microbial group.

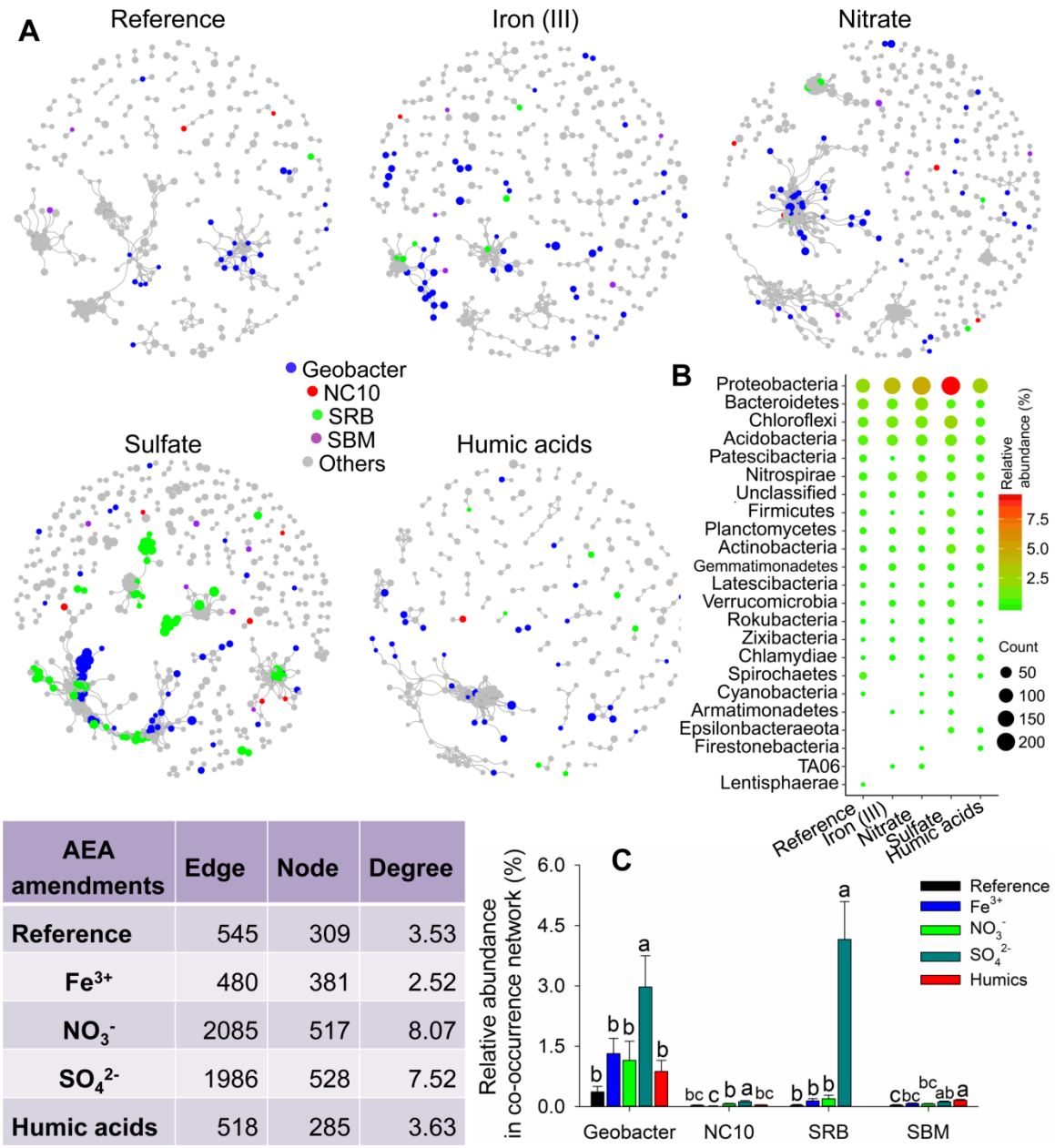

AEA amendments	Edge	Node	Degree
Reference	545	309	3.53
Fe^{3+}	480	381	2.52
NO_3^-	2085	517	8.07
SO_4^{2-}	1986	528	7.52
Humic acids	518	285	3.63

Fig. S8 The bacterial co-occurrence networks based on ASV (Amplicon Sequence Variants) correlation analysis under different electron acceptor amendments (A). The ASV with relative abundance above 0.01% was selected. A connection stands for a strong (Pearson's r>0.6) and significant (p<0.01) correlation. The size of each node is proportional to the relative abundance. (B) The relative abundances and amounts of nodes contributed into co-occurrence networks grouped by phyla. (C) Relative abundances of *Geobacter*, NC10, SRB (sulfate reducing bacteria), and SBM (syntrophic bacteria with methanogens) shown in the co-occurrence networks in each electron acceptor amendment. Lowercase letters: significant difference at p<0.05 for each microbial group.

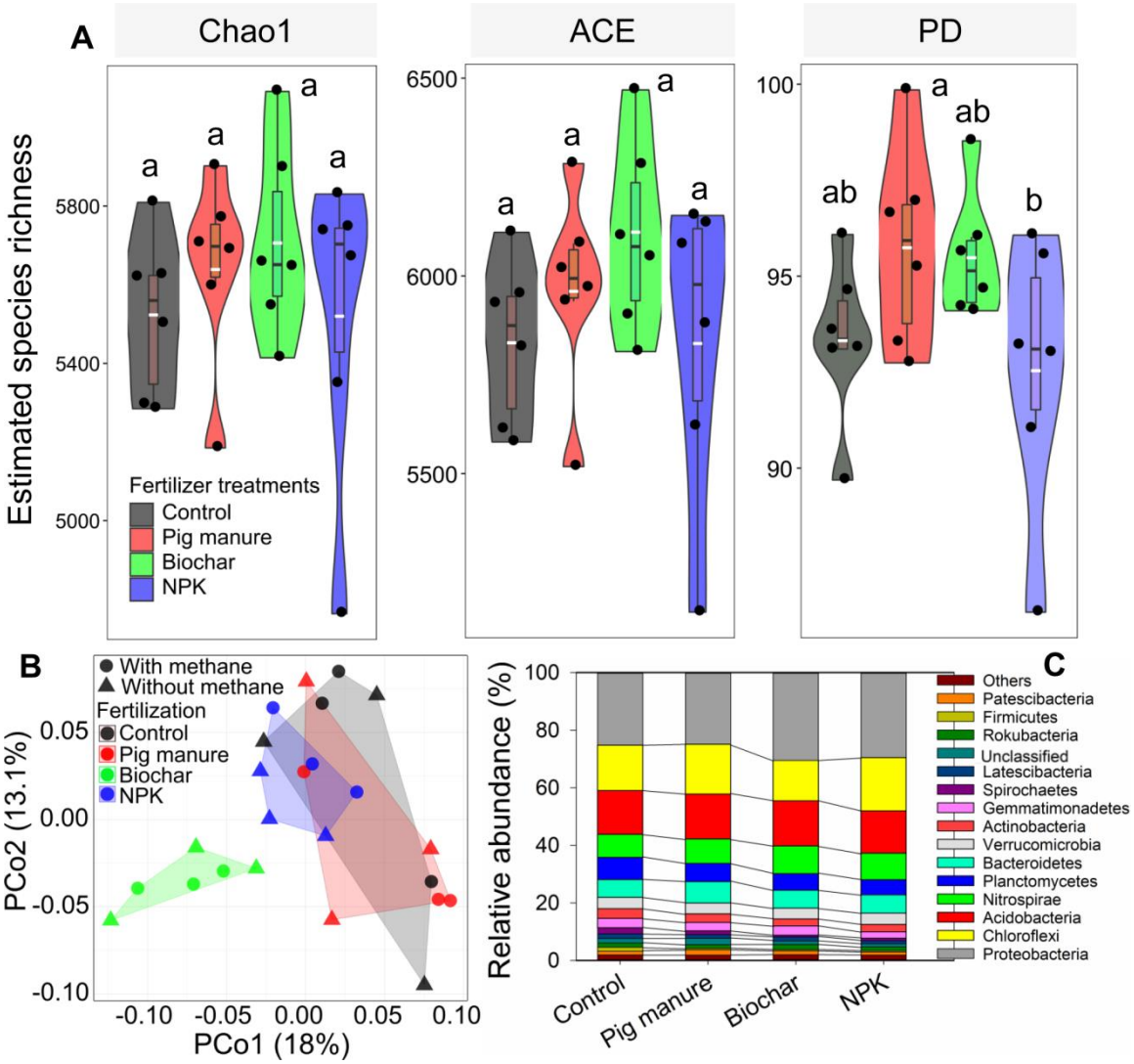

Fig. S9 Bacterial communities in paddy soils under different fertilization treatments. (A) Alpha diversity (α-diversity) was calculated as Chao1, Abund-based Coverage Estimator metric (ACE), and Faith's Phylogenetic Diversity (PD). The horizontal black lines within boxes represent the median, and the white lines represent the mean. The tops and bottoms of boxes represent the 75th and 25th quartiles, respectively. The upper and lower whiskers represent a 95% confidence interval. Lowercase letters represent significance at p<0.05. (B) Principal Coordinates Analysis (PCoA) using the unweighted Unifrac distance metric. (C) Relative abundance of the top 15 phyla.

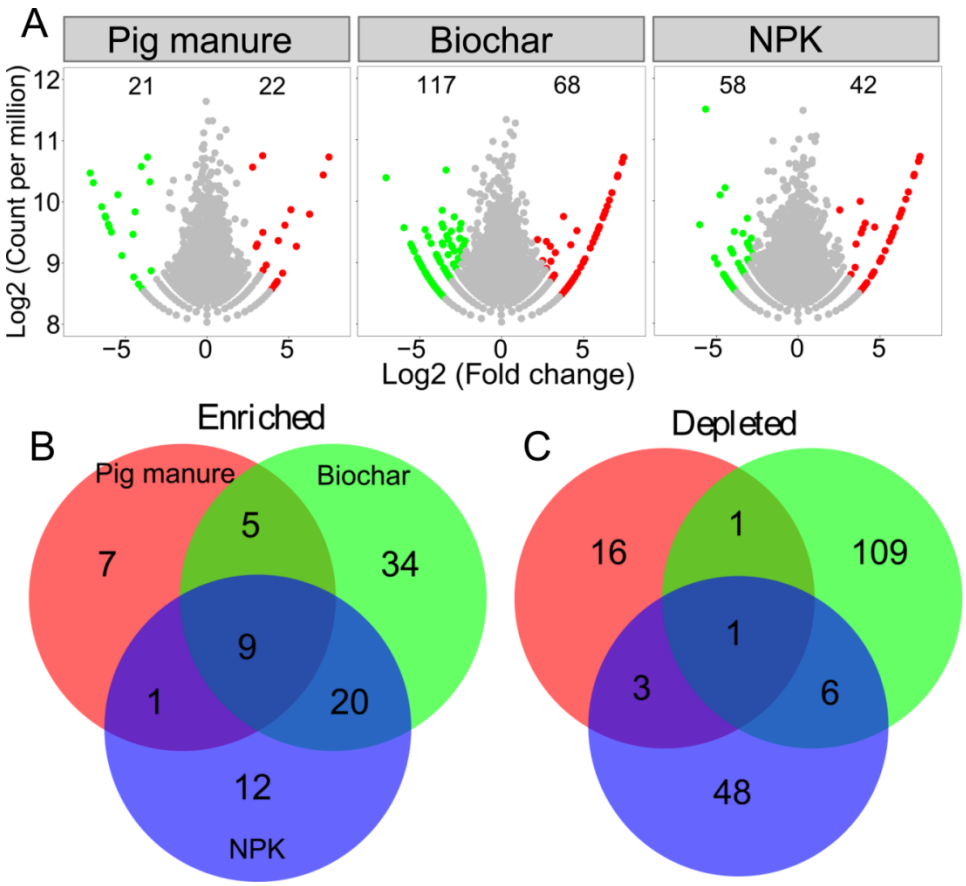

Fig. S10 Enrichment and depletion of ASV (Amplicon Sequence Variants) under different fertilization in paddy soils. (A) Enrichment and depletion in each fertilization treatment as compared with the control. Each point represents an individual ASV, and the position along the x axis represents the abundance fold change compared with the control. (B) Numbers of differentially enriched ASV between each fertilization as compared with the control. (C) Numbers of differentially depleted ASV between each fertilization as compared with the control.

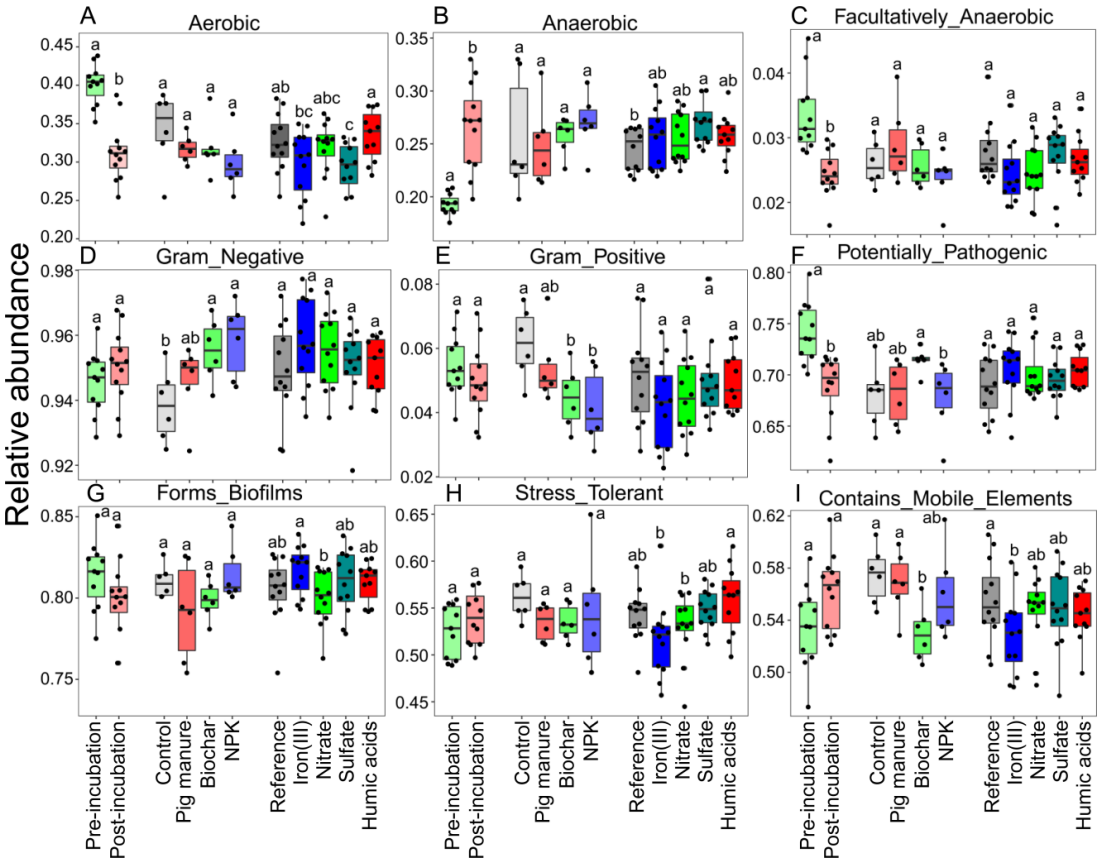

Fig. S11 Functional community profiles based on BugBase prediction. Lowercase letters: significant difference at $p<0.05$ under anaerobic incubation, fertilization treatments, and electron acceptor amendments.

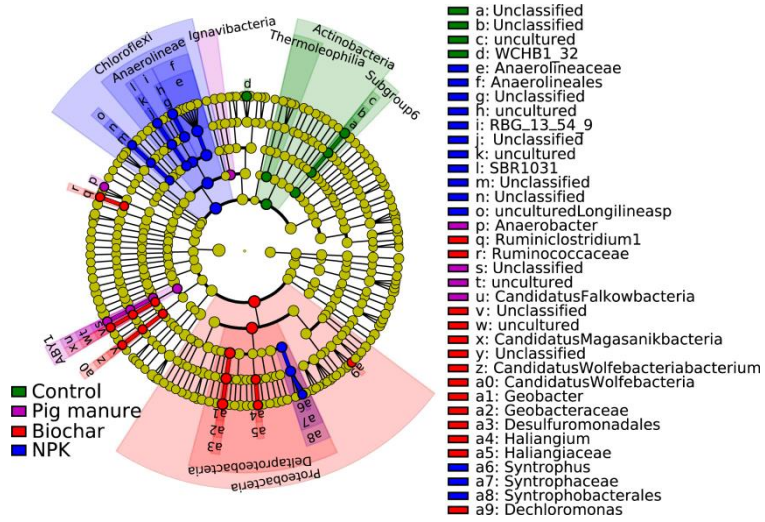

Fig. S12 Linear discriminant analysis effect size (LEfSe) results revealed bacterial biomarkers (from phylum to genus level) sensitive to fertilization treatments (Control, Pig manure, Biochar, NPK). LEfSe was performed to investigate biomarkers (across five taxonomic levels, from phylum to genus) within soil bacterial communities specifically enriched in each fertilization treatment and AEA amendment, based on $p<0.05$ and an LDA score >2.0. There are five circular rings in the cladogram; each circular ring deposits all taxa within a taxonomic level, the circular ring from inside to outside represents phylum, class, order, family, and genus, respectively. Each node on a circular ring represents a taxon affiliating within the respective taxonomic level. Taxa having a significantly higher relative abundance in a certain treatment within each soil type were color-coded within the cladogram according to the SILVA 138 taxonomy.

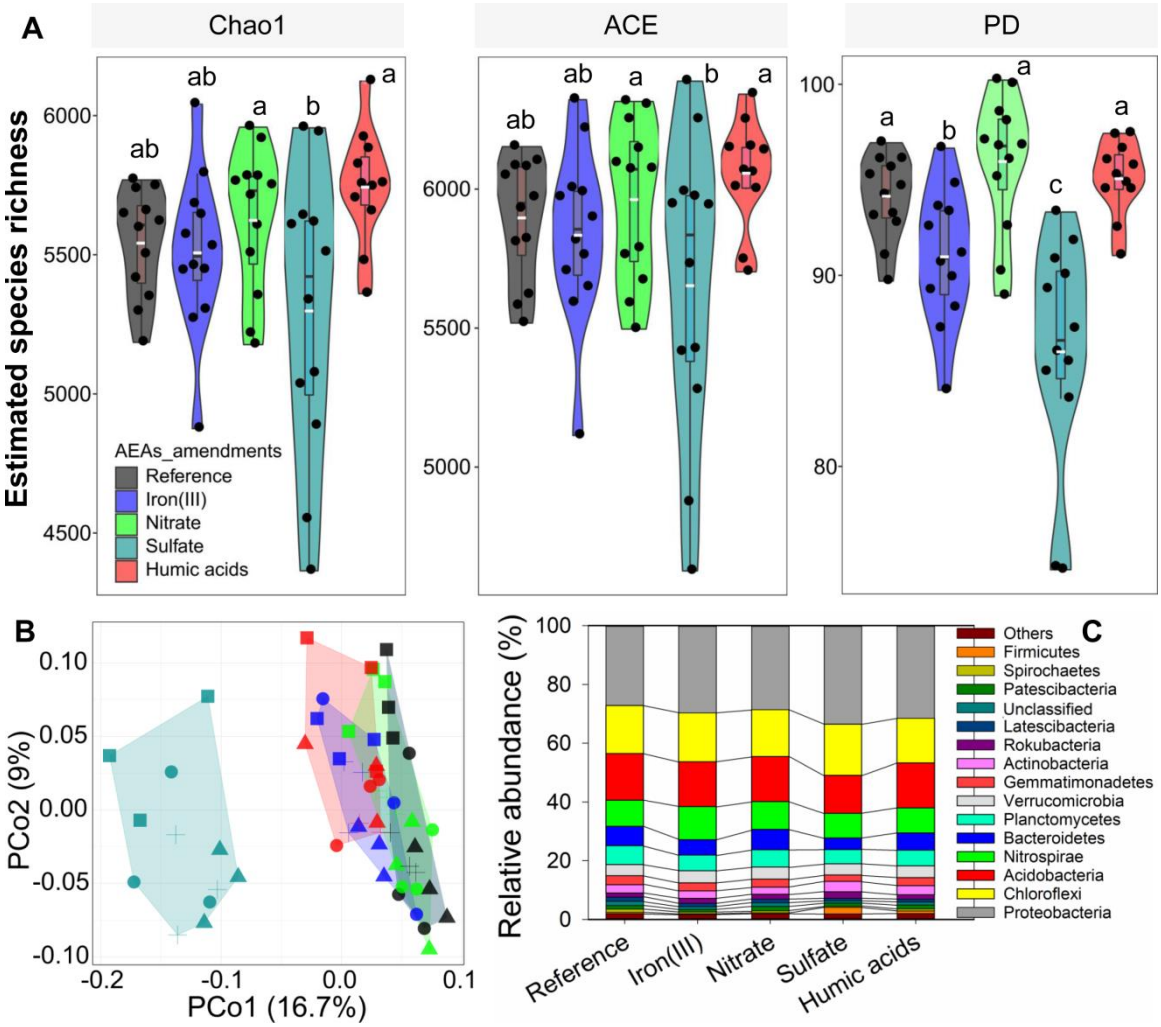

Fig. S13 Bacterial communities in paddy soils with different electron acceptor amendments. (A) Alpha diversity (α-diversity), i.e. estimated species richness, was calculated as Faith's Phylogenetic Diversity. The horizontal lines within boxes represent the median. The tops and bottoms of boxes represent the 75th and 25th quartiles, respectively. The upper and lower whiskers represent a 95% confidence interval. Lowercase letters represent significance at p<0.05. (B) Principal Coordinates Analysis (PCoA) using the unweighted Unifrac distance metric. Circle: the control; up triangle: pig manure; square: biochar; cross lines: NPK. (C) Relative abundance of top the 15 phyla.

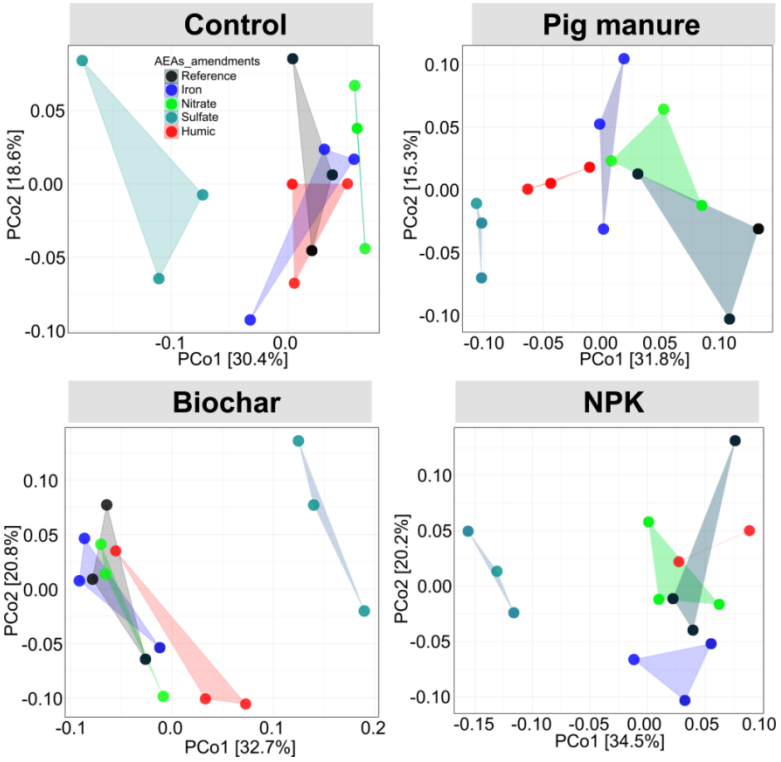

Fig. S14 Principal Coordinates Analysis (PCoA) of electron acceptor amendments under each fertilization treatment by using the unweighted Unifrac distance metric.

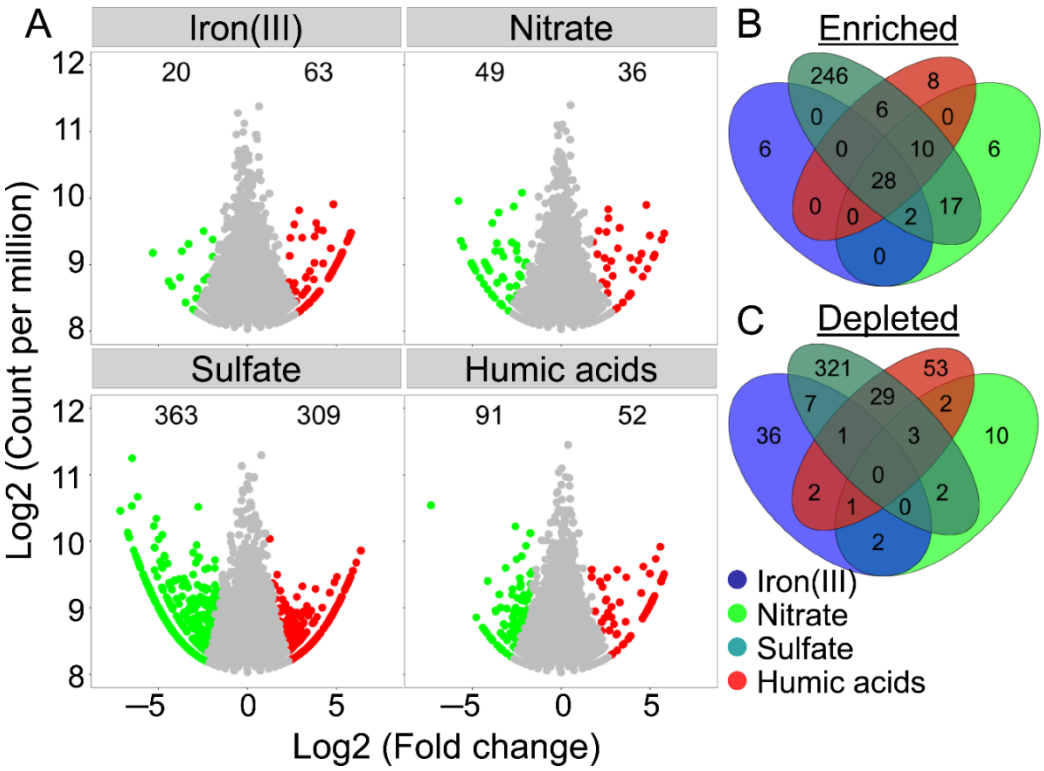

Fig. S15 Different electron acceptor amendments have enriched and depleted ASV (Amplicon Sequence Variants). (A) Enrichment and depletion in each electron acceptor amendment as compared with the reference. Each point represents an individual ASV, and the position along the x axis represents the abundance fold change compared with reference. (B) Numbers of differentially enriched ASV between each electron acceptor amendment as compared with the reference. (C) Numbers of differentially depleted ASV between each electron acceptors amendments.

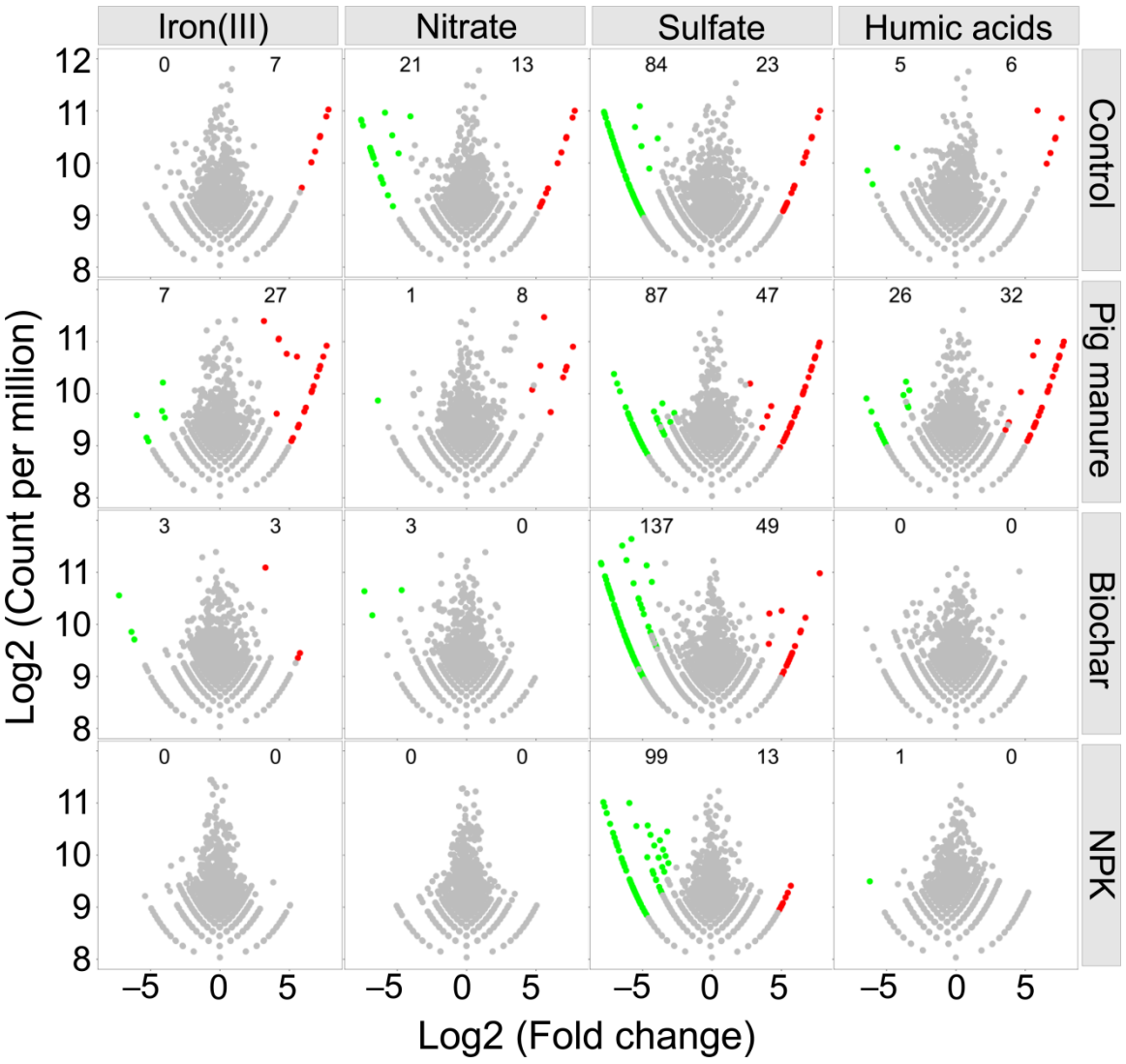

Fig. S16 Different fertilized paddy soils nested with different electron acceptor amendments are enriched and depleted for certain ASV (Amplicon Sequence Variants). Enrichment and depletion in each fertilization treatments were as compared with the reference. Each point represents an individual ASV, and the position along the *x* axis represents the abundance fold change compared with the control.

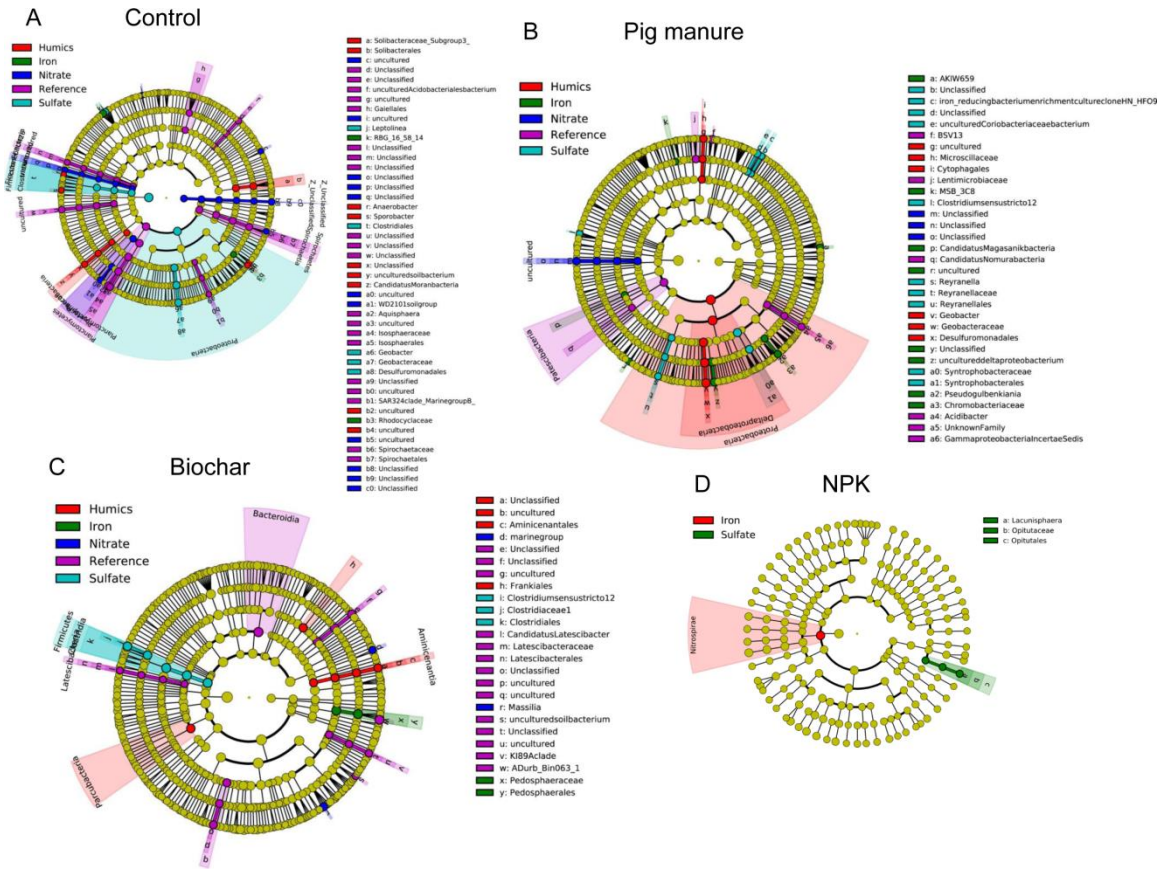

Fig. S17 LEfSe results revealed bacterial biomarkers (from phylum to genus level) sensitive to electron acceptors amendments under each fertilization treatment. There are five circular rings in the cladogram, each circular ring deposit all taxa within a taxonomic level, the circular ring from inside to outside represents phylum, class, order, family, and genus, respectively. The node on the circular ring represents a taxon, affiliating within the taxonomic level. Taxa that had significantly higher relative abundance in a certain treatment within each soil type were color-coded within the cladogram according to the SILVA 138 taxonomy.

Supplementary tables

Table S1 Grouping of the PLFA to microbial groups: four groups were distinguished through factor analysis and relevant factor loadings

Fatty acids	Factor 1	Factor 2	Factor 3	Factor 4	Microbial group
10Me16:0	**0.91**	0.223	0.137	0.137	**Actinobacteria**
10Me18:0	**0.874**	0.142	0.22	-0.046	**Actinobacteria**
18:2ω6,9	0.181	0.064	0.198	**0.868**	**Fungi**
16:1ω5c	**0.733**	0.544	-0.095	0.009	**Gram-negative**
16:1ω7c	**0.776**	0.556	-0.003	0.101	**Gram-negative**
18:1ω7c	**0.887**	0.181	0.211	0.168	**Gram-negative**
18:1ω9c	**0.592**	0.107	0.429	0.355	**Gram-negative**
a15:0	**0.746**	0.576	0.04	0.23	**Gram-negative**
cy19:0	**0.242**	0.019	0.873	0.124	**Gram-negative**
i15:0	**0.763**	0.525	0.086	0.237	**Gram-negative**
i16:0	**0.865**	0.328	0.125	0.111	**Gram-negative**
a16:0	0.009	**0.674**	0.432	0.211	**Gram-positive**
a17:0	0.404	**0.868**	0.106	-0.012	**Gram-positive**
cy17:0	0.397	**0.876**	-0.025	-0.109	**Gram-positive**
i14:0	0.13	**0.681**	-0.165	0.414	**Gram-positive**
i17:0	0.412	**0.858**	0.093	0.019	**Gram-positive**

Table S2 Observed bacterial ASVs under different fertilization treatments and AEA amendments

Treatments		Sequence reads	Observed ASVs
Field fertilization treatments	**AEA amendments**		
Control	Without $^{13}CH_4$	7633	3695
Control	Without $^{13}CH_4$	7633	3251
Control	Without $^{13}CH_4$	7633	3635
Pig manure	Without $^{13}CH_4$	7633	3748
Pig manure	Without $^{13}CH_4$	7633	3651
Pig manure	Without $^{13}CH_4$	7633	3693
Control	$^{13}CH_4$	7633	3609
Control	$^{13}CH_4$	7633	3306
Control	$^{13}CH_4$	7633	3624
Pig manure	$^{13}CH_4$	7633	3766
Pig manure	$^{13}CH_4$	7633	3587
Pig manure	$^{13}CH_4$	7633	3318
Control	$^{13}CH_4 + Fe^{3+}$	7633	3536
Control	$^{13}CH_4 + Fe^{3+}$	7633	3411
Control	$^{13}CH_4 + Fe^{3+}$	7633	3694
Pig manure	$^{13}CH_4 + Fe^{3+}$	7633	3641
Pig manure	$^{13}CH_4 + Fe^{3+}$	7633	3698
Pig manure	$^{13}CH_4 + Fe^{3+}$	7633	3571
Control	$^{13}CH_4 + NO_3^-$	7633	3746
Control	$^{13}CH_4 + NO_3^-$	7633	3355
Control	$^{13}CH_4 + NO_3^-$	7633	3701
Pig manure	$^{13}CH_4 + NO_3^-$	7633	3718
Pig manure	$^{13}CH_4 + NO_3^-$	7633	3829
Pig manure	$^{13}CH_4 + NO_3^-$	7633	3628
Biochar	Without $^{13}CH_4$	7633	3831
Biochar	Without $^{13}CH_4$	7633	3707
Biochar	Without $^{13}CH_4$	7633	3670
NPK	Without $^{13}CH_4$	7633	3673
NPK	Without $^{13}CH_4$	7633	3816
NPK	Without $^{13}CH_4$	7633	2785
Biochar	$^{13}CH_4$	7633	3653
Biochar	$^{13}CH_4$	7633	3591
Biochar	$^{13}CH_4$	7633	3760
NPK	$^{13}CH_4$	7633	3745
NPK	$^{13}CH_4$	7633	3579
NPK	$^{13}CH_4$	7633	3726
Biochar	$^{13}CH_4 + Fe^{3+}$	7633	3472
Biochar	$^{13}CH_4 + Fe^{3+}$	7633	3805
Biochar	$^{13}CH_4 + Fe^{3+}$	7633	3482
NPK	$^{13}CH_4 + Fe^{3+}$	7633	3555
NPK	$^{13}CH_4 + Fe^{3+}$	7633	3298
NPK	$^{13}CH_4 + Fe^{3+}$	7633	3803
Biochar	$^{13}CH_4 + NO_3^-$	7633	3220
Biochar	$^{13}CH_4 + NO_3^-$	7633	3671
Biochar	$^{13}CH_4 + NO_3^-$	7633	3639

NPK	$^{13}CH_4 + NO_3^-$	7633	3770
NPK	$^{13}CH_4 + NO_3^-$	7633	3468
NPK	$^{13}CH_4 + NO_3^-$	7633	3689
Control	$^{13}CH_4 + SO_4^{2-}$	7633	3445
Control	$^{13}CH_4 + SO_4^{2-}$	7633	3084
Control	$^{13}CH_4 + SO_4^{2-}$	7633	2839
Pig manure	$^{13}CH_4 + SO_4^{2-}$	7633	3627
Pig manure	$^{13}CH_4 + SO_4^{2-}$	7633	3761
Pig manure	$^{13}CH_4 + SO_4^{2-}$	7633	3762
Biochar	$^{13}CH_4 + SO_4^{2-}$	7633	2485
Biochar	$^{13}CH_4 + SO_4^{2-}$	7633	3200
Biochar	$^{13}CH_4 + SO_4^{2-}$	7633	3314
NPK	$^{13}CH_4 + SO_4^{2-}$	7633	3367
NPK	$^{13}CH_4 + SO_4^{2-}$	7633	3662
NPK	$^{13}CH_4 + SO_4^{2-}$	7633	3689
Control	$^{13}CH_4$ + Humic acids	7633	3613
Control	$^{13}CH_4$ + Humic acids	7633	3636
Control	$^{13}CH_4$ + Humic acids	7633	3805
Pig manure	$^{13}CH_4$ + Humic acids	7633	3738
Pig manure	$^{13}CH_4$ + Humic acids	7633	3772
Pig manure	$^{13}CH_4$ + Humic acids	7633	3556
Biochar	$^{13}CH_4$ + Humic acids	7633	3330
Biochar	$^{13}CH_4$ + Humic acids	7633	3584
Biochar	$^{13}CH_4$ + Humic acids	7633	3842
NPK	$^{13}CH_4$ + Humic acids	7633	3744
NPK	$^{13}CH_4$ + Humic acids	7633	3817
Control	Unincubated soil	7633	3479
Control	Unincubated soil	7633	3522
Control	Unincubated soil	7633	3503
Pig manure	Unincubated soil	7633	3193
Pig manure	Unincubated soil	7633	3144
Pig manure	Unincubated soil	7633	3436
Biochar	Unincubated soil	7633	2988
Biochar	Unincubated soil	7633	3324
Biochar	Unincubated soil	7633	3699
NPK	Unincubated soil	7633	3454
NPK	Unincubated soil	7633	3484

Table S3 Permutational multivariate analysis of variance results using unweighted UniFrac as a distance metric for pre-/post-incubation nested with fertilizer treatments

Factor	Degree of freedom	Sums of squares	Mean squares	F.Model	Variation (R2)	P value
Pre-/post-incubation	1	0.36	0.36	2.44	0.10	<0.001
Fertilizer treatments	3	0.52	0.17	1.16	0.14	0.071
Pre-/post-incubation: Fertilizer treatments	3	0.44	0.15	0.98	0.12	0.57
Residuals	16	2.39	0.15		0.64	
Total	23	3.71			1.00	

Table S4 Wilcoxon signed ranks test for phyla between pre-incubation and post-incubation samples

Taxa	Pre-incubation_Relative_Abundance	Post-incubation_Relative_Abundance	Z	Sig. (2-tailed)
Proteobacteria	0.302	0.277	-1.883a	0.060
Chloroflexi	0.105	0.166	-3.059b	0.002
Acidobacteria	0.163	0.150	-1.961a	0.050
Nitrospirae	0.107	0.087	-1.412a	0.158
Bacteroidetes	0.050	0.066	-1.961b	0.050
Planctomycetes	0.073	0.060	-2.040a	0.041
Verrucomicrobia	0.044	0.039	-1.883a	0.060
Actinobacteria	0.029	0.029	-.549a	0.583
Gemmatimonadetes	0.030	0.027	-1.334a	0.182
Patescibacteria	0.025	0.015	-1.961a	0.050
Rokubacteria	0.017	0.014	-1.804a	0.071
Spirochaetes	0.006	0.013	-2.040b	0.041
Latescibacteria	0.008	0.013	-2.746b	0.006
Firmicutes	0.002	0.009	-3.059b	0.002
Armatimonadetes	0.004	0.004	-.078a	0.937
Chlamydiae	0.010	0.004	-2.667a	0.008
FCPU426	0.003	0.003	-1.412a	0.158
Zixibacteria	0.002	0.002	-1.255b	0.209
Firestonebacteria	0.000	0.001	-3.059b	0.002
Cyanobacteria	0.002	0.001	-.784b	0.433
TA06	0.001	0.001	-.706b	0.480
BRC1	0.001	0.001	-.392b	0.695
Dadabacteria	0.001	0.001	-.157b	0.875
Lentisphaerae	0.000	0.000	-1.604b	0.109
Omnitrophicaeota	0.000	0.000	.000c	1.000
Caldiserica	0.000	0.000	-2.824b	0.005
Fibrobacteres	0.000	0.000	-2.701b	0.007
Elusimicrobia	0.000	0.000	-2.366b	0.018
LCP-89	0.000	0.000	-.943b	0.345
Epsilonbacteraeota	0.000	0.000	-.943b	0.345
WPS-2	0.000	0.000	-1.682a	0.093

Note: a, based on negative ranks. b, based on positive ranks. c, the sum of negative ranks equals the sum of positive ranks.

Table S5 Topological properties of the co-occurrence networks

Treatments	The Erdős–Rényi random networks							
	Bacterial co-occurrence network				Co-occurrence network associated with methane cycling			
	Average degree	**Average path length**	**Network diameter**	**Clustering coefficient**	**Average degree**	**Average path length**	**Network diameter**	**Clustering coefficient**
Pre-incubation	4.181	4.341±0.029	9.123±0.680	0.010±0.003	-	-	-	-
Post-incubation	11.233	2.984±0.002	5.009±0.094	0.015±0.001	-	-	-	-
Control	1.986	8.531±0.320	21.047±2.060	0.003±0.003	12.663	2.624±0.002	4.043±0.203	0.033±0.002
Pig manure	2.16	7.968±0.221	19.343±1.682	0.003±0.002	10.896	2.654±0.003	4.265±0.442	0.035±0.002
Biochar	1.825	9.461±0.440	23.790±2.523	0.002±0.002	15.538	2.460±0.001	4.000±0.000	0.042±0.002
NPK	2.533	6.799±0.130	16.041±1.336	0.004±0.002	7.357	2.988±0.008	5.395±0.505	0.030±0.003
Reference	3.528	4.601±0.056	10.072±0.811	0.011±0.004	3.732	4.128±0.054	8.921±0.795	0.018±0.006
Iron(III)	2.52	6.141±0.160	14.522±1.398	0.006±0.004	4.864	3.562±0.025	7.193±0.550	0.022±0.005
Nitrate	8.066	3.224±0.005	5.802±0.423	0.016±0.002	12.331	2.507±0.002	4.012±0.109	0.045±0.002
Sulfate	7.523	3.331±0.006	6.061±0.275	0.014±0.002	6.743	3.142±0.003	5.924±0.395	0.025±0.003
Humic acids	3.635	4.442±0.055	9.644±0.780	0.013±0.005	3.433	3.983±0.084	8.706±0.805	0.026±0.010
Treatments	**The real-world networks**							
	Bacterial co-occurrence network				Co-occurrence network associated with methane cycling			
	Average degree	**Average path length**	**Network diameter**	**Clustering coefficient**	**Average degree**	**Average path length**	**Network diameter**	**Clustering coefficient**
Pre-incubation	4.180	2.660	9.000	0.760	-	-	-	-
Post-incubation	11.230	5.660	16.000	0.760	-	-	-	-
Control	1.990	1.900	7.000	0.970	12.663	6.155	16.000	0.679
Pig manure	2.160	1.000	1.000	1.000	10.896	5.073	13.000	0.757
Biochar	1.820	1.000	2.000	1.000	15.538	4.552	13.000	0.877
NPK	2.530	3.090	9.000	0.830	7.357	3.218	8.000	0.761
Reference	3.530	2.640	8.000	0.730	3.732	3.701	11.000	0.782
Iron(III)	2.520	2.590	10.000	0.680	4.864	3.565	11.000	0.719
Nitrate	8.070	3.060	12.000	0.780	12.331	4.179	17.000	0.819
Sulfate	7.520	4.500	17.000	0.770	6.743	3.325	10.000	0.789
Humic acids	3.630	4.140	11.000	0.730	3.433	2.671	8.000	0.777

Note:

Average degree: how many nodes connected to one certain node, the higher the degree of a node in the graph, the higher the centrality of its degree.

Average path length: the average distance between any two nodes in the network reflects the degree of separation between the nodes in the network. Real networks usually have the smallest average path.

Network diameter: it is the shortest distance between the two most distant nodes in the network. In other words, once the shortest path length from every node to all other nodes is calculated, the diameter is the longest of all the calculated path lengths.

Clustering coefficient: relations between nodes in the network.

Table S6 The compositions of ^{13}C enriched biomarkers under fertilization treatments (A), and alternative electron acceptor (AEA) amendments (B) in paddy soil

A:

Source of Variation	DF	SS	MS	F	P
Fertilizer treatments	3	0.553	0.184	5.952	<0.001
^{13}C-PLFA	15	2.591	0.173	5.577	<0.001
Fertilizer treatments: ^{13}C-PLFA	45	2.264	0.0503	1.624	0.011
Residual	256	7.93	0.031		
Total	319	13.338	0.0418		

B:

Source of Variation	DF	SS	MS	F	P
AEA amendments	4	1.643	0.411	14.558	<0.001
^{13}C-PLFA	15	2.591	0.173	6.124	<0.001
AEA amendments:^{13}C-PLFA	60	2.334	0.0389	1.379	0.048
Residual	240	6.77	0.0282		
Total	319	13.338	0.0418		

Table S7 Permutational multivariate analysis of variance results using unweighted UniFrac as a distance metric for fertilizer treatments with and without CH_4

Factor	Degree of freedom	Sums of squares	Mean squares	F.Model	Variation (R2)	P value
Fertilizer treatments	3	0.58	0.19	1.45	0.18	<0.001
with/without CH_4	1	0.13	0.13	0.97	0.04	0.515
Fertilizer treatments: with/without CH_4	3	0.37	0.12	0.92	0.11	0.843
Residuals	16	2.14	0.13		0.66	
Total	23	3.22			1.00	

Table S8 Permutational multivariate analysis of variance results using unweighted UniFrac as a distance metric for fertilizer treatments and electron acceptor (AEA) amendments

Factor	Degree of freedom	Sums of squares	Mean squares	F.Model	Variation (R2)	P value
Fertilizer treatments	3	0.84	0.28	2.20	0.10	<0.001
AEA amendments	4	1.09	0.27	2.15	0.13	<0.001
Fertilizer treatments: AEA amendments	12	1.51	0.13	1.00	0.18	0.523
Residuals	40	5.07	0.13		0.60	
Total	59	8.51			1.00	

Table S9 LefSE analysis revealed bacterial biomarkers (from phylum to genus level) sensitive to fertilization

Kingdom	Phylum	Class	Order	Family	Genus	logarithm value	Fertilizer treatments	LDA	P-value
Bacteria	Chloroflexi	Anaerolineae				5.153	NPK	4.398	0.014
Bacteria	Chloroflexi					5.223	NPK	4.386	0.027
Bacteria	Proteobacteria	Deltaproteobacteria				5.114	Biochar	4.337	0.006
Bacteria	Proteobacteria					5.390	Biochar	4.323	0.048
Bacteria	Chloroflexi	Anaerolineae	Anaerolineales			4.968	NPK	4.236	0.044
Bacteria	Chloroflexi	Anaerolineae	Anaerolineales	Anaerolineaceae		4.968	NPK	4.236	0.044
Bacteria	Proteobacteria	Deltaproteobacteria	Desulfuromonadales	Geobacteraceae	Geobacter	4.614	Biochar	4.221	0.001
Bacteria	Proteobacteria	Deltaproteobacteria	Desulfuromonadales			4.614	Biochar	4.221	0.001
Bacteria	Proteobacteria	Deltaproteobacteria	Desulfuromonadales	Geobacteraceae		4.614	Biochar	4.221	0.001
Bacteria	Bacteroidetes	Bacteroidia	Bacteroidales	Prolixibacteraceae	WCHB1_32	4.051	Control	3.869	0.027
Bacteria	Chloroflexi	Anaerolineae	RBG_13_54_9			4.491	NPK	3.865	0.021
Bacteria	Chloroflexi	Anaerolineae	RBG_13_54_9	uncultured	Unclassified	4.356	NPK	3.767	0.007
Bacteria	Chloroflexi	Anaerolineae	RBG_13_54_9	uncultured		4.356	NPK	3.767	0.007
Bacteria	Bacteroidetes	Ignavibacteria				4.223	Pig manure	3.689	0.025
Bacteria	Actinobacteria					4.532	Control	3.637	0.046
Bacteria	Acidobacteria	Subgroup6				4.363	Control	3.542	0.032
Bacteria	Chloroflexi	Anaerolineae	SBR1031			3.982	NPK	3.533	0.013
Bacteria	Chloroflexi	Anaerolineae	SBR1031	uncultured		3.982	NPK	3.533	0.013
Bacteria	Chloroflexi	Anaerolineae	SBR1031	uncultured	Unclassified	3.982	NPK	3.533	0.013
Bacteria	Proteobacteria	Deltaproteobacteria	Syntrophobacterales			4.177	NPK	3.485	0.039
Bacteria	Proteobacteria	Deltaproteobacteria	Syntrophobacterales	Syntrophaceae		4.177	NPK	3.485	0.039
Bacteria	Actinobacteria	Thermoleophilia				4.088	Control	3.470	0.042
Bacteria	Patescibacteria	ABY1				3.776	Pig manure	3.461	0.021
Bacteria	Proteobacteria	Gammaproteobacteria	Betaproteobacteriales	Rhodocyclaceae	Dechloromonas	3.685	Biochar	3.458	0.007
Bacteria	Proteobacteria	Deltaproteobacteria	Myxococcales	Haliangiaceae		3.772	Biochar	3.439	0.020
Bacteria	Proteobacteria	Deltaproteobacteria	Myxococcales	Haliangiaceae	Haliangium	3.772	Biochar	3.439	0.020
Bacteria	Patescibacteria	ABY1	CandidatusFalkowbacteria	unculturedParcubacteriagroupbacterium	Unclassified	3.641	Pig manure	3.389	0.018
Bacteria	Patescibacteria	ABY1	CandidatusFalkowbacteri			3.641	Pig manure	3.381	0.018

			a						
Bacteria	Patescibacteria	ABY1	CandidatusFalkowbacteria	unculturedParcubacteriagroupbacterium		3.641	Pig manure	3.362	0.018
Bacteria	Firmicutes	Clostridia	Clostridiales	Ruminococcaceae	Ruminiclostridium1	3.546	Biochar	3.358	0.019
Bacteria	Firmicutes	Clostridia	Clostridiales	Ruminococcaceae		3.546	Biochar	3.357	0.019
Bacteria	Patescibacteria	ABY1	CandidatusMagasanikbacteria			3.438	Biochar	3.355	0.023
Bacteria	Patescibacteria	ABY1	CandidatusMagasanikbacteria	uncultured	Unclassified	3.438	Biochar	3.355	0.023
Bacteria	Patescibacteria	ABY1	CandidatusMagasanikbacteria	uncultured		3.438	Biochar	3.355	0.023
Bacteria	Firmicutes	Clostridia	Clostridiales	Clostridiaceae1	Anaerobacter	3.490	Pig manure	3.353	0.047
Bacteria	Patescibacteria	Parcubacteria	CandidatusWolfebacteria	CandidatusWolfebacteriabacterium		3.512	Biochar	3.349	0.002
Bacteria	Patescibacteria	Parcubacteria	CandidatusWolfebacteria	CandidatusWolfebacteriabacterium	Unclassified	3.512	Biochar	3.349	0.002
Bacteria	Patescibacteria	Parcubacteria	CandidatusWolfebacteria			3.512	Biochar	3.347	0.002
Bacteria	Acidobacteria	Subgroup6	unculturedAcidobacterialesbacterium	Unclassified	Unclassified	4.052	Control	3.311	0.038
Bacteria	Acidobacteria	Subgroup6	unculturedAcidobacterialesbacterium			4.052	Control	3.311	0.038
Bacteria	Acidobacteria	Subgroup6	unculturedAcidobacterialesbacterium	Unclassified		4.052	Control	3.311	0.038
Bacteria	Proteobacteria	Deltaproteobacteria	Syntrophobacterales	Syntrophaceae	Syntrophus	3.458	NPK	3.225	0.034
Bacteria	Chloroflexi	KD4_96	unculturedLongilineasp	Unclassified	Unclassified	3.417	NPK	3.180	0.035
Bacteria	Chloroflexi	KD4_96	unculturedLongilineasp			3.417	NPK	3.180	0.035
Bacteria	Chloroflexi	KD4_96	unculturedLongilineasp	Unclassified		3.417	NPK	3.180	0.035

Table S10 LefSE analysis revealed bacterial biomarkers (from phylum to genus level) sensitive to electron acceptor amendments

Kingdom	Phylum	Class	Order	Family	Genus	logarithm value	AEAs amendments	Fertilizer treatments	LDA	P-value
Bacteria	Epsilonbacteraeota	Campylobacteria	Campylobacterales	Sulfurospirillaceae		3.110	Humic acids	Control	3.268	0.034
Bacteria	Acidobacteria	Subgroup17	uncultured	Unclassified	Unclassified	3.045	Humic acids	Control	3.346	0.034
Bacteria	Proteobacteria	Alphaproteobacteria	Rhizobiales	Beijerinckiaceae	Roseiarcus	3.620	Humic acids	Control	3.366	0.024
Bacteria	Proteobacteria	Alphaproteobacteria	uncultured	unculturedalphaproteobacterium		3.656	Humic acids	Control	3.399	0.023
Bacteria	Acidobacteria	Holophagae	Holophagales	Holophagaceae		3.903	Humic acids	Control	3.402	0.046
Bacteria	Proteobacteria	Gammaproteobacteria	Betaproteobacteriales	A21b		3.620	Humic acids	Control	3.411	0.024
Bacteria	Chloroflexi	JG30_KF_CM66	uncultured	Unclassified		3.620	Humic acids	Control	3.439	0.024
Bacteria	Spirochaetes	Spirochaetia				3.111	Humic acids	Control	3.455	0.020
Bacteria	Planctomycetes	Phycisphaerae				4.530	Humic acids	Control	3.860	0.047
Bacteria	Nitrospirae	Nitrospira	Nitrospirales	Nitrospiraceae	Leptospirillum	4.530	Humic acids	Control	3.916	0.047
Bacteria	Rokubacteria	NC10	Methylomirabilales	Methylomirabilaceae	Sh765B_TzT_35	3.740	Humic acids	Pig manure	3.418	0.038
Bacteria	Bacteroidetes	Ignavibacteria	SJA_28			3.740	Humic acids	Pig manure	3.421	0.038
Bacteria	Acidobacteria	Thermoanaerobaculia	Thermoanaerobaculales	Thermoanaerobaculaceae		3.740	Humic acids	Pig manure	3.443	0.038
Bacteria	Actinobacteria	Coriobacteriia	OPB41	uncultured	Unclassified	4.752	Humic acids	Pig manure	4.407	0.026
Bacteria	Chloroflexi	Ktedonobacteria	Ktedonobacterales	Ktedonobacteraceae		4.752	Humic acids	Pig manure	4.423	0.026
Bacteria	Patescibacteria	Parcubacteria	CandidatusYanofskybacteria	uncultured		4.752	Humic acids	Pig manure	4.431	0.026
Bacteria	Chloroflexi	Ktedonobacteria	Ktedonobacterales	Ktedonobacteraceae	HSBOF53_F07	5.239	Humic acids	Pig manure	4.644	0.013
Bacteria	Proteobacteria	Alphaproteobacteria	Elsterales			5.504	Humic acids	Pig manure	4.664	0.026
Bacteria	Acidobacteria	Aminicenantia				3.906	Humic acids	Biochar	3.476	0.017
Bacteria	Acidobacteria	Aminicenantia	Aminicenantales	uncultured	Unclassified	3.906	Humic acids	Biochar	3.498	0.017
Bacteria	Acidobacteria	Aminicenantia	Aminicenantales	uncultured		3.906	Humic acids	Biochar	3.506	0.017
Bacteria	Acidobacteria	Aminicenantia	Aminicenantales			3.906	Humic acids	Biochar	3.540	0.017
Bacteria	Actinobacteria	Actinobacteria	Frankiales			4.113	Humic acids	Biochar	3.703	0.038

Bacteria	Patescibacteria	Parcubacteria				4.116	Humic acids	Biochar	3.774	0.031
Bacteria	Bacteroidetes	Ignavibacteria	SJA_28			3.513	Iron	Control	3.381	0.013
Bacteria	Proteobacteria	Alphaproteobacteria	Rhizobiales			4.355	Iron	Control	3.839	0.047
Bacteria	Proteobacteria	Deltaproteobacteria	DeltaproteobacteriaIncertaeSedis	Syntrophorhabdaceae	Syntrophorhabdus	3.572	Iron	Pig manure	3.309	0.022
Bacteria	Bacteroidetes	Ignavibacteria	Ignavibacteriales	Ignavibacteriaceae	Ignavibacterium	3.572	Iron	Pig manure	3.315	0.022
Bacteria	Proteobacteria	Gammaproteobacteria	Betaproteobacteriales	Chromobacteriaceae		3.678	Iron	Pig manure	3.335	0.040
Bacteria	Proteobacteria	Gammaproteobacteria	Betaproteobacteriales	B1_7BS	uncultured	3.217	Iron	Pig manure	3.345	0.029
Bacteria	Proteobacteria	Alphaproteobacteria	uncultured	unculturedalphaproteobacterium		3.219	Iron	Pig manure	3.460	0.032
Bacteria	Acidobacteria	Holophagae	Holophagales	Holophagaceae		3.615	Iron	Pig manure	3.569	0.017
Bacteria	Chloroflexi	JG30_KF_CM66	unculturedsoilbacterium	Unclassified	Unclassified	4.479	Iron	Pig manure	3.854	0.043
Bacteria	Chloroflexi	JG30_KF_CM66	uncultured	Unclassified		4.479	Iron	Pig manure	3.868	0.043
Bacteria	Verrucomicrobia	Verrucomicrobiae	Pedosphaerales			4.628	Iron	Biochar	3.871	0.045
Bacteria	Verrucomicrobia	Verrucomicrobiae	Pedosphaerales	Pedosphaeraceae		4.628	Iron	Biochar	3.951	0.045
Bacteria	Nitrospirae					5.523	Iron	NPK	4.833	0.045
Bacteria	Actinobacteria	MB_A2_108	uncultured			3.304	Nitrate	Control	3.165	0.028
Bacteria	Epsilonbacteraeota	Campylobacteria	Campylobacterales	Sulfurospirillaceae	Sulfurospirillum	3.021	Nitrate	Control	3.265	0.049
Bacteria	Proteobacteria	Deltaproteobacteria	Syntrophobacterales	Syntrophobacteraceae	Desulforhabdus	3.353	Nitrate	Control	3.301	0.045
Bacteria	Bacteroidetes					3.290	Nitrate	Control	3.320	0.012
Bacteria	Acidobacteria	Holophagae	Subgroup7	uncultured		3.290	Nitrate	Control	3.370	0.012
Bacteria	Rokubacteria	NC10	Methylomirabilales	Methylomirabilaceae	Sh765B_TzT_35	3.290	Nitrate	Control	3.381	0.012
Bacteria	Acidobacteria	Thermoanaerobaculia	Thermoanaerobaculales	Thermoanaerobaculaceae		3.290	Nitrate	Control	3.387	0.012
Bacteria	Armatimonadetes	DG_56				3.706	Nitrate	Control	3.423	0.036
Bacteria	Dadabacteria	Dadabacteriia	Dadabacteriales			3.290	Nitrate	Control	3.438	0.012

Bacteria	Actinobacteria	Coriobacteriia	OPB41	uncultured	Unclassified	3.845	Nitrate	Control	3.489	0.029
Bacteria	Proteobacteria	Deltaproteobacteria	Myxococcales	P3OB_42		4.102	Nitrate	Control	3.687	0.047
Bacteria	Actinobacteria	Thermoleophilia	Solirubrobacterales	Solirubrobacteraceae		4.207	Nitrate	Control	3.760	0.020
Bacteria	Patescibacteria	Parcubacteria	CandidatusNomurabacteria	CandidatusNomurabacteriabacterium	Unclassified	4.207	Nitrate	Control	3.792	0.020
Bacteria	Rokubacteria	NC10	Rokubacteriales	uncultured	Unclassified	4.207	Nitrate	Control	3.810	0.020
Bacteria	Acidobacteria	Subgroup18	unculturedAcidobacteriabacterium	Unclassified		4.207	Nitrate	Control	3.810	0.020
Bacteria	Proteobacteria	Gammaproteobacteria	Betaproteobacteriales	Burkholderiaceae	uncultured	4.207	Nitrate	Control	3.810	0.020
Bacteria	Acidobacteria	Subgroup11	unculturedAcidobacteriumsp	Unclassified		4.207	Nitrate	Control	3.821	0.020
Bacteria	Proteobacteria	Deltaproteobacteria	Syntrophobacterales	Syntrophobacteraceae	Desulforhabdus	3.953	Nitrate	Pig manure	3.343	0.032
Bacteria	Bacteroidetes					3.953	Nitrate	Pig manure	3.367	0.032
Bacteria	Acidobacteria	Subgroup17	uncultured	Unclassified	Unclassified	3.953	Nitrate	Pig manure	3.370	0.032
Bacteria	Acidobacteria	Holophagae	Subgroup7	uncultured		3.953	Nitrate	Pig manure	3.406	0.032
Bacteria	Acidobacteria	Holophagae	Holophagales	Holophagaceae	marinegroup	3.173	Nitrate	Biochar	3.390	0.030
Bacteria	Proteobacteria	Gammaproteobacteria	Betaproteobacteriales	Burkholderiaceae	Massilia	3.828	Nitrate	Biochar	3.567	0.039
Bacteria	Chloroflexi	KD4_96	uncultured	Unclassified		3.334	Reference	Control	3.232	0.045
Bacteria	Planctomycetes	Planctomycetacia	Isosphaerales	Isosphaeraceae		3.334	Reference	Control	3.243	0.045
Bacteria	Chloroflexi	Ktedonobacteria	Ktedonobacterales	Ktedonobacteraceae	JG30a_KF_32	3.334	Reference	Control	3.253	0.045
Bacteria	Proteobacteria	Deltaproteobacteria	Myxococcales	Archangiaceae		2.988	Reference	Control	3.257	0.039
Bacteria	Actinobacteria	Actinobacteria	Frankiales	Sporichthyaceae	CandidatusPlanktophila	3.334	Reference	Control	3.258	0.045
Bacteria	Patescibacteria	Parcubacteria	CandidatusYanofskybacteria	CandidatusYanofskybacteriabacterium	Unclassified	3.334	Reference	Control	3.284	0.045
Bacteria	Proteobacteria	Gammaproteobacteria	Betaproteobacteriales	SC_I_84	unculturedbetaproteobacteriu	3.967	Reference	Control	3.301	0.034

					m					
Bacteria	Proteobacteria	Gammaproteobacteria	Betaproteobacteriales	B1_7BS	uncultured	2.988	Reference	Control	3.304	0.039
Bacteria	Proteobacteria	Alphaproteobacteria	Holosporales	Holosporaceae		2.988	Reference	Control	3.305	0.039
Bacteria	Verrucomicrobia	Verrucomicrobiae	S_BQ2_57soilgroup	uncultured		3.967	Reference	Control	3.318	0.034
Bacteria	Chloroflexi	Anaerolineae	RBG_13_54_9	unculturedCaldilineaceaebacterium		3.967	Reference	Control	3.348	0.034
Bacteria	Planctomycetes	Phycisphaerae	Tepidisphaerales	CPla_3termitegroup		4.071	Reference	Control	3.469	0.045
Bacteria	Chloroflexi	Ktedonobacteria	Ktedonobacterales	Ktedonobacteraceae		4.066	Reference	Control	3.502	0.037
Bacteria	Caldiserica	Caldisericia	Caldisericales			4.041	Reference	Control	3.503	0.042
Bacteria	Chloroflexi	Ktedonobacteria	Ktedonobacterales	Ktedonobacteraceae	HSBOF53_F07	4.066	Reference	Control	3.503	0.037
Bacteria	Proteobacteria	Alphaproteobacteria	Elsterales			4.066	Reference	Control	3.533	0.037
Bacteria	Bacteroidetes	Bacteroidia	Cytophagales			4.066	Reference	Control	3.568	0.037
Bacteria	Proteobacteria	Deltaproteobacteria	RCP2_54			4.310	Reference	Control	3.730	0.019
Bacteria	Proteobacteria	Deltaproteobacteria	Desulfovibrionales			4.485	Reference	Control	3.953	0.021
Bacteria	Chloroflexi	Anaerolineae	Anaerolineales	Anaerolineaceae	GWD2_49_16	4.548	Reference	Control	4.161	0.043
Bacteria	Actinobacteria	Acidimicrobiia	uncultured	uncultured	Unclassified	4.548	Reference	Control	4.178	0.043
Bacteria	FCPU426	uncultured	Unclassified	Unclassified	Unclassified	4.553	Reference	Control	4.178	0.027
Bacteria	Patescibacteria	Berkelbacteria	uncultured			4.548	Reference	Control	4.196	0.043
Bacteria	Rokubacteria	NC10	Rokubacteriales			4.982	Reference	Control	4.422	0.028
Bacteria	Planctomycetes	Phycisphaerae	Tepidisphaerales	CPla_3termitegroup	unculturedplanctomycete	4.974	Reference	Control	4.445	0.019
Bacteria	Proteobacteria	Alphaproteobacteria	Rhizobiales	Methyloligellaceae	uncultured	5.026	Reference	Control	4.446	0.020
Bacteria	Planctomycetes	Phycisphaerae	Tepidisphaerales	WD2101soilgroup	unculturedsoilbacterium	4.974	Reference	Control	4.452	0.019
Bacteria	Actinobacteria	MB_A2_108	uncultured			3.619	Reference	Pig manure	3.095	0.046
Bacteria	Chloroflexi	KD4_96	uncultured	Unclassified		3.619	Reference	Pig manure	3.126	0.046
Bacteria	Bacteroidetes	Ignavibacteria	Kryptoniales	MSB_3C8	unculturedChloroflexibacteri	3.619	Reference	Pig manure	3.150	0.046

					um					
Bacteria	Chloroflexi	Ktedonobacteria	Ktedonobacterales	Ktedonobacteraceae	JG30a_KF_32	3.317	Reference	Pig manure	3.291	0.049
Bacteria	Proteobacteria	Gammaproteobacteria	Acidiferrobacterales			3.895	Reference	Pig manure	3.581	0.040
Bacteria	Armatimonadetes	DG_56				4.217	Reference	Pig manure	3.807	0.042
Bacteria	Spirochaetes	Spirochaetia				4.456	Reference	Pig manure	4.218	0.042
Bacteria	Latescibacteria	Latescibacteria	Latescibacterales	Latescibacteraceae	CandidatusLatescibacter	2.980	Reference	Biochar	3.004	0.031
Bacteria	Latescibacteria	Latescibacteria				2.980	Reference	Biochar	3.027	0.031
Bacteria	Latescibacteria	Latescibacteria	Latescibacterales			2.980	Reference	Biochar	3.035	0.031
Bacteria	Latescibacteria	Latescibacteria	Latescibacterales	Latescibacteraceae		2.980	Reference	Biochar	3.080	0.031
Bacteria	Proteobacteria	Gammaproteobacteria	KI89Aclade	uncultured	Unclassified	3.351	Reference	Biochar	3.114	0.036
Bacteria	Proteobacteria	Gammaproteobacteria	KI89Aclade			3.351	Reference	Biochar	3.119	0.036
Bacteria	Proteobacteria	Gammaproteobacteria	KI89Aclade	uncultured		3.351	Reference	Biochar	3.150	0.036
Bacteria	Proteobacteria	Alphaproteobacteria	uncultured	uncultured		3.738	Reference	Biochar	3.342	0.020
Bacteria	Proteobacteria	Alphaproteobacteria	uncultured	uncultured	Unclassified	3.738	Reference	Biochar	3.357	0.020
Bacteria	Proteobacteria	Alphaproteobacteria	uncultured			3.812	Reference	Biochar	3.360	0.021
Bacteria	Acidobacteria	Subgroup6	uncultured			4.013	Reference	Biochar	3.439	0.030
Bacteria	Proteobacteria	Gammaproteobacteria	Betaproteobacteriales	SC_I_84	unculturedsoilbacterium	3.201	Reference	Biochar	3.457	0.042
Bacteria	Acidobacteria	Subgroup6	uncultured	Unclassified		4.013	Reference	Biochar	3.463	0.030
Bacteria	Acidobacteria	Subgroup6	uncultured	Unclassified	Unclassified	4.013	Reference	Biochar	3.502	0.030
Bacteria	Verrucomicrobia	Verrucomicrobiae	Pedosphaerales	Pedosphaeraceae	ADurb_Bin063_1	4.468	Reference	Biochar	3.851	0.050
Bacteria	Bacteroidetes	Bacteroidia				4.718	Reference	Biochar	4.228	0.042
Bacteria	Armatimonadetes	Chthonomonadetes	Chthonomonadales	Chthonomonadaceae		4.555	Sulfate	Control	4.137	0.025
Noblasthit	Unclassified	Unclassified	Unclassified			4.470	Sulfate	Control	4.139	0.025
Bacteria	Bacteroidetes	Bacteroidia	Chitinophagales	Chitinophagaceae		4.470	Sulfate	Control	4.163	0.025
Bacteria	Proteobacteria	Deltaproteobacteria	Sva0485			4.470	Sulfate	Control	4.170	0.025
Bacteria	Caldiserica	Caldisericia	Caldisericales	LF045		5.998	Sulfate	Control	4.234	0.020

Bacteria	Spirochaetes	Leptospirae	Leptospirales			4.844	Sulfate	Control	4.459	0.045
Bacteria	Dadabacteria	Dadabacteriia	Dadabacteriales	uncultured	Unclassified	4.844	Sulfate	Control	4.463	0.045
Bacteria	Proteobacteria	Alphaproteobacteria	Sphingomonadales	Sphingomonadaceae	Sphingomonas	4.844	Sulfate	Control	4.497	0.045
Bacteria	Patescibacteria	Parcubacteria	CandidatusNomurabacteria	CandidatusNomurabacteriabacterium		5.494	Sulfate	Control	4.732	0.039
Bacteria	Planctomycetes	Planctomycetacia	Isosphaerales	Isosphaeraceae		2.941	Sulfate	Pig manure	3.274	0.044
Bacteria	Proteobacteria	Deltaproteobacteria	Myxococcales	Archangiaceae		2.941	Sulfate	Pig manure	3.305	0.044
Bacteria	Proteobacteria	Gammaproteobacteria	Betaproteobacteriales	SC_I_84	unculturedbetaproteobacterium	3.186	Sulfate	Pig manure	3.331	0.027
Bacteria	Proteobacteria	Alphaproteobacteria	Holosporales	Holosporaceae		3.657	Sulfate	Pig manure	3.356	0.038
Bacteria	Verrucomicrobia	Verrucomicrobiae	S_BQ2_57soilgroup	uncultured		3.447	Sulfate	Pig manure	3.363	0.027
Bacteria	Chloroflexi	Anaerolineae	RBG_13_54_9	unculturedCaldilineaceaebacterium		3.657	Sulfate	Pig manure	3.373	0.038
Bacteria	Proteobacteria	Alphaproteobacteria	Rhizobiales	Beijerinckiaceae	Roseiarcus	3.447	Sulfate	Pig manure	3.394	0.027
Bacteria	Proteobacteria	Alphaproteobacteria	Rhizobiales	Xanthobacteraceae	Pseudolabrys	3.447	Sulfate	Pig manure	3.410	0.027
Bacteria	Proteobacteria	Gammaproteobacteria	Betaproteobacteriales	A21b		4.061	Sulfate	Pig manure	3.664	0.034
Bacteria	Chloroflexi	JG30_KF_CM66	unculturedsoilbacterium			4.436	Sulfate	Pig manure	3.912	0.031
Bacteria	Firmicutes	Clostridia	Clostridiales	Clostridiaceae1	Clostridiumsensustricto12	4.194	Sulfate	Biochar	3.876	0.026
Bacteria	Firmicutes	Clostridia	Clostridiales	Clostridiaceae1		4.205	Sulfate	Biochar	3.911	0.025
Bacteria	Firmicutes	Clostridia				4.656	Sulfate	Biochar	4.323	0.047
Bacteria	Firmicutes	Clostridia	Clostridiales			4.656	Sulfate	Biochar	4.325	0.047
Bacteria	Firmicutes					4.656	Sulfate	Biochar	4.357	0.047
Bacteria	Verrucomicrobia	Verrucomicrobiae	Opitutales	Opitutaceae		4.225	Sulfate	NPK	4.287	0.040
Bacteria	Verrucomicrobia	Verrucomicrobiae	Opitutales	Opitutaceae	Lacunisphaera	4.225	Sulfate	NPK	4.541	0.040
Bacteria	Verrucomicrobia	Verrucomicrobiae	Opitutales			4.225	Sulfate	NPK	4.556	0.040

Declaration

I, hereby, declare that this Ph.D. dissertation has not been presented to any other examining body either in its present or a similar form. I also affirm that I have not applied for a Ph.D. at any other higher school of education. I solemnly declare that this dissertation was undertaken independently and without any unauthorized aid.

Göttingen

Lichao Fan